PRELIMINARY DESIGN STUDY OF A LUNAR LOCAL SCIENTIFIC SURVEY MODULE (LSSM)

FINAL TECHNICAL REPORT

MOBILITY SYSTEM ANALYSIS AND DESIGN

D2-83012-1

Prepared for

NATIONAL AERONAUTICS AND SPACE ADMINISTRATION

GEORGE C. MARSHALL SPACE FLIGHT CENTER

Under

CONTRACT NAS8-11411, MOD. 2

June 1966

X66 23302 (ACCESSION NUMBER)	(THRU)
360 (PAGES)	2D (CODE)
CR-77969 (NASA CR OR TMX OR AD NUMBER)	11 (CATEGORY)

U. S. Government Agencies and Contractors Only

Prepared for The Boeing Company by General Motors Corporation, Defense Research Laboratories, Santa Barbara, California, as TR66-17

THE BOEING COMPANY
SPACE DIVISION
SEATTLE, WASHINGTON

(D2-83012-1) PRELIMINARY DESIGN STUDY OF A LUNAR LOCAL SCIENTIFIC SURVEY MODULE (LSSM) Final Technical Report (General Motors Corp.) 360 p

N75-74973

Unclas
00/98 28203

PRELIMINARY DESIGN STUDY OF A LUNAR LOCAL SCIENTIFIC SURVEY MODULE (LSSM)

FINAL TECHNICAL REPORT: LSSM MOBILITY SYSTEM

D2-83012-1

Prepared For
The Boeing Company
Seattle, Washington

Under

P.O. No. K-634755-9548, Change No. 2
(NASA Prime Contract 8-11411)

GM DEFENSE RESEARCH LABORATORIES
SANTA BARBARA, CALIFORNIA

TR66-17

JULY 1966

FOREWORD

This document is one of the final reports identified in the accompanying document tree presenting the results of a Preliminary Design Study of a Lunar Local Scientific Survey Module (LSSM). This study was performed for the National Aeronautics and Space Administration, Marshall Space Flight Center, Huntsville, Alabama under Contract NAS 8-11411, Modification No. 2, by The Boeing Company with the assistance of General Motors Corporation — Defense Research Laboratories and A. C. Electronics Division, Radio Corporation of America, and the Garrett Corporation — AiResearch Division.

The NASA Technical Supervisor for the contract was Mr. Lynn L. Bradford, Advanced Systems Office, Marshall Space Flight Center.

BACKGROUND

The Apollo Applications Program (AAP) has been proposed to extend the capabilities of Apollo systems to extensive Earth and lunar orbital, and lunar surface, scientific operations. In a typical AAP lunar surface mission, two flights will be made to the lunar surface. The first will deliver a LEM-Shelter, together with scientific and operational support equipment. The second flight will deliver two astronaut-scientists in a LEM-Taxi to the vicinity of the LEM-Shelter. A key element of support equipment delivered by the first flight will be surface mobility aids to extend the astronaut's range of exploration. These mobility aids may include one or two lunar local scientific survey modules (LSSM's) and/or a lunar manned flying system (MFS). The LSSM, a manned lunar surface vehicle, will transport a pressure-suited astronaut and an extensive inventory of scientific equipment on sorties of up to 6 hours duration within an area of 8-kilometer radius about the lunar landing site.

LSSM GENERAL DESCRIPTION

The baseline LSSM vehicle, as illustrated below, is a six-wheeled semi-articulated vehicle capable of traversing the lunar surface under direct control or an on-board pressure-suited crew member. The forward unit provides crew station, life support (PLSS) stowage, and space for carrying a cargo of scientific equipment or a second astronaut. The aft unit carries equipment for communications, navigation, drive system electronics, and power. The LSSM is designed to provide transportation of an astronaut-scientist and a 320-kilogram (700 pound) load of scientific equipment for round trips of up to 26 kilometers in traversed distance on the lunar surface.

The four-wheeled forward unit and the two-wheeled aft unit are connected by a flexible frame to provide freedom of pitch and roll movement between the two units. Ackermann-type steering is used on both front and rear wheel pairs.

The 1.02-meter (40-inch)-diameter wheels are of flexible-wire-frame construction. Each wheel is mounted on a parallel arm suspension with torsion bar springing and a viscous damper. The wheels are driven by individual electric motors through a harmonic drive gear reduction.

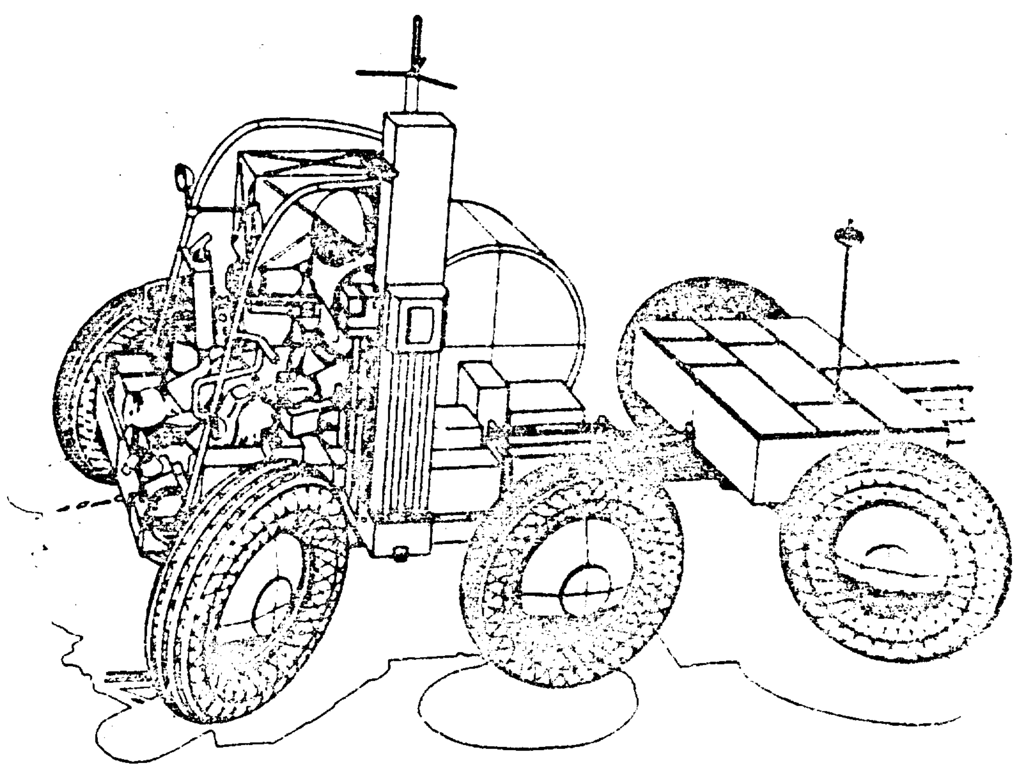

Electric power is provided by two 3-kilowatt-hour silver-zinc storage batteries that are recharged betweensorties from the LEM-Shelter power system. A 50-watt SNAP 27 radioisotope power system supplies the small amounts of power required during lunar storage, when the LSSM cannot be dependent on the LEM-Shelter.

Communications are provided by S-band and VHF equipment adapted from LEM designs. Direct two-way voice communication with Earth is provided, as well as a 1.6 kilobit-per-second telemetry capability for vehicle monitoring and scientific data transmission.

A piloting mode of navigation is provided by an odometer distance measurement system and an inertial measurement unit for heading information.

All of the electrical and electronic equipment is packaged on the aft unit and uses a passive thermal control system. Elements of this system include the thermally insulated compartment, a segmented horizontal space radiator, and a two-phase wax heat sink. The heat-sink material permits spreading the high heat-rejection loads of the 6-hour sorties over a 24-hour duty cycle, thus minimizing radiator area requirements.

The crew station provides a seat with adjustable foot position for a range of astronaut sizes, a folding boarding platform, a side-arm controller for vehicle throttle, brake and steering functions, and a control and display panel. The seat and support structure (roll bar) fold for stowage on the LEM-Shelter.

Life support is provided by the astronaut's pressure suit and three portable life support system (PLSS) units. One of these is worn by the astronaut and used for operations off the vehicle. The other two units are vehicle-mounted and provide for on-board operations and an emergency reserve."Y" connections on the suit permit rapid and reliable transfer from one unit to another.

The LSSM provides for a variety of both vehicle-mounted and vehicle-transported scientific equipment. Major elements include a 3-meter drill (20 kilograms) in the first category and the emplaced scientific station (ESS) (136 kilograms) in the second category.

LSSM OPERATION AND PERFORMANCE

After delivery to the lunar surface as part of the total lunar exploration payload, the LSSM may remain in its stowed position on the LEM-Shelter for up to six months. During this storage period, critical system parameters are monitored by telemetry transmission to Earth using the LSM-Shelter S-band equipment. A signal umbilical connecting the LSSM telemetry system to the LEM-Shelter communications system is provided for this purpose.

The operational mission begins with arrival of the two-man exploration crew in a LEM-Taxi. The LSSM is unloaded from the LEM-Shelter by the men using mechanical unloading aids as necessary. The LSSM tie-down and unloading system is currently considered an element of payload integration hardware, and not an element of the LSSM system. Technical consideration of requirements in these areas are included in this study, but no resource allocations are provided.

The operational mission involves a series of one-man, 6-hour sorties within an 8-kilometer radius of the LEM-Shelter. The sorties vary in distance traversed and scientific activity accomplished within the two principal constraints of 6-hour duration and 6-kilowatt-hour energy reserve in the fully charged LSSM batteries. Typical extremes are a 26-kilometer traverse distance combined with 1.3 hours of scientific observation, and a 16-kilometer traverse distance combined with 3 hours of activity to drill a 3-meter hole and install an emplaced scientific station.

The LSSM is capable of performing its mission in a wide variety of lunar terrain conditions. Drawbar pull-to-weight ratio ranges from 0.56 in hard soils to 0.13

in extremely soft soils (bearing pressure of 1 psi per foot sinkage). Average velocity capability ranges from 7.2 kilometers per hour across maria profiles to 5.6 kilometers per hour across typical uplands profiles. Maximum design speed on level, smooth terrain is 16 kilometers per hour. The vehicle is capable of negotiating 130-centimeter-high step obstacles and 142-centimeter-wide crevices. The vehicle is statically stable to 52 degrees in roll and 62 degrees in pitch, and is dynamically stable for all conditions of speed and turning radius on any slopes expected to be encountered in the lunar maria or uplands.

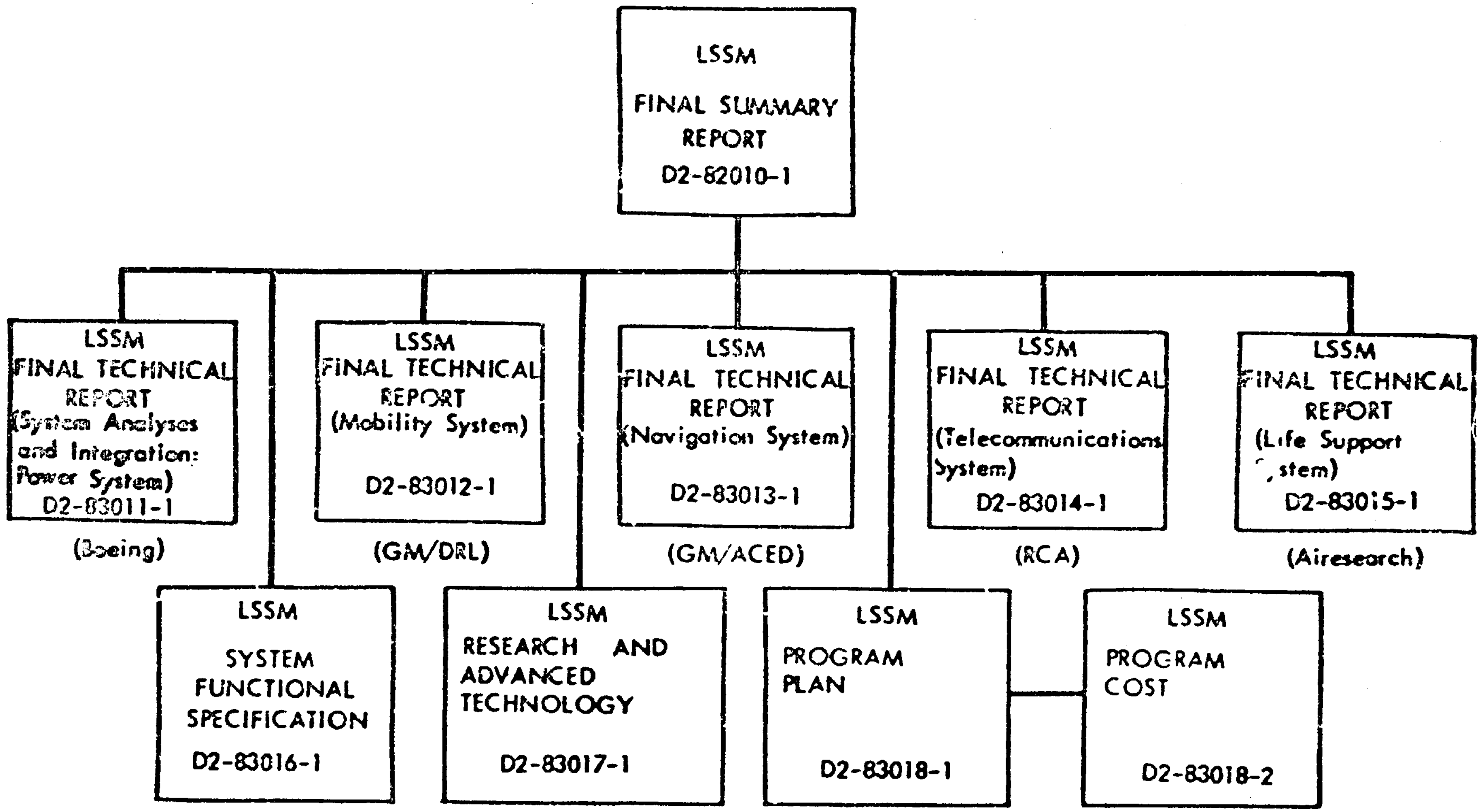

LSSM FINAL REPORTS DOCUMENT TREE

TABLE OF CONTENTS

TABLE OF CONTENTS CONTINUED

LIST OF ILLUSTRATIONS

LIST OF ILLUSTRATIONS (CONTINUED)

LIST OF ILLUSTRATIONS (CONTINUED)

LIST OF ILLUSTRATIONS (CONTINUED)

LIST OF ILLUSTRATIONS (CONTINUED)

LIST OF ILLUSTRATIONS (CONTINUED)

1.0 INTRODUCTION

1.1 GENERAL

This document reports the technical work accomplished by GM Defense Research Laboratories (GM DRL), General Motors Corporation, under Boeing Purchase Order K-634755-9548, Change #2 (NASA Prime Contract NAS 8-11411), on the Preliminary Design Study of a Lunar "Local Scientific Survey Module" (LSSM).

The major objectives of the program were to conduct a preliminary design of the selected LSSM concept with emphasis on the mobility system, and to perform a performance analysis of the derived design.

To accomplish these technical objectives, the following approach was taken and the results are reported herein:

- A review was made of existing lunar surface wheeled vehicle concepts to determine the best approach to LSSM design.

- A range of feasible LSSM conceptual configurations was defined and their performance characteristics determined.

- Based on system restraints and performance requirements, a selection was made of the conceptual approach considered most promising for LSSM baseline design. The configuration selected was a 6 x 6 semi-articulated vehicle consisting of a 2-wheel unit connected to a 4-wheel unit through a flexible frame coupling. All wheels would be individually powered.

- The major mobility subsystems, consisting of wheels, wheel drive mechanisms, suspension, steering, chassis-frame and electric drive system, were designed to given performance and environmental requriements, and incorporated into a complete mobility system assembly.

- An overall LSSM system conceptual design was performed to achieve integration of all LSSM subsystems including power, communications, navigation, crew accommodations and scientific equipment, in addition to the mobility system.

- A detailed mobility performance analysis of the baseline LSSM was performed including characteristics pertaining to soft ground mobility, obstacle capability, maneuverability and dynamic ride behavior.

- Design and functional specifications were prepared for the mobility system.

- Failure mode and reliability analyses were performed for the mobility system.

1.2 REQUIREMENTS

Major requirements affecting LSSM concept selection and the design of the mobility system were:

- Maximum LSSM system mass 2500 lbm (1140 kg).
- Maximum mass without cargo or operator 1540 lbm (700 kg).
- Ability to transport up to 700 lbm (318 kg) of specified scientific equipment, or a second astronaut in place of the cargo.
- Speed of at least 5 km/hr on level soft soil ($k_\phi = 0.5$, $n = 0.5$).
- Speed of at least 8 km/hr on level compacted soil ($k_\phi = 6.0$, $n = 1.25$).
- Ability to negotiate all soil and slope combinations specified in Engineering Lunar Model Surface (ELMS), KSC TR-83-D.
- Average speed capability over ELMS should be at least 5 km/hr.
- Maximum mobility and maneuverability over as wide a range of possible lunar surface conditions as practicable.
- 200 km (125 miles) total travel in 14 day (earth) period, maximum sortie distance of 25 km (16 miles), minimum operational radius of 8 km (5 miles) from LEM/Shelter.
- Lunar day or night operational capability.
- Capable of being stored in standby mode for at least 6 months.
- Compatible with volume constraints of LEM/Shelter.
- Capable of being unloaded and deployed on the lunar surface by one astronaut.
- Capable of withstanding all handling, transportation, launch, flight, staging and operational loads.
- Mission success and crew safety are prime design objectives.

2.0 REVIEW OF EXISTING WHEELED VEHICLE CONCEPTS

2.1 APPROACH

In order to assist in the formulation of LSSM vehicle concepts compatible with system and mission requirements, a literature search was conducted to gather together as many previously proposed lunar wheeled vehicle concepts as possible. This review was limited to wheeled vehicle concepts since studies performed during the MOLAB Program had shown that, on the basis of locomotion efficiency and reliability in the expected lunar environment, wheels would be the most practical mode of locomotion over the lunar surface.

From a review of the references listed in Figure 2.1.1, it was determined that at least forty-seven (47) wheeled vehicle concepts had been previously considered or proposed for lunar use. These are summarized in Figure 2.1.2 according to proposing organization, literature source, vehicle type, and available characteristics.

EFERENCES

(1) Lunar Soft Landing Study for NASA, Army Ballistic Missile Agency, Section III, ABMA DLS-N-26-59, 17 December 1959.

(2) Grumman Project 344, Summary Report, Studies of Lunar Logistics System Payload Performance, Supplement 1, Study of LLS Payloads Compatible with a Modified LEM.

(3) Lunar Logistics System Study, Vol. X, MTP-M-63-I, George C. Marshall Space Flight Center, NASA, March 15, 1963.

(4) Grumman Project 344, Summary Report, Studies of Lunar Logistics System Payload Performance, PDR-344-2b, January 7, 1963.

(5) Final Report, Payload Performance Study, Lunar Logistics System, NSL 62-150, Northrop Space Laboratories, December 1962.

(6) Final Report, Initial Concept of Lunar Exploration Systems for Apollo, The Boeing Company, Aerospace Division, D2-100057-3B, November, 1963.

(7) Lunar Surface Vehicle Subsystem for a Lunar Base, GM DRL, Report TR 63-233, October 1963.

(8) An Integrated Moonmobile - Spacesuit Concept, A. B. Hazard, Aerojet General, SAE Paper 424D, October 9, 1961.

(9) San Francisco Examiner, June 15, 1964.

(10) Aviation Week, June 4, 1962, Pages 54-57.

(11) Lunar Surface Vehicle, American Machine and Foundry, ASTIA Report AD 255019, Pages 9-14.

(12) JPL Seminar Proceedings, Status of Designs of Lunar Surface Vehicles, Pages 6 and 7.

(13) SAE Paper 632 L, Pages 6 and 7, January 14, 1963.

(14) Surface Exploration of the Moon, P. A. E. Stewart, Spaceflight, Vol III, No. 2, March 1961.

Figure 2.1.1 Literature Search References

REFERENCES

(15) Presentation to NASA Headquarters Staff, GM Defense Research Laboratories, S62-205, March 20, 1962.

(16) Technical Data on Advanced Lunar Exploration Vehicles, GM Defense Research Laboratories, TR 65-21, March 1965.

(17) AES/LSSM Analysis and Conceptual Design, The Boeing Company, Aerospace Division, D2-83221-1, June 1965.

(18) Final Presentation, Grumman LEM Utilization, Grumman Aircraft Engineering Company, 15 July 1965.

(19) Lunar Shelter/Rover Conceptual Design and Evaluation, ALSS-MOLAB Studies, NASA CR-61049, Hayes International Corporation, November 1964.

(20) System Approach to Lunar Surface Exploration, The Bendix Corporation, Session V, Paper 2; 11th Annual Meeting of AAS, May 1965.

Literature Search References

Figure 2.1.1 (Continued)

Concept No.	Proposed by	Source	Vehicle Type	Available Characteristics	Comments
1	ABMA	(1)	2 x 2 with Stabilizing Wheel	Wheel Diam. = 16 ft. Wheel Width = 5 ft. Weight = 1450 lb.	Unmanned Rover. Mission= 1 Lunar Day Range = 50 miles
2	Grumman	(2) Pgs. 5-6 thru 5-8 & Fig. 15	Wheeled - 6 x 6 - Articulated 3 units	Cabin Vol. - 320 ft.^{3} Total Vol. -620 ft.^{3} Weight - 6935 lb.	2- man extended surface exploration mission, range of 740 miles. Variable geometry capability (wheel).
3	Grumman	(2) Pgs. 5-13 & Fig. 20	Wheeled - 4 x 4 - Articulated, Goer-type	Cabin Vol. - 440 ft.^{3} Total Vol. - N.A. Weight - 3149 to 6935 lb.	Mobile Shelter and power unit for 2-man crew, 10.5 day "stay-time". Variable geometry capability (wheel).
4	Grumman	(2)Pgs. 5-17 & Fig. 23	Wheeled - 4 x 4 Rigid Frame Skid Steering	Length- 174 inches Width - 174 inches Cabin Vol. -1010 ft.^{3} Total Vol. - 1010 ft.^{3} Weight - 6935 lb.	Large Mobile shelter for 2-man crew, variable geometry capability (wheel).
5	NASA	(3) Pgs. 126-156 & Figs. 40 & 41	Wheeled- 4 x 4 Rigid Frame Ackermann or Skid Steering	Length - 21.7 inches Width - 135 inches Wheel Diam. - 78 inches Wheel Width - 14 inches Tread - 121 inches Cabin Vol. - 343 ft.^{3} Total Vol. - 450 ft.^{3} Weight - 10,740 lb.	30 day Scientific mission with 2-man crew, Rigid Wheels, 280 mile range
6	NASA	(3) Pgs. 164-174 & Fig. 48	Wheeled - 4 x 4 Rigid Frame Ackermann Steering	Length - 142 inches Width - 100 inches Wheel Diam. - 48 inches Wheel Width - 8 inches Tread - 92 inches Cabin Vol. - 150 ft.^{3} Total Vol. - 200 ft.^{3} Weight - 5,000 lb.	7 day Scientific mission 2-man crew 230 mile range

Figure 2.1.2 Summary of Existing Wheeled Vehicle Concepts

Concept No.	Proposed by	Source	Vehicle type	Available Characteristics	Comments
7	Grumman	(4) Pages 6-6, 6-7 & 6-8 Fig. 6-13	Wheeled - 4 x 4 Articulated (with controlled pitch)	Wheel Diam. - 150 inches (eff.) Cabin Vol. - None Weight - 1500 lb.	Manned or unmanned capability, Spacesuit operation for short term (24 hr) One-man crew in manned mode.
8	Grumman	(4) Pages 6-8 and 6-9 Fig. 6-15	Same as above	Same as above except Cabin Vol. - 100 ft.^{3} (eff.) Weight - 2370 lb.	Manned or unmanned capability, Emergency shelter provided. Not suitable for long term use. 2-man crew 100 miles range manned. 338 miles range unmanned.
9	Grumman	(4) Pages 6-9, 6-10, & 6-11 Figs. 6-13 6-17, 6-18	Wheeled - 8 x 8 Articulated Train, 4 units (with controllable pitch).	Wheel Diam. - 150 inches (eff.) Weight - 4500 lb. + 2000 lb. radiation protection (lunar soil)	Remote or manned capability 7-day mission with 2-man crew, 229 mile range Manned.
10	Grumman	(4) Pages 6-11, 6-12, 6-13 Fig. 6-20	Wheeled - 6 x 6 Articulated 3 unit (controllable pitch)	Weight - 23,000 lb.	Long range exploration vehicle can be modified to an unmanned surface modification vehicle. 28-day mission with 3-man crew. 1450 mile range
11	Northrop	(5) Pages VII-24 thru VII-35, Fig. VII-15	Wheeled - 4 x 4 Rigid Frame Ackermann front	Length - 240 inches Width - 156 inches Cabin Vol. - 1500 ft.^{3} Total Vol. - 2300 ft.^{3} Wheel Diam. - 80 inches Weight - 25,000 lb.	Long range exploration vehicle for 2-man crew. 2,000 mile range (hard surface and 1,000 mile range soft ground.)

Figure 2.1.2 Summary of Existing Wheeled Vehicle Concepts (Continued)

Concept No.	Proposed by	Source	Vehicle Type	Available Characteristics	Comments
12	Northrop	(5) Pages VII-35 Fig. VII-16	4-Wheel Tractor w/ 2-wheel trailer 6 x 6 Ackermann on front of 4 x 4	Width - 120 inches Wheel Diam. - (4) 80" (2) 60" Cabin Vol. - 400 $ft.^3$ Weight - 25,000 lb.	Multi-purpose vehicle Shelter module on 2-wheel trailer. Tractor may be detached from shelter. 2-man crew.
13	Boeing (AMF)	(6) Pages 527, 531 Fig. 7.10-1	Wheeled 4 x 4 Articulated Goer-type	Length - 197 inches Width - 108 inches Wheel Diam. - 64 in. Wheel Width - 12 inches Tread - 96 inches Cabin Vol. - 175 $ft.^3$ Weight - 4415-4745 lb.	Multi-purpose vehicle 8-day roving
14	GM DRL	(7) Pages 19, 20, 24 Figs. 18, 21, 22, 23, 24.	Wheeled 4 x 4 Flexible frame Articulated (Controlled pitch)	Length - 180 inches Width - 120 inches Wheel Diam. - 66 in. Wheel Width - 18 in. Tread - 102 inches Cabin Vol. - 400 $ft.^3$ Weight - 5000 lb.	Scientific Mission 5-day roving capability for 2-man crew 200 mile range
15	GM DRL	(7) Pages 19, 20, Fig. 27, 29 & 30	Wheeled 4 x 4 Rigid Frame Ackermann Steering	Length - 168 inches Width - 120 inches Wheel Diam. - 66 in. Wheel Width - 18 in. Tread - 102 inches Cabin Vol. - 400 $ft.^3$ Weight 5000 lb.	Multi-purpose vehicle 8-day roving
16	GM DRL	(7) Pages 19, 21, 25 Fig. 27, 28 & 31	Wheeled 6 x 6 Semiflexible frame Articulated	Length - 264 inches Width - 120 inches Wheel Diam. - 66 in. Wheel Width - 18 in. Tread - 102 inches Cabin Vol. - 400 $ft.^3$ Weight - 8000 lb.	Scientific exploration mission, 8-day roving capability, 2-man crew 300 mile range

Figure 2.1.2 Summary of Existing Wheeled Vehicle Concepts (Continued)

Concept No.	Proposed by	Source	Vehicle Type	Available Characteristics	Comments
17	GM DRL	(7) Pages 19, 21, 24 & 25, Figs. 18, 19, 20	Wheeled 6 x 6 Flexible frame Articulated	Length - 264 inches Width - 120 inches Wheel Diam. - 66 in. Wheel Width - 18 in. Tread - 102 inches Cabin Vol. - 250 ft.^{3} Weight - 8000 lb.	Multi-purpose vehicle 8 day roving
18	GM DRL	(7) Pages 19, 22 & 25, Figs. 32 & 33	Wheeled 6 x 6 Flexible frame Articulated	Length - 576 inches Width - 204 inches Wheel Diam. - 144 in. Wheel Width - 30 in. Tread - 174 inches Cabin Vol. - 1000 ft. Weight - 24,000 lb.	Scientific exploration mission, 30-day mission capability, Nuclear power 4-man crew
19	Aerojet-General	(3) Page 74	Integrated Moon mobile spacesuit, wheeled Moon mobile 4 x 4 articulated & hard shell spacesuit.	Weight - Vehicle 3000 lb. Spacesuit - 350 lb. ea.	Lunar Surface exploration mission, 2-man crew Rigid tires. Crew wears hardshell spacesuits attached to vehicle. Range 500 miles.
20	Lockheed	(9)	Wheeled 4 x 4 Rigid frame Ackermann steering.	Wheel Diam. - 142 inches Weight - 12,000 lb.	Multi-purpose vehicle 4-man crew Rigid wheels
21	Bendix	(10) Pages 54-57	Wheeled 4 x 4 Rigid frame, Differential or skid steering	Length - 144 inches Width - 82 inches Cabin Vol. - 1 man - 5 ft.^{3} 2 men - 175 ft.^{3} 3 men - 249 ft.^{3} Weight - 1 man - 4600 lb. 2 men - 5400 lb. 3 men - 6000 lb.	System involves a modular rover as support for life support capsule to be mounted on moon. Powered by fuel cells. Modular rover wt. is 2350 lb. 1 man capsule wt. is 2246 lb. 2 man capsule wt. is 3022 lb. 3 man capsule wt. is 3609 lb.

Figure 2.1.2 Summary of Existing Wheeled Vehicle Concepts (Continued)

Concept No.	Proposed by	Source	Vehicle Type	Available Characteristics	Comments
22	Bendix	(10) Pages 54 & 57	Wheeled 3 x 3 Rigid Frame Ackermann front wheel.	Length - 244 inches Width - 144 inches Wheel Diam. - 60 in. Wheel Width - 12 in. Cabin Vol. - None Weight - 1, 756 lb.	Unmanned rover Nuclear power 500 mile range
23	AMF	(11)	Wheeled 4 x 4	Weight - 15, 000 lb.	Same as 29.
24	Hughes	(12)	Wheeled 4 x 4 Rigid frame	None	Collapsible wheels for space saving fuel cell or nuclear power
25	Space-General	(12) p. 8	Wheeled 4 x 4	Length - 240 inches Width - 144 inches Weight - 3000 lb.	Has accomodations for various attachments to accomplish various missions.
26	Chrysler	(13) p. 6-7	Wheeled 4 x 4 Rigid frame	Length - 80 inch wheel base Wheel Diam. - 60 in. Weight - 3800 lb.	Has smaller side wheels used to increase obstacle crossing capacity.
27	Tinsley	(14) p. 42	Wheeled Rolling device	Diameter - 384 inches	An inflatible spherical cabin inside the single wheel. Gyro stabilized.
28	GM DRL	(15) Pages 135-143	Wheeled 6 x 6 Flexible frame	Over-all length - 3 ft. Wheel Diam. - 9 inches Weight - 36 lb.	Local scientific investigation Unmanned lunar roving vehicle. Excursion capability to about 1000 ft.
29	GM DRL	(15) Pages 149-151 & 158	Wheeled 3 x 3 Articulated front wheel	Wheel Diam. - 18 inches Wheel Base - 42 inches Weight - 225 lbs.	Local Scientific investigation Unmanned lunar roving vehicle. Excursion is about 50-65 miles.
30	GM DRL	(15) (19) P. 153 &158	Wheeled 4 x 4 Rigid frame Ackermann steering	Wheel Diam. - 18 inches Wheel Width - 5 inches Weight - 243 lbs.	Same as above. Excursion 50-65 miles

Fig. 2.1.2 Summary of Existing Wheeled Vehicle Concepts (Con't.)

Concept No.	Proposed by	Source	Vehicle Type	Available Characteristics	Comments
31	GM DRL	(15) Pages 155, 157, & 158	Wheeled 6 x 6 Flexible frame Articulated	Over-all length - 72 in. Wheel Diam. - 18 in. Wheel Width - 9 inches Weight - 275 lbs.	Same as Concept 29 Excursion 60-70 miles
32	GM DRL	(15) (19) Page 160	Wheeled 6 x 6 Flexible frame Articulated	Wheel Base - 66-135 in. Wheel Diam. - 22-45 in. Weight - 450 lbs.	Same as above. Excursion - 250 miles minimum
33	GM DRL	(16)	6 x 6 Semi-flexible frame Articulated	Length - 20.2 ft. Wheel Diam. - 60 inches Weight - 6400 lb.	LESA vehicle, 14-day mission, 2-man crew Range - 200 miles
34	GM DRL	(16)	8 x 8 Semi-flexible frame Articulated	Length - 32.1 ft. Wheel Diam. - 60 inches Weight - 10,300 lb.	LESA vehicle, same as above with additional trailer 42-day mission, 2-man crew Range - 600 miles
35	GM DRL	(16)	10 x 10 Semi-flexible frame Articulated	Length - 44.0 ft. Wheel Diam. - 60 inches Weight - 15,800 lb.	LESA vehicle, same as above with another additional trailer. 84-day mission 2-man crew Range - 1600 miles
36	Boeing (GM DRL)	(17) Page 95-102	Wheeled 6 x 6 Semi-flexible frame Articulated	Over-all length - 192 in. Wheel Diam. - 48 inches Wheel Width - 12 inches Weight - 2200 lbs.	Extended stay time Scientific exploration Radial excursion -250 miles minimum.
37	Boeing (GM DRL)	(17)	Wheeled 4 x 4 Rigid frame Ackermann steering	None	Manned Rover 1-man crew

Figure 2.1.2 Summary of Existing Wheeled Vehicle Concepts (Continued)

Concept No.	Prepared by	Source	Vehicle Type	Available Characteristics	Comments
38	Boeing (GM DRL)	(17)	Wheeled 6 x 6 Semi-flexible frame	None	Manned Rover 1-man crew
39	Boeing (GM DRL)	(17)	Wheel 4 x 4 Semi-flexible frame	None	2-man crew
40	Grumman	(18) P. 31	Wheeled 3 x 3 Ackermann front wheel	Weight - 300 lb. Payload - 200 lb.	Extended stay time Short range rover 1-man crew Range - 2 miles ECS: Pressure suit- back Pack.
41	Grumman	(18) P. 32	Wheeled 4 x 4 Rigid frame	Weight - 900 lb. Payload - 300 lb.	Extended Stay time Scientific investigation Medium Range Rover. 1-man crew Range - 4-6 miles ECS: plug in & pressure suit
42	Grumman	(18) P. 33	Wheeled 4 x 4 Rigid frame	Weight - 2100 lb. Payload - 400 lb.	Extended Stay time Medium range rover 1-man crew Range - 4-6 miles ECS: Pressurized cabin
43	Hayes International Corp.	(19) Pages 58-73	Wheeled 4 x 4 Rigid frame Ackermann steering	Wheel Diam. - 40 in. Wheel Width - 10 in. Wheel Base - 72 in. Weight - 1500 lbm.	Lunar traversing vehicle 1-man crew, space suit operation, Range - 5 miles
44	Bendix	(20) Pages 10, 13, 15	Wheeled 4 x 4 Articulated (Modified)	Weight - 150 lbm	Unmanned Rover RPU power Range - 8 km radius from shelter.

Figure 2.1.2 Summary of Existing Wheeled Vehicle Concepts (Continued)

Concept No.	Proposed by	Source	Vehicle Type	Available Characteristics	Comments
45	Bendix	(20) Pages 10, 13, 16, 17	Wheeled 4 x 4 Rigid Frame Variable Geometry Skid steering	Weight - 675- 1500 lbm	Manned Rover 1-man crew Space suit operation Range - 273 to 378 km.
46	Bendix	(20) Pages 10, 17, 20 & 21	Wheeled 4 x 4 Rigid frame Variable Geometry Skid steering	Weight - 2000 lbm	Extended time Rover 1-man crew Life Support Cabin
47	Bendix	(20) Pages 21, 25, 26 & 27	Wheeled 4 x 4 Rigid frame Skid steering Variable Geometry	Weight - 7100 lbm Wheel Diam. - 80 inches	Manned Rover 2-man crew 14 day, 80 km radius mission.

Figure 2. 1. 2 Summary of Existing Wheeled Vehicle Concepts (Continued)

2.2 DISCUSSION

These concepts encompassed both rigid - and articulated - frame types ranging from gyro-stabilized single wheel devices (1 x 1) to train - type vehicles for extended lunar exploration (10 x 10). Masses ranged from about 50 lbm to 25,000 lbm. As would be expected, the large majority of the proposed concepts were of the 4-wheel variety, with 6-wheel versions next in popularity. This is not surprising because, unless the lunar surface is radically different from what so far has been considered, vehicle concepts based on either four or six wheels would strike a reasonable balance between performance and simplicity for most missions.

Insofar as LSSM application was concerned, simple analyses based on system constraints and performance requirements resulted in the conclusion that only 4 x 4's and 6 x 6's should be seriously considered. Concepts with less than four wheels were eliminated on the basis of one or more of the following factors:

- o Stability considerations
- o Poor obstacle capability
- o Poor payload carrying capacity.

Concepts with more than six wheels were considered not practical for LSSM application on the basis of the following:

- o Undue design complexity
- o Poor maneuverability characteristics
- o Difficulties of stowage in LEM/Shelter envelope unless wheel diameters were kept small.
- o Mobility performance in the softer soils would be poor due to small wheel diameters.

3.0 ASSEMBLY OF LSSM CONCEPTUAL CONFIGURATIONS

3.1 APPROACH TO BASELINE SELECTION

Conceptual layouts (both in the stowed and operational configurations) were prepared of ten 4 x 4 and 6 x 6 designs, ranging in size from the smallest considered practical to the largest that could be stowed within the available LEM/Shelter space envelope.

These concepts encompassed the following mobility configurations:

- o 4 x 4, rigid frame, fixed wheel geometry
- o 4 x 4, rigid frame, variable wheel geometry
- o 4 x 4, articulated frame
- o 6 x 6, semi-flexible frame
- o 6 x 6, fully-flexible frame

All concepts utilized flexible wheels with diameters ranging from 36 to 48 inches. For the 4 x 4's, primary steering modes considered included front-wheel Ackermann, double Ackermann and frame articulation. In the case of the 6 x 6's, double Ackermann, combined Ackermann-articulated, and double frame-articulation were considered.

The ten configurations can be described briefly as follows:

CONCEPT NO.	DESCRIPTION
(1)	Large 4 x 4, rigid frame, trailing arm rear suspension (rear suspension arms rotated at deployment to achieve large wheelbase)
(2)	Large 4 x 4, GOER-type articulated frame
(3)	Large 6 x 6, semi-flexible frame (4-wheel unit forward)
(4)	Large 6 x 6, semi-flexible frame (2-wheel unit forward)
(5)	Large 6 x 6, articulated in pitch only
(6)	Large 6 x 6, fully flexible frame

CONCEPT NO.	DESCRIPTION
(7)	Small 4 x 4, rigid frame
(8)	Small 4 x 4, GOER-type articulated frame
(9)	Small 6 x 6, semi-flexible frame
(10)	Small 6 x 6, articulated in pitch only

The dimensional characteristics for these concepts are given in Figure 3.1.1. Some of the typical configurations considered are shown in the sketches of Figure 3.1.2.

A simplified mobility performance analysis was conducted for each of the concepts listed. Included were estimations of drawbar pull to weight ratio over ELMS and Annex G soft soils, locomotion energy requirements over the ELMS Maria and Uplands models, obstacle performance, turning radius and static stability. In order to make the necessary calculations, vehicle masses were estimated based on parametric subsystem data contained in Boeing Document D2-83221-1 entitled "AES/LSSM Analysis and Conceptual Design", dated June 1965. For these mass estimates it was assumed that all "large" vehicles carried 270 kg (594 lbm) of scientific equipment; the "small" ones 150 kg (330 lbm). The estimated mass breakdowns for the ten concepts is shown in Figure 3.1.3. In addition, equal wheel loadings were assumed in all cases.

Drawbar pull was calculated for the softest specified ELMS soil ($k_\phi = 0.5$, $n = 0.5$, $\phi = 32^\circ$) and for a very weak soil used in the Surveyor Lunar Roving Vehicle (SLRV) study ($k_\phi = 0.083$, $n = 1.0$, $\phi = 20^\circ$). Step obstacle and crevice crossing capabilities were estimated on the basis of model studies previously conducted in the MOLAB and SLRV programs. Turning radius and off-tracking could be calculated from the known vehicle geometries. Calculations of static pitch and roll stability limits were based on center-of-gravity heights estimated from the mass breakdowns of Figure 3.1.3. Locomotion energy requirements were estimated by scaling results previously obtained for vehicles of similar size and mass. These requirements assumed

CHARACTERISTICS	CONCEPT NO. (1)	(2)	(3)	(4)	(5)
Wheelbase (in)	112	95	58/62	62/58	60/60
Tread (in)	82	85	82	82	60
Wheel Dia (in)	48	48	40	40	45
Wheel Width (in)	10	10	10	9	11
O. A. Length (in)	160	144	160	160	165
O. A. Width (in)	92	92	92	92	80
GRD. Clearance (in)	22	24	18	18	19
	(6)	(7)	(8)	(9)	(10)
Wheelbase (in)	67.5/67.5	85	80	54/54	54/54
Tread (in)	69	60	48	48	48
Wheel Dia (in)	45	40	40	36	36
Wheel Width (in)	11	10	10	9	9
O. A. Length (in)	130	125	120	144	144
O. A. Width (in)	80	70	58	57	57
GRD. Clearance (in)	20	20	18	16	17

Figure 3.1.1 - Dimensional Characteristics of LSSM Conceptual Configurations

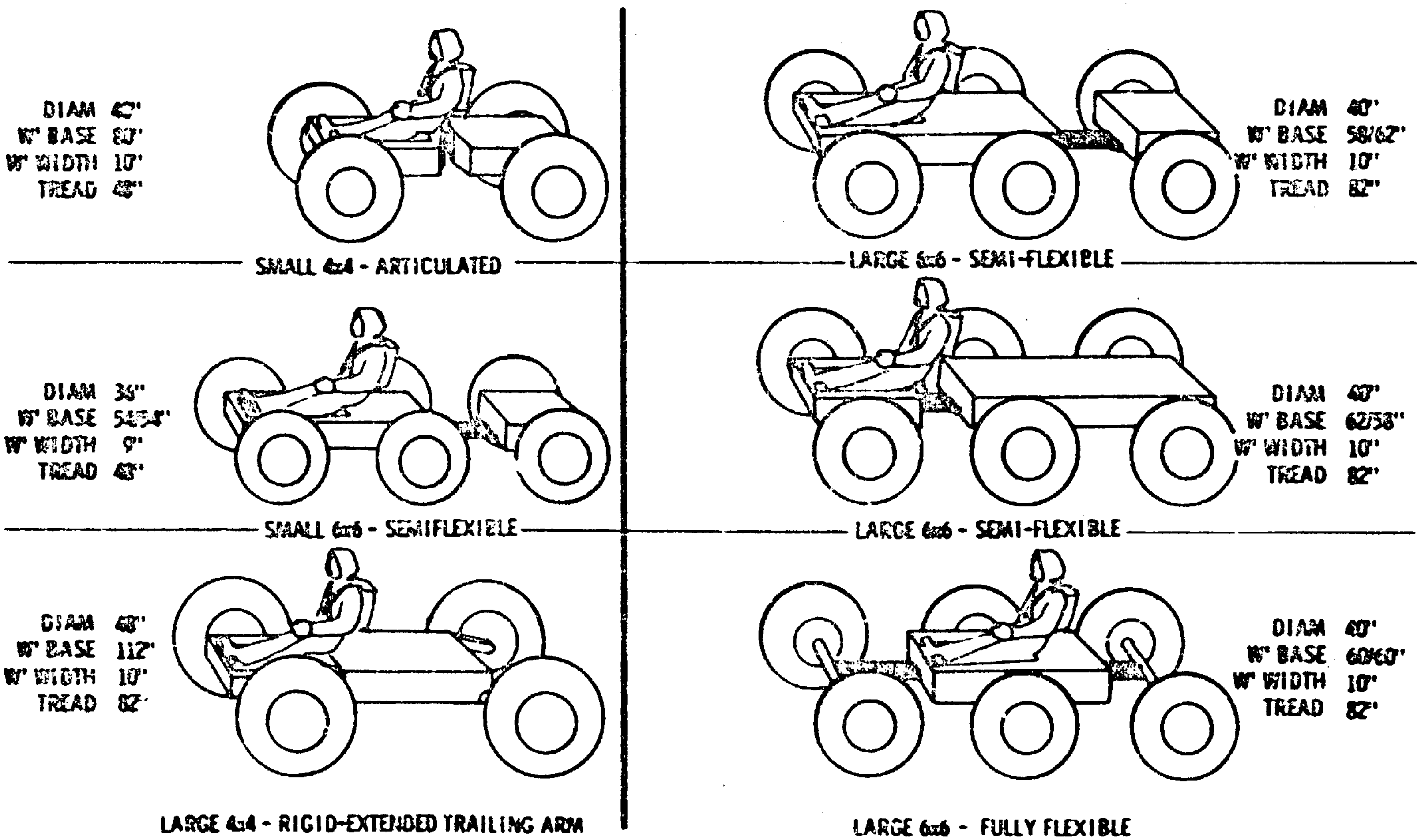

Figure 3.1.2 — Typical LSSM Configurations Considered

	CONCEPT NO.				
	(1)	(2)	(3)	(4)	(5)
System	LBM	LBM	LBM	LBM	LBM
Mobility	504	504	509	509	543
Power	220	220	220	220	220
Astrionics	139	139	139	139	139
Crew	88	88	88	88	88
Scientific	594	594	594	594	594
Astronaut	200	200	200	200	200
PLSS (3)	145	145	145	145	145
TOTAL	1890	1890	1895	1895	1929

	(6)	(7)	(8)	(9)	(10)
System	LBM	LBM	LBM	LBM	LBM
Mobility	543	271	271	286	286
Power	220	198	198	198	198
Astrionics	139	114	114	114	114
Crew	88	66	66	66	66
Scientific	594	330	330	330	330
Astronaut	200	200	200	200	200
PLSS (3)	145	145	145	145	145
TOTAL	1929	1324	1324	1340	1340

Figure 3.1.3 - Estimated Mass Breakdown
For LSSM Conceptual Configurations

a traverse half over the ELMS Maria; and half over the ELMS Uplands. In addition, all concepts were assumed to have a drive system efficiency of 40% and a 35% contingency factor was added to allow for energy expenditure due to surface roughness. A summary of the estimated performance characteristics is shown in Figure 3.1.4.

A preliminary design review was held to evaluate and compare the proposed conceptual configurations. The purpose was to reduce the number of practical approaches to baseline LSSM design as much as possible.

Based on factors such as estimates of mobility performance, mission requirements, payload carrying capacity, available mass, complexity and growth potential, it was decided that only the large 4 x 4 rigid frame and 6 x 6 semi-flexible frame configurations should be further considered for LSSM design. These concepts are depicted below with their major dimensional characteristics.

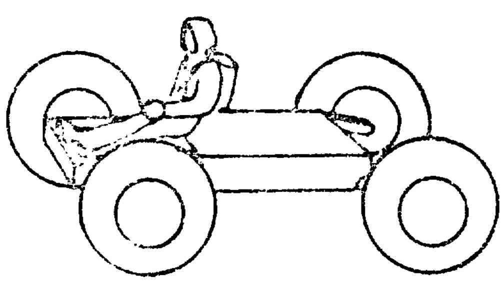

(Concept 1)
Large 4 x 4 - Rigid-Extended Trailing Arm

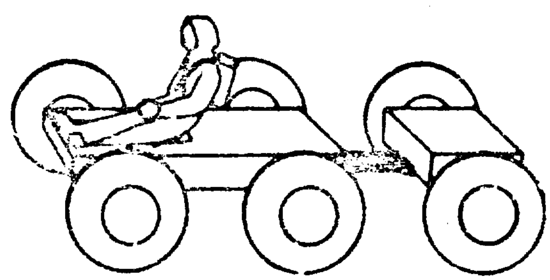

(Concept 3)
Large 6 x 6 - Semi-Flexible

	Concept 1	Concept 3
Overall Length	160 in (406 cm)	160 in (406 cm)
Overall Width	92 in (234 cm)	92 in (234 cm)
Wheelbase	112 in (284 cm)	58/62 in (147/157 cm)
Wheel Diameter	48 in (122 cm)	40 in (102 cm)
Wheel Width	10 in (25.4 cm)	10 in (25.4 in)

Characteristics	Concept No. 1	2	3	4	5	6	7	8	9	10
Gross Vehicle Mass (lbm)	1890	1890	1895	1895	1929	1929	1324	1324	1340	1340
DP/W Ratio										
$k_{\phi} = 0.083$, $n = 1$, $\phi = 20^{o}$	0.18	0.18	0.18	0.18	0.20	0.20	0.18	0.18	0.20	0.20
$k_{\phi} = 0.5$, $n = 0.5$, $\phi = 32^{o}$	0.54	0.54	0.56	0.56	0.57	0.57	0.55	0.55	0.57	0.57
Step Obstacle Height (in.)	19	19	64	64	28	74	16	16	58	22
Crevice Width (in.)	45	45	60	60	40	78	38	38	54	32
Turning Radius (in.)	303	172	204	204	189	209	229	178	156	156
Off-Tracking (in.)	22	0	10	10	10	17	17	0	10	10
Roll Stability (degrees)	50^{o}	50^{o}	52^{o}	52^{o}	44^{o}	44^{o}	44^{o}	38^{o}	44^{o}	44^{o}
Pitch Stability (degrees)	58^{o}	58^{o}	61^{o}	61^{o}	62^{o}	62^{o}	54^{o}	53^{o}	65^{o}	65^{o}
Locomotion Energy (kw-hr/km)	120	120	112	112	96	96	71	71	60	60

Figure 3.1.4 - Performance Summary of LSSM Conceptual Configurations

3.2 PERFORMANCE COMPARISON OF LSSM CONCEPTS

A more comprehensive performance analysis was then performed for these concepts, including soft ground, slope climbing and obstacle capability, locomotion energy requirements, stability and maneuverability. The majority of the calculations were made for a gross vehicle mass of 1800 lbm (816 kg), which was the estimated baseline mass at the time this work was conducted, with all wheels equally loaded. Center of gravity heights above the ground were estimated to be 32 inches for the 6 x 6 and 34 inches for the 4 x 4, due to the larger wheel diameter. Wheel deflections on hard surface were 1.67 inches in both cases.

The equations and techniques to evaluate soft ground and slope climbing (drawbar-pull to weight ratio) capability, stability, maneuverability and energy requirements are given in Sections 5.2 and 5.4 of this report. The only important difference between the present analysis and the baseline LSSM mobility analysis in Section 5.0 is the fact that in this case a drive system efficiency of 40% was assumed, constant over the entire speed range, whereas for baseline evaluation the drive system efficiency was a known function of speed.

Figure 3.2.1 compares the total motion resistance of the 4 x 4 concept with 48 inch diameters with that of the 6 x 6 with 40 inch wheels. The comparison was made for two soils; the softest ELMS ($k_\phi = 0.5$, $n = 0.5$, $\phi = 32^\circ$), and the very weak soil previously used in the SLRV studies ($k_\phi = 0.083$, $n = 1.0$, $\phi = 20^\circ$) Motion resistance has been plotted as a function of vehicle mass, with the range of interest for LSSM design indicated. Although absolute differences between the two concepts do not appear to be large, they could be significant in terms of energy requirements since these are a direct function of resistance.

Figure 3.2.2 shows test results obtained from single wheel tests conducted under controlled conditions in the GM DRL soil bin. They illustrate the effect on motion resistance of multiple passes made by a wheel running in the same rut. It can be seen that there is a decrease in resistance on both the second

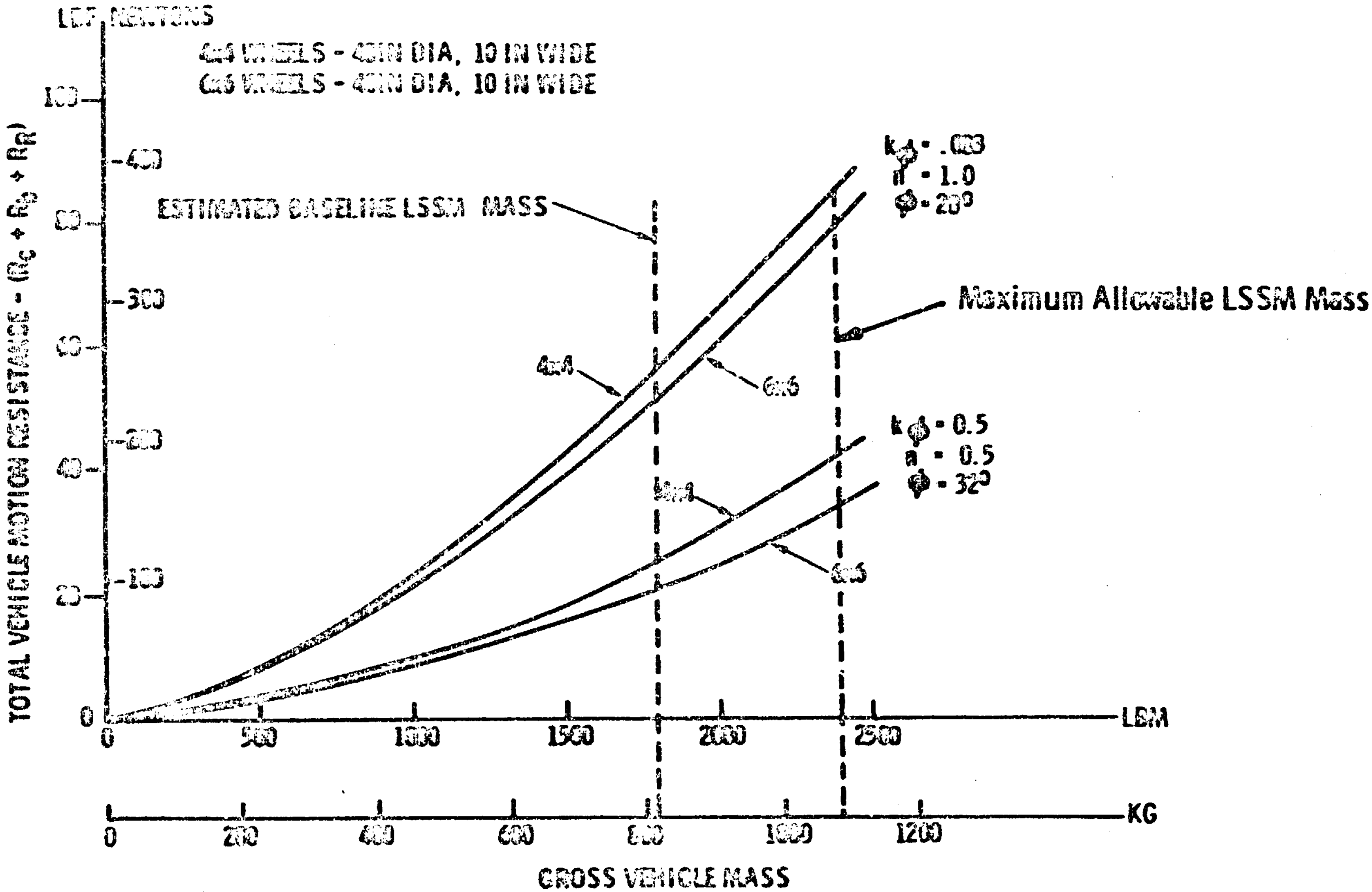

Figure 3.2.1- Comparison of Motion Resistance, 4x4 versus 6x6

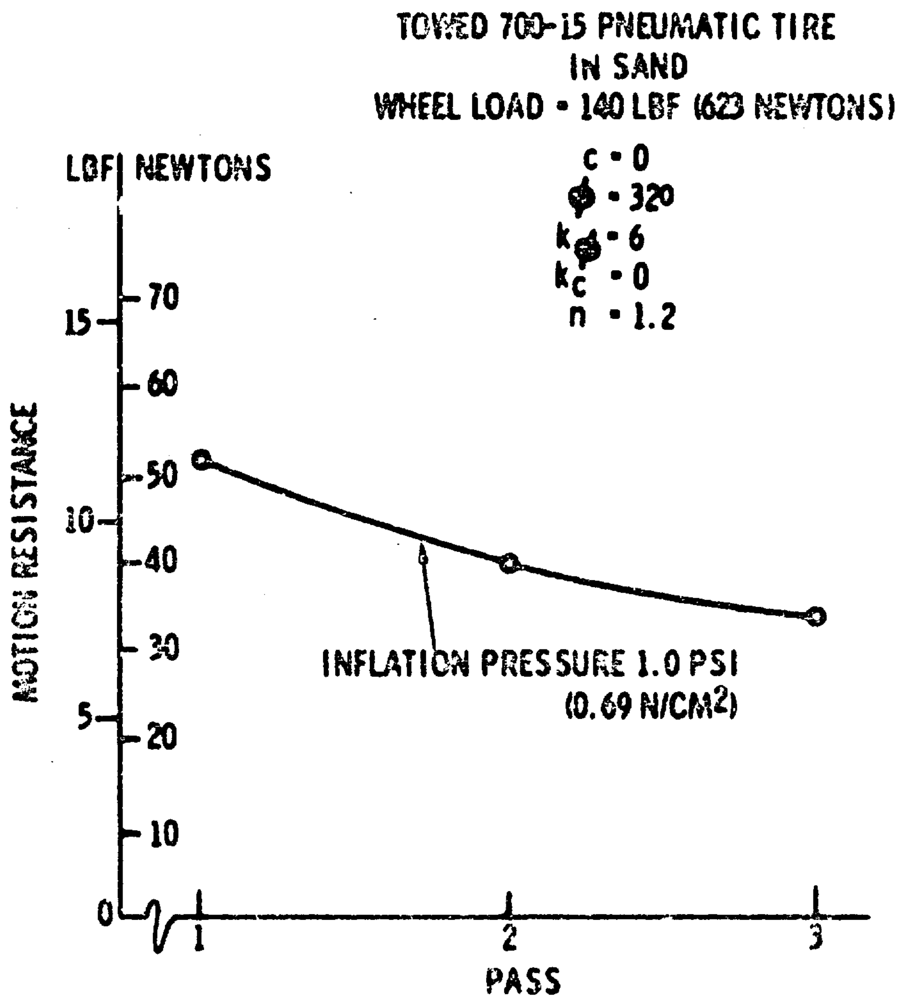

Figure 3.2.2 - Multiple Pass Test Results

and third passes. Since all calculations of motion resistance, drawbar pull and locomotion energy are based on the assumption that all wheels operate in virgin soil, it can be deduced that in the case of tracking wheels the advantages of a 6 x 6 over a 4 x 4 are greater than can be indicated by the usual analytical techniques. The inflation pressure used for these tests was 1.0 psi, as compared to the estimated LSSM ground pressure of 0.5 - 0.7 psi.

The impact of the loss of drive to one wheel due to mechanical or electrical failure is graphically presented in Figure 3.2.3 for the 6 x 6 and 4 x 4 LSSM concepts in terms of drawbar-pull-to-weight ratio. Note that in the very soft (k_ϕ = 0.083) soil, loss of drive to one of 4 x 4 wheels results in a reduction of DP/W ratio of more than one-half. Even in a very compact soil (k_ϕ = 6), where the drawbar pull capability of the two concepts is equal when all wheels are driven, degradation for the 4 x 4 is much greater than for the 6 x 6.

The chart of Figure 3.2.4 summarizes the estimated capabilities of the 4 x 4 and 6 x 6 concepts over the obstacles specified in "Annex G, Mobility Criteria, April 1964", an attachment to the statement-of-work. (The obstacles and their modes of negotiation are depicted in Figures 5.3.1 and 5.3.2 of this report. Perhaps the cases of greatest interest are Obstacle 2 - Mode 2 which represents crevice crossing, and Obstacle 2 - Mode 5 which is the case of a vehicle climbing a vertical step obstacle.) The capabilities shown are based on model test results obtained for 4 x 4 and 6 x 6 concepts during the MOLAB program. The results shown are somewhat idealized as they do not consider the effect of suspension, unusually high c.g., or unequal axle load distribution. They are, however, indicative of the relative performance of the LSSM concepts under consideration.

Estimated peak torque requirements as a function of step height, based on model test results, are plotted in Figure 3.2.5 for a 6 x 6 semi-flexible frame vehicle with 40 inch wheels and a 4 x 4 rigid-frame vehicle with 48 inch wheels. For a given obstacle height, the 6 x 6 concept requires significantly less torque than

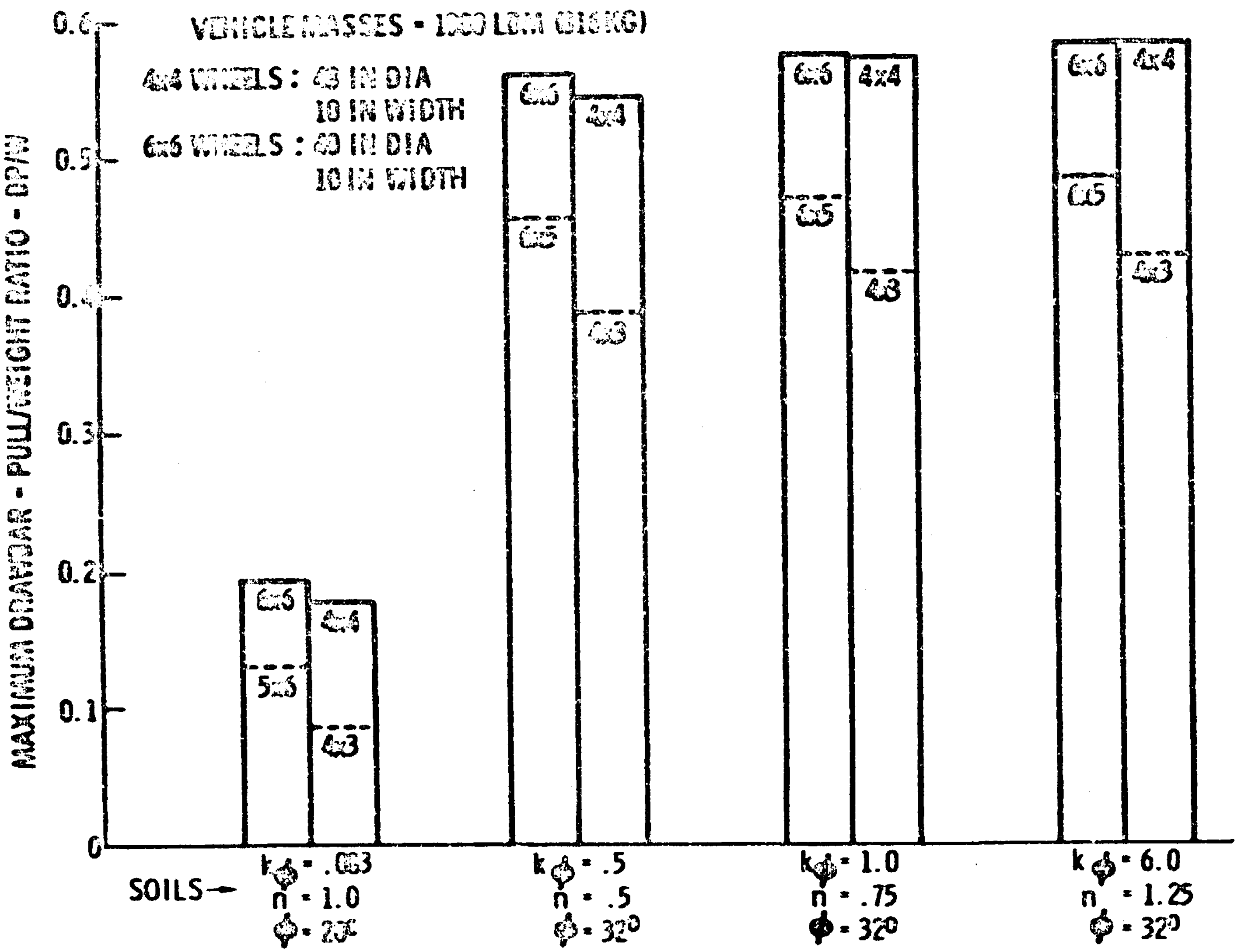

Figure 3.2.3 - Performance Degradation Due to Loss of Drive to One Wheel

CONFIGURATION	4x4 RIGID FRAME		6x6 SEMI-FLEXIBLE	
OBSTACLE 1	IN.	CM	IN.	CM
MODE 1 (HEIGHT)	26	66	36	91
MODE 2 (HEIGHT)	19	48	22	56
MODE 3 (HEIGHT)	22	56	18	46
(LENGTH)	70	178	70	178
OBSTACLE 2				
MODE 1 (WIDTH)	43	122	86	218
MODE 2 (WIDTH)	46	117	60	152
MODE 3 (HEIGHT)	19	48	32	81
(WIDTH)	48 - 112	122-284	40-120	101-304
MODE 4 (HEIGHT)	86	218	110	280
MODE 5 (HEIGHT)	20	51	60	152

Figure 3.2.4- Estimated Obstacle Performance of 4x4 and 6x6 Concepts

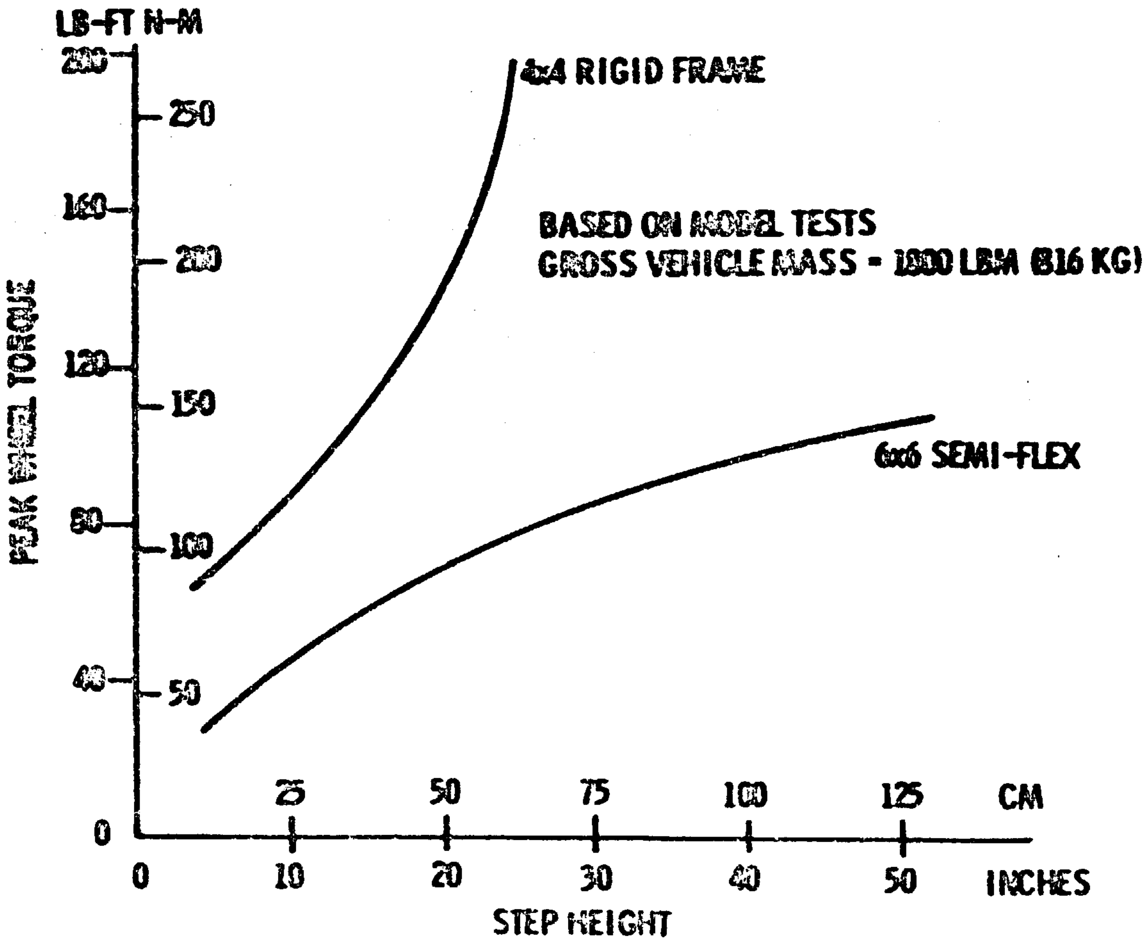

Figure 3.2.5- Peak Wheel Torque vs Step Height (Obstacle 2, Mode 5)

the 4 x 4. Furthermore, the torque requirements of the 4 x 4 increase rapidly as step height increases, in comparison to the 6 x 6. Designing the 4 x 4 for a step height capability of 50 cm (20 inches) and the 6 x 6 for a capability of 100 cm (40 inches) would result in a significantly larger drive system for the 4 x 4.

In addition to the results illustrated, calculations were made of drawbar pull to weight (DP/W) ratio, turning radius, pitch and roll stability and locomotion energy. The results of the performance analysis are summarized in Figure 3.2.6. It can be seen from this and previously illustrated results that the 6 x 6 semiflexible frame concept is superior to the 4 x 4 rigid frame configuration in all aspects of mobility performance. Furthermore, qualitative assessments of failure mode operation and system reliability also appeared to favor the 6 x 6, due to inherent subsystem redundancies. Since the 4 x 4 appeared to have little if any advantage from the points-of-view of factors such as mass, design simplicity or payload carrying capacity, the 6 x 6 semiflexible frame configuration was selected for LSSM baseline design.

CONFIGURATION	4x4 RIGID FRAME	6x6 SEMI-FLEX
DRAWBAR PULL/WEIGHT RATIO		
$k_\phi = 0.083,\ n = 1.0,\ \phi = 20^0$	0.178	0.184
$k_\phi = 0.5\ \ n = 0.5,\ \phi = 32^0$	0.539	0.555
STEP OBSTACLE CAPABILITY	20.2 IN. (51 CM)	60 IN. (152 CM)
CREVICE CROSSING CAPABILITY	45.6 IN. (116 CM)	60 IN. (152 CM)
TURNING RADIUS (MINIMUM)	*303 IN. (7.7 M)	196 IN. (5.0 M)
ROLL STABILITY (STATIC)	50^0	52^0
PITCH STABILITY (STATIC)	58^0	61^0
**LOCOMOTION ENERGY	139 W-HR/KM	129 W-HR/KM

* BASED ON ACKERMANN STEER, FRONT WHEELS ONLY

** BASED ON: (1) 50% MARIA, 50% UPLANDS
(2) 40% DRIVE SYSTEM EFFICIENCY
(3) 35% ALLOWANCE PER ELMO

Figure 3.2.6- Estimated Performance Characteristics of Conceptual LSSM Designs

4.0 DESCRIPTION OF BASELINE LSSM CONCEPT

4.1 DISCUSSION OF ALTERNATE LSSM CONFIGURATIONS

Two alternate versions of the 6 x 6 semiflexible frame configuration were originally considered for baseline design.

Both consisted of a four-wheel forward unit coupled to a two-wheel aft unit through a flexible frame, which permits the two units to pitch and roll relative to each other. This feature permits the wheels to maintain contact with the ground and provide traction even over severely undulating terrain, and also greatly enhances obstacle crossing capability. In both cases, the crew station and accommodations for scientific equipment were located on the forward unit; the aft unit carried a thermal compartment which housed navigation, telecommunications, drive electronics and power systems. All major dimensions such as wheel size, overall length and width, wheel base, etc. were identical. The only important differences between the two versions were in steering and suspension design.

One version (Figure 4.1.1) was similar to MOLAB in that it incorporated Ackermann-type steering of the front wheels of the forward unit and articulated steering of the aft unit. In the second version (Figure 4.1.2) the wheels of the aft unit were also Ackermann steered.

With respect to suspension design, the first version had parallel arm-type suspensions at the front wheels, and trailing arm suspensions on the center and aft sets of wheels. The second version incorporated identical parallel arm-type suspensions throughout.

In the early stages of the study, the decision was made to utilize the first version as the baseline LSSM concept. This was due largely to two factors:

- o Articulated steering of the aft unit permitted a wider thermal compartment since there would be no wheel encroachment as in the case of Ackermann steering.
- o Due to chassis geometry, trailing arm suspensions appeared to be simpler to install at the center and rear wheels than parallel

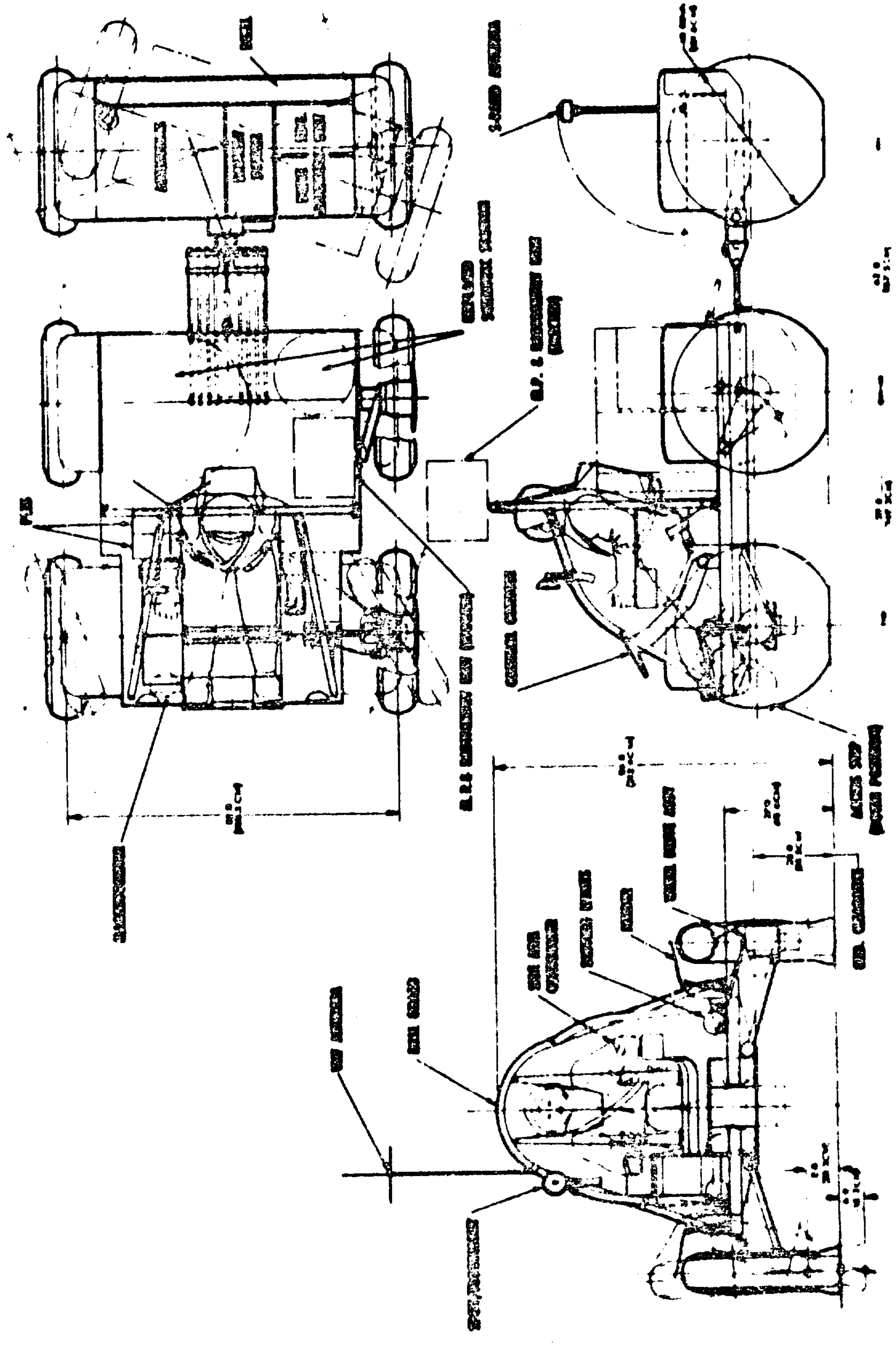

Figure 4.1.1- Early Baseline LSSM Concept

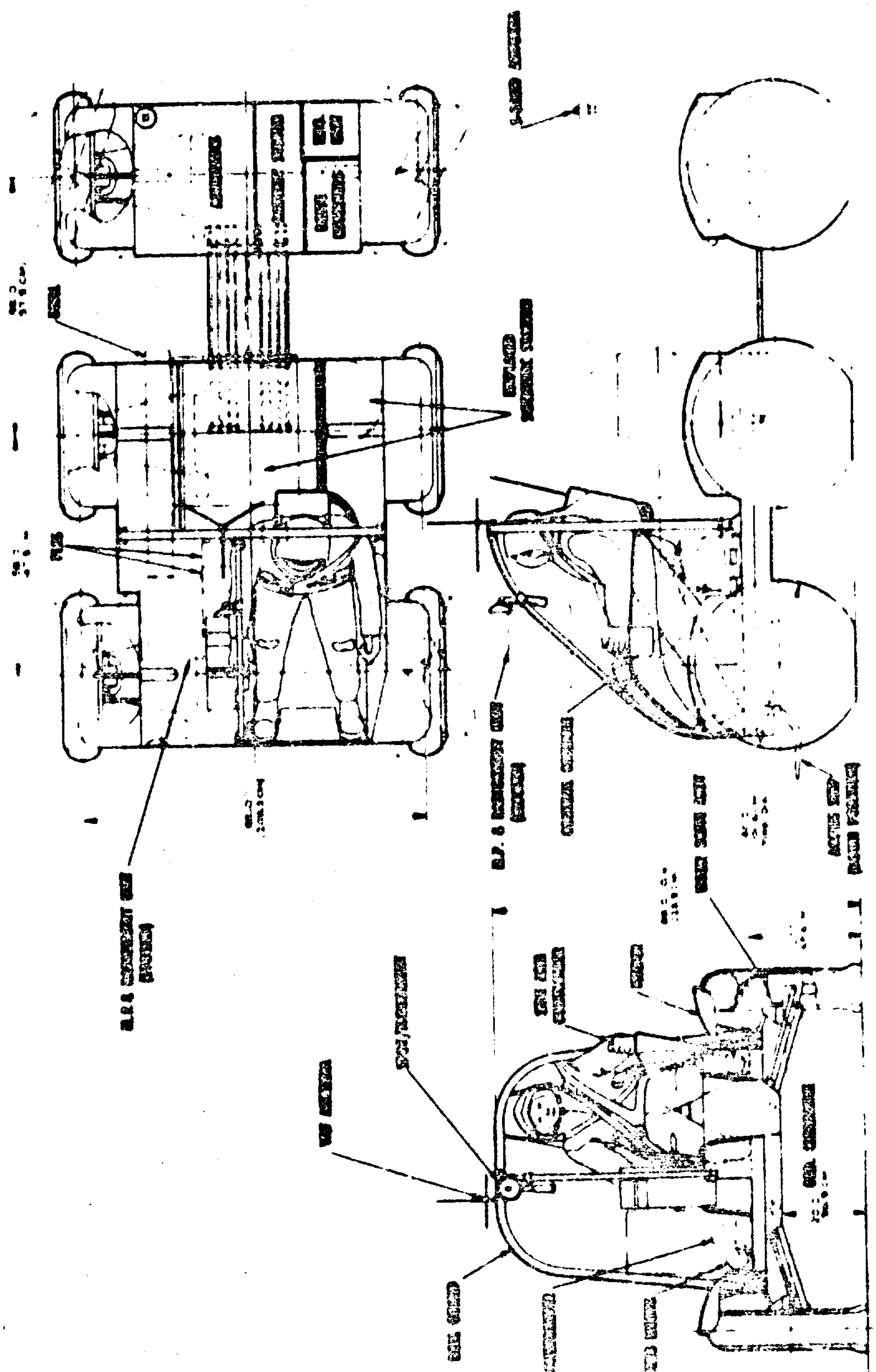

Figure 4.1.2- Early Alternate LSSM Concept–
Double Ackermann

However, as preliminary design of the mobility system progressed and system requirements became better defined, it was determined that the major objections to the second version were not critical.

Since use of identical steering mechanisms for the forward and aft units and identical suspensions at all wheels would result in a simpler design and greatly reduce development and testing requirements, the concept with double-Ackermann steering and parallel arm-type suspensions throughout was redefined as the baseline LSSM.

4.2 BASELINE LSSM CONFIGURATION SUMMARY

The baseline LSSM as it finally evolved in the course of this study is shown in its operational mode in Figures 4.2.1, 4.2.2 and 4.2.3. The crew accommodations system including seat, controls, displays, roll bar and PLSS, and scientific equipment are located on the forward unit. Batteries, power distribution and regulation equipment, drive electronics, telecommunications and navigation equipment are located in a thermal compartment on the aft unit.

In order to stow the LSSM in the LEM/Shelter space envelope (Figure 4.2.4), it is necessary to collapse the vehicle by sliding the flexible frame assembly into the forward unit chassis. In addition, crew station roll bar, controls and display console and antennas are either collapsed or folded to satisfy envelope constraints. The SNAP-27 is attached to the forward unit frame and provides power for heating during transit and storage. Life support systems and scientific equipment are placed on the vehicle only after deployment on the lunar surface.

A mass summary of the baseline LSSM is given in Figure 4.2.5 for two cases; when carrying maximum scientific payload and during a typical sortie.

The general characteristics of the baseline LSSM (typical sortie case) are given in Figure 4.2.6.

Figure 4.2.1 - Artist's Concept of Baseline LSSM

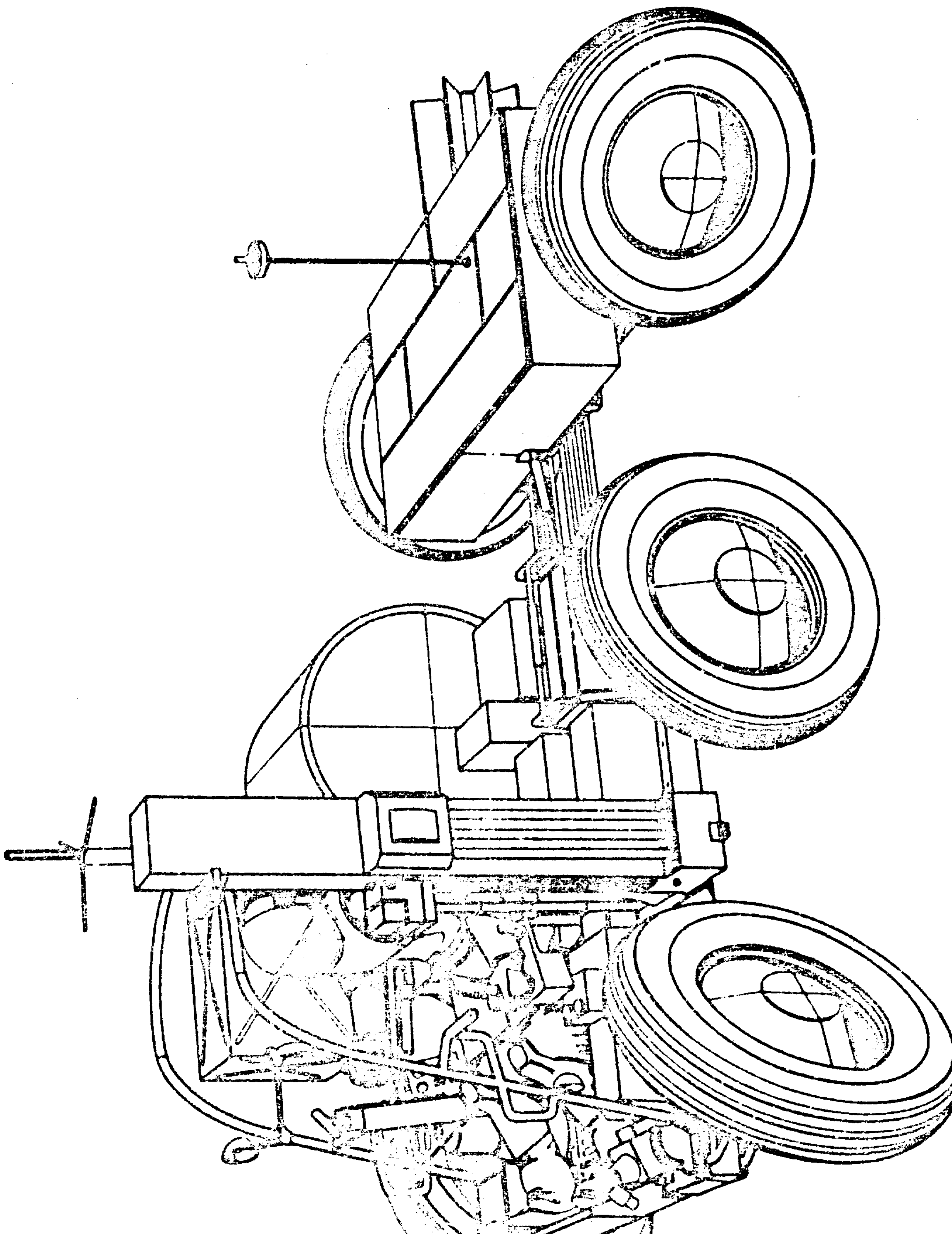

Figure 4.2.2- Artist's Con··pt of Baseline LSSM

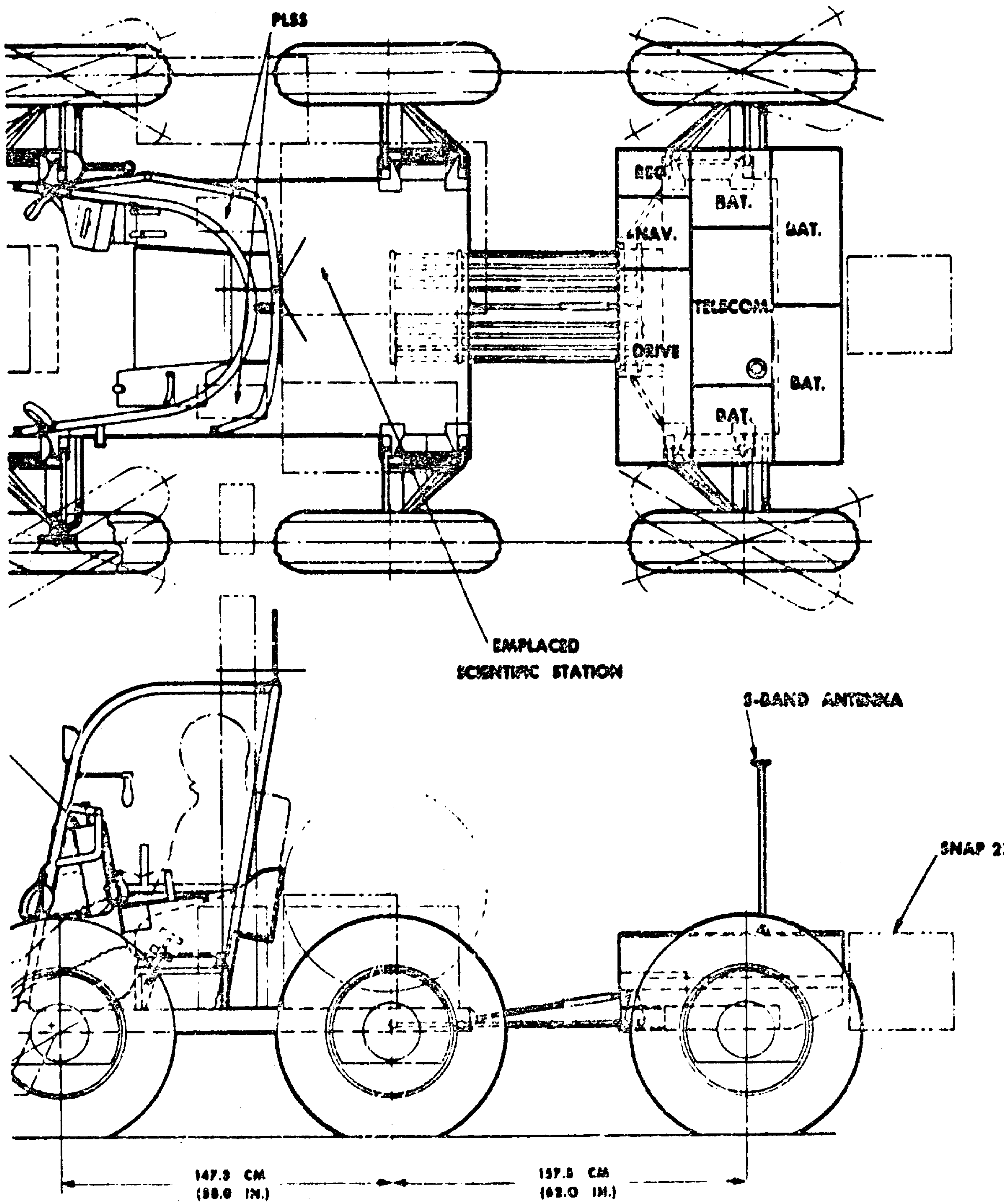

Figure 4.2.3 - Baseline LSSM Concept, Deployed

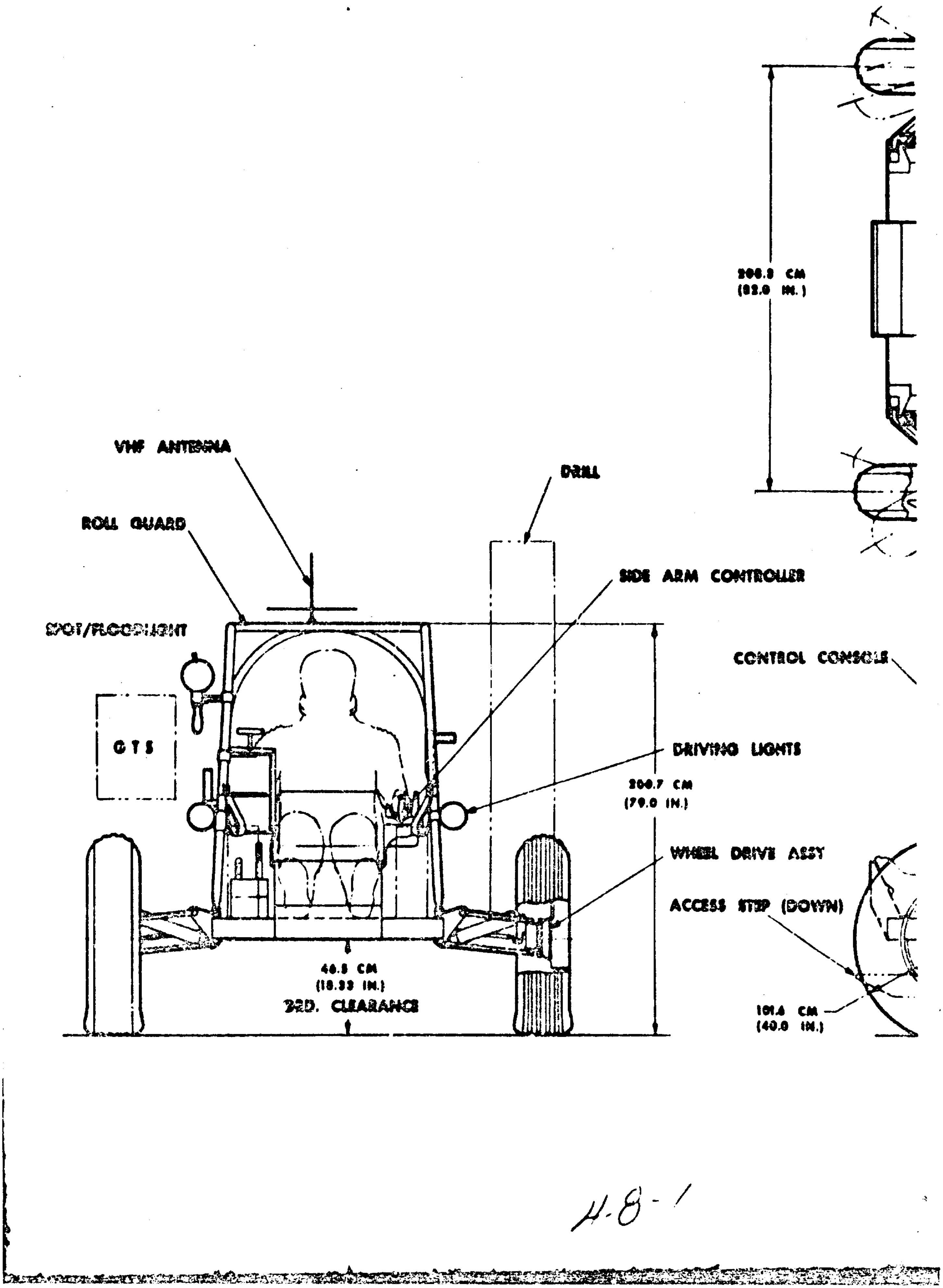

VHF ANTENNA
DRILL
ROLL GUARD
SIDE ARM CONTROLLER
SPOT/FLOODLIGHT
CONTROL CONSOLE
G T S
DRIVING LIGHTS
200.7 CM
(79.0 IN.)
WHEEL DRIVE ASSY
ACCESS STEP (DOWN)
46.5 CM
(18.32 IN.)
GRD. CLEARANCE
101.6 CM
(40.0 IN.)

4-8-1

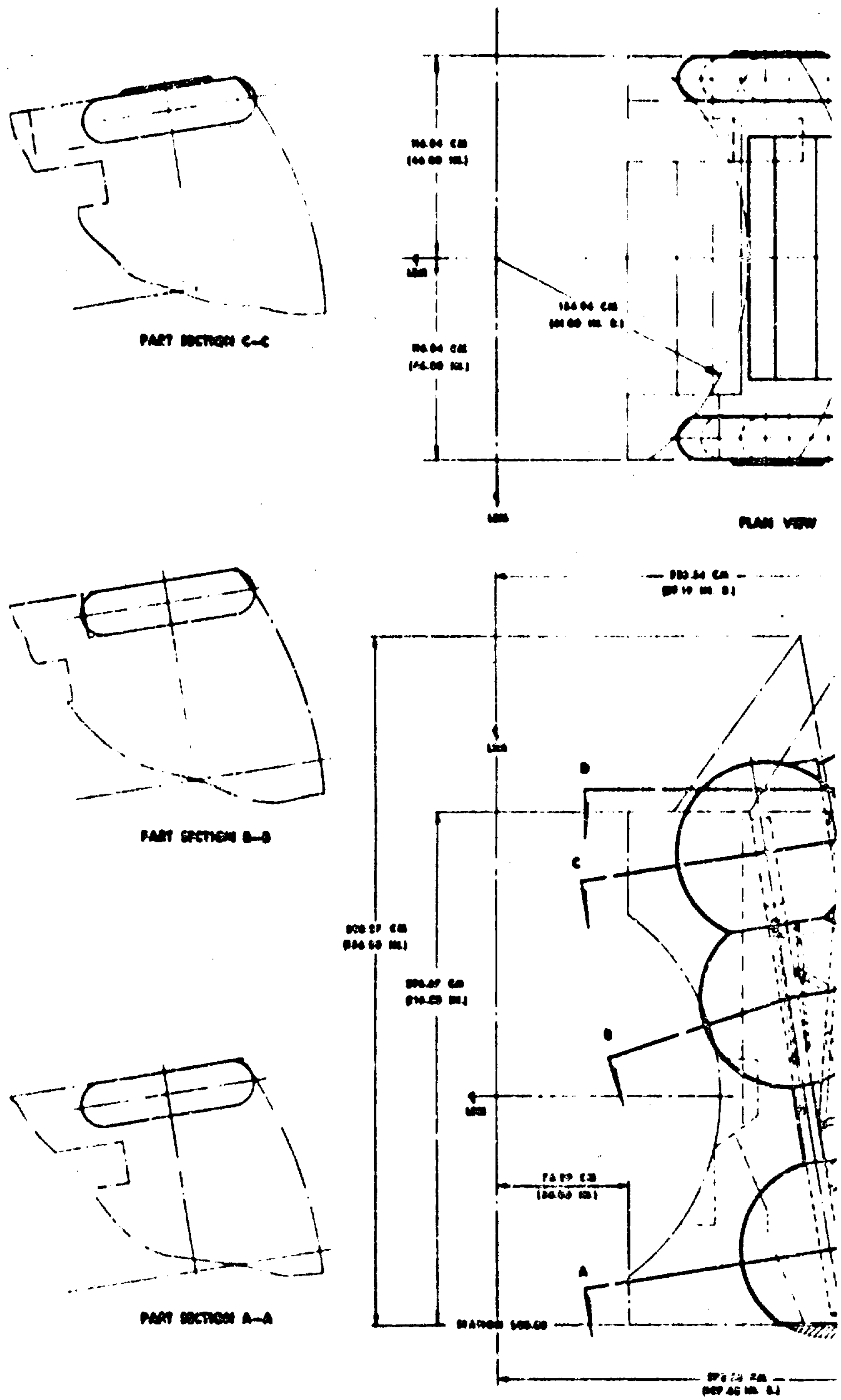

Figure 4.2.4 - S

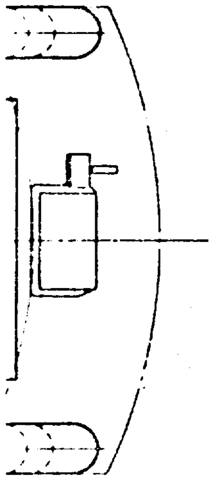

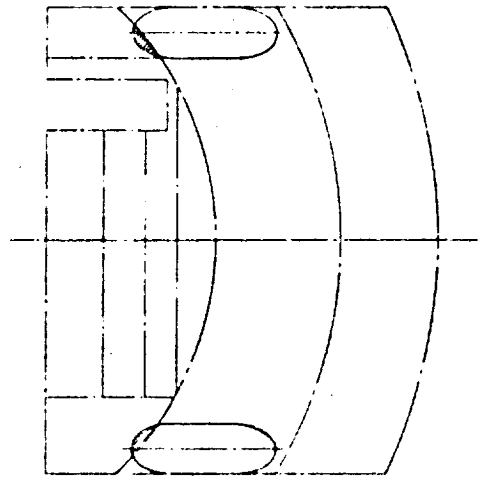

SECTION D—D

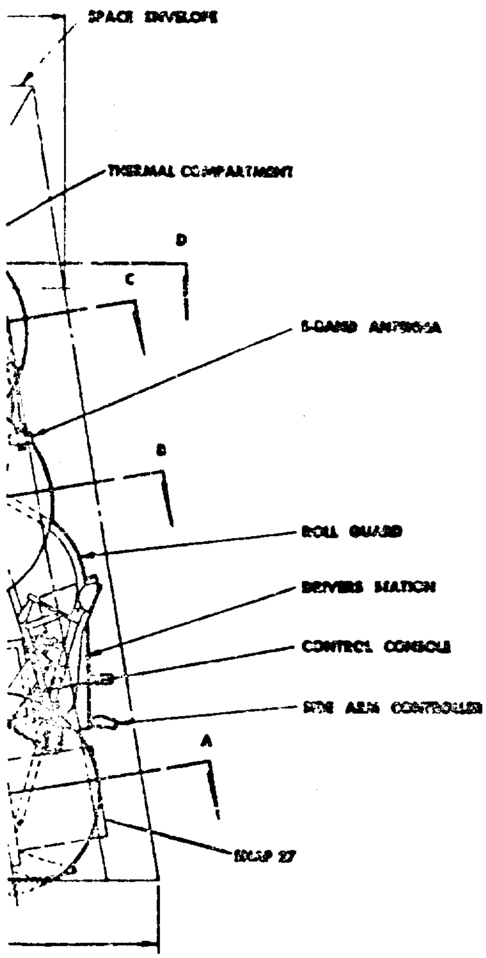

pace Envelope (LSSM Stowed)

2

Description	Maximum Payload LBM	Maximum Payload KG	Typical Sortie LBM	Typical Sortie KG
Mobility System	603	274	603	274
Crew System	56	25	56	25
Power System	304	138	304	138
Astrionics	113	51	113	51
Thermal Compartment Structure & Insulation	63	29	63	29
*Empty Vehicle Mass	1139	517	1139	517
Astronaut + PLSS	320	145	320	145
Spare PLSS (2)	135	61	135	61
Scientific Equipment	705	320	576	261
Gross Vehicle Mass	2299	1043	2170	984

* SNAP 27 Included With Scientific Equipment

Figure 4.2.5 Baseline LSSM Mass Summary

Gross Vehicle Mass (with Crew)	984 kg (2170 lbm)
C.G. Height Above Ground - Overall	0.82 m (32.2 in.)
Forward Unit	0.88 m (34.8 in.)
Aft Unit	0.67 m (26.4 in.)
Axle Load Distribution	
Front	30.9%
Center	37.1%
Rear	32.0%
Overall Length	406 cm (160 in.)
Overall Width	234 cm (92 in.)
Wheel Diameter	101.6 cm (40 in.)
Wheel Width	25.4 cm (10 in.)
Wheel Deflection (at Nominal Load)	4.3 cm (1.67 in.)
Average Ground Pressure	
Hard Surface	0.7 psi
Soft Soil ($k_\phi = 0.5$, $n = 0.5$)	0.5 psi
Wheel Base	147/158 cm (58/62 in.)
Wheel Tread	209 cm (82 in.)
Ground Clearance	45.7 cm (18 in.)
Hang-Up Radius (Between Axles)	35.5/41.9 cm (14/16.5 in.)
(Between Wheels)	132.1 cm (52 in.)
Angle of Approach	90^o +
Angle of Departure (Less SNAP 27)	90^o+
Basic Platform Area - Total	4.61 m^2 (49.6 ft^2)
Forward Unit	3.56 m^2 (38.3 ft^2)
Aft Unit	1.05 m^2 (11.3 ft^2)

Figure 4.2.6 Baseline LSSM General Characteristics

5.0 BASELINE LSSM MOBILITY PERFORMANCE ANALYSIS

5.1 INTRODUCTION

This part of the report on mobility analysis of the baseline LSSM covers the following aspects of vehicle performance:

- o Mobility over soft ground
- o Obstacle capability
- o Maneuverability
- o Dynamic ride behavior over rough terrain

Each subject is discussed separately under individual sections, and the results summarized.

The evaluation of mobility in soft soils was largely based on mathematical models of soil-vehicle relationships developed by M. G. Bekker and extended by the Land Locomotion Laboratory of the Army Tank Automotive Center. Obstacle capability was determined by means of scale-model tests. The analysis of maneuverability was by means of equations standard in automotive engineering, modified to the "non-standard" LSSM baseline design. Dynamic performance over rough terrain was evaluated by means of an extensive analog computer program.

5.2 SOFT GROUND MOBILITY

5.2.1 General

The soft ground mobility performance analysis included:

- o Tractive performance
- o Motion resistance
- o Drawbar-pull capability or gradeability
- o Drive power and torque requirements
- o Locomotion energy requirements

The evaluation of locomotion performance in soft soils was based on analytical and experimental methods developed by M. G. Bekker for the purpose of evaluating terrain-vehicle systems in off-the-road locomotion. In this approach, mathematical models of the soil-vehicle relationship were formulated to express vehicle performance characteristics, i.e., thrust, motion resistance, gradeability, etc. Laboratory scale model experiments were also utilized in this approach to solve mobility problems which were not readily amenable to analytical treatment. Most of the mobility computations were performed with the aid of the 7040 digital computer, making it possible to perform extensive parametric analyses.

5.2.2 Vehicle Characteristics

All calculations following were performed for the baseline LSSM as described in the previous section of the report. Gross vehicle mass was taken as 2170 lbm (984 kg) with the following axle load distribution on level ground:

- o Front - 30.9%
- o Center - 37.1%
- o Rear - 32.0%

The assumption was made that the two wheels on one axle would be equally loaded. Other vehicle characteristics pertinent to these calculations were:

- o Wheel dimensions - 40 in. O.D. x 10 in. wide
- o Wheel deflection rate - 36 lb/in.
- o Coefficient of rolling resistance - 0.04

The latter value is the resistance due to wheel flexure and was determined by means of tests on the GM DRL rolling road. The actual values measured on a 60 inch wire frame wheel, over a wide range of loadings, varied between 0.02 to 0.04.

5.2.3 Surface Characteristics

In order to evaluate mobility performance, in addition to knowing the pertinent vehicle parameters such as mass, load distribution, size and form of the contact area and power characteristics, it is necessary to quantitatively describe the terrain characteristics that affect performance. In this study, calculations were based mainly on the terrain characteristics of the Engineering Lunar Model Surface (ELMS), given in Annex A of the statement-of-work. Combinations of soil values specified were: $\left[k_\phi = 0.5,\ n = 0.5,\ \phi = 32^\circ\right]$, $\left[k_\phi = 1.0,\ n = 0.75,\ \phi = 32^\circ\right]$, $\left[k_\phi = 3.0,\ n = 1.0,\ \phi = 32^\circ\right]$ and $\left[k_\phi = 6.0,\ n = 1.25,\ \phi = 32^\circ\right]$, where ϕ = soil angle of friction, and k_ϕ and n are vertical deformation parameters by means of which vehicle sinkage can be calculated. Another soil given for consideration (Annex G of statement-of-work) had the characteristics of a very weak soil $\left[k_\phi = 0.05,\ n = 1.0,\ \phi = 20^\circ\right]$. In all cases, the soils were considered to be non-cohesive ($c = 0$, $k_c = 0$). In addition to the given characteristics, it was necessary to make the following assumptions to complete the necessary calculations:

- o Soil specific weight, $\gamma = 0.01$ lb/cu. in.
- o Soil deformation modulus, $K = 0.5$
- o Coefficient of friction between wheel and hard surface, $\mu = 0.8$

The assumptions were necessary for the following reasons:

- o Motion resistance due to bulldozing is dependent on the soil specific weight. The value chosen, $\gamma = 0.01$ lb/cu. in., corresponds to the specific weight of loose, dry sand, adjusted to "lunar weight".

- o The value, K, is required to define the form of the soil thrust - slip curve. Tests conducted by GM DRL indicate that a value of $K = 0.5$ is reasonable for dry loose sand.

- In order to evaluate performance over a hard, non-deformable surface, the coefficient of friction between wheel and surface must be known. A value of $\mu = 0.8$ was selected to permit the vehicle to negotiate the 35 degree slopes specified in the ELMS.

5.2.4 Baseline LSSM Mobility Calculations

Two of the most important measures of vehicle mobility performance are its drawbar pull capability, which determines its ability to climb slopes, accelerate, tow loads, etc., and the energy consumption required for locomotion.

Drawbar pull is defined as the excess thrust a vehicle is capable of developing over and above that required to overcome motion resistance. The thrust (or gross tractive effort) a vehicle can develop depends on the shearing characteristics of the soil.

It has been suggested that the shear stress-strain relationships of soils can be expressed generally by:

$$\tau = \left[\frac{c + p \tan \phi}{Y}\right] \left[\exp(-K_2 + \sqrt{K_2^2 - 1})\, K_1 j - \exp(-K_2 - \sqrt{K_2^2 - 1})\, K_1 j\right] \qquad (5.1)$$

where

τ = soil shearing strength (lb/in.^{2})

K_1, K_2 = soil deformation parameters (in^{-1}, dimensionless)

j = horizontal soil deformation (in.)

Y = maximum value of quantity in brackets (dimensionless)

c = soil cohesion (lb/in.^{2})

ϕ = soil angle of friction (degrees)

p = ground contact pressure (lb/in.^{2})

Since for most soils, particularly dry granular soils, the stress-strain curve does not exhibit a peak and then a decay (as per Equation 5.1), other investigators have suggested a simpler equation:

$$\tau = (c + p \tan \phi)(1 - e^{-j/K}) \qquad (5.2)$$

where K is a soil deformation modulus (in.) that can readily be determined from conventional shear vane tests. As was stated previously K = 0.5 provides a close fit between analytical and experimental results. This is illustrated in Figure 5.2.1. For comparison purposes, curves derived from Equation(5.1) using values of K_1 and K_2 suggested in Annex A are also included.

The tractive effort (or thrust) developed at the wheel-surface interface can be found by integrating the shear stress along the ground contact area.

Assuming a uniform ground pressure over the contact area, integrating Equation (5.2) yields:

$$H = \left[c\,A + W_n \tan \phi \right] \left[1 + \frac{K}{sl} \left(\exp\left(- \frac{sl}{K} \right) - 1 \right) \right] \tag{5.3}$$

where

s = wheel slip (%)

l = length of ground contact area (in.)

H = tractive effort or thrust (lb.)

A = ground contact area (in.^{2})

W_n = wheel load normal to the surface (lb.)

and other terms are as defined previously.

Thus the thrust developed by each wheel can be found as a function of slip if the soil parameters ϕ and K, and the ground contact length and wheel load normal to the surface are known (c = 0 in all cases).

A thrust-slip curve for the complete vehicle can be developed by taking the H-s curves for each individual wheel and adding the values of H at each value of slip.

Thrust versus slip curves for the baseline LSSM are shown in Figure 5.2.2 covering all soil conditions considered in this study. Note that these curves are for level surfaces and thrust is expressed as a percent of vehicle weight.

To determine drawbar pull capacity, the resistances encountered by the vehicle must also be known. Total motion resistance is composed of the following factors:

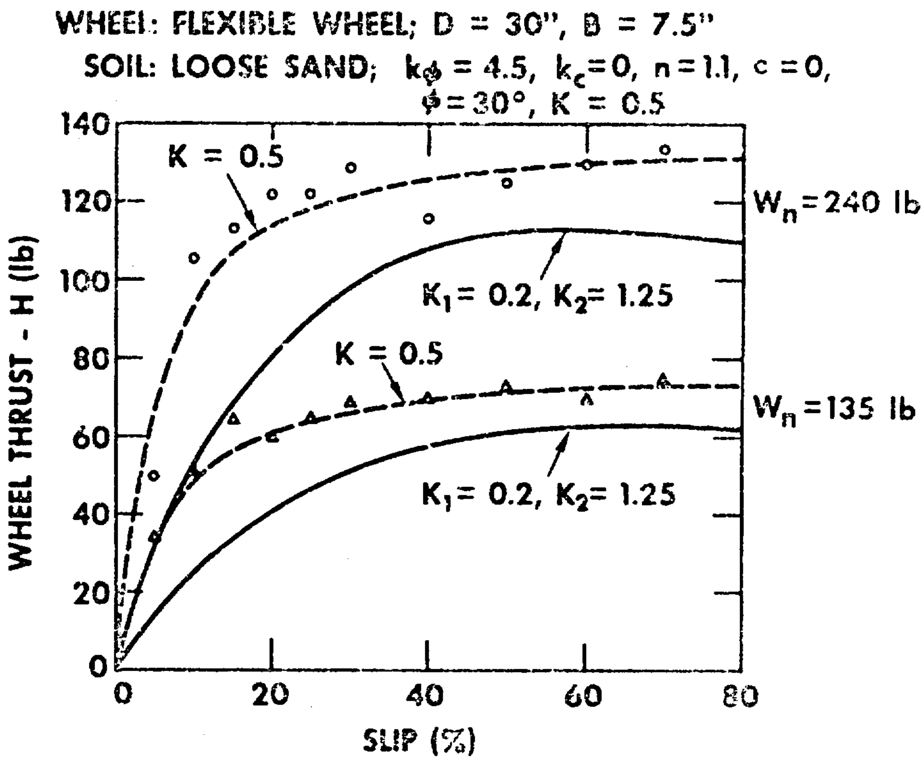

Figure 5.2.1 - Wheel Thrust in Soft Soil

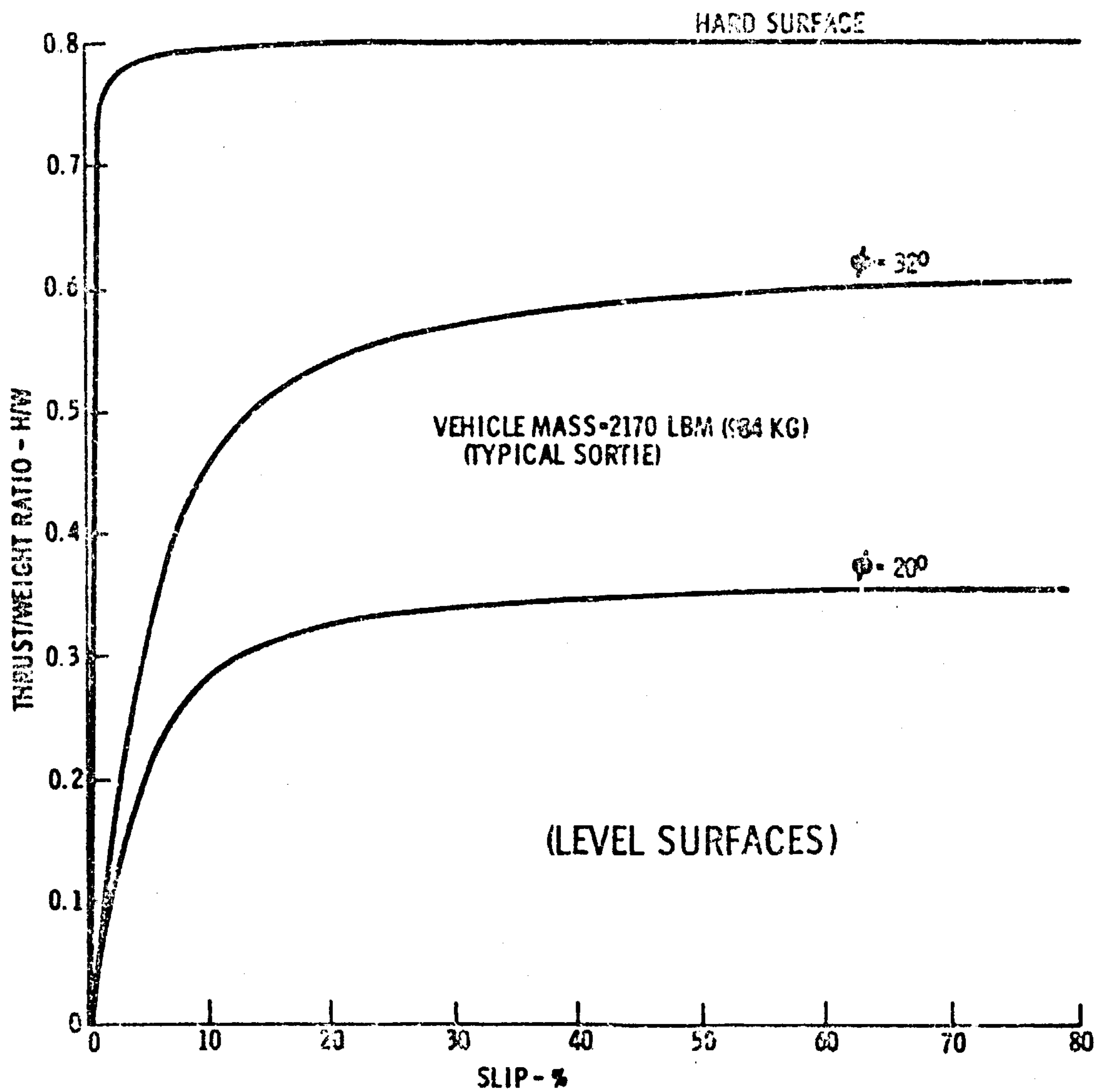

Figure 5.2.2 - LSSM Thrust/Weight Ratio vs Slip

- **Rolling Resistance Due to Wheel Flexure**

  This is a loss that takes place entirely within the wheel and can be expressed by

$$R_r = f W_n \tag{5.4}$$

where f = a coefficient determined by experimentation and W_n is the wheel load normal to the surface. As was stated above, a value of f = 0.04 has been established for this study.

- **Motion Resistance Due to Soil Deformation**

  This is composed of two factors; resistance due to soil compaction and resistance due to soil bulldozing. The latter can be determined from the following equation:

$$R_b = 1/2 \gamma b z^2 \tan^2 (45^\circ + \phi/2) + 2 c b z \tan (45^\circ + \phi/2) \tag{5.5}$$

where R_b = bulldozing resistance (lb.)

γ = specific soil weight (lb/in.^{3})

b = width of ground contact area (in.)

z = wheel sinkage (in.)

For the postulated soil models, c = o and γ has been assumed to be equal to 0.01.

The equation to be used to calculate compaction resistance depends on whether the whel is considered to be flexible or rigid.

For a rigid wheel,

$$R_c = \frac{1}{(3-n)^{(2n+2)/(2n+1)} (n+1) (k_c + b k_\phi)^{1/(2n+1)}} \left[\frac{3 W_n}{\sqrt{D}} \right]^{\frac{(2n+2)}{(2n+1)}} \tag{5.6}$$

where R_c = compaction resistance (lb.)

n = exponent of soil sinkage (dimensionless)

k_c = cohesive modulus of soil deformation (lb/in.$^{n+1}$)

k_ϕ = frictional modulus of soil deformation (lb/in.$^{n+2}$)

D = wheel diameter (in.)

W_n = wheel load normal to ground surface (lb.)

b = width of ground contact area (in.)

For a flexible wheel

$$R_c = \frac{1}{(n+1)(k_c + bk_\phi)^{1/n}} \left[\frac{W_n}{\ell}\right]^{\frac{n+1}{n}} \tag{5.7}$$

where ℓ = length of ground contact area in inches and the other terms are as described previously. For the postulated soils, $k_c = o$.

To determine whether the flexible or rigid wheel equation should be used, it is necessary to determine the critical ground pressure above which a flexible wheel behaves like a rigid wheel. This critical pressure can be found from:

$$p_{crit} = \frac{W_n (n+1)}{b\left[\frac{3W_n}{(3-n)\, bk_\phi \sqrt{D}}\right]^{1/(2n+1)} \sqrt{D - \left[\frac{3W_n}{(3-n)\, bk_\phi \sqrt{D}}\right]^{2/(2n+1)}}} \tag{5.8}$$

where p_{crit} = critical ground pressure and all other terms are as previously described. If this value of p_{crit} is greater than the ground contact pressure calculated for the case of a flexible wheel, then the wheel can be treated as a high deflection flexible wheel; if lower, the wheel must be considered as a rigid wheel.

o **Motion Resistance Due to Slopes**

This is the downhill component of the vehicle weight and is calculated by

$$R_g = W \sin \theta \tag{5.9}$$

where R_g = grade resistance (lb.)

W = vehicle weight (lb.)

θ = angle of the slope from the horizontal (degrees)

If the vehicle is going downhill, R_g has a negative value.

The total motion resistance then can be expressed by:

$$R_t = R_r + R_b + R_c + R_g \tag{5.10}$$

Curves of motion resistance on level surfaces are given as a function of wheel load in Figure 5.2.3 for the ELMS and Annex G soils. The range of interest for LSSM lies between wheel loads of 55-65 lbf. As an added matter of interest,

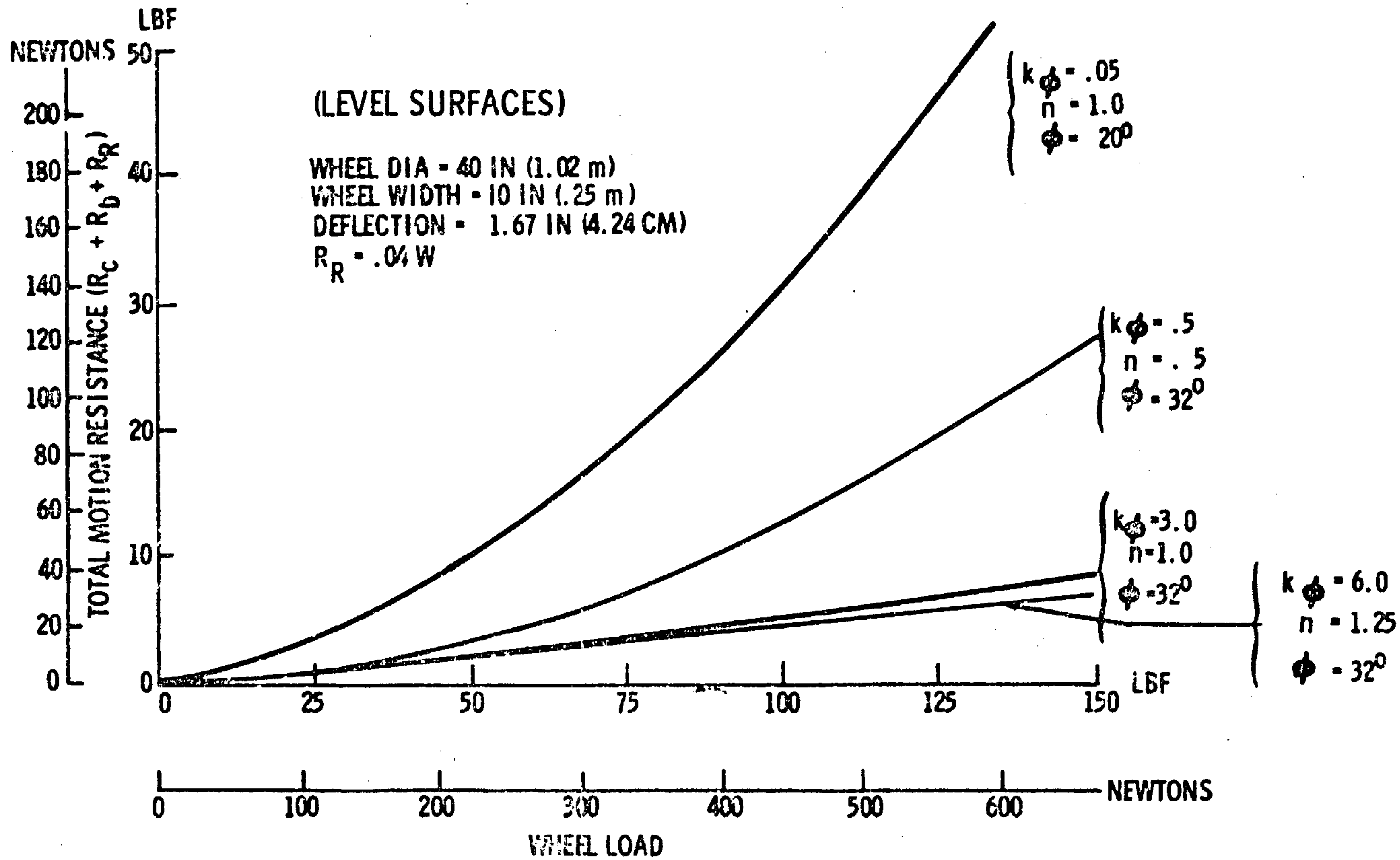

Figure 5.2.3 - LSSM Wheel Motion Resistance vs Load

Figure 5.2.4 illustrates the correlation between results derived analytically by means of the above equations, and from tests conducted in dry sand. Also clearly illustrated is the superiority of flexible wheels over rigid wheels from the point-of-view of motion resistance.

Drawbar pull as a function of wheel slip can now be calculated from the relationship:

$$DP = H - R_t \tag{5.11}$$

Figure 5.2.5 shows the drawbar capability of the baseline LSSM plotted in terms of drawbar pull - to - weight ratio versus wheel slip, for three soil models. Again, the calculations are for level surfaces. The results indicate that the LSSM would be able to negotiate slopes as follows:

(1) For soil $k_\phi = 0.05$, $n = 1.0$, $\phi = 20^\circ$ - Slope = 7.5°.

(2) For soil $k_\phi = 0.5$, $n = 0.05$, $\phi = 32^\circ$ - Slope = 27°

(3) For soil $k_c = 3.0$, $n = 1.0$, $\phi = 32^\circ$ - Slope = 29°

The large difference in capability in Case (1) as compared to the others is mainly due to the difference in soil friction angle, ϕ, which results in a large difference in available tractive effort or thrust. The slope climbing capability for the LSSM on a hard, non-deformable surface would depend on the coefficient of friction between wheels and surface. For example, assuming sufficient torque were available, the coefficient of friction required for climbing a hard surface 35° slope would be at least $\mu = 0.7$.

To estimate steady - state locomotion energy requirements over smooth terrain, it is necessary only to know the values of the above elements of motion resistance, the efficiency of the vehicle drive system, and the wheel slip relative to the ground contact surface. The equation for this case is

$$E_S = \frac{0.00123\ R_t}{\eta\ (1 - s)} \tag{5.12}$$

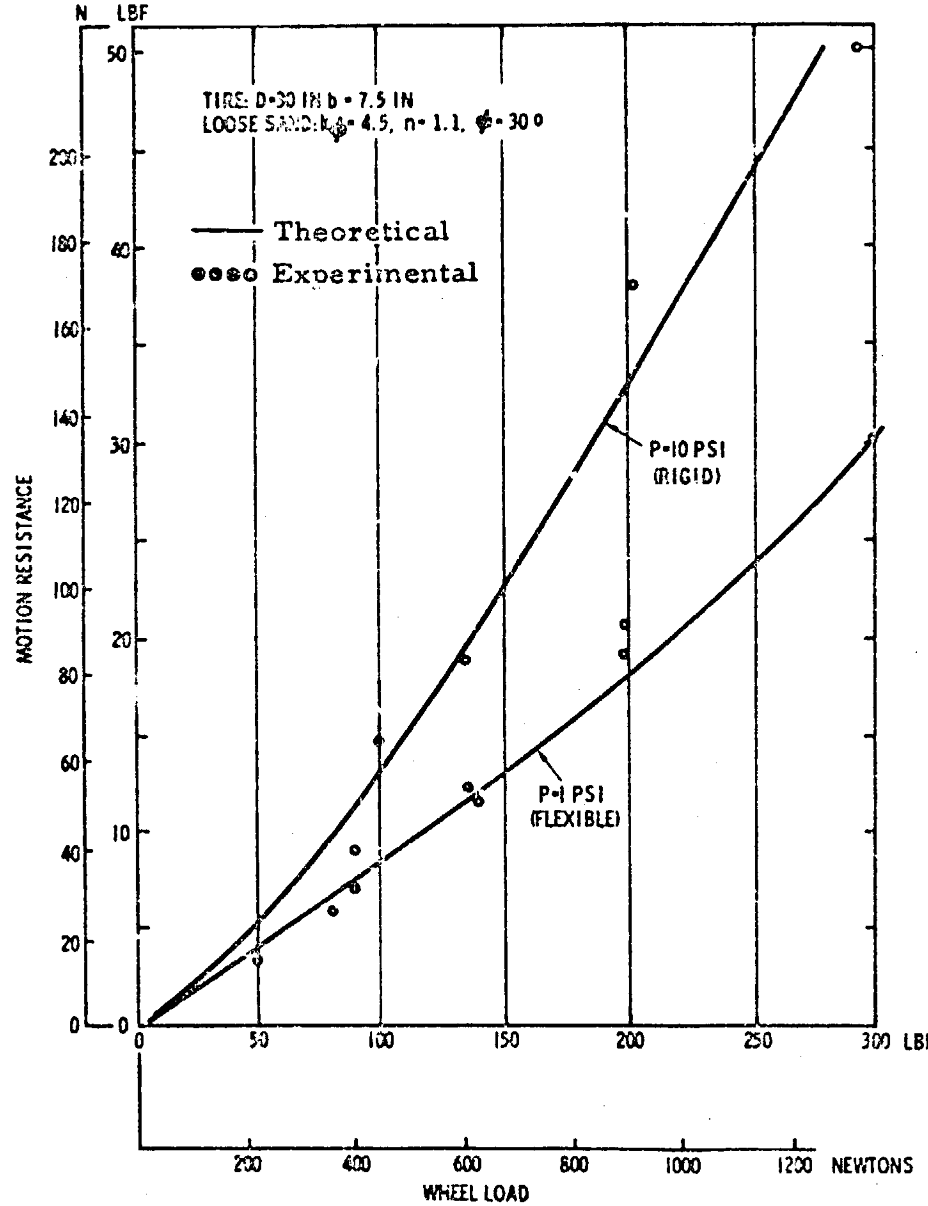

Figure 5.2.4 - Comparison of Rigid and Flexible Wheels in Sand
(Theoretical and Experimental)

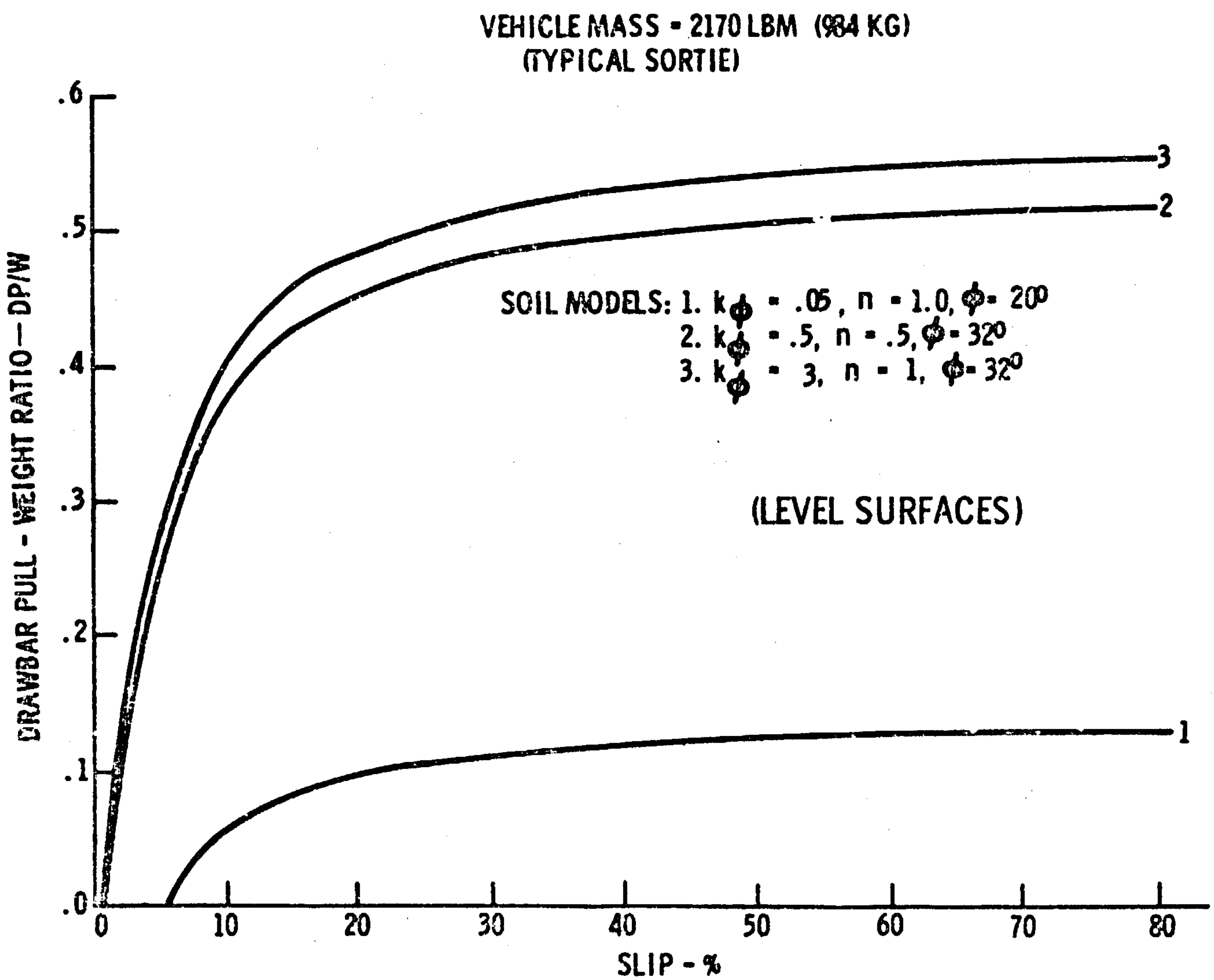

Figure 5.2.5 - LSSM Drawbar Pull-Weight Ratio vs Slip

where E_s = steady-state energy (kw-hr/km)

R_t = total steady-state motion resistance (lb.)

$= R_r + R_b + R_c + R_g$ (5.12)

η = drive system efficiency (dimensionless)

s = slip (dimensionless)

The value of η depends on the specific design of the drive system and in the case of the LSSM will vary with wheel speed.

To determine the value of slip, it is necessary to know the shearing characteristics of the soil. For steady-state operation, the thrust H developed by the vehicle must equal the total motion resistance R_t developed by all wheels. Therefore, knowing R_t, the average wheel slip can be found from the vehicle thrust-slip curve.

ıus, all factors affecting the steady-state energy can easily be determined ıce the terrain and vehicle characteristics are specified. GM DRL has 'epared a 7040 digital computer program which permits rapid calculation the necessary resistance and slip factors. The following vehicle parameters 'e inputs to the program:

- o Nominal wheel load, as determined for level surface - $W_i (i = 1, 2, \ldots, 6)$ (lbf)
- o Wheel diameter - D_i (in)
- o Wheel width - B_i (in)
- o Wheel spring (deflection rate) - ψ_i (lb/in)
- o Coefficient of wheel rolling resistance - f_i (dimensionless)

he operational mass of the LSSM is presently estimated at 2170 lbm dis-buted as per 5.2.2. The pair of wheels on each axle are assumed to be ually loaded. All wheels are 40 inches in diameter with a maximum section idth of 10 inches. The wheel spring rate is estimated at 36. lb/in and as ›inted out previously, the coefficient "f" is taken equal to 0.04.

he values and distribution for the soil parameters ϕ, k_ϕ, and n, and slopes , used to calculate energy in this study, are given by the ELMS Maria and plands models. In all cases, c and k_c are zero. The form of the thrust-ip curve for ELMS soils was assumed to be represented by Equation 5.2.

he steps carried out to calculate locomotion energy requirements for each ›mbination of soil type and slope are as follows:

(1) Calculate wheel normal loading for each wheel

$$W_{n_i} = W_i \cos \Theta \qquad (5.13)$$

The effect of weight shift due to slopes or suspension deflection is neglected. Calculations have shown that these have negligible effect on vehicle energy requirements.

(2) Calculate average ground pressure under each wheel.

(a) Calculate wheel deflection: $\Delta_i = W_{n_i} / \psi_i$ (5.14)

(b) Calculate ground contact length for each wheel on non-deformable surface:

$$\ell_i' = 2\sqrt{\Delta_i (D_i - \Delta_i)} \quad (5.15)$$

(c) Calculate ground contact width for each wheel on non-deformable surface:

$$b_i' = 2\sqrt{\Delta_i (B_i - \Delta_i)} \quad (5.16)$$

(d) Calculate ground contact area for each wheel on non-deformable surface. Experimental data shows that the area is nearly elliptical in shape and can be approximated by

$$A_i' = \frac{\pi}{4} b_i' \ell_i' \quad (5.17)$$

(e) Calculate average ground pressure on hard surface

$$p_i' = W_{n_i} / A_i' \quad (5.18)$$

(3) Calculate p_{crit} from Equation (5.8). If p_{crit} is greater than p_i' as calculated above, the wheel can be considered flexible; if $p_{crit} < p_i'$ then rigid wheel equations must be used. In the case of LSSM, the wheels can be considered flexible.

(4) Calculate wheel sinkage z for each soil-slope combination.

(a) In the first approximation, calculate sinkage using average ground pressure calculated in Step 2e above:

$$z_i' = \left[p_i' / k_\phi \right]^{1/n} \quad (5.19)$$

(b) Correct ground contact length for specified soil condition: (see sketch below)

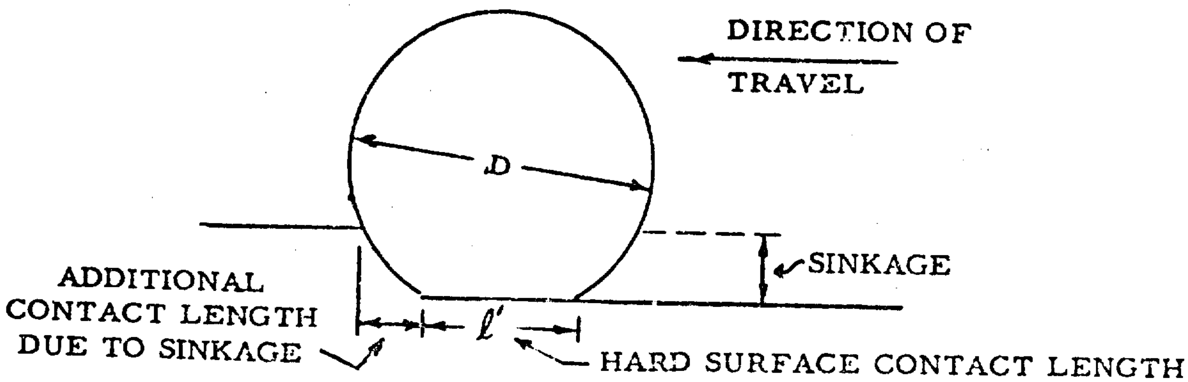

The corrected length is given by:

$$\ell_i = \ell_i/2 + \sqrt{(\Delta_i + z_i')(D_i - \Delta_i - \Delta z_i')} \qquad (5.20)$$

(c) Correct ground contact width for specified soil condition. In a manner similar to above, this can be determined to be:

$$b_i = 2\sqrt{(\Delta_i + z_i')(B_i - \Delta_i - z_i')} \qquad (5.21)$$

(d) Recalculate ground contact area:

$$A_i = \frac{\pi}{4} \ell_i b_i \qquad (5.22)$$

(e) Recalculate average ground pressure:

$$p_i = W_{n_i}/A_i \qquad (5.23)$$

(f) Recalculate sinkage

$$z_i = \left[p_i/k_\phi\right]^{1/n} \qquad (5.24)$$

(g) Iterate above corrections until two consecutive calculations of sinkage are within 3% of each other.

(5) Calculate the rolling resistance R_r for each wheel and sum up for all wheels.

$$\sum R_{r_i} = \sum f\, W_{n_i} \tag{5.25}$$

(6) Calculate bulldozing resistance R_b for each wheel using Equation (5.5) and sum up for all wheels.

(7) Calculate compaction resistance R_c for each wheel and sum up for all wheels. Use Equation (5.7) if wheel is flexible; Equation (5.6) if rigid.

(8) Calculate grade resistance R_g for total vehicle.

$$R_g = W\sin\Theta \qquad \text{where } W = \text{weight of vehicle} \tag{5.26}$$

(9) Add totals of R_r, R_b, and R_c to R_g to determine total vehicle steady state motion resistance.

$$R_t = R_r + R_b + R_c \pm R_g \tag{5.27}$$

(10) Calculate thrust H as a function of slip.

(a) Using Equation (5.3) determine H as a function of slip for each wheel. GM DRL assumes K = 0.5 for all ELMS surfaces, including the 35° hard surface. The value of tan ϕ, or μ for this 35° surface is assumed to be 0.8. The ground contact length, ℓ, has previously been determined for each soil and slope combination in Step 4.b above.

(b) The H versus Slip curve for the complete vehicle is then obtained by adding the separate H values for each wheel at each value of slip. This results in a thrust versus "average" slip relationship.

(11) Determine "average" wheel slip. For steady-state operation, the thrust H must equal the total external motion resistance, R_t. Therefore, knowing R_t for the vehicle from Step 9, the value of slip can be read directly from the Thrust-Slip curve derived in Step 10.b above. This is only for those cases where R_t is a positive number, in which case drive power must be applied. In cases where the vehicle is going downhill, it is possible for R_t to have a negative value; that is, $R_g > R_c + R_b + R_r$. In these cases brakes are applied to prevent acceleration and no drive energy is expended.

(12) Calculate required wheel torque as follows:

(a) For any surface condition, take total vehicle motion resistance, R_t, and divide by the number of wheels to obtain average R_t per wheel.

(b) Multiply this average R_t by the effective wheel radius where the effective radius is equal to $(D/2 - \Delta)$. This is the required value of wheel torque.

(13) Determine average wheel speed. This depends on the torque-speed characteristics of the drive system. The present LSSM drive system output torque-speed and power/speed characteristics are shown in Figure 5.2.6.

These have been derived from the following minimum requirements:

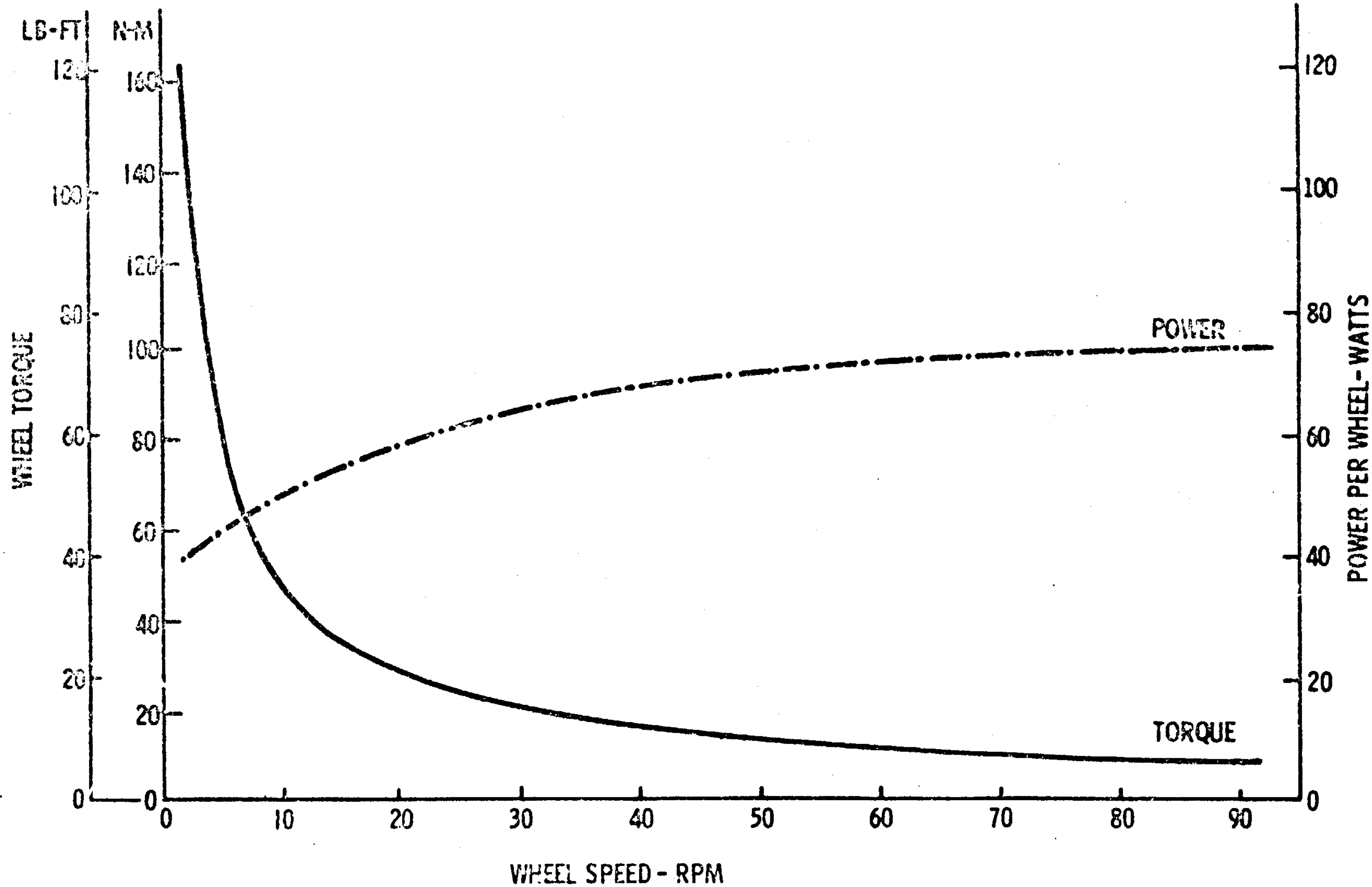

Figure 5.2.6 - Wheel Net Torque and Power Characteristics

- A maximum vehicle velocity of 16 km/hr (10 mph) over hard level surface (this represents a wheel speed of about 92 rpm).
- An 8 km/hr (5 mph) velocity over compacted soil with characteristics $k_\phi = 6.0$ and $n = 1.25$.
- Maximum continuous duty requirements (69 ft-lb of torque) correspond to climbing a 35 degree hard surface slope at a wheel speed of about 5 rpm.
- Maximum intermittent duty torque of 120 ft-lb at 2 rpm to climb a vertical step obstacle 40 inches high.

Where R_t is positive, the wheel speed is found from the torque-speed curve for the corresponding torque value calculated in Step 12. b.

(14) Determine vehicle speed. For the cases where R_t has a positive value, this can be determined by:

Speed = (Average Wheel Speed) (Effective Wheel Radius) (1-Slip)

The value of slip is that found in Step 11, and the wheel speed is that found from Step 13. The effective wheel radius is calculated by finding the average of all wheel deflections and subtracting this value from the undeflected wheel radius. The value of Δ is that used in Step 12. b.

To determine vehicle speed for the cases where R_t has a negative value, that is, coming down high angle slopes, the following procedure is used:

(a) Assume that the vehicle is maintained at a constant speed; that is, braking is applied to prevent acceleration.

(b) Assume that the speed of the vehicle coming down the 35° slope (non-deformable surface) is the same as the speed going up the slope. The braking power for this case is then ($-R_t$) times (vehicle speed).

(c) Assume that this value of braking power is available for all other slope-soil combinations. Then the vehicle speed for each condition can be found by dividing the braking power by the corresponding value of $-R_t$.

(15) Determine distance vehicle travels for each slope-soil combination. If a total traverse of one kilometer is assumed, then the distance travelled for each condition is simply equal to the percent occurrence whibh is specified in the ELMS models.

(16) Calculate travel time for each slope-soil combination. This is equal to the distance (Step 15) divided by the vehicle velocity over each surface condition.

(17) Calculate net steady-state locomotion energy for each slope-soil combination. This is equal to:

$$E_S = \frac{(0.00123)R_t \text{ (Distance)}}{(1-s)} \qquad (5.28)$$

where E_S = net energy over given surface (kw-hr)

Distance = distance travelled per kilometer over given surface condition (Km)

s = slip (0 - 1.0)

R_t = total motion resistance (lb)

(only the cases where R_t is positive are considered; that is, where drive power must be supplied for locomotion.)

(18) Energy dissipated by the suspension dampers must also be considered because this must be provided by the drive system. An analog computer program for LSSM operating over an undulating terrain similar to that shown in Ranger 7 photographs established damping power as a function of vehicle speed. This is discussed in Section 5.5 of this report.

Energy for damping that must be supplied can be determined for each travel segment (slope-soil combination) by multiplying travel time (Step 16) for the segment by the damping power required at the calculated vehicle velocity (Step 14).

As in the case for so-called steady-state energy, damping energy is considered only for those cases where drive power must be supplied. That is, if R_t for the vehicle has a negative value, damping energy (E_d) is neglected because it is not supplied by the power system.

(19) Add net steady-state and damping energies for each soil-slope combination ($E_S + E_d$).

(20) Determine gross energy due to R_t and damping requirements. This depends on drive system efficiency which in turn depends on the specific drive system. For LSSM, the overall efficiency is a combination of electric drive system and wheel drive mechanism efficiencies. The overall efficiency as a function of wheel speed is shown in Figure 5.2.7.

Therefore, dividing the results from Step (19) by the efficiency at a corresponding wheel speed gives the gross value of ($E_{R_t} + E_d$).

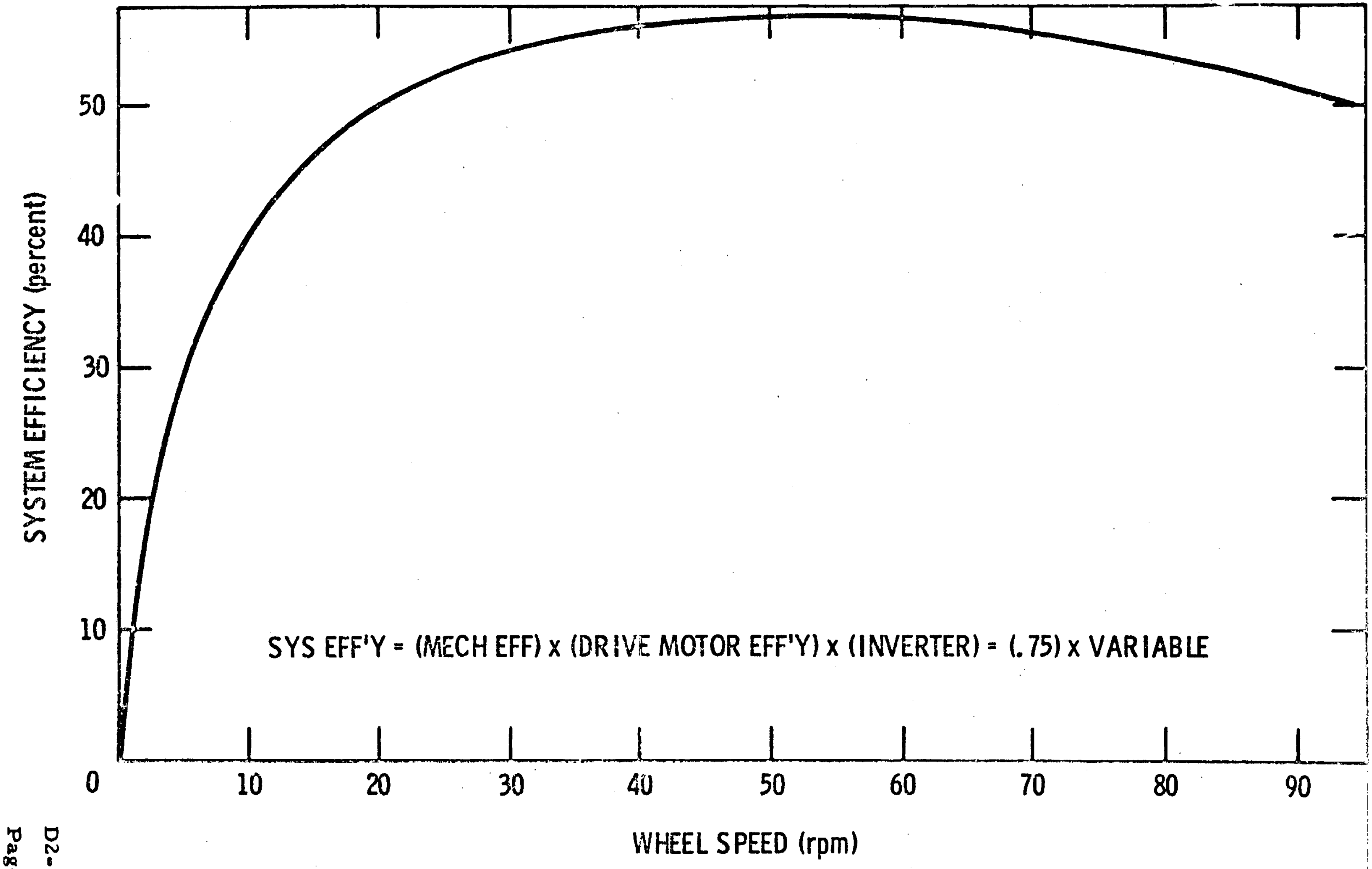

Figure 5.2.7 - Baseline LSSM Overall Drive System Efficiency

(21) In addition to the factors so far discussed, energy is also required to accelerate, brake and steer the vehicle, and to overcome losses due to surface roughness. These latter losses are reflected in increased wheel flexing and slippage, and in impact energy absorbed by the vehicle and ground surface. Since no simple analytical methods are presently available to treat these factors in a rational manner, it is necessary to provide an energy reserve. At the present time, GM DRL is using a reserve of 35% of the gross value of $(E_{R_t} + E_d)$ as calculated in Step (20).

(22) Calculate average velocity capability over ELMS. This is accomplished by adding the travel time for all travel segments. The average velocity is the reciprocal of this value since a total traverse of one kilometer was assumed.

Figures 5.2.8 and 5.2.9 show the results of the locomotion energy calculation procedure for the ELMS Maria and Uplands models. Similar calculations were made for the maximum estimated LSSM mass of 2300 lbm. This condition reflects a maximum scientific equipment payload of 705 lbm.

The results are summarized in Figure 5.2.10. (Note that the average velocities shown do not reflect possible limitations that might exist due to ride performance over rough surfaces.)

LOCOMOTION ENERGY TABULATION

VEHICLE CONCEPT Baseline LSSM, 6x5 Semi-Flex 40-in. Dia Wheels, 10-in. Width
VEHICLE MASS 2170 LSM (Typical Sortie)
WHEEL LOADS @ 0° Slope, 55.9 LBF (Front), 67.2 LBF (Center), 57.9 LBF (Rear)

Surface Model ELMS - Maria			Vehicle Motion Resistance					Average % Slip	Slip Factor (1-s)	Distance Traveled per km (km)	Steady State Locomotion Energy (watt-hr/km)	Wheel Torque (lb-ft)	Wheel Speed (rpm)	Vehicle Linear Velocity (km/hr)	Travel Time (hrs/km)	Wheel Damping Power (watts)	Wheel Damping Energy (watt-hr/km)	Vehicle Damping Energy (watt-hr/km)	Net Locomotion Energy (watt-hr/km)	Overall Efficiency	Total Locomotion Energy (watt-hr/km)
Slope (degrees)	Percent Occurrence	Soil Values	R_c	R_b	R_r	R_{slope}	Total														
0	11	k_ϕ=0.5	16.46	0.792	14.48	0	31.74	0.9	0.991	0.11	4.332	8.09	50.6	8.80	0.0125	13.24	0.166	0.996	5.328	0.567	9.397
+1	11.25	M=0.5	16.46	0.792	14.48	6.32	38.05	1.1	0.989	0.1125	5.322	9.69	43.4	7.53	0.0149	10.31	0.154	0.924	6.256	0.563	11.112
-1	11.25	ϕ=32°	16.46	0.792	14.48	-6.32	25.42	0.7	0.993	0.1125	3.541	6.47	59.5	10.36	0.0109	17.14	0.187	1.122	4.663	0.565	8.253
+2	13.25	K=0.5	16.45	0.791	14.47	12.64	44.35	1.3	0.987	0.1225	6.749	11.29	37.9	6.57	0.0187	8.14	0.152	0.912	7.661	0.557	13.754
-2	13.25	γ=0.01	16.45	0.791	14.47	-12.64	19.08	0.5	0.995	0.1225	2.890	6.06	73.9	12.69	0.0095	25.39	0.241	1.446	4.336	0.547	7.927
+3	8		16.44	0.790	14.46	18.95	50.64	1.5	0.985	0.08	5.059	12.89	32.8	5.87	0.0141	6.40	0.090	0.540	5.598	0.548	10.215
-3	8	c=0	16.44	0.790	14.46	-18.95	12.74	0.3	0.997	0.08	1.256	3.24	91.6	16.01	0.0050	38.83	0.193	1.158	2.416	0.508	4.756
+4	5	k_c=0	16.42	0.789	14.45	25.26	56.91	1.7	0.983	0.05	3.531	16.49	29.2	5.04	0.0099	5.32	0.053	0.318	3.879	0.539	7.197
-4	5		15.42	0.789	14.45	-25.26	6.40	0.2	0.998	0.05	0.394	3.63	91.6	16.04	0.0031	38.73	0.120	0.720	1.114	0.508	2.193
+5	3.75		7.07	0.166	14.43	31.56	53.21	1.7	0.983	0.0375	2.496	13.55	31.2	5.38	0.0070	5.97	0.042	0.252	2.748	0.544	5.051
-5	3.75	k_ϕ=1.0	7.07	0.166	14.43	-31.56	-9.90	-	-	0.0375	0	-	-	16.04	0.0023	0	0	0	0		0
+7.5	1.5	M=0.75	7.04	0.165	14.36	47.26	68.82	2.3	0.977	0.015	1.300	17.53	25.4	4.35	0.0035	4.45	0.016	0.096	1.396	0.525	2.659
-7.5	1.5		7.04	0.165	14.36	-47.26	-25.70	-	-	0.015	0	-	-	7.62	0.0020	0	0	0	0		0
+10	0.9		2.79	0.030	14.26	62.87	79.95	3.0	0.970	0.009	0.912	20.38	16.7	2.85	0.0032	2.50	0.008	0.048	0.360	0.478	2.008
-10	0.9	k_ϕ=3.0	2.79	0.030	14.26	-62.87	-45.79	-	-	0.009	0	-	-	4.28	0.0021	0	0	0	0		0
+12.5	0.6	M=1.0	2.77	0.030	14.14	78.30	95.30	3.9	0.961	0.006	0.732	24.31	14.7	2.48	0.0024	2.06	0.005	0.030	0.702	0.461	1.653
-12.5	0.6		2.77	0.030	14.14	-78.35	-61.43	-	-	0.006	0	-	-	3.19	0.0019	0	0	0			0
+15	0.5		2.75	0.030	13.99	93.71	110.47	5.0	0.950	0.005	0.715	28.21	12.7	2.12	0.0024	1.84	0.004	0.024	0.739	0.445	1.661
-15	0.5		2.75	0.030	13.99	-93.71	-76.94	-	-	0.005	0	-	-	2.54	0.0020	0	0	0	0		0
+17.5	0.25		2.72	0.030	13.81	108.87	125.43	6.5	0.935	0.0025	0.413	32.07	10.7	1.77	0.0014	1.41	0.002	0.012	0.425	0.413	1.029
-17.5	0.25		2.72	0.030	13.81	-108.87	-92.31	-	-	0.0025	0	-	-	2.12	0.0012	0	0	0	0		0
+20	0.25		2.69	0.029	13.61	123.83	140.16	8.6	0.914	0.0025	0.472	35.88	9.2	1.49	0.0017	1.19	0.002	0.012	0.494	0.369	1.244
-20	0.25		2.69	0.029	13.61	-123.83	-107.50	-	-	0.0025	0	-	-	1.82	0.0014	0	0	0	0		0
+25	0.15	k_ϕ=6.0	1.68	0.018	13.13	152.01	168.04	17.6	0.824	0.0015	0.376	43.14	7.6	1.10	0.0014	0.98	0.001	0.006	0.382	0.359	1.064
-25	0.15	M=1.25	1.68	0.018	13.13	-153.01	-137.98	-	-	0.0015	0	-	-	1.42	0.0011	0	0	0	0		0
+30	0.1	μ=0.8	0	0	12.54	181.03	193.59	0.3	0.997	0.001	0.233	49.83	6.5	1.17	0.0009	0.99	0.001	0.006	0.245	0.335	0.731
-30	0.1	μ=0.8	0	0	12.54	-181.03	-168.47	-	-	0.001	0	-	-	1.16	0.0009	0	0	0	0		0
											40.760				0.1388		1.437	8.622	49.382		91.904

ASSUME TOTAL TRAVERSE = 1 km

LOCOMOTION ENERGY PER WHEEL	15.317 w hr/km
LOCOMOTION ENERGY PER VEHICLE	91.904 w hr/km
TOTAL LOCOMOTION ENERGY + 35%	124.07 w hr/km
AVERAGE VEHICLE VELOCITY	7.2 km/hr

Figure 5.2.8

LOCOMOTION ENERGY TABULATION

VEHICLE CONCEPT Baseline LSSM, 6x6 Semi-Flex 40-in. Dia Wheels, 10-in. Width
VEHICLE MASS 2170 LBM (Typical Sortie)
WHEEL LOADS @ 0° Slope 55.9 LBF (Front), 67.2 LBF (Center), 57.9 LBF (Rear)

Surface Model ELMS - Uplands			Vehicle Motion Resistance					Average % Slip	Slip Factor (1-s)	Distance Traveled per km (km)	Steady State Locomotion Energy (watt-hr/km)	Wheel Torque (lb-ft)	Wheel Speed (rpm)	Vehicle Linear Velocity (km/hr)	Travel Time (hrs/km)	Wheel Damping Power (watts)	Wheel Damping Energy (watt-hr/km)	Vehicle Damping Energy (watt-hr/km)	Net Locomotion Energy (watt-hr/km)	Overall Efficiency	Total Locomotion Energy (watt-hr/km)
Slope (degrees)	Percent Occurence	Soil Values	R_c	R_b	R_r	R_{Slope}	Total														
0	9.5	k_ϕ=0.5	16.46	0.792	14.48	0	31.74	0.9	0.991	0.089	3.741	8.08	50.6	8.80	0.0108	13.24	0.143	0.858	4.599	0.567	8.111
+1	5.4		16.46	0.792	14.48	6.32	38.05	1.1	0.989	0.054	2.555	9.69	43.4	7.53	0.0072	10.31	0.274	0.444	2.999	0.583	5.327
-1	5.4	M=0.5	16.46	0.792	14.48	-6.32	25.42	0.7	0.993	0.054	1.700	6.47	69.5	10.36	0.0052	17.14	0.089	0.534	2.234	0.565	3.954
+2	5.9	ϕ=32°	16.45	0.791	14.47	12.64	44.35	1.3	0.987	0.059	3.300	11.29	37.9	8.57	0.0090	8.14	0.073	0.438	3.696	0.557	6.639
-2	5.9	K=0.5	16.45	0.791	14.47	-12.64	18.08	0.5	0.995	0.059	1.392	4.68	73.9	12.69	0.0048	25.39	0.117	0.702	2.094	0.547	3.828
+3	6.2	γ=0.01	16.44	0.790	14.46	18.95	50.54	1.5	0.965	0.062	3.920	12.89	32.8	5.67	0.0109	6.4	0.070	0.420	4.340	0.548	7.920
-3	6.2		16.44	0.790	14.46	-18.93	12.74	0.3	0.997	0.062	.975	2.24	91.6	16.01	0.0039	38.63	0.151	0.906	1.881	0.508	3.703
+4	6.3	C=0	16.42	0.789	14.45	25.26	56.91	1.7	0.983	0.063	4.487	14.44	29.2	5.04	0.0125	5.32	0.068	0.336	4.883	0.539	9.058
-4	6.3	k_c=0	16.42	0.789	14.45	-25.29	6.40	0.2	0.998	0.063	.197	1.63	91.6	16.04	0.0039	38.73	0.151	0.906	1.403	0.508	2.762
+5	6.2	k_ϕ=1.0	7.07	0.166	14.43	31.56	53.21	1.7	0.983	0.062	4.127	13.55	31.2	5.38	0.0115	5.97	0.067	0.402	4.529	0.544	8.325
-5	6.2	M=0.75	7.07	0.166	14.43	-31.56	-9.00	-	-	0.032	0	-	-	16.04	0.0039	0	0	0	0		0
+7.5	5.5		7.04	0.165	14.36	47.26	68.82	2.3	0.977	0.055	4.738	17.52	25.4	4.35	0.0127	4.45	0.056	0.338	5.102	0.525	9.718
-7.5	5.5		7.04	0.165	14.36	-47.26	-25.70	-	-	0.055	0	-	-	7.62	0.0072	0	0	0	0		0
+10	4.2		2.79	0.030	14.26	62.87	79.95	3.0	0.970	0.042	4.238	20.33	16.7	2.85	0.0147	2.50	0.037	0.222	4.478	0.478	9.368
-10	4.2	k_ϕ=3.0	2.79	0.030	14.26	-62.87	-45.70	-	-	0.042	0	-	-	4.28	0.0098	0	0	0	0		0
+12.5	2.65	M=1.0	2.77	0.030	14.14	78.36	95.30	3.9	0.961	0.0265	3.231	24.31	14.7	2.48	0.0107	2.06	0.022	0.132	3.363	0.461	7.295
-12.5	2.65		2.77	0.030	14.14	-78.36	-61.43	-	-	0.0265	0	-	-	3.19	0.0083	0	0	0	0		0
+15	1.35		2.75	0.030	13.99	93.71	110.47	5.0	0.950	0.0135	1.931	25.21	12.7	2.12	0.0064	1.84	0.012	0.072	2.003	0.445	4.501
-15	1.35		2.75	0.030	13.99	-93.71	-76.94	-	-	0.0135	0	-	-	2.544	0.0053	0	0	0	0		0
+17.5	0.55		2.72	0.030	13.81	108.37	125.43	6.5	0.935	0.0055	.908	32.07	10.7	1.77	0.0031	1.41	0.004	0.074	.932	0.413	2.257
-17.5	0.55		2.72	0.030	13.81	-108.37	-92.31	-	-	0.0035	0	-	-	2.12	0.0026	0	0	0	0		0
+20	0.4		2.69	0.029	13.61	123.83	140.16	8.6	0.914	0.004	.754	35.83	9.2	1.49	0.0027	1.19	0.003	0.018	.772	0.389	1.984
-20	0.4		2.69	0.029	13.61	-123.83	-107.50	-	-	0.004	0	-	-	1.82	0.0022	0	0	0	0		0
+22.5	0.3	k_ϕ=6.0	1.91	0.018	13.38	138.55	153.86	11.7	0.883	0.003	.643	39.44	8.2	1.24	0.0023	1.08	0.003	0.018	.861	0.370	1.788
-22.5	0.3	M=1.25	1.91	0.018	13.38	-133.55	-123.25	-	-	0.003	0	-	-	1.59	0.0019	0	0	0	0		0
+25	0.2		1.88	0.018	13.13	153.01	168.04	17.6	0.824	0.002	.502	43.14	7.6	1.10	0.0018	.36	0.002	0.012	.514	0.359	1.432
-25	0.2		1.88	0.018	13.13	-153.01	-137.98	-	-	0.002	0	-	-	1.42	0.0014	0	0	0	0		0
+35	0.1	μ=0.8	0	0	11.88	207.67	219.55	0.9	0.991	0.001	.273	56.81	5.7	1.00	0.0010	.76	0.001	0.006	.279	0.312	0.594
-35	0.1	μ=0.8	0	0	11.86	-207.67	-195.70	-	-	0.001	0	-	-	1.00	0.0010	0	0	0	0		
											43.918				0.1785		1.141	6.843	50.764		98.853

ASSUME TOTAL TRAVERSE = 1 km

LOCOMOTION ENERGY PER WHEEL	13.471 w hr km
LOCOMOTION ENERGY PER VEHICLE	98.853 w hr km
TOTAL LOCOMOTION ENERGY + 35%	133.46 w hr km
AVERAGE VEHICLE VELOCITY	5.6 km hr

Figure 5.2.9

	MASS 2170 LBM (984 KG)	MASS 2300 LBM (1043 KG)
	TYPICAL SORTIE	MAX. PAY LOAD
ENERGY		
• MARIA	124.1 W.HR/KM	137.3 W.HR/KM
• UPLANDS	133.5 W.HR/KM	145.6 W.HR/KM
AVERAGE VELOCITY		
• MARIA	7.2 KM/HR	6.7 KM/HR
• UPLANDS	5.6 KM/HR	5.2 KM/HR

Figure 5.2.10- LSSM Energy and Average Velocity Comparison

5.3 LSSM OBSTACLE PERFORMANCE

5.3.1 General

A test program was conducted utilizing a 1/2 - scale model of the LSSM configuration to determine performance over the types of obstacles specified in Annex G of the statement-of-work. The specified obstacles and their modes of negotiation are shown in Figures 5.3.1 and 5.3.2. The cases of greatest interest are Obstacle 2 - Mode 2, which represents the simple case of crossing a crevice of any depth, and Obstacle 2 - Mode 5, which is the case of a vehicle climbing a vertical step obstacle.

The 1/2 scale LSSM was essentially the same mobility model used in the MOLAB program with appropriate dimensional modifications. Figure 5.3.3 shows the model negotiating a step obstacle. Tests were conducted early in the program before subsystem and payload mass characteristics had been clearly defined. Tests were conducted at equal wheel loading with the vertical center-of-gravity of the forward unit 35 inches above the ground line, and that of the aft unit 27 inches above. (All values given are in terms of full-size equivalents.) Loads and v.c.g.'s were simulated by mounting adjustable weights at appropriate points on the model. Although the model was equipped with suspensions, it was necessary to lock them out because they were too soft for LSSM simulation. In most cases, incorporation of a suspension would improve obstacle performance. The coefficient between the wheels and plywood obstacle course was on the order of 0.7.

Results of the tests performed under the above conditions are given below:

Obstacle 1	IN.	CM	Obstacle 2	IN.	CM
Mode 1 (height)	26	66	Mode 1 (width)	58	147
Mode 2 (height)	21	53	Mode 2 (width)	56	142
Mode 3 (height)	19	48	Mode 3 (height)	32	81
			(width)	40 - 120	101 - 304
			Mode 4 (height)	72	183
			Mode 5 (height)	51	130

Mobility Over Annex G Obstacles
(Model Test Results)

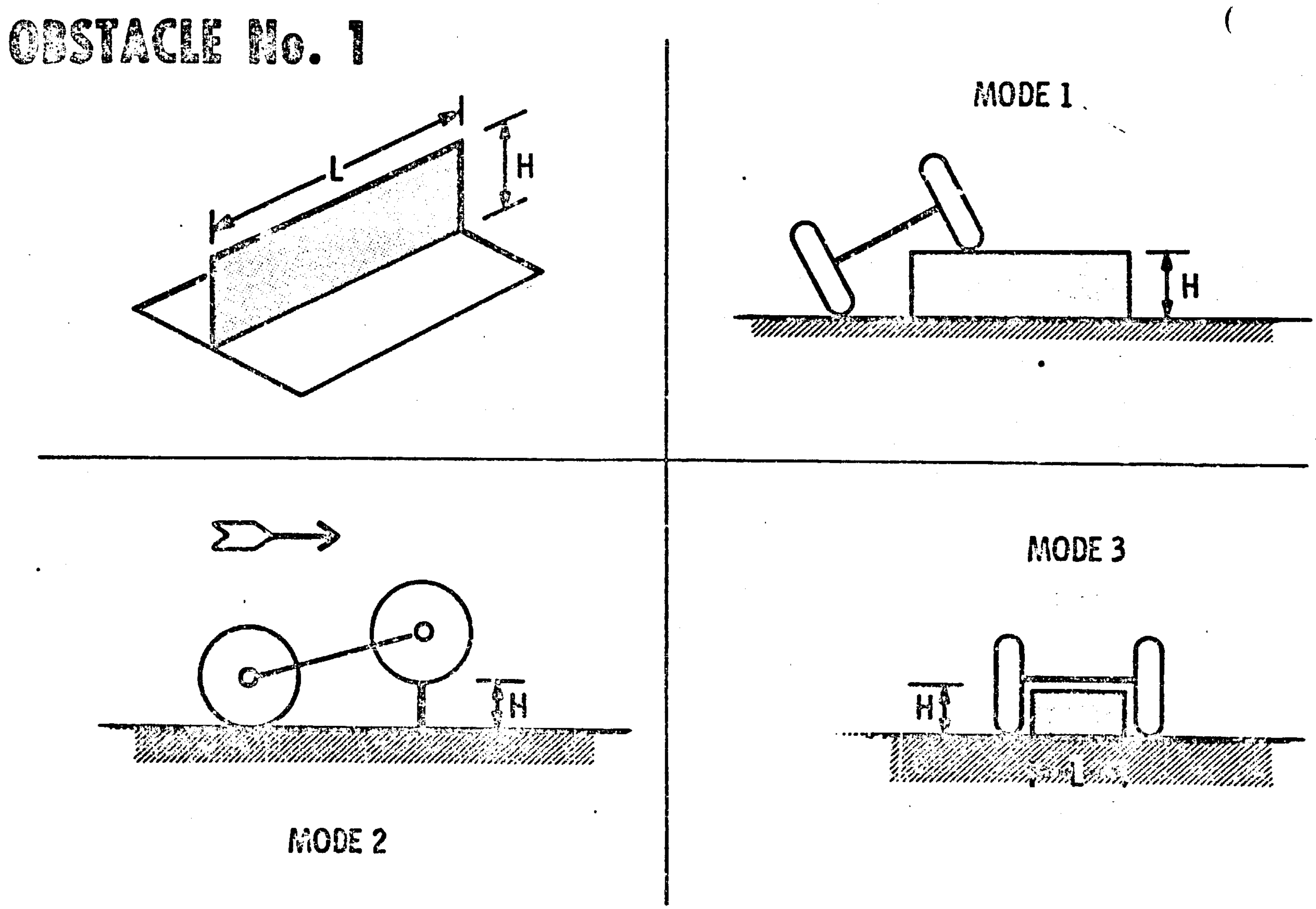

Figure 5.3.1 - Standard Obstacles and Modes of Negotiation

OBSTACLE NO. 2

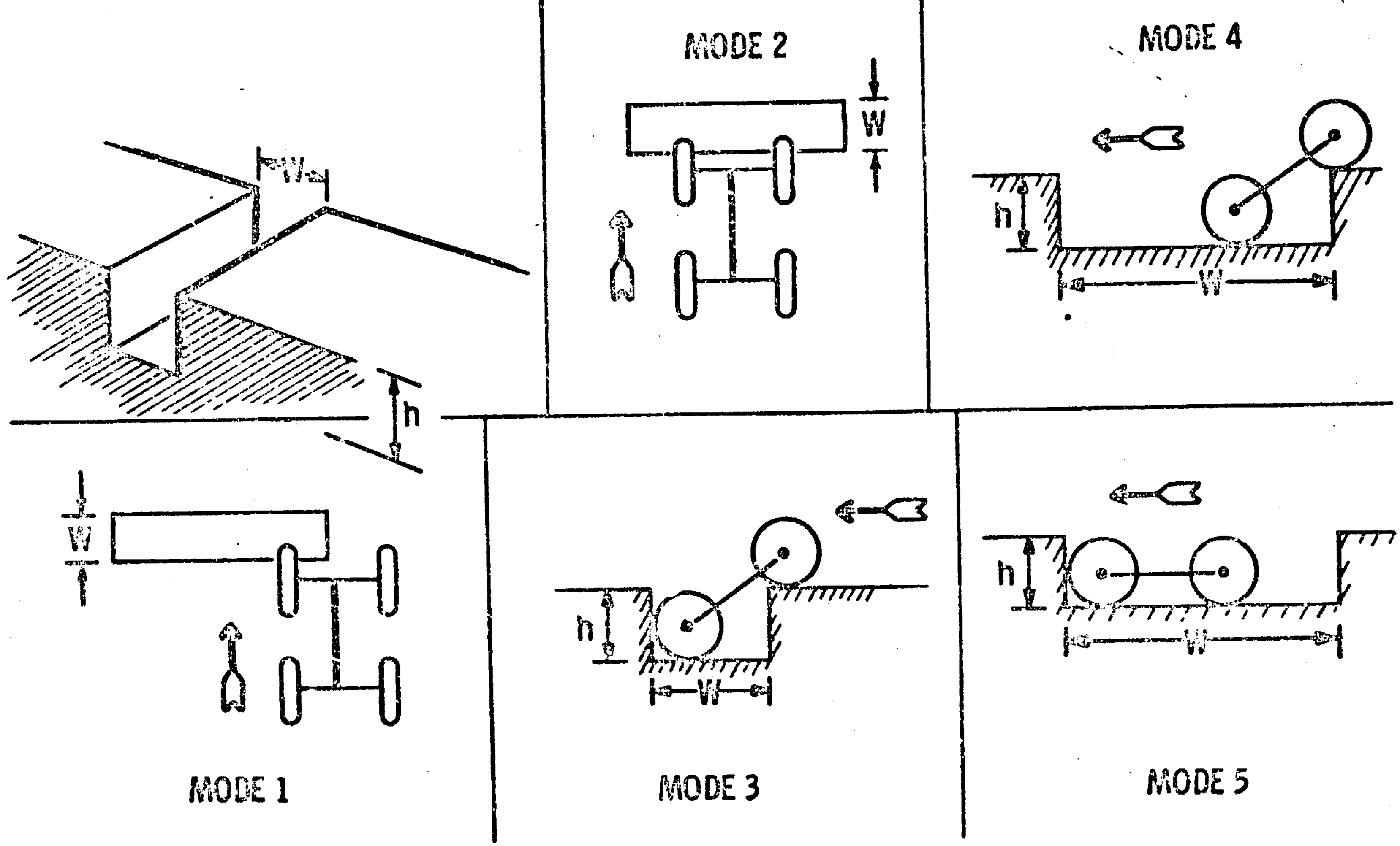

Figure 5.3.2 - Standard Obstacles and Modes of Negotiation

Figure 5.3.3- Obstacle Tests of 1/2-Scale Model LSSM

At the present time, axle loadings for baseline LSSM are estimated to be as follows: Front - 31%, Center - 37%, Rear - 32%. Extensive tests conducted and reported during the MOLAB study indicated that overloading of the center axle has negligible effect on step obstacle capability, and might even improve crevice crossing. The present estim es for the vertical centers-of-gravity are: Front unit - 34.9 inches, Aft unit - 26.4 inches. These are very slightly lower than the values used in the model tests, and the differences would have no effect on the results.

The effect of coefficient of friction on step climbing ability is illustrated in Figure 5.3.4. Note the coefficient of 0.7 permitted the LSSM to develop its fullest capability. A reduction in coefficient to a value of 0.6 would reduce the maximum step from 51 inches to about 45 inches.

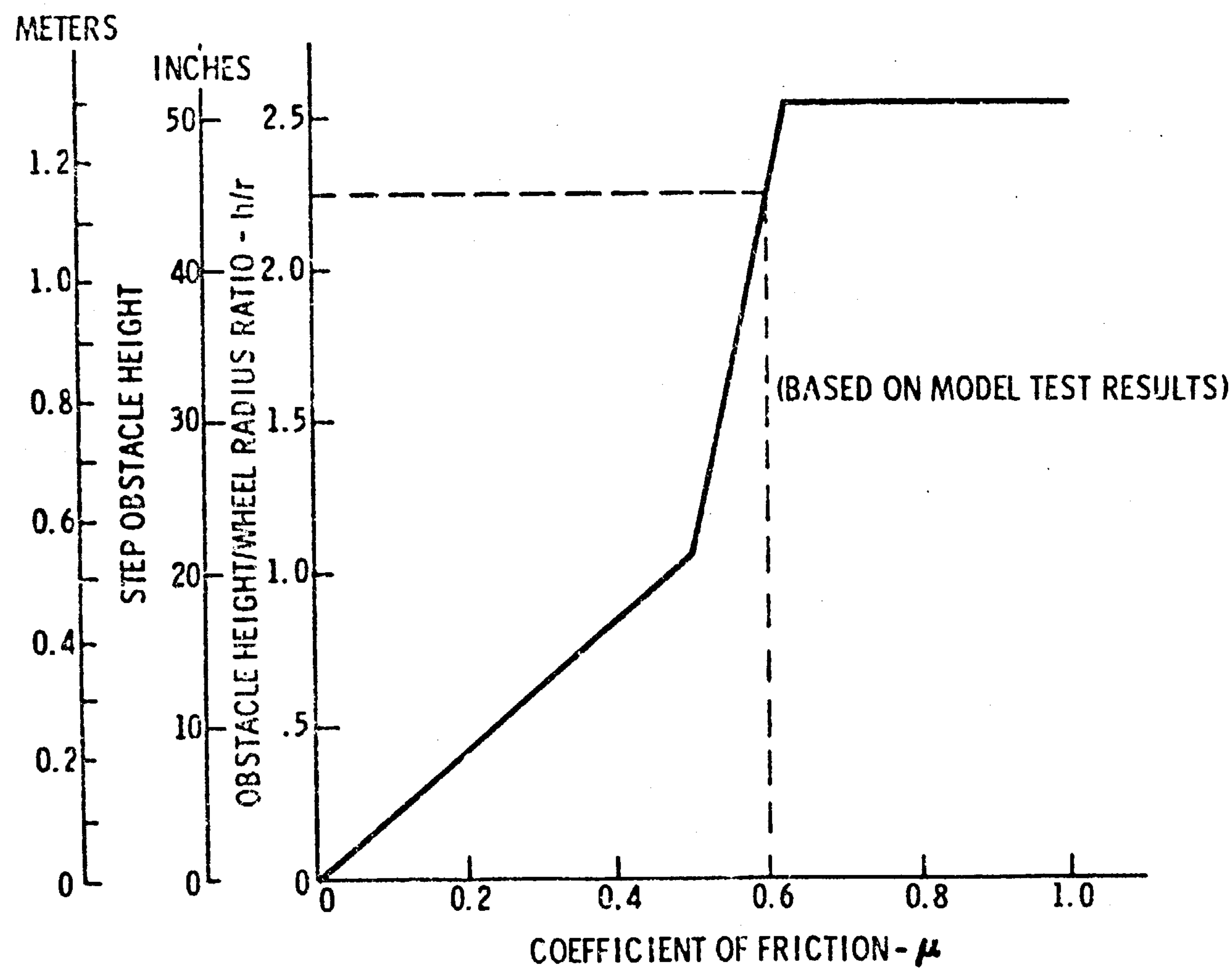

Figure 5.3.4 - LSSM Step Obstacle Climbing Capability
(Obstacle 2 Mode 5)

5.4 LSSM MANEUVERABILITY

5.4.1 Introduction

This part of the report describes studies performed on the baseline LSSM relating to maneuverability. Topics included are:

- o Steering characteristics
- o Tracking characteristics
- o Braking characteristics
- o Roll stability
- o Pitch stability

5.4.2 Steering Characteristics

The steering characteristics for LSSM were established so a common center of rotation resulted for all wheels during a turn. The geometry is illustrated in the sketch of Figure 5.4.1.

Equations relating the wheel steering angles to the physical dimensions of the LSSM were derived from the geometry, and turning radius determined for each of the four steered wheels as a function of wheel angle. The turning radius is defined as the outside (wall-to-wall) turning radius, which for this vehicle is that of the outside aft unit wheel, due to the slightly longer aft wheel base.

The minimum turning radius depends on the position of the inside aft unit wheel which has a maximum steering angle, limited by chassis and suspension geometry, of 25 degrees.

The equationfor determining the wall-to-wall turning radius is:

$$R = \frac{L_2}{\sin\alpha} + \frac{b}{2} + l' \qquad (5.29)$$

where

L_2 = aft wheel base

α = angle of aft unit outside wheel

b = wheel width

l' = distance from steering pivot to wheel centerline

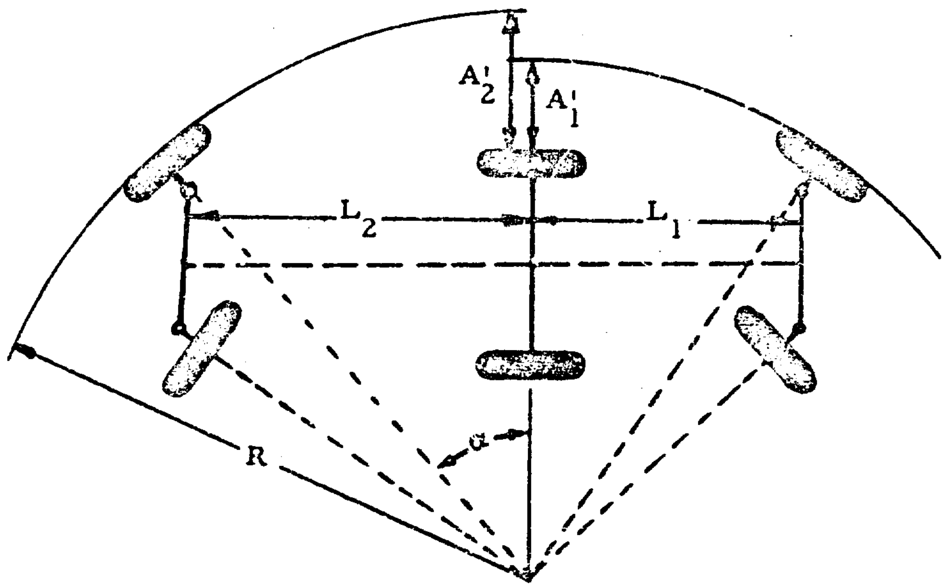

L_1 = Forward Unit Wheel Base

L_2 = Aft Unit Wheel Base

R = Wall-to-Wall Turning Radius

A'_1 = Forward-to-Center Wheel Off-Tracking

A'_2 = Aft-to-Center Wheel Off-Tracking

α = Steering Angle

Figure 5.4.1 - LSSM Steering Geometry Characteristics

The steering angles of the other steered wheels are determined from

$$\sin \alpha_i = \frac{\text{Wheelbase}}{\left[\begin{array}{l}\text{Distance from Common Steering} \\ \text{Center to Steering Pivot}\end{array}\right]} \qquad (5.30)$$

The results of this analysis are shown in Figures 5.4.2 and 5.4.3. The minimum wall-to-wall turning radius is seen to be 18.9 ft (6.1 meters). These graphs also indicate the angular relationship the steered wheels must have for synchronization at any turning radius.

5.4.3 Tracking Characteristics

Due to steering geometry, in turns a certain amount of off-tracking occurs between consecutive wheels (see Figure 5.4.1). The equation for determining the off-tracking of the outside front and rear wheels, relative to the outside center wheel, is:

$$A' = \frac{L}{\sin \alpha} \left[\left(\frac{L}{\sin \alpha} \right)^2 - L^2 \right]^{1/2}$$

where A' = off-tracking

L = distance from center wheel to wheel under consideration

α = steering angle of wheel under consideration

The tracking characteristics of the baseline LSSM are shown in Figure 5.4.4. The amount of off-tracking for the front and rear wheels is 8 and 9 inches respectively, or just under a wheel width.

5.4.4. LSSM Braking Characteristics

The braking capability of LSSM is affected by the vehicle velocity and the coefficient of friction on hard surfaces, or soil shear strength and motion resistance in soft soils. The minimum stopping distance for a vehicle on level ground, assuming constant deceleration and neglecting wheel drive mechanism resistances, is given by:

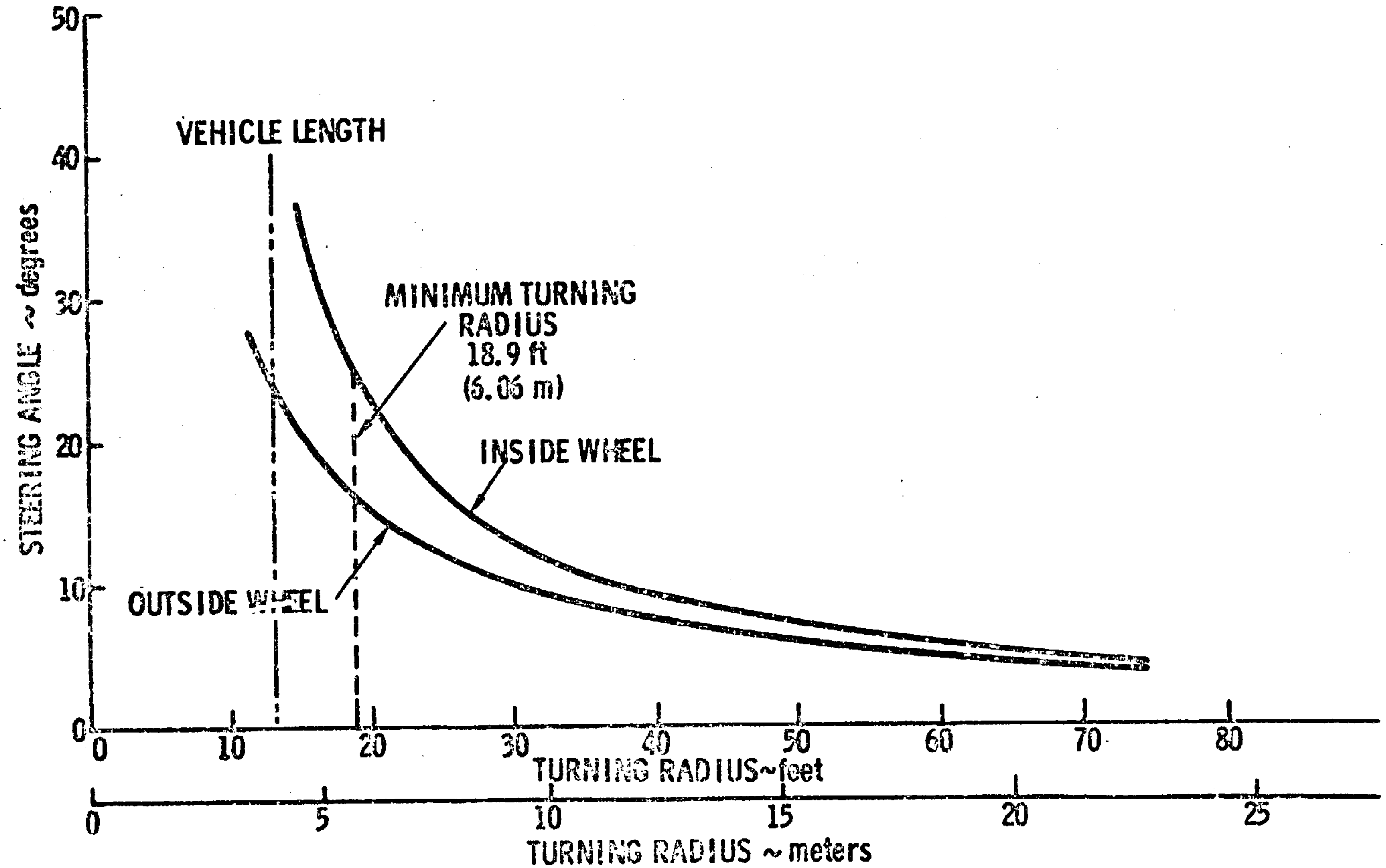

Figure 5.4.2 - LSSM Steering Angle vs Turning Radius - Rear Axle Wheels

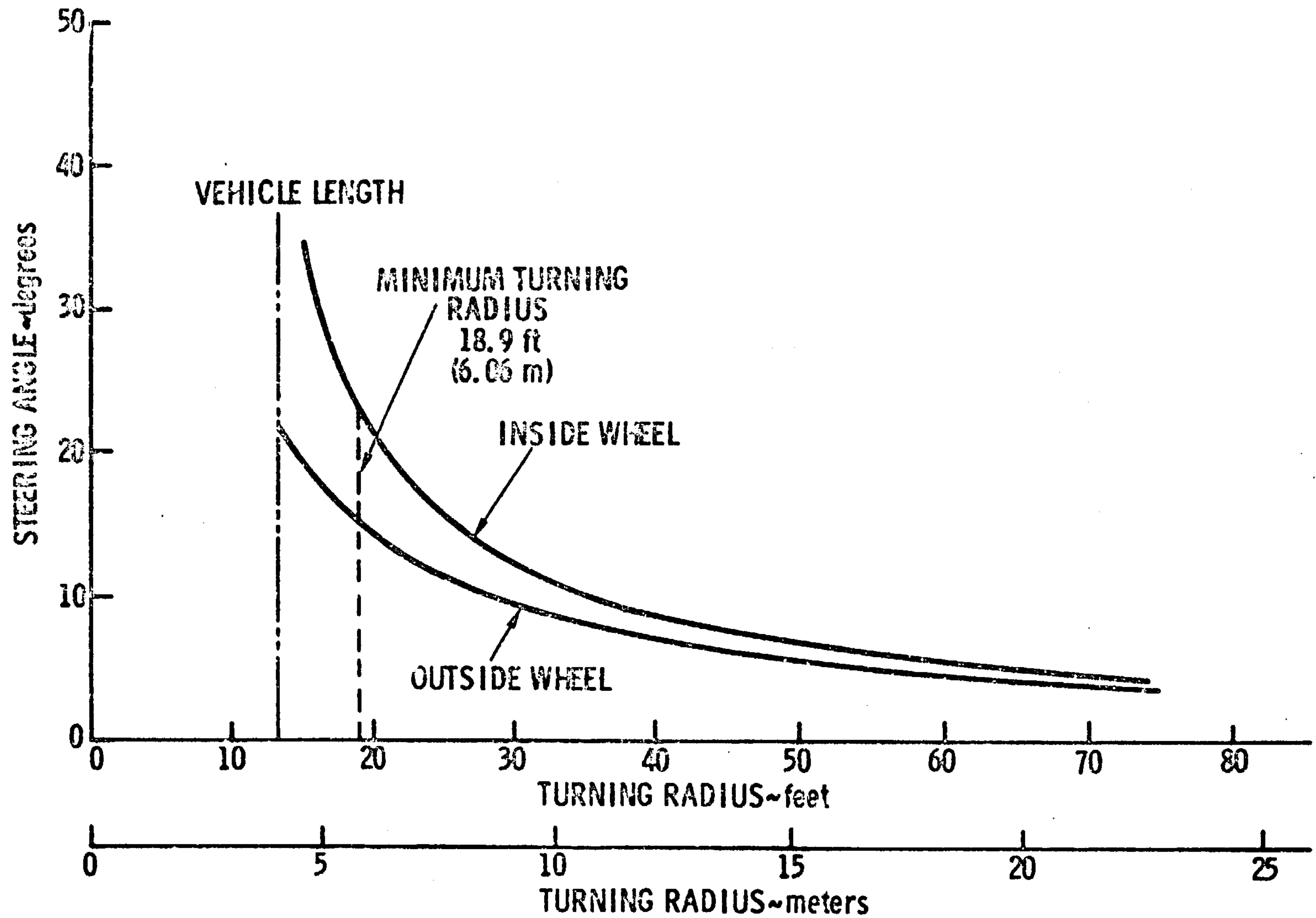

Figure 5.4.3 - LSSM Steering Angle vs Turning Radius - Front Axle Wheels

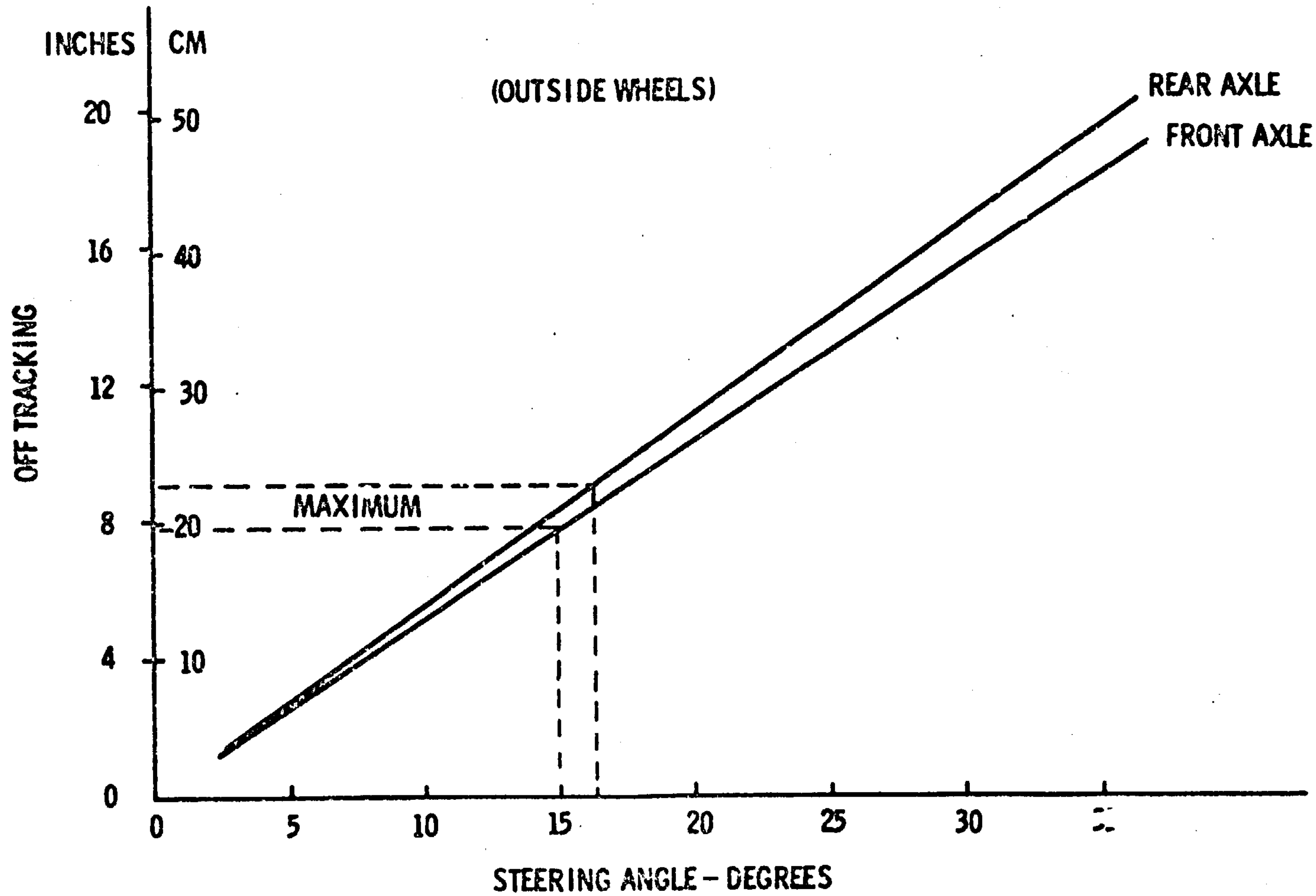

Figure 5.4.4 - LSSM Tracking Characteristics
(Double Ackermann)

$$S = \left[\frac{\gamma' m}{F + \sum R_t}\right] \left[\frac{v^2}{2}\right] \qquad (5.31)$$

where ϕ = soil angle of friction

m = vehicle mass

F = $W\tan\phi$ for soils and μW for hard surfaces

$R_t = R_c + R_b + R_r$ for soils and R_r for hard surfaces

v = vehicle velocity

γ' = inertia mass factor for rotating parts in the wheels. This was used as 1.04 for LSSM (similar to conventional vehicles).

W = vehicle "lunar weight"

μ = coefficient of friction

The braking distances for the baseline LSSM on hard surfaces was determined over a range of coefficients of friction from 0.1 to 1.0. A family of curves was generated for constant vehicle velocities of 5, 10, and 15 km/hr. These are shown in Figure 5.4.5. For a coefficient of friction of 0.6 and a speed of 15 km/hr, the required stopping distance is on the order of 27 feet.

Braking distances were also determined for the LSSM travelling at a velocity of 5 km/hr over soft soils with the following characteristics:

- o $k_\phi = 0.083$, $n = 1.0$, $\phi = 20^\circ$
- o $k_\phi = 0.5$, $n = 0.5$, $\phi = 32^\circ$
- o $k_\phi = 3.0$, $n = 1.0$, $\phi = 32^\circ$

These calculations were made for a range of slopes and the results are plotted in Figure 5.4.6. The results illustrate that stopping distances are greatest for soils where low shearing forces are developed (function of ϕ), even though the soil may be very soft as compared to the others.

Figure 5.4.7 shows an attempt to correlate braking properties of soft soils to the coefficient of friction on non-deformable surfaces. The technique used was based on the following relationship:

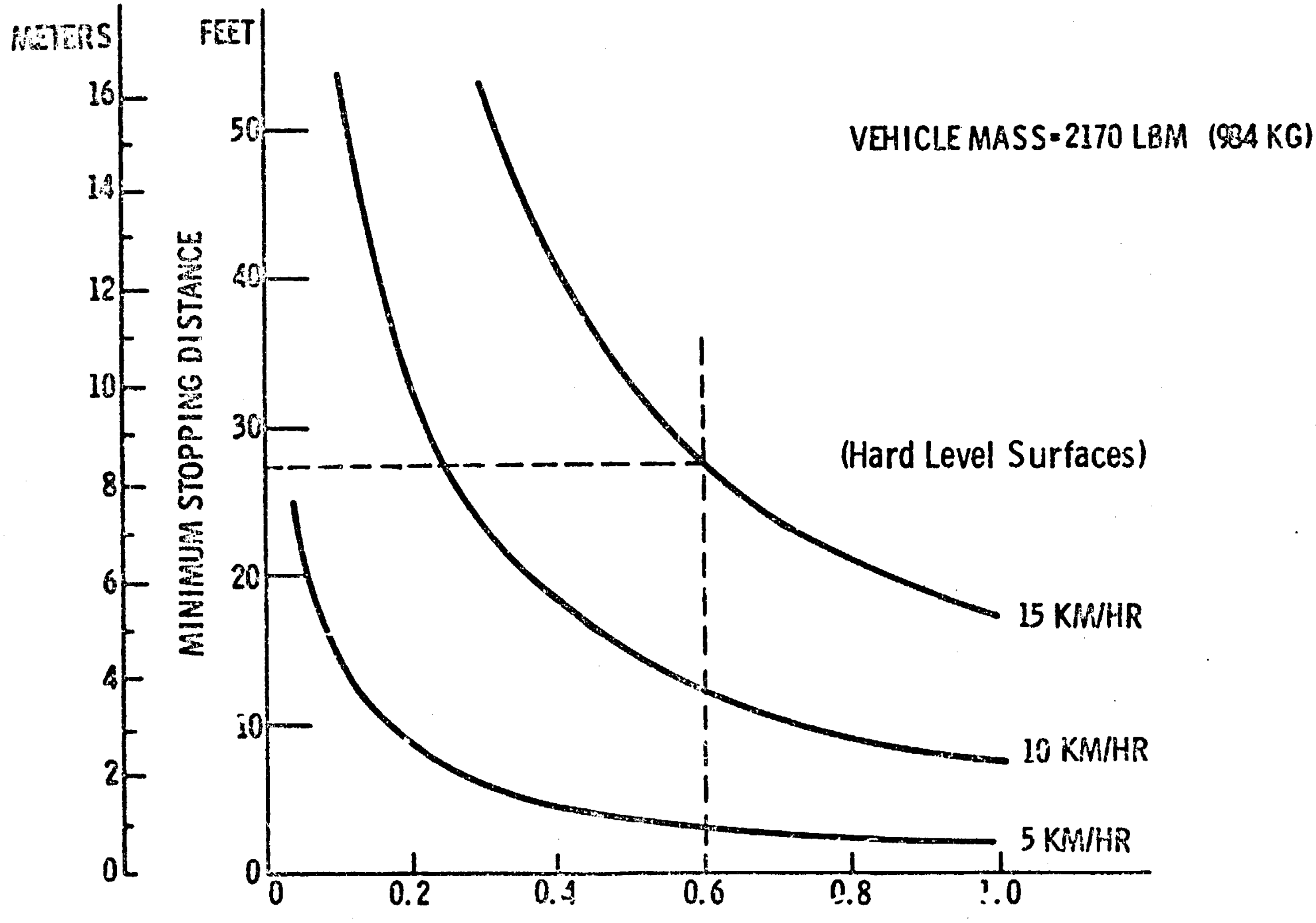

Figure 5.4.5 - LSSM Braking Characteristics

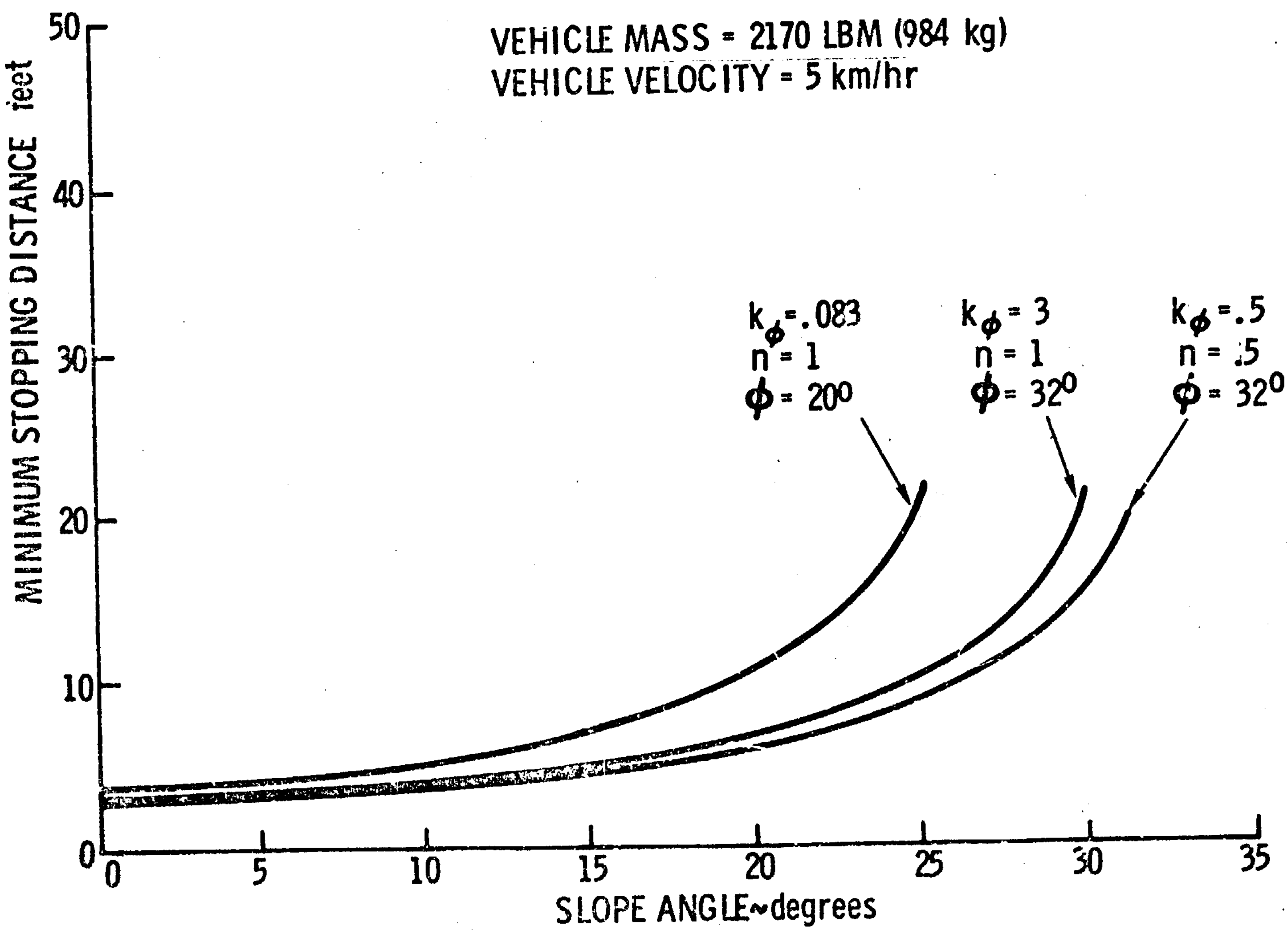

Figure 5.4.6 - LSSM Braking Characteristics - Soft Soils

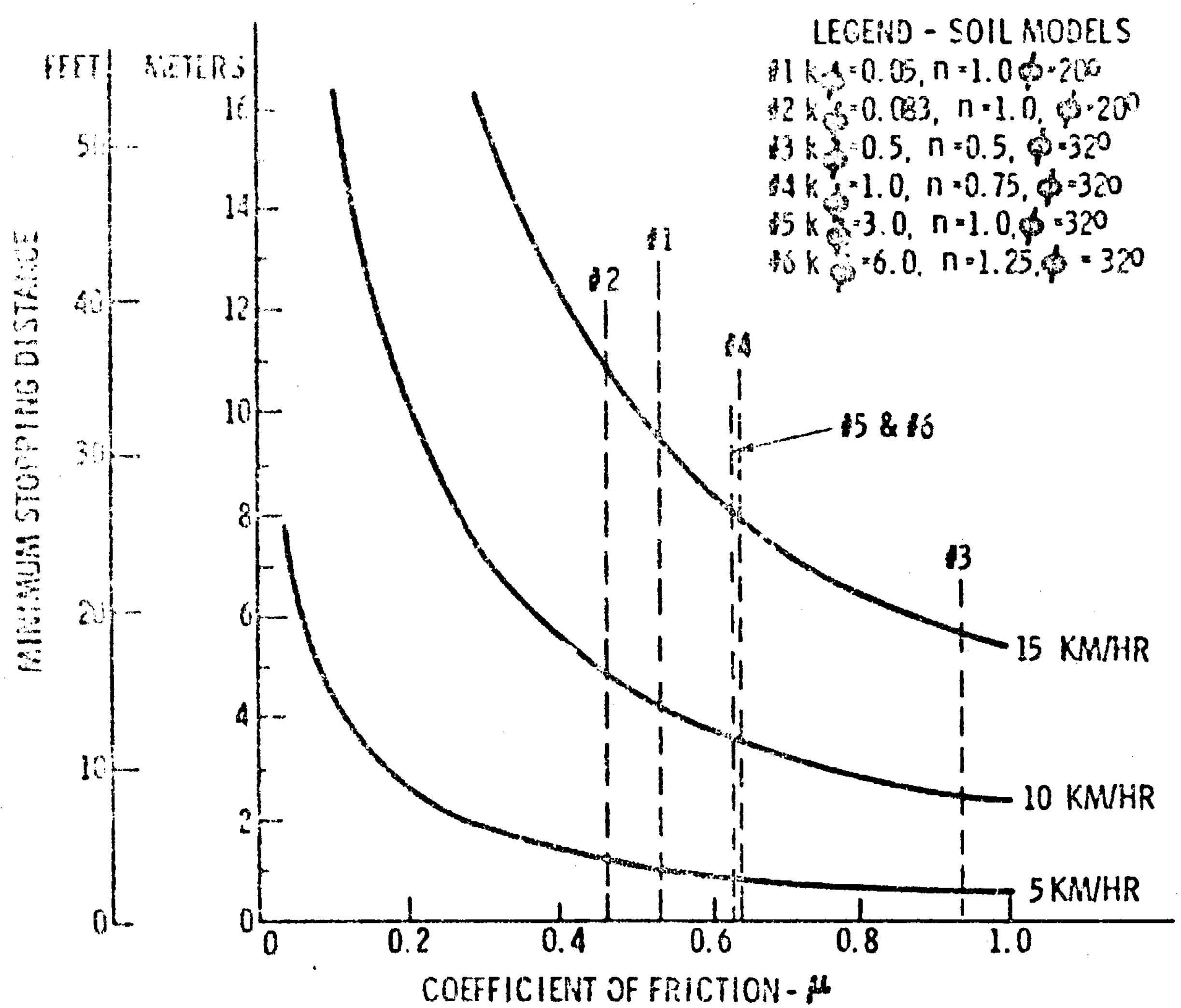

Figure 5.4.7 - LSSM Braking Characteristics
(Level Surfaces)

$$W \tan \phi + R_c + R_b + R_r = \mu W + R_r \quad \text{(from Eq. 5.31)}$$

On this basis, each soil can be said to have an "equivalent" coefficient of friction as shown.

5.4.5 Vehicle Stability

Static Stability: The static stability characteristics of the LSSM were determined as a function of slope angle and azimuth orientation. The results were plotted in polar coordinates and are presented in Figure 5.4.8. This polar plot illustrates the static stability characteristics regardless of the direction of vehicle travel. Zero degrees azimuth corresponds to the vehicle travelling straight up the slope; 180 degrees is coming down. From the results shown, the following can be seen.

- For coefficients of friction less than 1.0, the LSSM will always slide rather than overturn.
- Up to an angle of approach to the slope (azimuth) of 32 degrees, the LSSM will tend to overturn in pitch rather than in roll.
- The minimum slope angle at which the vehicle will roll over is 52°.
- The minimum slope angle at which the vehicle will overturn in pitch is 62°.

Roll Stability in Turns: In the lunar environment, the lateral stability of a vehicle is seriously effected when maneuvering, because the overturning forces due to lateral accelerations at the center of gravity are the same as on earth, while the restoring forces dependent upon vehicle weight are reduced to a 1/6-th factor. This problem becomes even more severe when turns are negotiated on straight continuous side slopes. Therefore, the problem of LSSM lateral (or roll) stability was investigated for side slope operation. Equations of equilibrium were set-up for the case of the vehicle overturning about the ground contact points of the wheels, and the limiting velocity determined as a function of vehicle turning radius and slope. The equation for this case is:

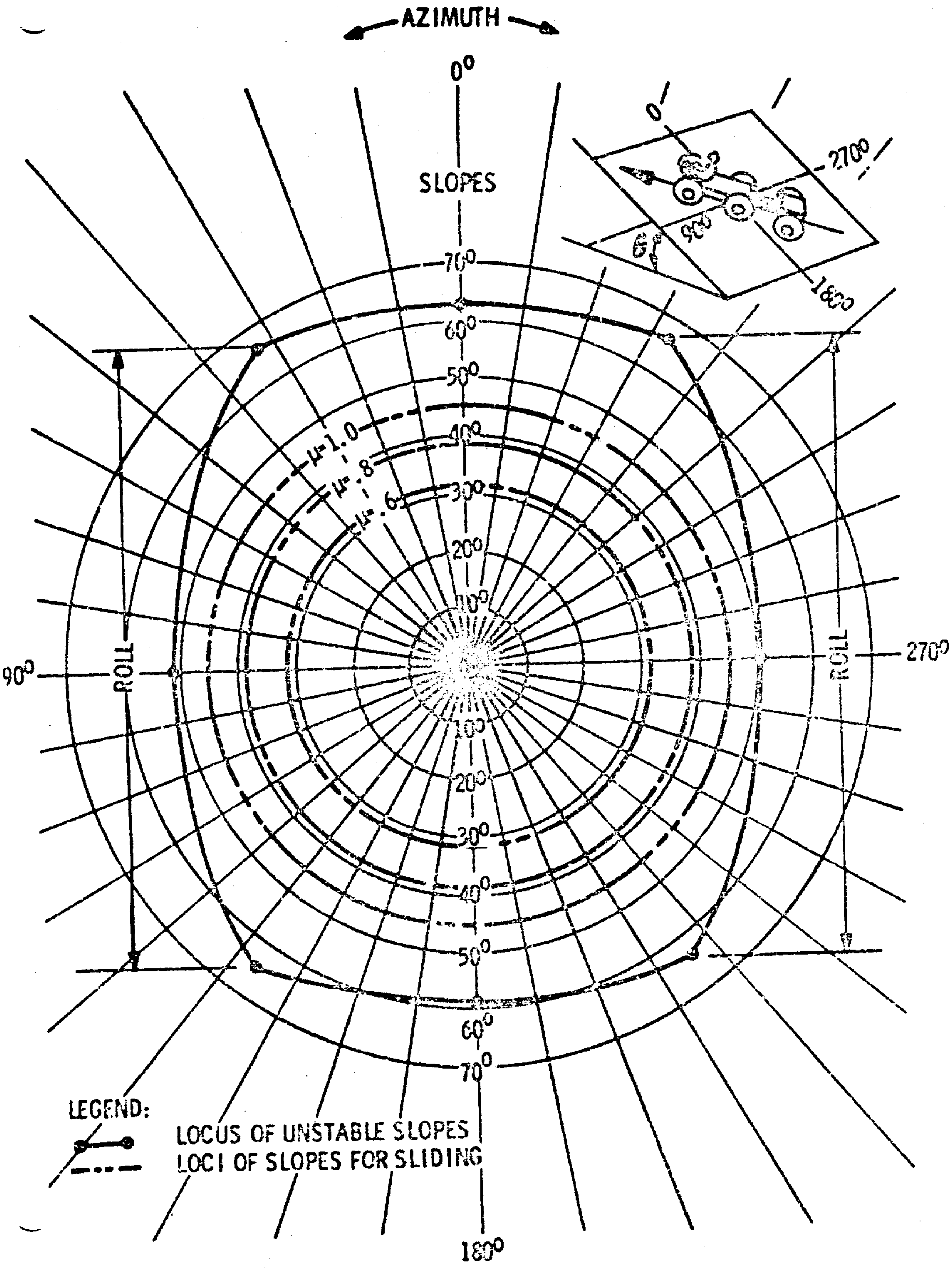

Figure 5.4.8 - Vehicle Static Slope Stability as a Function of Azimuth Orientation (Polar Plot)

$$v = \left[g\,R'\left(\frac{t}{h} \cos\theta + \sin\theta \right) \right]^{1/2} \tag{5.32}$$

where v = limiting velocity

g = lunar gravity

R' = vehicle turning radius measured at the c.g.

t = lateral distance from wheel contact to c.g.

h = height of c.g. above ground

θ = slope angle

Overturning will occur only if the friction of coefficient at the wheels is large enough to prevent sliding. Sliding takes place if the lateral acceleration forces developed during a turn are greater than the friction forces. The equation of equilibrium for sliding is as follows:

$$v = \left[g\,R'\left(\mu \cos\theta + \sin\theta \right) \right]^{1/2} \tag{5.33}$$

where μ is the coefficient of friction and the other terms are as in Equation (5.32).

The results obtained are summarized in Figures 5.4.9 and 5.4.10. Figure 5.4.9 shows that even for a coefficient of 1.0, sliding always occurs before the vehicle can become unstable. Calculations show that the coefficient of friction would have to be on the order of 1.3 before instability can take place. (These results assume a smooth surface, and do not take the presence of obstacles into account). Figure 5.4.10 shows the turning radius at which sliding takes place as a function of friction coefficient and slope angle. Calculations were for the case of a vehicle travelling at a velocity of 5 km/hr and turning up - slope. For the down - slope case, results would be much more conservative.

Pitch Stability: With respect to pitch stability, overturning moments are produced by tractive or braking forces resulting from accelerating or decelerating the vehicle. The worst cases are for operation on slopes, in which case the limiting accelerations can be expressed by:

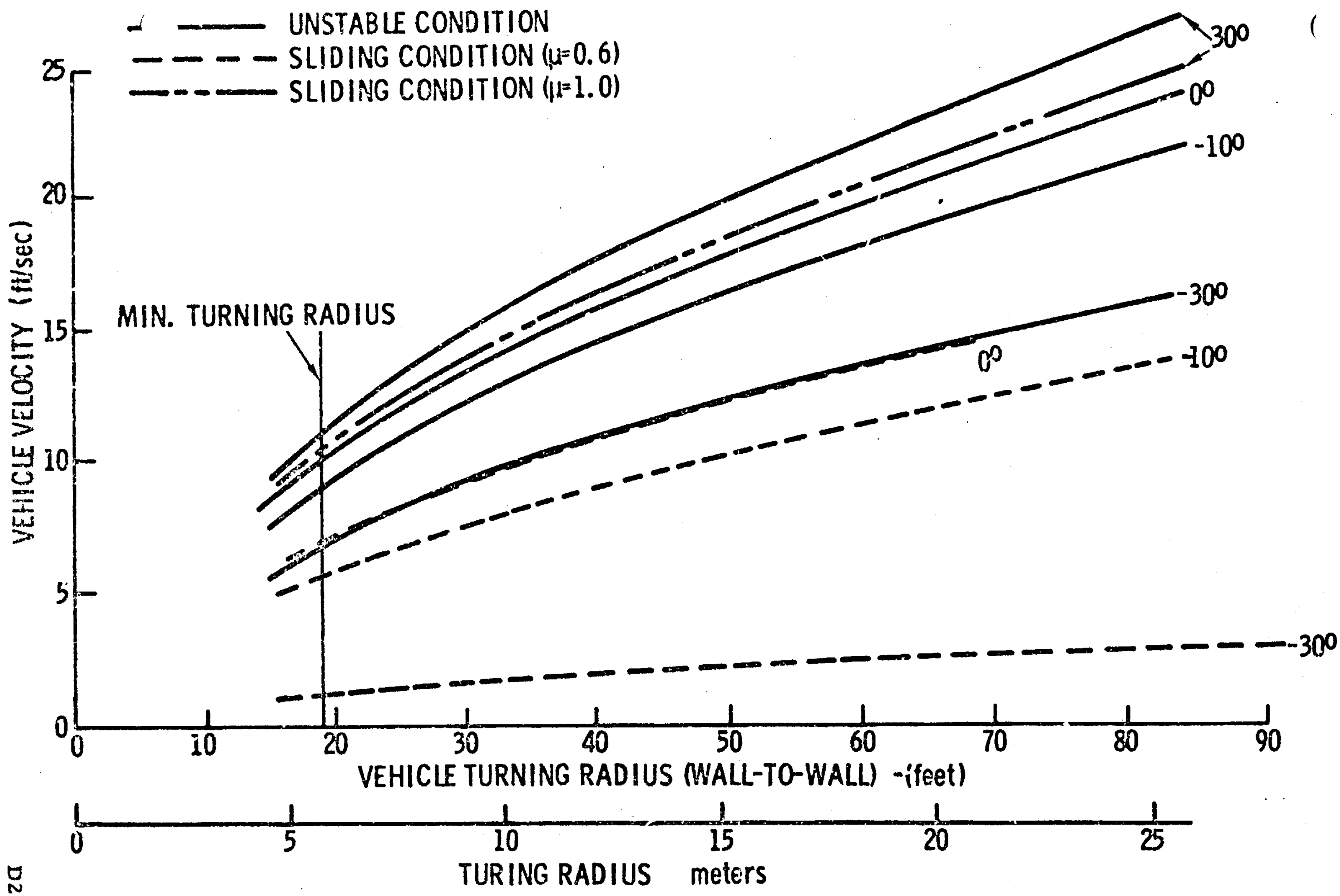

Figure 5.4.9 - LSSM Roll Stability Characteristics

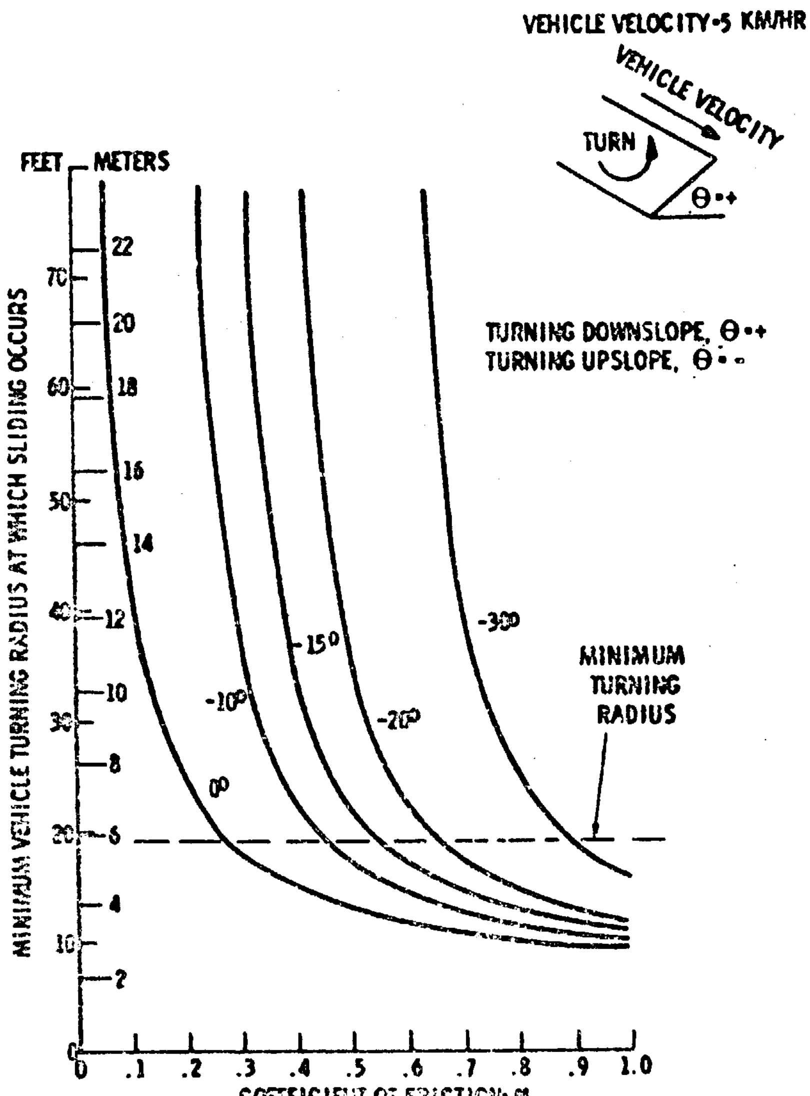

Figure 5.4.10- LSSM Lateral Sliding Characteristics (Continous Slopes)

$$a = g\left[\frac{x}{h}\cos\theta - \sin\theta\right] \quad (5.34)$$

where x = the longitudinal distance from the front axle of the vehicle to the center-of-gravity. This equation applies equally for accelerating up or decelerating (braking) down the slope. Figure 5.4.11 illustrates that, as in the case for roll stability, the LSSM will always slide rather than overturn unless the coefficient of friction is significantly greater than 1.0. It can also be seen from this graph that at zero acceleration, the vehicle becomes unstable only if the slope angle exceeds 62 degrees.

Limiting accelerations at which sliding takes place can be determined from:

$$a = g\left[\mu\cos\theta - \sin\theta\right] \quad (5.35)$$

The results of this calculation are given in Figure 5.4.12 as a function of coefficient of friction.

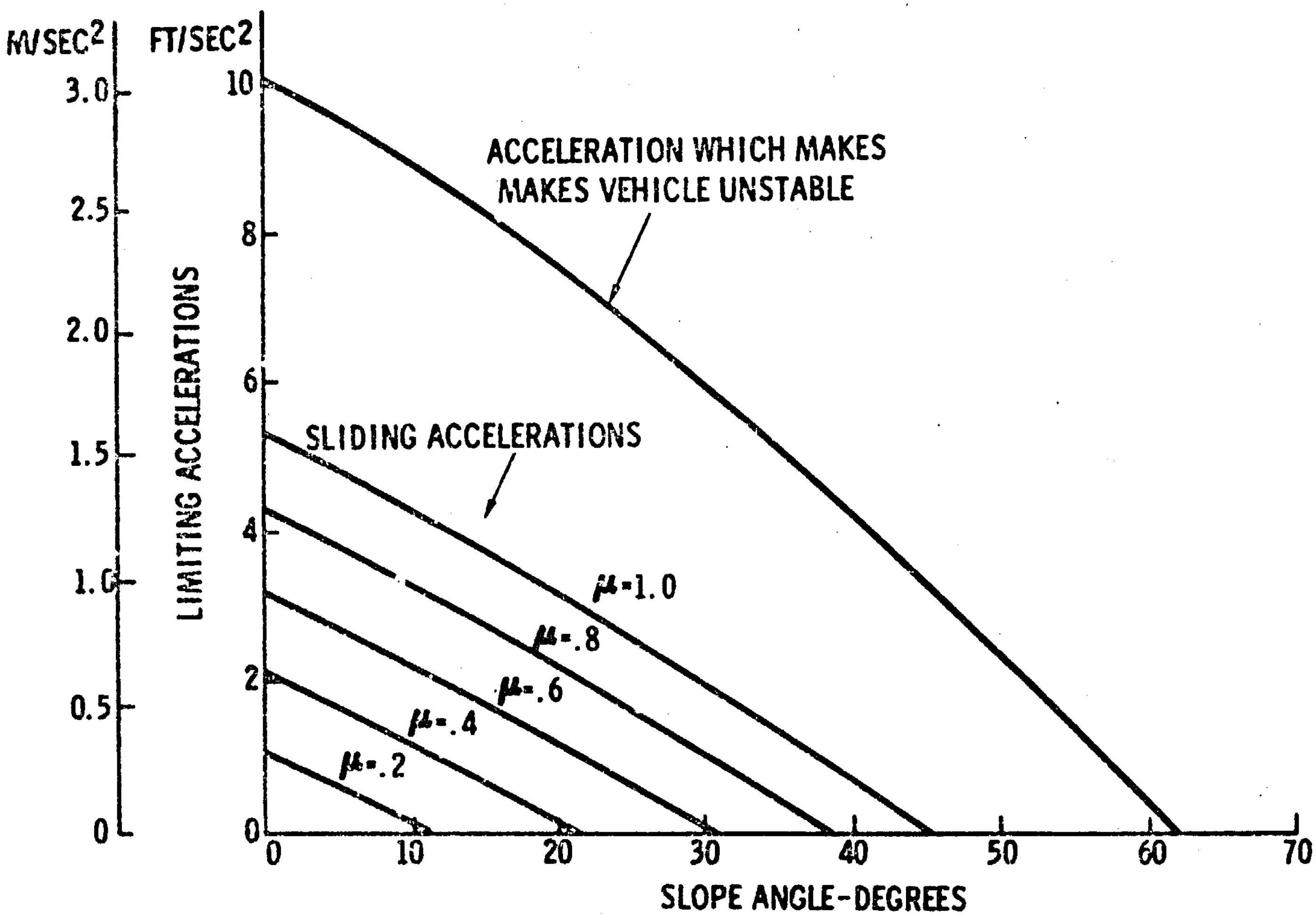

Figure 5.4.11 - LSSM Pitch Stability Characteristics

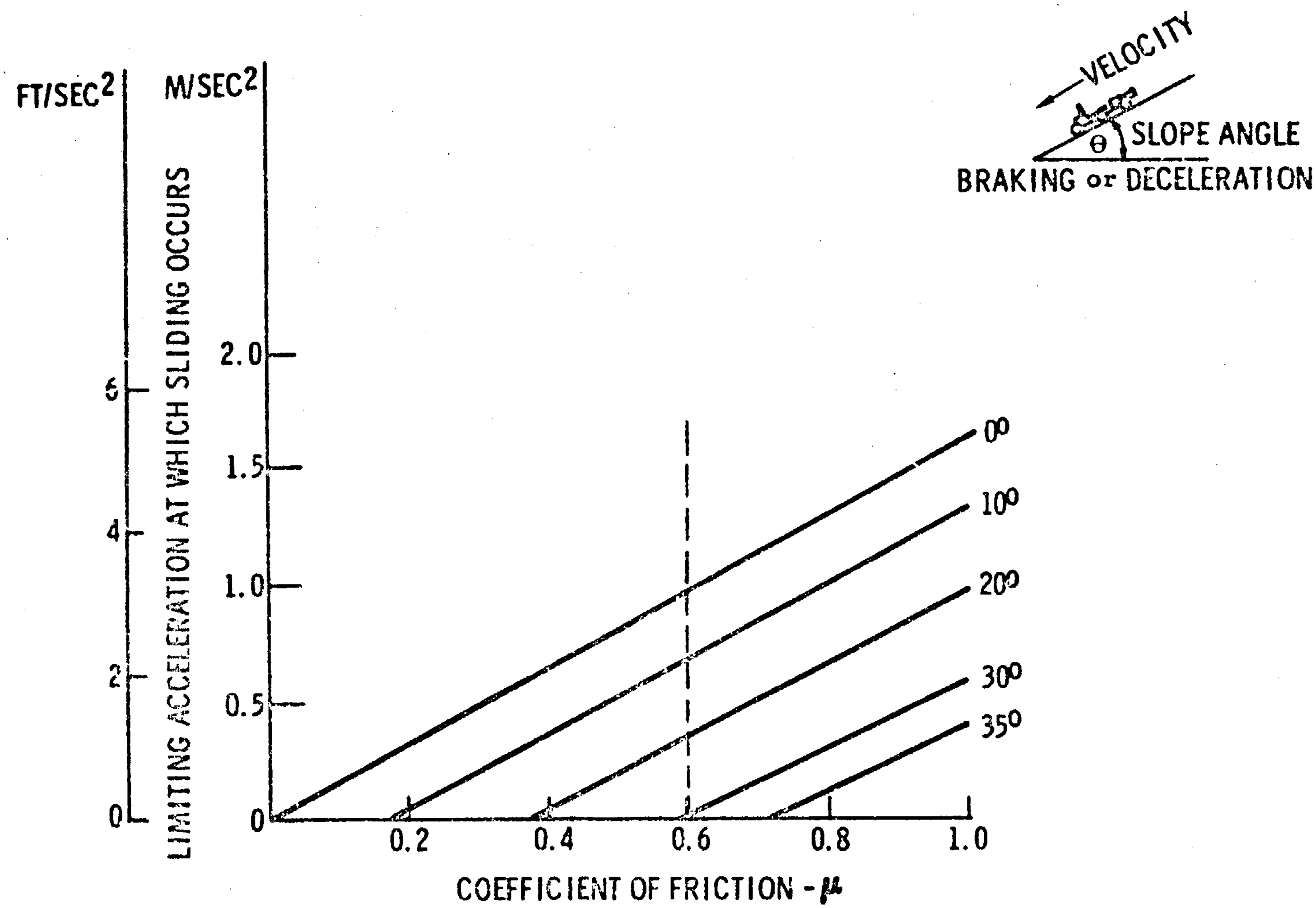

Figure 5.4.12 - LSSM Pitch Stability Characteristics

5.5 DYNAMIC PERFORMANCE ANALYSIS

5.5.1 Introduction

The objective of this study was to determine the steady-state and the transient responses of a 6 x 6 semi-flexible frame vehicle traveling with linear, constant speed over hard ground. Four aspects were of particular interest:

- o Optimization of steady-state performance by varying the damping and spring rates of the wheel suspensions.
- o Determining the influence of vehicle speed and terrain roughness on steady-state performance of the optimized vehicle.
- o Compare the steady-state ride performance of the vehicle with optimized flexible wheels (with and without suspensions) with one equipped with rigid wheels.
- o Evaluate the transient response and stability of the vehicle when hitting a 'bump'.

To this end, equations of motion of all forces and moments were programmed on a PACE 231-R analog computer and the outputs evaluated as a function of terrain and vehicle velocity inputs.

5.5.2 The Vehicle

The elements of the vehicle are considered to consist of two rigid compartments connected by a massless, continuous elastic beam, and a pitch limiter. The forward unit is support by four wheels (two axles) and the aft unit by two wheels (one axle). Figure 5.5.1 is a line diagram illustrating the possible motions of the vehicle elements. It contains six wheel masses and two compartment masses. To describe the motion of the masses, a datum plane and a coordinate system are defined. A "normal" axis is one proceeding along a line normal to the datum plane; a "forward" or "roll" axis is identical with a linear movement of the vehicle parallel to the datum plane, and a "side" or "pitch" axis is orthogonal to the vertical and forward axes. The rectangular system of normal, forward, and side axes are connected to the moving vehicle. Because the vehicle moves linearly with constant speed, one can visualize the vehicle and the coordinate system as standing still and the ground moving with constant speed underneath the vehicle.

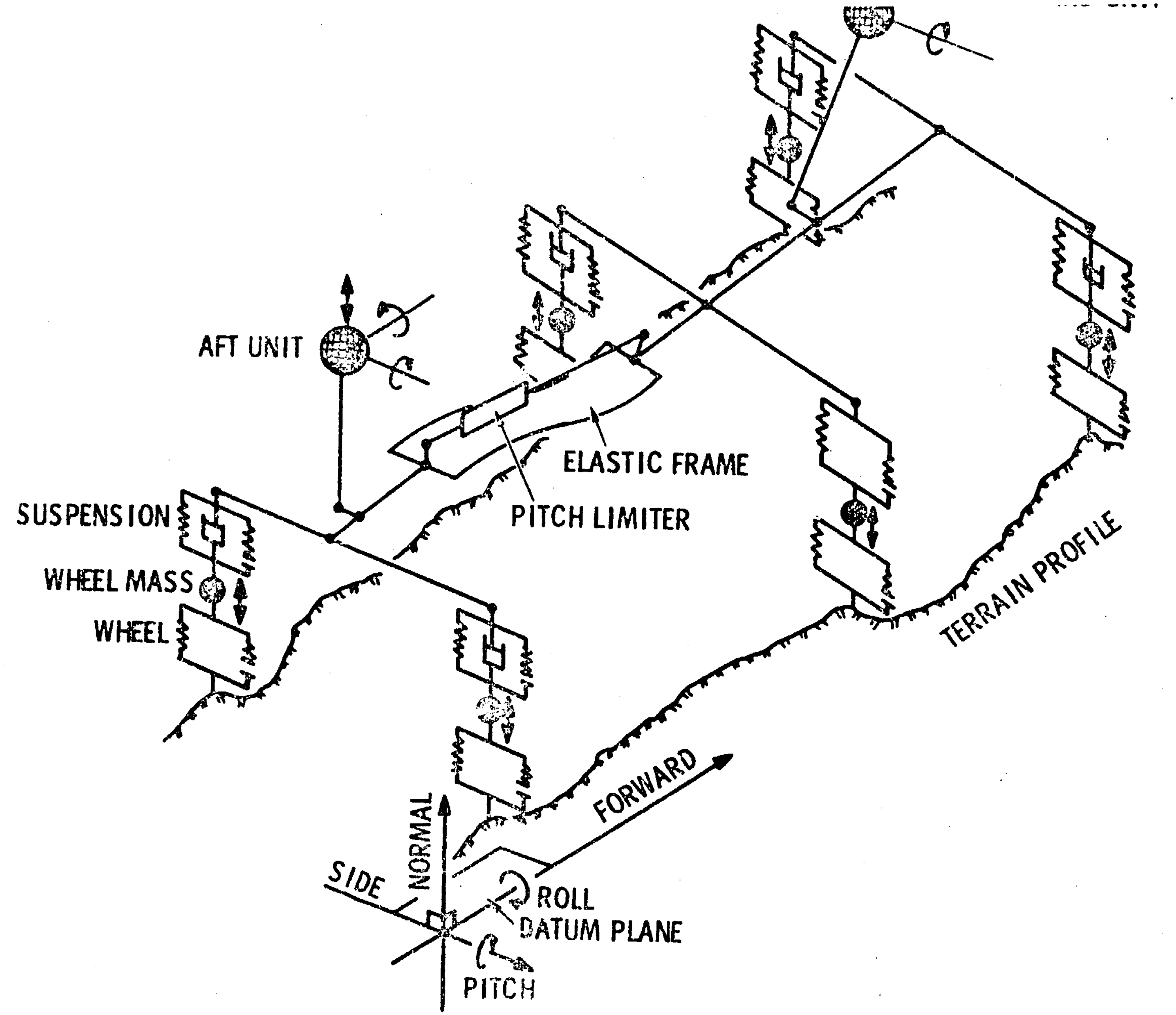

Figure 5.5.1 - Definition of Vehicle Motions

The movements of the masses are as follows: The six wheel masses move forward with constant speed and are allowed to accelerate only vertically. The two compartment masses can accelerate vertically, and also pitch and roll. Therefore, there are a total of 12 degrees of freedom for the vehicle.

Three wheel - suspension combinations were investigated:

1. Flexible Wheel with Suspension

This model consists of:

- A spring symbolizing the elastic properties of the wheel. The spring is allowed to bottom, at which time a second, very stiff spring is engaged. The spring can also lose contact with the ground. The wheels are point follower.
- A wheel mass.
- A suspension consisting of a bottoming spring and a linear viscous damper.

2. Flexible Wheel without Suspension

With the removal of the suspensions, the "mathematical model" vehicle would lack a source of energy dissipation and the dynamics of the undamped model vehicle would probably not reflect the dynamics of the real vehicle, where in addition to the suspension damping numerous other sources of energy dissipation exist, for instance, at the interface of wheel and soil, in the tires, in the elastic frame, and chassis. To restore the damping capability of the unsuspended vehicle, an arbitrary damping rate was assigned to the wheels. A damping rate of 2 lb-sec/in. was chosen for this study. (For comparison, a pneumatic tire of about half the size of the LSSM wheel has a damping rate of about 20 lb-sec/in).

3. Rigid Wheel with Suspension

This model is composed of a wheel mass and a suspension system similar to that for the flexible wheel.

Analog models of the three wheel-suspension combinations are illustrated in

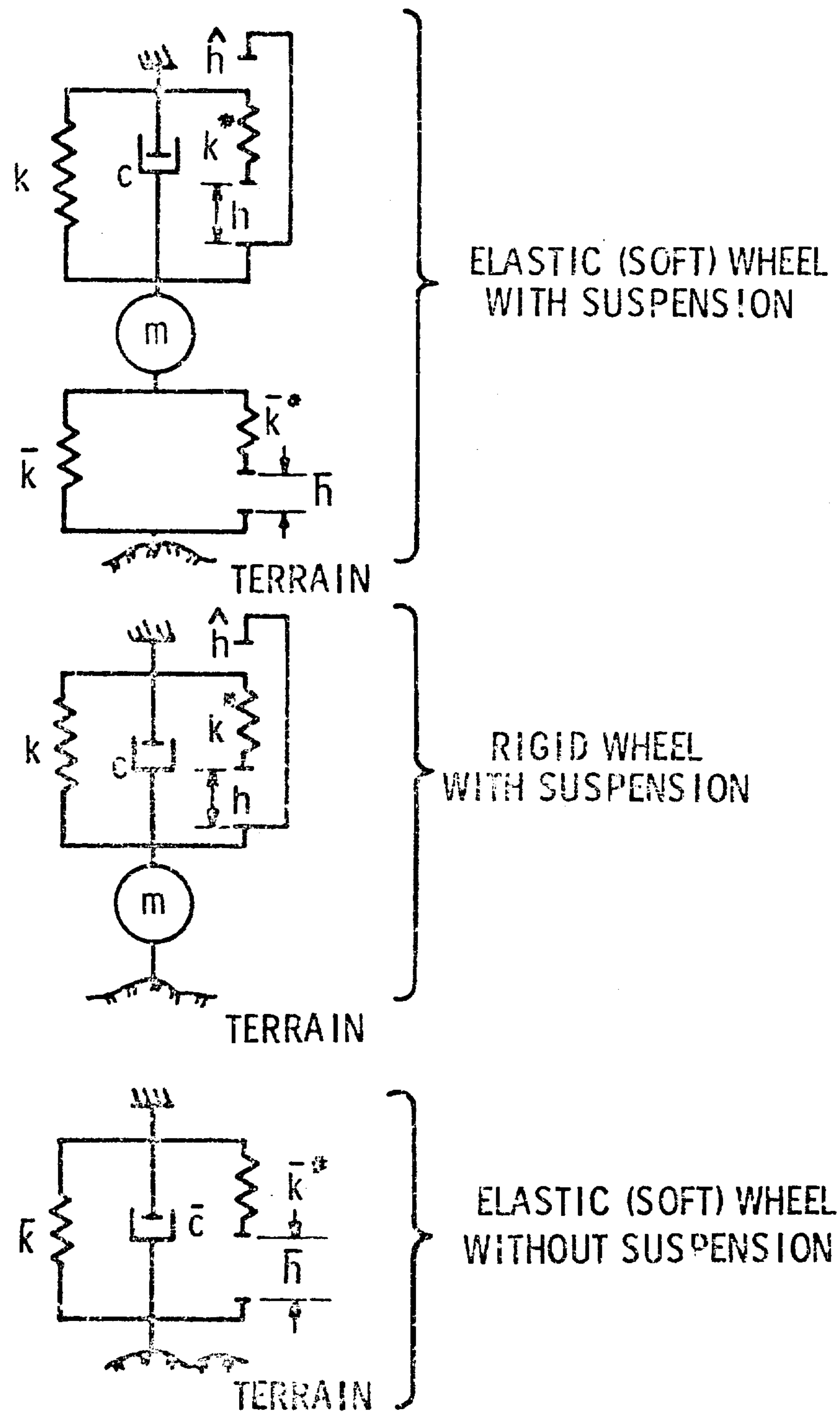

Figure 5.5.2- Line Diagrams of Three Wheel Types

Figure 5.5.2. The wheels are point followers and are able to lose contact with the ground.

5.5.3 The Terrain

Three types of terrain models were considered necessary to cover roughnesses ranging from relatively smooth, undulating hills to small, sharp 'bumps'; a "random" terrain, a terrain with small, periodic obstacles, and a terrain with a single obstacle.

The random terrain consists of elevation variations which are stable over relatively large distance. They do not contain obstacles such as large rocks, abrupt holes, etc. Furthermore, superimposed slowly varying elevations such as rolling hills were not considered. The roughness of the random terrain can be described quantitatively in terms of its power spectral density (PSD). Figure 5.5.3 presents the power spectral densities of the terrains used in this study. The ordinate has units of ft^3/cycle and the abscissa, spatial frequency, has units of cycle/ft. The area under a PSD-curve represents the mean square of the terrain roughness. The curves exhibit essentially similar characteristic features.

The curve with an RMS value of 1.0 ft. follows closely the curve describing lunar terrain as interpreted from Ranger VII photograph P979. For comparison, curves of an extremely rough terrain (Bonito Lava Flow, Arizona) and of very smooth terrains (Grass Runway and Concrete Taxiway) are also plotted. An additional terrain was derived from the 1.0 ft. terrain simply by shifting the PSD-curve downward until an RMS value of 0.5 ft. was obtained.

In this study the two terrain profiles underneath the left and the right side of the vehicle are completely uncorrelated although they exhibit the same statistical properties and follow the same PSD-curve. In reality there could be a correlation between the terrain tracks depending on the auto-correlation function of the terrain and the distance between the wheels. The extent of track correlation has yet to be investigated and, therefore, is not taken into account in this study.

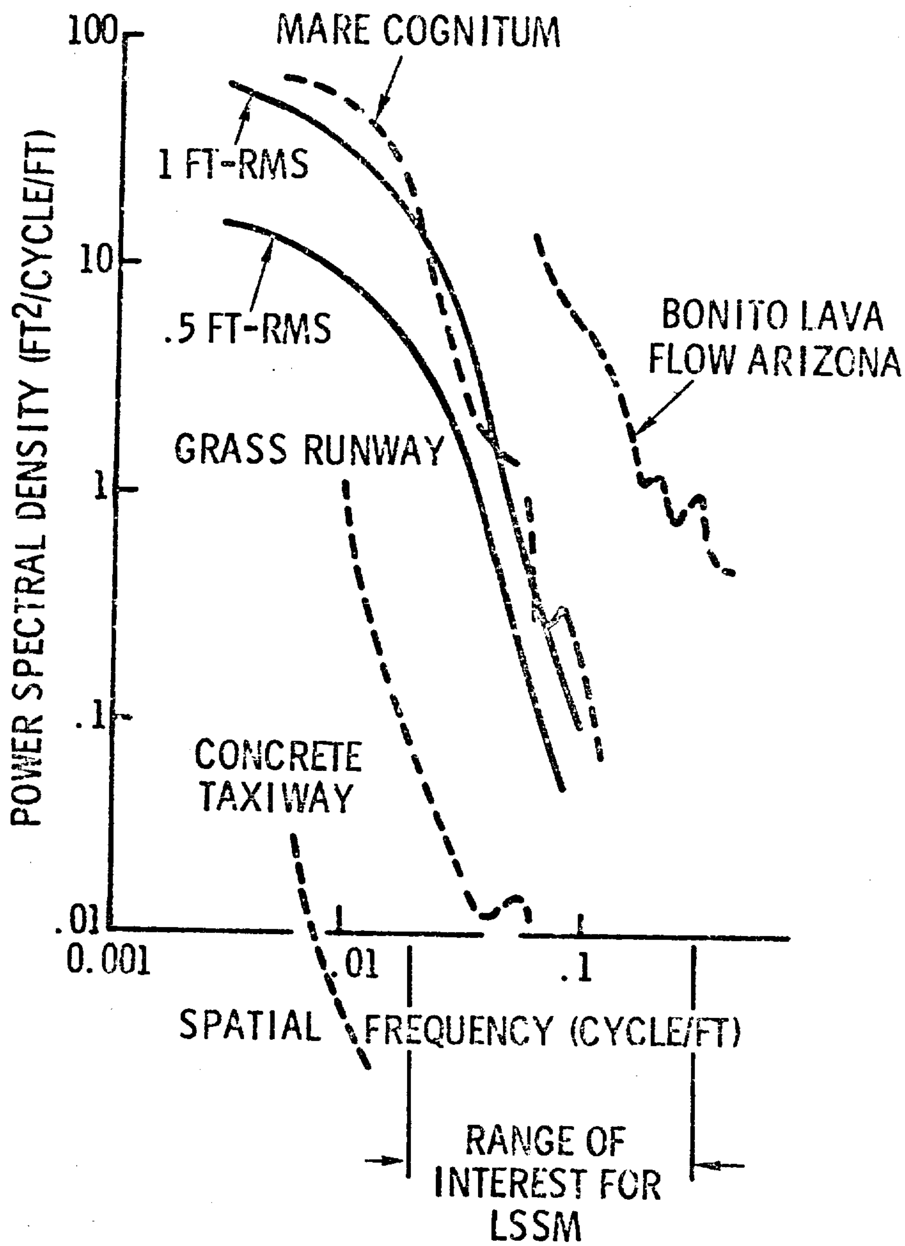

Figure 5.5.3- PSD Curves of Random Terrains

The wavelength range and spectral levels of interest to the designer of a lunar vehicle are dependent upon the natural frequency, the velocity, and the size of the vehicle he is considering. Using a summary of all existing lunar vehicle designs, a rough estimate yields a natural vehicle frequency of about 1 cps. Consequently, frequencies below 0.3 cps scarcely affect the dynamic performance of these vehicles. Lunar vehicles are likely to travel at speeds below 10 mph. Therefore, the minimum spatial frequency of interest is (0.3) (3600/10) (5280) = 0.02 cycles/ft. Accordingly, the spatial frequency range below 0.02 cycles/ft. does not affect lunar vehicle dynamics. This range can be pictured as gently rolling terrain.

An upper limit of the frequency range of interest is found by considering the power of terrain wavelengths smaller than the footprint of the wheel. Vehicle footprint lengths range between 1 ft. and 3 ft., depending on the wheel diameter, the soil condition, and the wheel load. Therefore, spatial frequencies larger than 0.3 to 1 cycle/ft. will be felt by the wheel only if the associated amplitudes are large enough to cause multiple contact within the footprint. Evidently, a terrain of the Mare Cognitum type yields very little power at frequencies higher than 0.3 cycles/ft. Therefore, terrain perturbations having wavelengths smaller than the footprint length apparently will not indent the wheel significantly.

Because the random terrains exhibit frequencies of significant power only in the low frequency range, a second type of terrain with increasingly higher power in the high-frequency range was added (a frequency analysis of this terrain was not performed). The upper sketch in figure 5.5.4 shows the profile of this terrain. It consists of triangular obstacles, equally distributed, with a height that is small compared to the wheel diameter (2 in; 1 in; 0.5 in.). In this phase of the study, the obstacles were assumed to be contacting the two wheels of one axle simultaneously. Consequently, only ch and vertical bounce of the vehicle was investigated on this terrain.

A third type of terrain consisted of a single bump on a tilted plane. This terrain permitted the study of transient motions and of the stability of the vehicle when

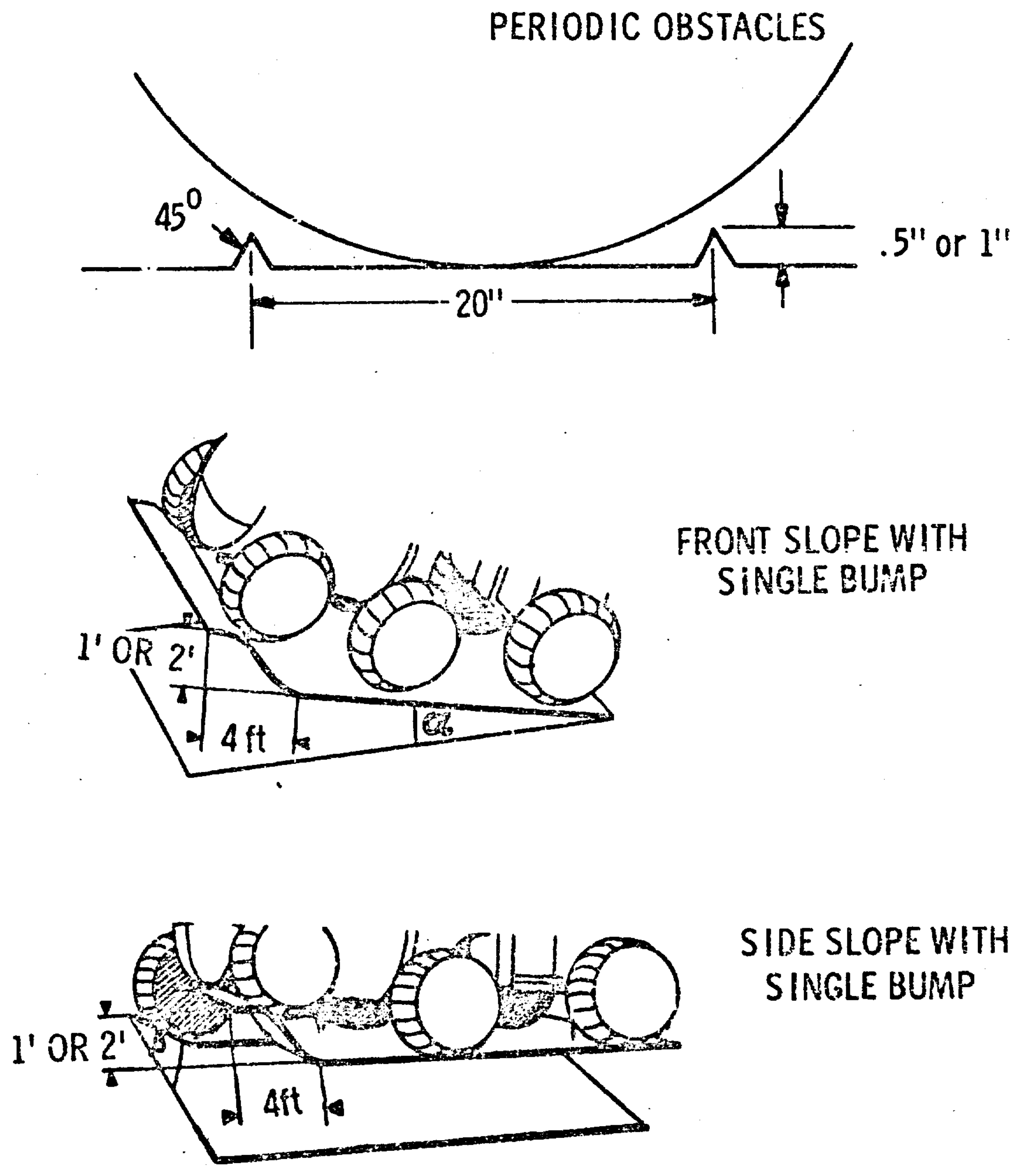

Figure 5.5.4- Obstacle Terraine

operating on a slope. Two slope types tilted at 30°, 15°, and 0° were investigated. These are illustrated by the bottom two sketches in Figure 5.5.4. The first type represents a side slope with a bump contacting the upper wheels of the vehicle. The second type represents a front slope with a bump contacting both wheels of one axle simultaneously. The 'slope' with an inclination of 0° is a horizontal plane with an obstacle contacting either one wheel or two wheels simultaneously. The form of the bump is sinusoidal; its height is less than the wheel radius (1 ft. and 2 ft.).

5.5.4 Notations

Following is a list of all notations used in this portion of the study, with a corresponding figure reference:

Angles (radians)

α	angle of forward slope	(see Fig. 4)
β	angle of side slope	(see Fig. 4)
θ_t	pitch angle of aft unit	(see Fig. 5)
θ_c	pitch angle of forward unit	(see Fig. 5)
ϕ_t	roll angle of aft unit	(see Fig. 5)
ϕ_c	roll angle of forward unit	(see Fig. 5)

Distances (in.)

a, b, $d_1 \ldots d_4$, e, f, g	see Fig. 5
$h_1 \ldots h_6$, $\bar{h}_1 \ldots \bar{h}_6$, $\hat{h}_1 \ldots \hat{h}_6$	see Fig. 8
ℓ, p, q	see Fig. 5

r,	wheel radius
ε_t, ε_c	(see Fig. 17)
$y_1 \ldots y_6$, $u_1 \ldots u_6$, $z_1 \ldots z_6$	(see Fig. 8)
z_t, z_c	(see Fig. 5)
δ_t, δ_c	(see Fig. 16)
h_p	(see Fig. 17)

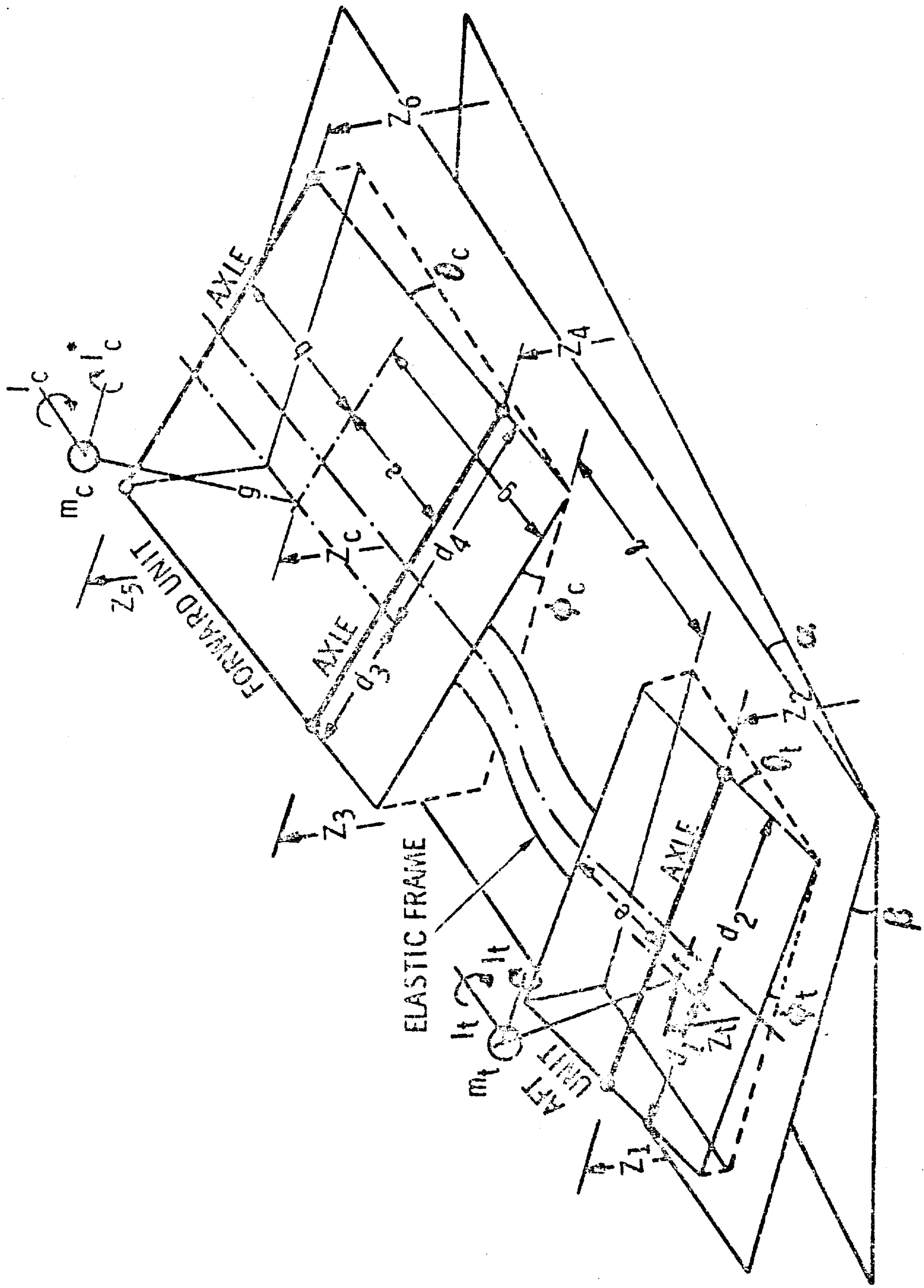

Figure 5.5.5- Dimensions, Angles, and Mass Locations of LSSM

Lunar Weights (lb.)

W_c,	Weight of the forward unit	(see Fig. 7)
W_t,	Weight of the aft unit	
W'_c,	W_c cos cos	
W''_c,	W_c sin	
W'''_c,	W_c cos sin	
W'_t	W_t cos cos	
W''_t,	W_t sin	
W'''_t,	W_t cos sin	
$W_1 \ldots W_6$,	Weight of wheel assembly, unsprung	(see Fig. 8)

Masses (lb. sec^2/in)

m_t,	aft unit (sprung)	(see Fig. 5)
m_c,	forward unit (sprung)	
$m_1 \ldots m_6$,	wheel assembly (unsprung)	(see Fig. 8)

Mass Moments of Inertia (in. lb. sec^2)

I_t,	aft unit, around c.g., roll axle	(see Fig. 5)
I_t^*,	aft unit, around c.g., pitch axle	
I_c,	forward unit, around c.g., roll axle	
I_c^*,	forward unit, around c.g., pitch axle	

Damping Rates (lb. sec/in)

$c_1 \ldots c_6$	suspension	(see Fig. 8)
c_p,	pitch limiter	(see Fig. 17)

Spring Rates (lb/in)

$k_1 \ldots k_6$,	suspension	(see Fig. 8)
$k_1{}^* \ldots k_6{}^*$,	suspension snubber	(see Fig. 8)
$\bar{k}_1 \ldots \bar{k}_6$,	wheel	(see Fig. 8)
$\bar{k}_1{}^* \ldots \bar{k}_6{}^*$,	wheel snubber	(see Fig. 8)
k_p, $k_p{}^*$,	pitch limiter	(see Fig. 17)

Forces (lb)

$S_1 \ldots S_6$,	wheel force between wheel and ground	(see Fig. 8)
$V_1 \ldots V_6$,	suspension force between suspension and compartment	(see Fig. 8)
V_t,	vertical force between aft unit and elastic frame	(see Fig. 16)
V_c,	vertical force between forward unit and elastic frame	(see Fig. 16)
P,	forward force between pitch limiter and compartments	(see Fig. 17)
H_t' & H_t'',	side forces at wheels of aft unit	(see Fig. 13)
H_c' & H_c'',	side forces at wheels of forward unit	(see Fig. 9)

Moments (in. lb.)

T_t,	torque between elastic frame and aft unit (roll)	(see Fig. 16)
T_c,	torque between elastic frame and forward unit (roll)	(see Fig. 16)
M_t,	moment between elastic frame and aft unit (pitch)	(see Fig. 16)
M_c,	moment between elastic frame and forward unit (pitch)	(see Fig. 16)

I,	surface moment of elastic frame (in^4)
Q,	torsion rate of elastic frame (in. lb/rad.)
E,	Young's modulus (lb/in^2)

5.5.5 Equations of Motion: General Remarks

The derivation of the equations of motion is based on the free-body principle. First, the vehicle is divided into a suitable number of elements and then forces are applied to re-establish equilibrium. Finally the equations of equilibrium are formulated for each element.

For practical reasons the vehicle has been divided into 10 elements (see Figure 5.5.6) as follows: 6 wheel assemblies, 1 forward unit, 1 elastic frame, 1 pitch damper, 1 aft unit.

All equations are based on the assumption of small angles, that is $\sin x = \tan x = x$ and $\cos x = 1$. To derive the equations of motion the vehicle is considered to be traveling over a hard surface sloped both in the forward and side directions. The tilted plane is the datum plane. Consequently, the weight forces of the masses have to be resolved into three components orthogonal to the datum plane (see Figure 5.5.7) as follows:

$$W' = W \cos\alpha \cos\beta$$

$$W'' = W \sin\alpha$$

$$W'' = W \cos\alpha \sin\beta$$

5.5.6 Equations of Motion for the Wheel Assembly

Figure 5.5.8 shows a schematic diagram of a wheel assembly. All points move in a direction normal to the datum plane. The following notations for the time dependent ordinates are defined as follows:

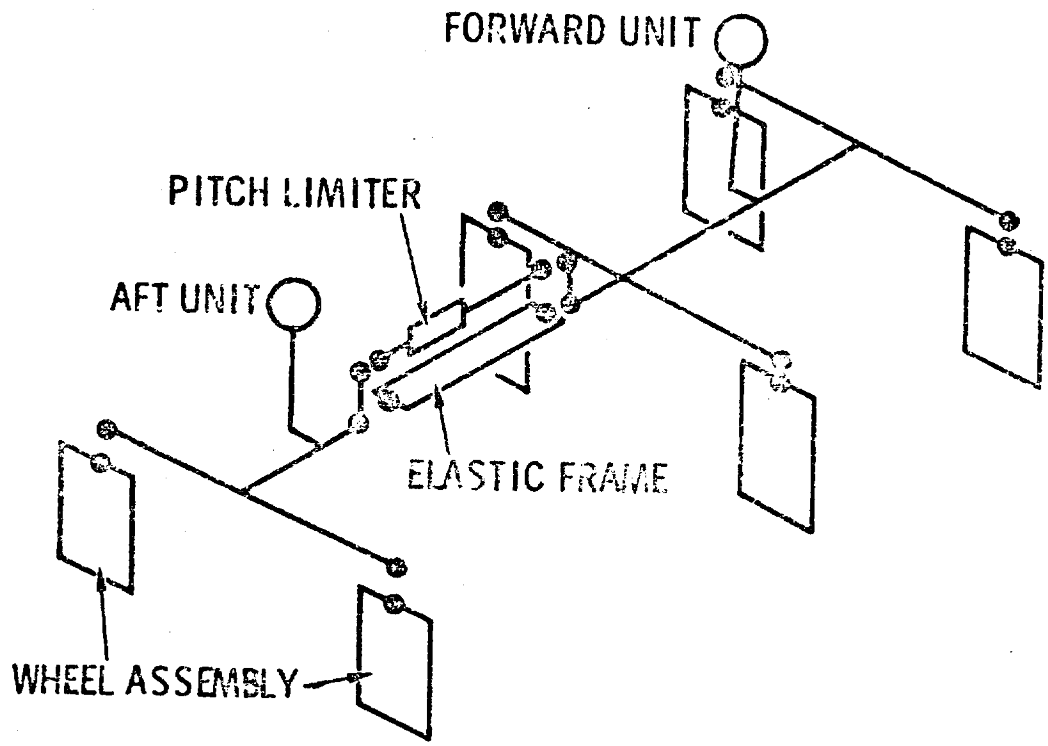

Figure 5.5.6- Ten Free-Bodied Elements of the Vehicle

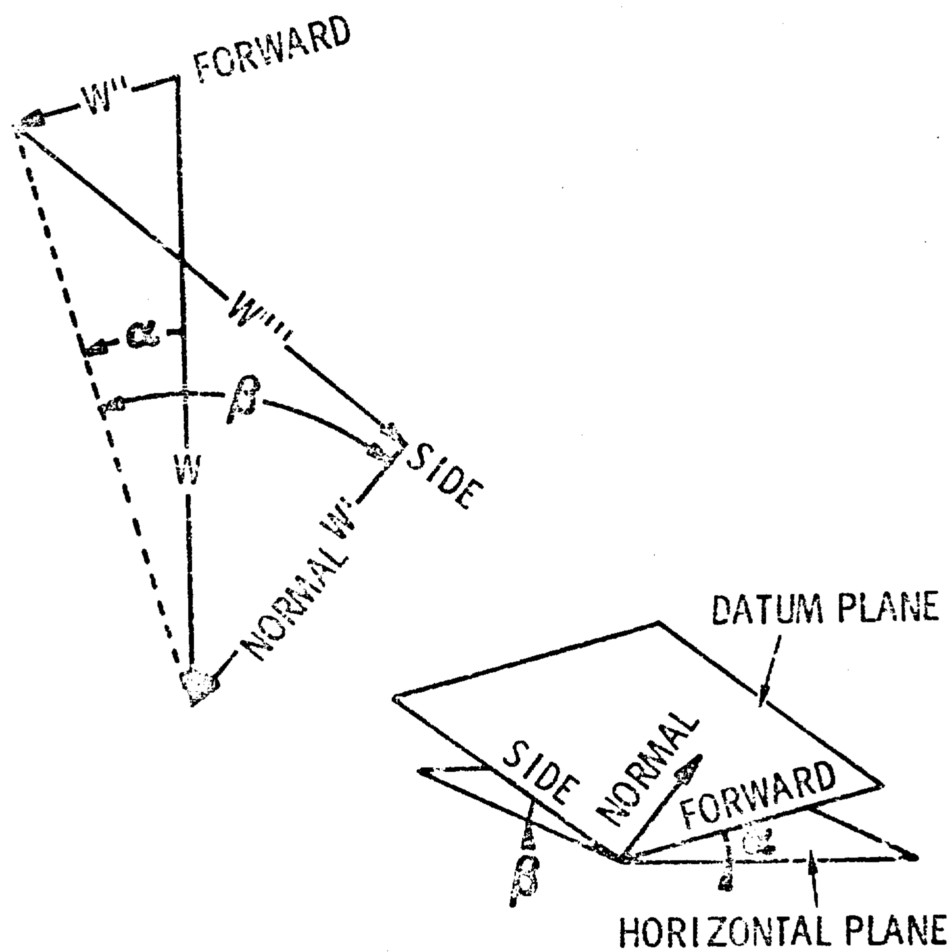

Figure 5.5.7- Weight Components

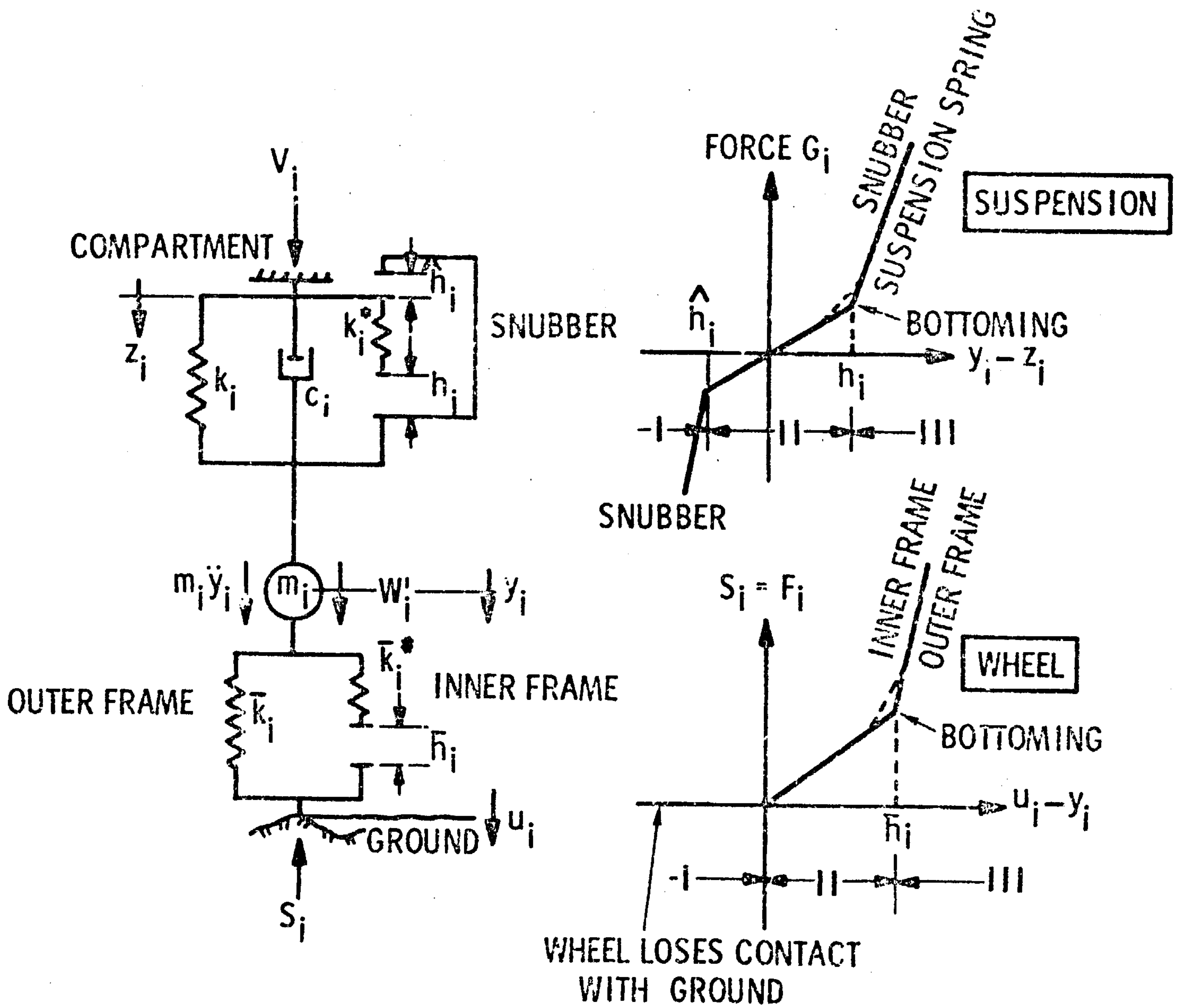

Figure 5.5.8- Forces and Spring Rates of a Wheel Assembly

$u_1 \ldots u_6$, distance of the terrain profile underneath the contact point from datum plane

$y_1 \ldots y_6$, distance of the masses from the datum plane

$z_1 \ldots z_6$, distance of the connection between wheel suspension and compartment from datum plane.

All springs and dampers are linear. The wheels are point followers. Forward thrust, slip, rolling resistances, and motor torque are not considered. Only mass forces, weight forces and spring and damper forces in the direction normal to the datum plane are taken into account.

The wheel operates over three ranges of spring rates as shown in Figure 5.5.8:

- o Range I: The wheel leaves the ground and the force S_i between wheel and ground is zero.
- o Range II: Only the outer spring frame of the wheel is deflected.
- o Range III: Outer and inner spring frames of the wheel are deflected (bottoming). - The suspension also operates over three ranges of spring rates as shown in Figure 5.5.8.
- o Range I: Only the suspension spring is deflected.
- o Ranges II and III. Both suspension spring and snubber are deflected (bottoming) in either direction.

The equations of equilibrium for a wheel-suspension assembly can be expressed as follows:

$$S_i - W_i' - m_i \ddot{Y}_i - V_i = O \qquad (1 - 6)$$

where

$$S_i = \begin{cases} O \text{ ------------------------- if } & u_i - y_i \leq O \\ \bar{k}_i (u_i - y_i) \text{ ----------------- if } & 0 < u_i - y_i \leq \bar{h}_i \\ \bar{k}_i (u_i - y_i) + \bar{k}_i^* (u_i - y_i - \bar{h}_i) \text{---if } & u_i - y_i > \bar{h}_i \end{cases} \qquad (7 - 12)$$

$$V_i = \begin{cases} k_i (y_i - z_i) + c_i (\dot{y}_i - \dot{z}_i) \text{---- if } -\hat{h}_i \leq y_i - z_i \leq h_i \\ k_i (y_i - z_i) + k_i^* (y_i - z_i - h_i) + c_i (\dot{y}_i - \dot{z}_i) \text{---if } y_i - z_i > h_i \\ k_i (y_i - z_i) + k_i^* (y_i - z_i - \hat{h}_i) + c_i (\dot{y}_i - \dot{z}_i) \text{---if } y_i - z_i < -h_i \end{cases} \qquad (13 - 18)$$

$$i = 1 \ldots 6$$

Equations (7) through (18) are valid for cases where the spring force - deflection characteristics can be expressed by linear functions. If this is not the case, the equations would be as follows:

$$S_i = F_i (u_i - y_i) \qquad (7 - 12)$$

$$V_i = G_i (y_i - z_i) + c_i (\dot{y}_i - \dot{z}_i) \qquad (13 - 18)$$

$$i = 1 - 6$$

where F_i and G_i denote functions of the displacements $(u_i - y_i)$ and $(y_i - z_i)$, respectively.

5.5.7 Equations of Motion for the Forward Unit

Figure 5.5.9 shows all forces and moments acting on the free-body of the forward unit. The weight forces are:

W'_c,	weight component normal to the datum plane
W''_c,	weight component in forward direction
W'''_c,	weight component in side direction

To understand the method of deriving the proper mass forces a simple case is considered. Figure 5.5.10 shows the compartment in a pitching mode. The rear and the front of the compartment can move only normally to the datum plane, according to the previous assumptions. Therefore, the mass is accelerated in the normal direction with $\ddot{z}_c$, in the forward direction with $q\dot{\theta}$, and around the axle A with $\ddot{\theta}$. Accordingly, the mass forces are:

$m_c q \ddot{\theta}_c$,	inertia force in the forward direction
$m_c q \ddot{\varphi}_c$,	inertia force in the side direction
$m_c \ddot{z}_c$,	inertia force in the normal direction
$I_c \ddot{\phi}_c$,	inertia moment in roll
$I^*_c \ddot{\theta}_c$,	inertia moment in pitch

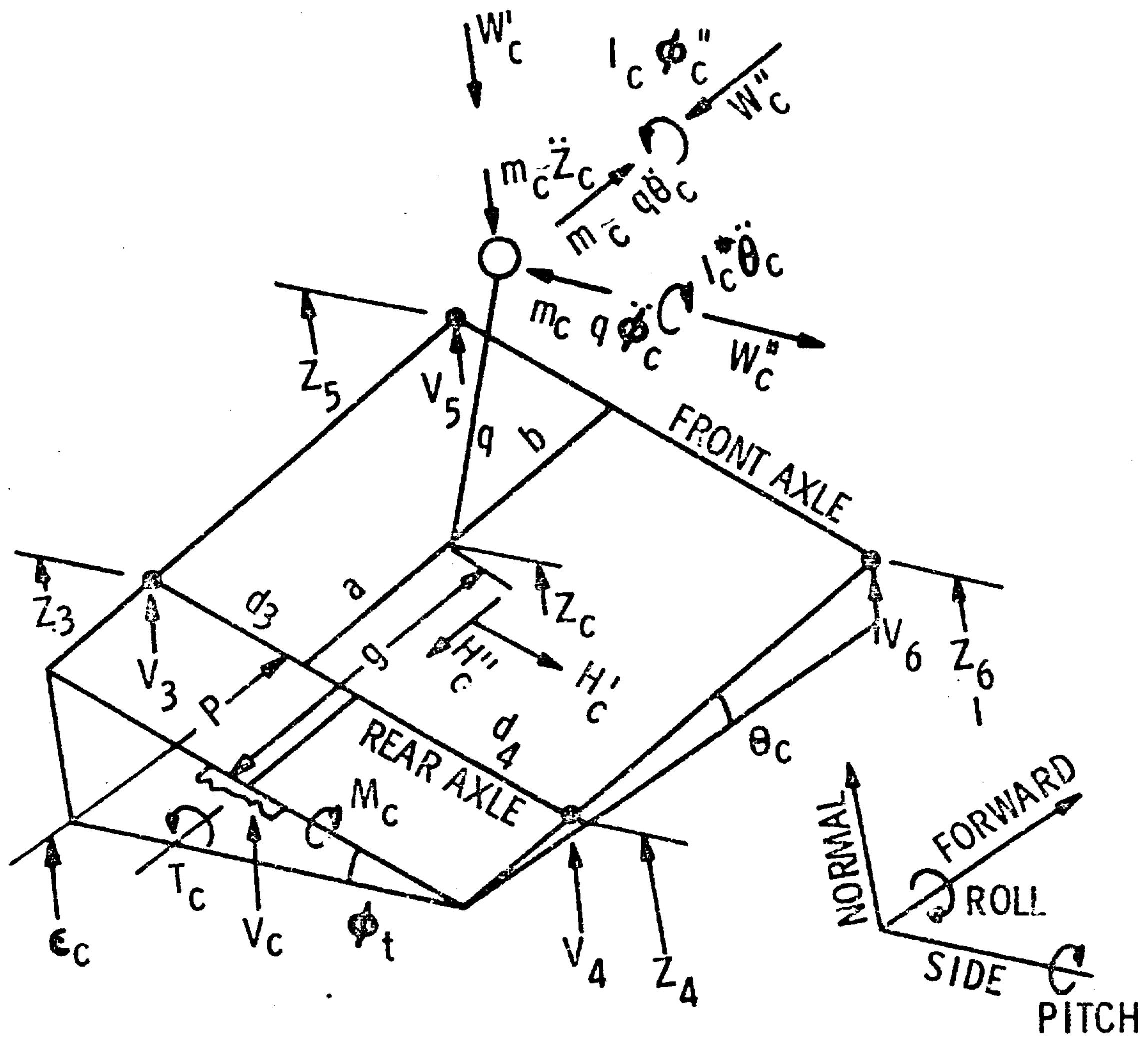

Figure 5.5.9- Forces and Moments of the Forward Unit

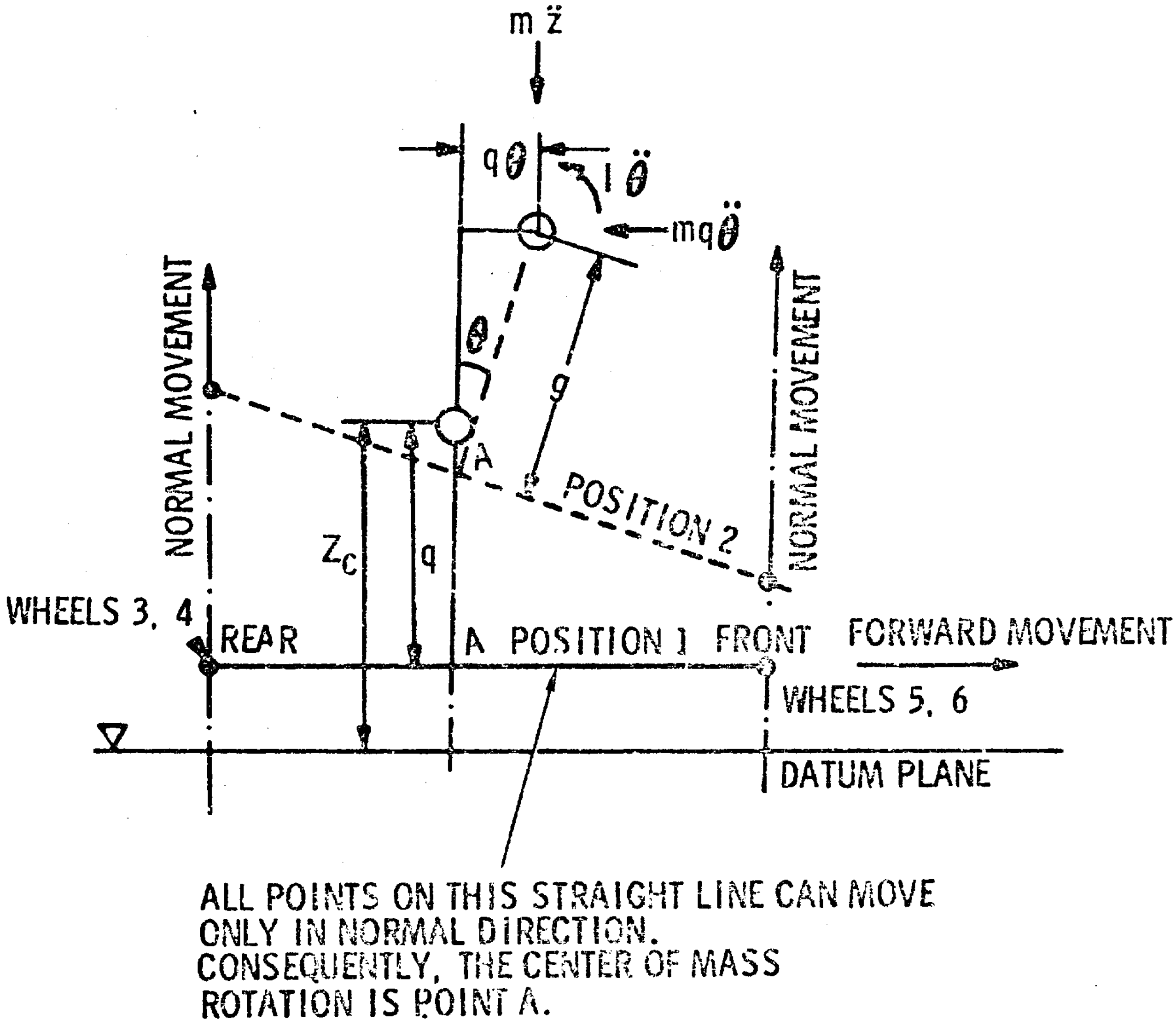

Figure 5.5.10- Inertia Forces of Pitching Forward Unit

From figure 5.5.9, the forces acting from the flexible frame are:

V_c, frame force normal to datum plane

M_c, pitch moment of frame

T_c, roll moment of frame

Frame forces in the side and forward directions are not considered in this study; it is assumed that these forces are counteracted within the compartments. Consequently, the forces $m_c q \ddot{\phi}_c$ and W_c''' acting in the side direction have to be counteracted by forces at the contact between the wheels and the ground. How these counter forces are distributed is unknown. To simplify the problem it has been assumed that the side forces at the wheel contact points are equally distributed and, consequently, add up to the resultant force H_c', as indicated in Figure 5.5.9. Similar considerations hold for the forward forces W_c'', and $m_c q\ddot{\theta}_c$. These counter forces add up to H_c'', acting at a distance r = wheel radius from the compartment.

Forces stemming from the wheels are:

$V_3 \ldots V_6$, wheel assembly forces in normal direction

The pitch limiter exerts a force P in the forward direction on the forward unit. (The magnitude of this force will be derived later.)

The equations of equilibrim are then easily derived from Figures 5.5.9, 11 and 12.

Since the sum of all forces in the forward direction equals zero,

$$m_c q \ddot{\theta}_c - W_c'' + P - H_c'' = 0 \tag{19}$$

Since the sum of all forces in the normal direction is zero,

$$V_3 + V_4 + V_5 + V_6 + V_c - W_c' - m_c \ddot{z}_c = 0 \tag{20}$$

Since the sum of all forces in the side direction is zero,

$$H_c' - m_c q \ddot{\phi}_c + W_c''' = 0 \tag{21}$$

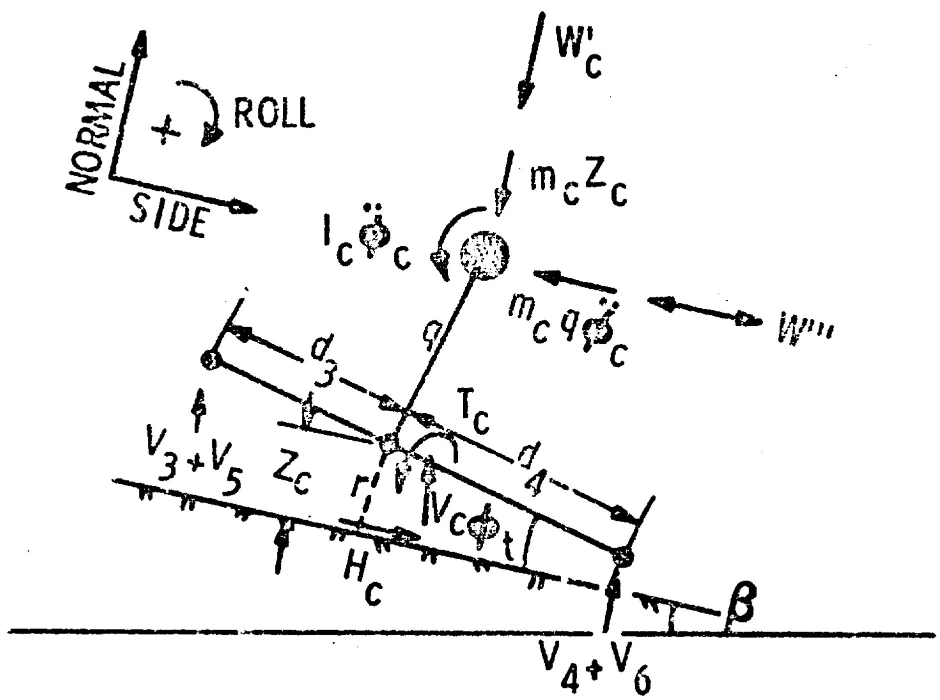

Figure 5.5.11- Forces and Moments of a Rolling Forward Unit

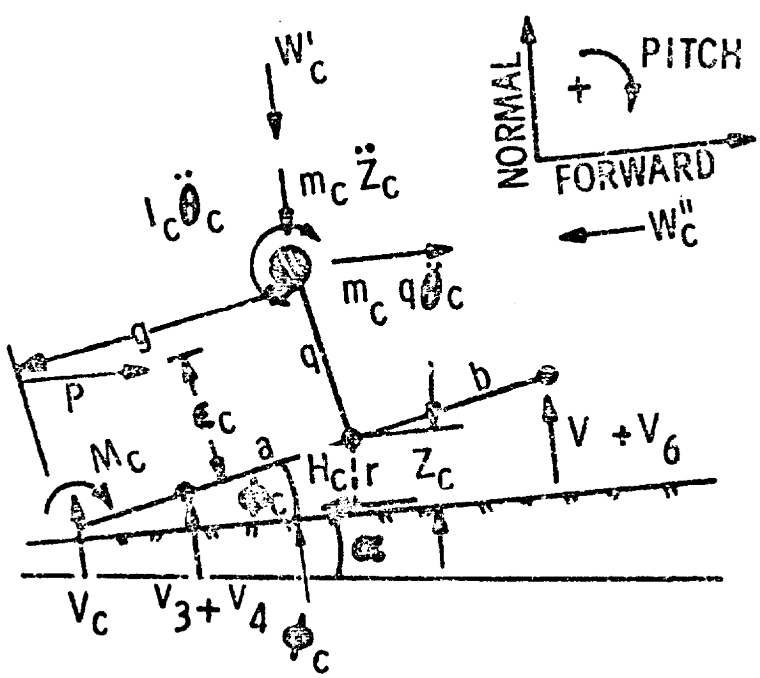

Figure 5.5.12- Forces and Moments of a Pitching Forward Unit

Since the sum of all moments in the roll direction is zero,

$$(V_3 + V_5)d_3 - (V_4 + V_6)d_4 - \frac{d_4 - d_3}{2} V_c - T_c - m_c q^2 \ddot{\phi}_c + W_c''' q - I_c \ddot{\phi}_c - H'_c r = 0 \tag{22}$$

Since the sum of all moments in the pitch direction is zero,

$$V_c g + M_c + (V_3 + V_4)a - (V_5 + V_6)b + I^*_c \ddot{\theta}_c + (m_c q \ddot{\theta}_c - W'''_c)q + P \varepsilon_c + H''_c r = 0 \tag{23}$$

5.5.8 Equations of Motion for the Aft Unit

Equations for the aft unit are derived in the same manner as for the forward unit (see Figures 5.5.13, 14, 15). The pitch and roll centers are always located at the axle.

In the forward direction,

$$m_t p \ddot{\theta}_t - W''_t - P - H''_t = 0 \tag{24}$$

In the normal direction,

$$V_1 + V_2 - V_t - W'_t - m_t \ddot{Z}_t = 0 \tag{25}$$

In the side direction,

$$W'''_t - m_t p \ddot{\phi}_t + H'_t = 0 \tag{26}$$

In roll,

$$V_1 d_1 + V_t \frac{d_2 - d}{2} - V_2 d_2 - H'_t r - m_t p^2 \ddot{\phi}_t + W'''_t p + T_t - I_t \ddot{\phi}_t = 0 \tag{27}$$

In pitch,

$$-(V_1 + V_2) f + V_t (f + e) + M_t + I^*_t \ddot{\theta}_t + m_t p^2 \ddot{\theta}_t - W''_t p - P \varepsilon_t + H''_t r = 0 \tag{28}$$

5.5.9 Equations of Motion for the Flexible Frame

The flexible frame connecting the two compartments is considered to be a massless, continuous beam of uniform cross section loaded at the ends by:

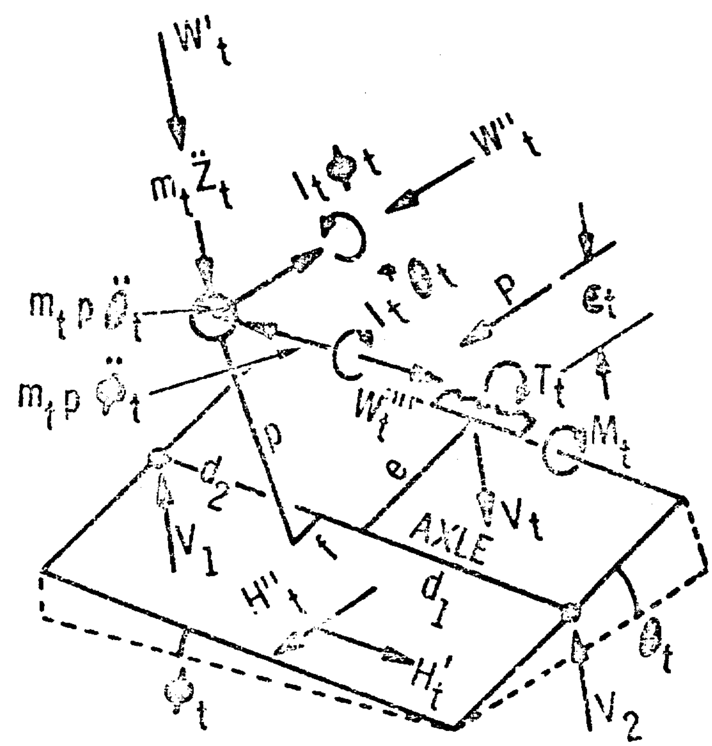

Figure 5.5.13- Forces and Moments of the Aft Unit

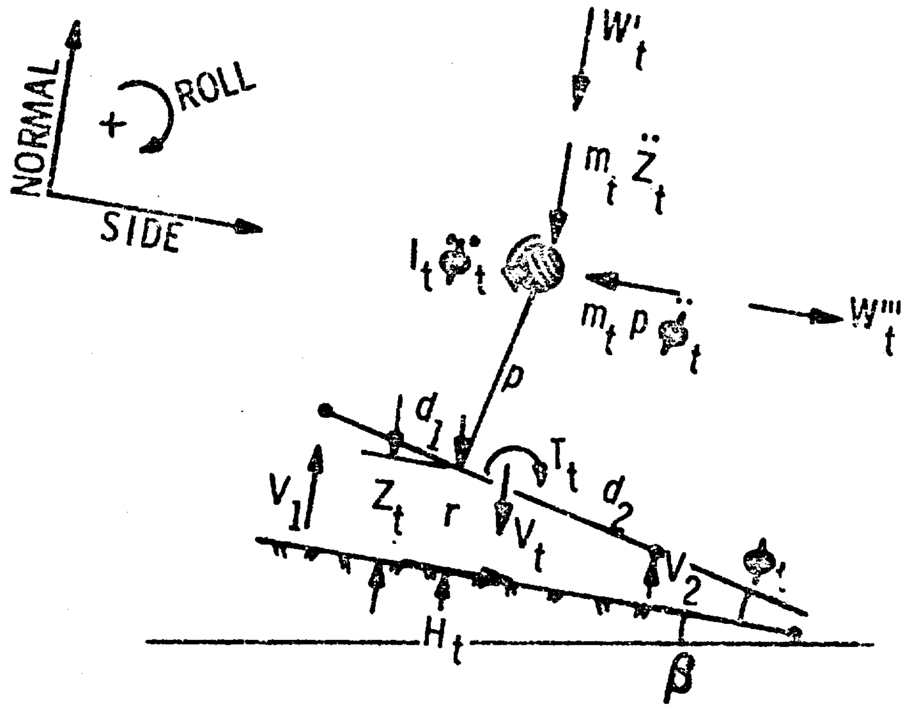

Figure 5.5.14- Forces and Moments of a Rolling Aft Unit

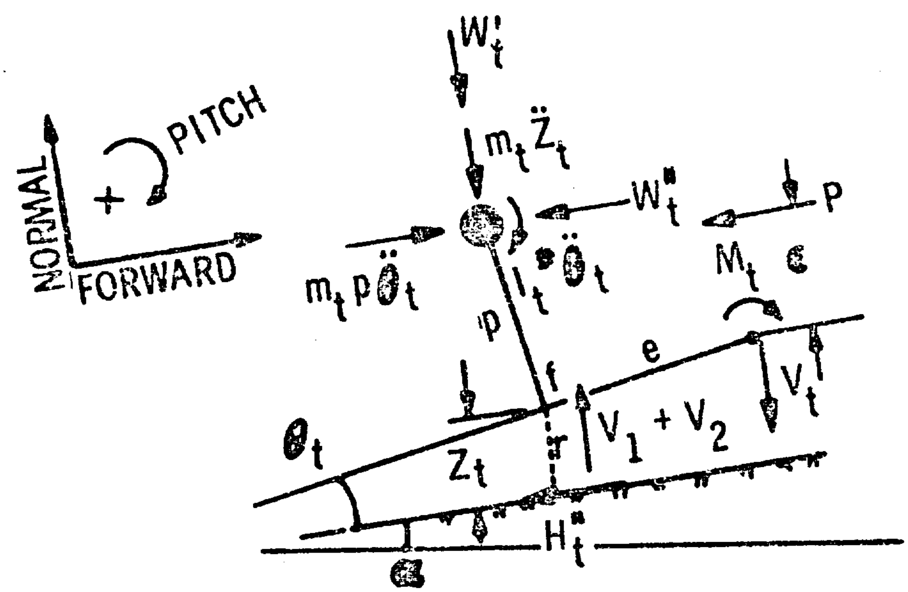

Figure 5.5.15- Forces and Moments of a Pitching Aft Unit

- forces V_c and V_t acting in the normal direction
- moments M_c and M_t acting in the pitch direction
- torques T_c and T_t acting in the roll direction

Forces in the forward and side directions are not considered, as explained above. The beam can be deformed by twisting in roll, by bending in pitch, and by moving the two beam ends in the normal direction. Because the angles and deflections are small, the principle of superposition can be employed. Figure 5.5.16 shows how, by superposition of two types of beam deflection, a general picture of beam deformation without torsion can be achieved. The equations of equilibrium for this general case are:

$$V_t - V_c = 0 \tag{29}$$

$$- M_t - M_c + V_c \ell = 0 \tag{30}$$

where

$$V_t = 12 \frac{m}{\ell^2} \delta_t - 12 \frac{m}{\ell^2} \delta_c + 6 \frac{m}{\ell} \theta_t + 6 \frac{m}{\ell} \theta_c \tag{31}$$

$$M_t = 6 \frac{m}{\ell} \delta_t - 6 \frac{m}{\ell} \delta_c + 4 m \theta_t + 2 m \theta_c \tag{32}$$

and

$$m = \frac{EI}{\ell} \tag{32a}$$

The equilibrium of torquesis simply expressed by (see Fig. 16)

$$T_c - T_t = 0 \tag{33}$$

where

$$T_t = Q (\phi_c - \phi_t) \tag{34}$$

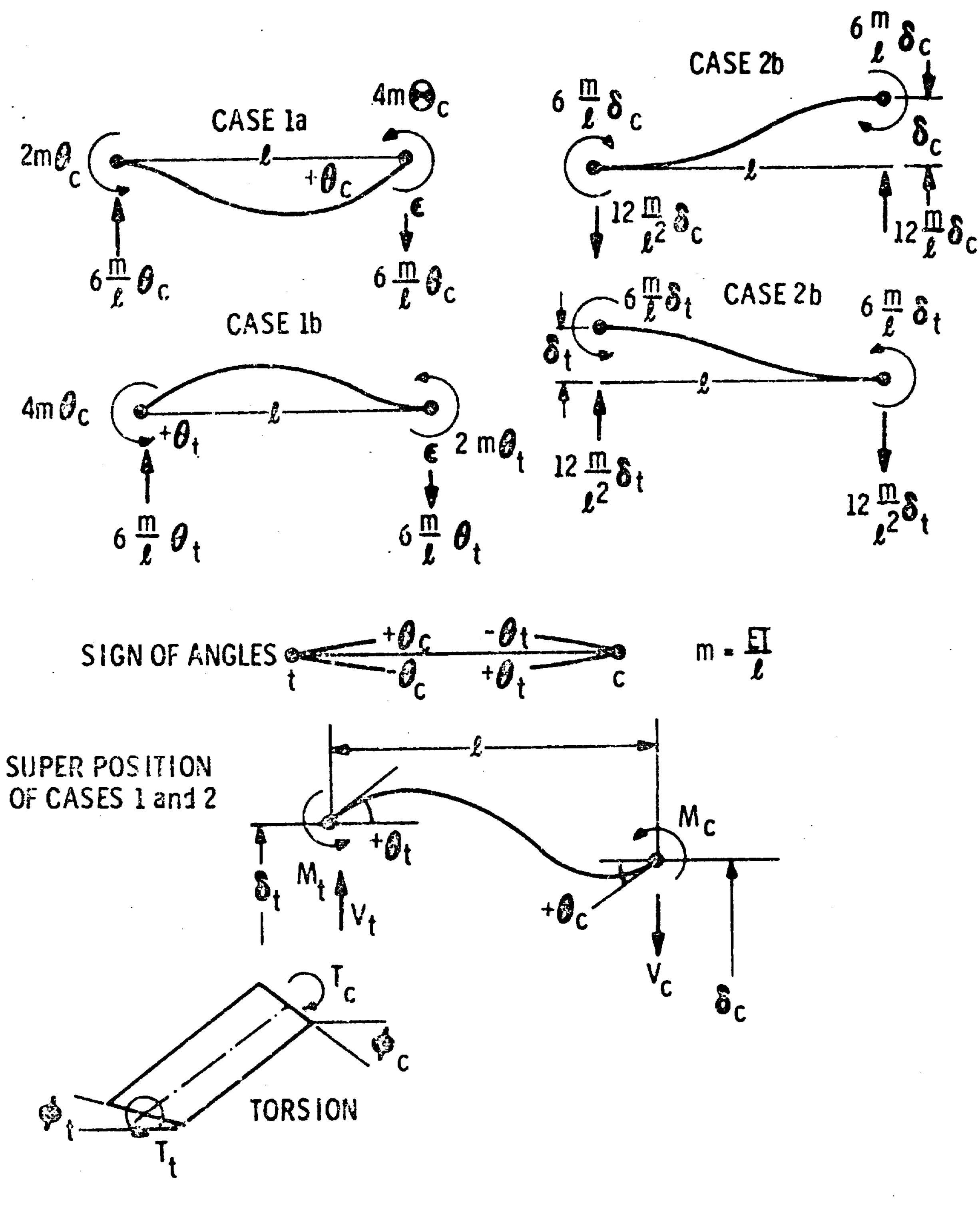

Figure 5. 5. 16- Forces and Moments of the Elastic Frame

5.5.10 Equations of Motion for the Pitch Limiter

The relative pitch between the forward and aft units is limited by a pitch limiter as shown in Figure 5.5.17. It is essentially a linear spring with snubbers at both ends. The spring is attached at both compartments and is constantly engaged. To prevent the continuous storage and release of energy in the spring, damping is added. From the spring characteristics and the geometry of the limiter, the following equations can be simply derived:

$$P = \begin{cases} k_p(\theta_c \varepsilon_c - \theta_t \varepsilon_t) + c_p(\dot{\theta}_c \varepsilon_c - \dot{\theta}_t \varepsilon_t) & \text{if } -h_p \leq \theta_c \varepsilon_c - \theta_t \varepsilon_t \leq h_p \\ k_p(\theta_c \varepsilon_c - \theta_t \varepsilon_t) + k_p^*(\theta_c \varepsilon_c - \theta_t \varepsilon_t - h_p) + c_p(\dot{\theta}_c \varepsilon_c - \dot{\theta}_t \varepsilon_t) .. & \\ & \text{if } -h_p > \theta_c \varepsilon_c - \theta_t \varepsilon_t > h_p \end{cases} \quad (35)$$

5.5.11 Geometrical Relationships

Other equations relating to geometrical relationships can be derived from the various vehicle dimensions:

$$\delta_t = z_t - \frac{d_2 - d_1}{2} \phi_t + (e + f)\theta_t \quad (36)$$

$$\delta_c = z_c - \frac{d_4 - d_3}{2} \phi_c - g\theta_c \quad (37)$$

$$z_1 = z_t + f\theta_t + d_1 \phi_t \quad (38)$$

$$z_2 = z_t + f\theta_t - d_2 \phi_t \quad (39)$$

$$z_3 = z_c - a\theta_c + d_3 \phi_c \quad (40)$$

$$z_4 = z_c - a\theta_c - d_4 \phi_c \quad (41)$$

$$z_5 = z_c + b\theta_c + d_3 \phi_c \quad (42)$$

$$z_6 = z_c + b\theta_c - d_4 \phi_c \quad (43)$$

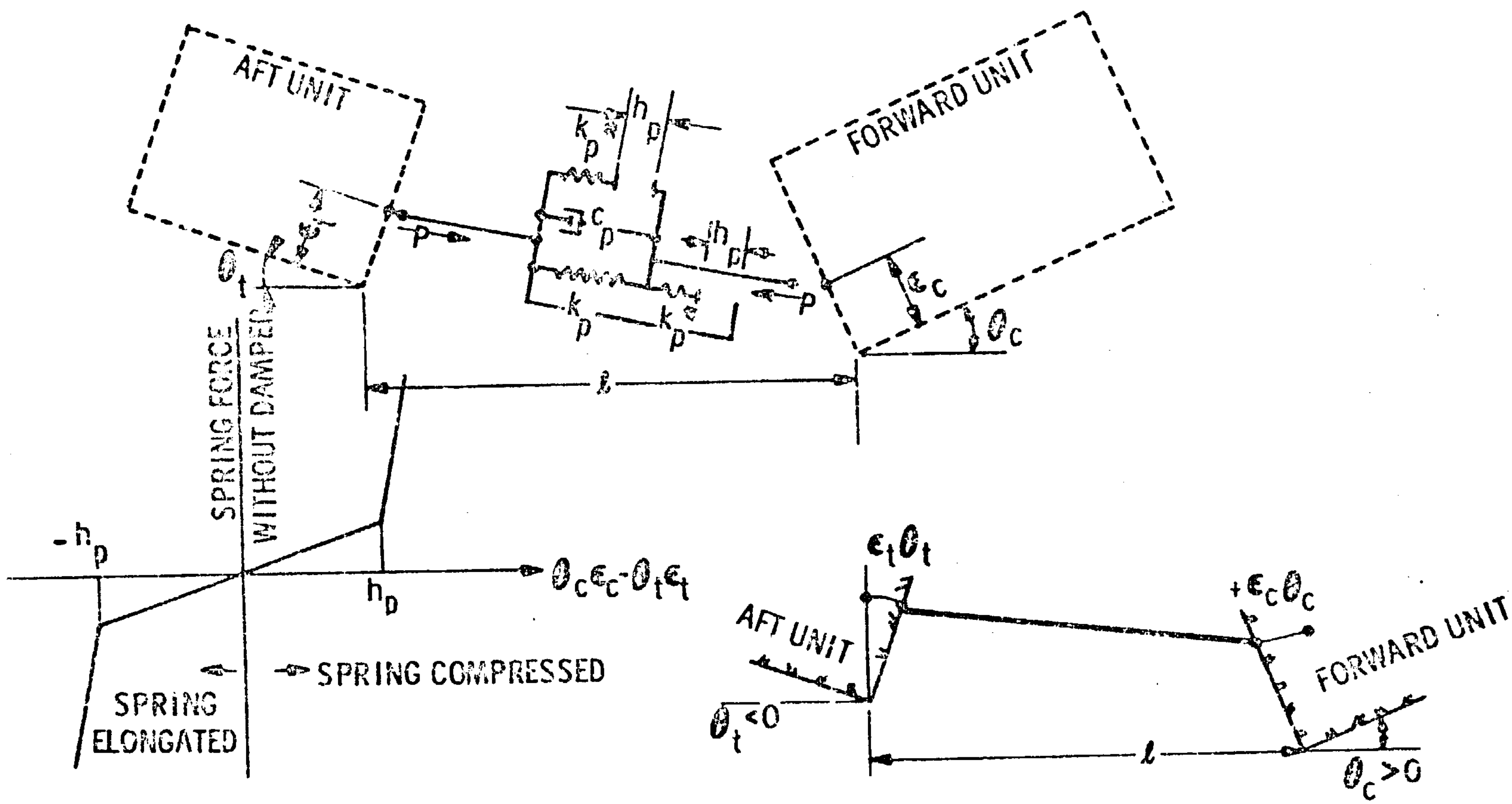

Figure 5.5.17 - Pitch Limiter

5.5.12 Human Tolerance to Vibration

The level of human tolerance to vibrations may limit the speed of the vehicle. Some of the most recent studies on this subject have been conducted by Pradko and others. * Figure 5.5.18 shows the findings insofar as they are relevant to the problem of defining human tolerance to random vibrations. Pradko vibrated persons seated (without cushions) on a shake table in the vertical, pitch, and roll modes by means of white-noise vibrations filtered through a 2 cps band-pass filter. The pitch and roll center was located in the contact area between seat and subject, and the center frequency was varied between 3 cps and 30 cps.

The frequency range of interest for the LSSM lies between 0.3 cps and 4.5 cps, as was discussed under the section on Terrain. From Figure 5.5.18 we estimate that in this frequency range the RMS levels of human tolerance to random vibrations will be:

- o Vertical - 0.25 g (100 in/sec^2)
- o Pitch - 6 rad/sec^2
- o Roll - 9 rad/sec^2

The pitch and roll tolerances cannot be applied immediately to our problem because the pitch and roll axes of the LSSM are not located at the seat. The actual locations of the pitch and roll axes of the forward unit chang with time, but very likely they may be found most of the time beneath the center of gravity in the plane of the wheel axles. To transfer Pradko's data to a rotation center located at a certain distance from the seat, it was assumed that the hips of the seated person exactly follow the motions of the rotating chair, as if this part of the body were connected rigidly to the seat.

* F. Pradko: Human Tolerance to Random and Sinusoidal Acceleration, U.S. Army Tank Automotive Command, Research and Engineering Directorate, 1965

* F. Pradko and R. A. Lee: Vibration Comfort Criteria, Society of Automotive Engineers Paper 660139, January 1966

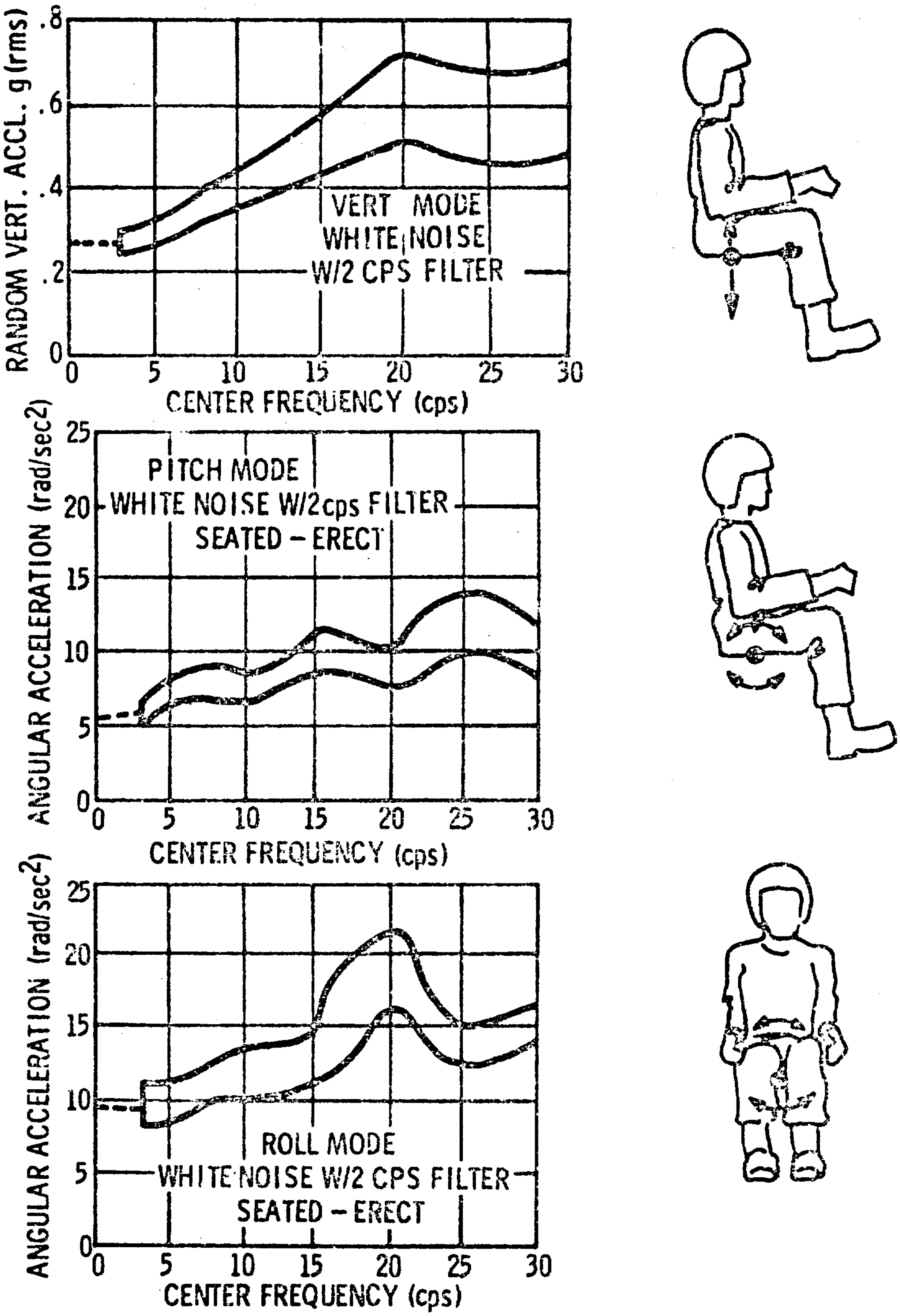

Figure 5.5.18 - Human Tolerance of Random Vibration

As the distance from the seat to the hips is approximately 0.7 ft, the horizontal acceleration of the hips associated with the tolerable pitch acceleration of 6 rad/sec^2 is (0.7) (6) = 4.2 ft/sec^2. If a distance of 2.7 ft. is assumed between the hips of the driver and the pitch and roll center of the LSSM (see Figure 5.5.19), the same horizontal acceleration for the case of the LSSM would be attained at a pitch acceleration of (0.7) (6)/(2.7) = 1.6 rad/sec^2. In the case of roll, the tolerance level would be 2.3 rad/sec^2.

To summarize, the following values can then be taken to represent the tolerance levels to random vibrations of an LSSM driver.

- Vertical - 100 in/sec^2 (RMS)
- Pitch - 1.6 rad/sec^2 (RMS)
- Roll - 2.3 rad/sec^2 (RMS)

These numbers represent performance on Earth, and how they might change in the low gravity field on the moon is unknown. Because the lunar gravitational acceleration of 65 in/sec^2 is less than the human tolerance to vertical vibrations on earth, it is conceivable that the tolerance level to vertical vibrations may be decreased considerably on the moon. The other two tolerance values may be unchanged on the moon because gravitational effects are not involved in essentially horizontal motions.

5.5.13 Vehicle Performance Evaluation

As was stated previously, the main objectives of this dynamics analysis program were to:

- Optimize the suspension system from the point-of-view of vehicle dynamic performance.
- Determine the influence of speed and terrain roughness.
- Compare rigid and flexible wheels and evaluate effect of eliminating the suspension system.
- Evaluate the transient response and stability of the LSSM when operating over "bumps".

In order to achieve the above, it was considered necessary to assess the following elements of vehicle response:

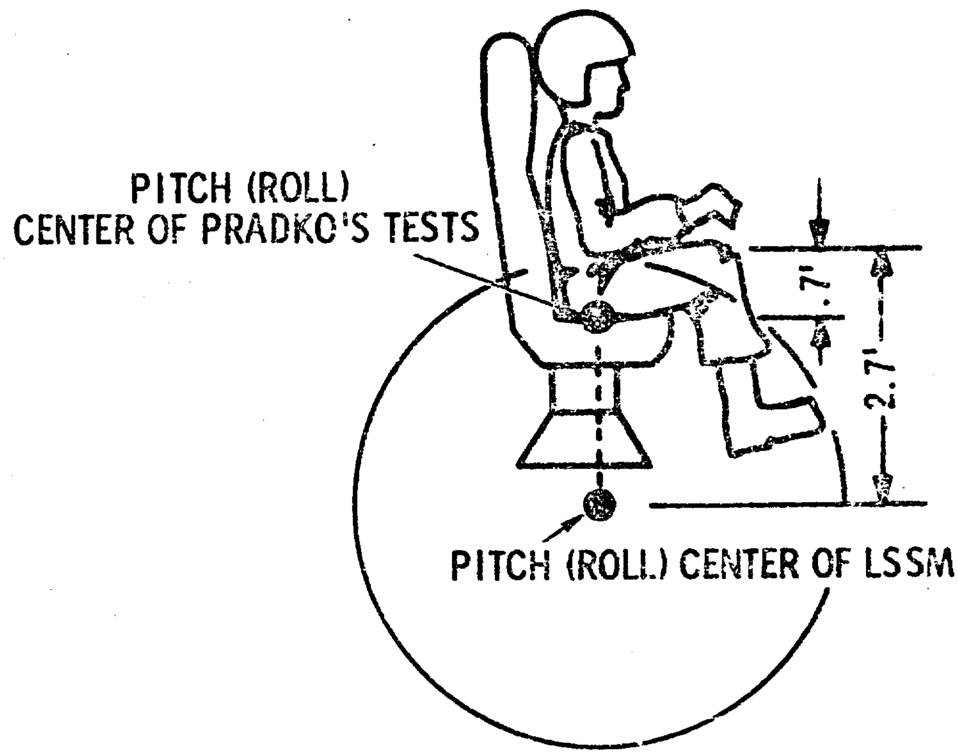

Figure 5.5.19 - Transformation of Pitch and Roll Center

- o The percentage of time one wheel or both wheels on one axle lose contact with the ground. (This information can be considered a measure of the controllability of the vehicle.)
- o The root-mean-square (rms) values of the vertical accelerations of the centers of gravity (cg) of both units.
- o The root-mean-square (rms) values of the pitch accelerations of both units.
- o The root-mean-square (rms) values of the roll accelerations of of both units. (These acceleration data permit an estimate of the ride comfort.)
- o The damping power dissipated by the dampers of the wheel suspensions. (This is an important part of the power requirements of the vehicle.)
- o The percentage of time the force between a wheel and the ground surpasses a certain limit. (This provides structural design information.)

The rms-values of accelerations were computer in a simplified manner by assuming that the accelerations were normally distributed even if wheel bottoming or wheel lift-offs occur. The assumption of normal distribution proved to be acceptable in all cases that were checked-out. Thus the rms-values could be computed by fully rectifying the output signal, smoothing it, and multiplying it by a constant factor of $\sqrt{\frac{\pi}{2}}$.

5.5.14 Vehicle Data for Computer Program

The LSSM vehicle data used for the dynamic performance analysis is listed below. In actuality, computer programs were conducted for vehicle masses of 2400 lbm and 1800 lbm. However, the 2400 lbm case was investigated early in the LSSM study, before vehicle characteristics were well-defined. Furthermore, the 1800 lbm vehicle underwent a much more thorough analysis. In any event no significant difference in results was discerned between the two cases. For these reasons, the program conducted with the 1800 lbm LSSM is reported here. Although a design iteration carried out after the completion of the dynamics study resulted in a fully-loaded LSSM with an estimated mass of 2170 lbm, it is felt that the results reported herein are reasonably applicable.

Dimensions (inches)	
a,	29.3
b,	28.7
d_1-d_4,	41.0
e	25

Lunar Weights (lb)	
W_c (sprung),	160
W_t (sprung),	80
W_1-W_6 (unsprung),	10

Dimensions (inches)	
f,	-1.5
g,	38.3
l,	28
p,	9.5
q,	14.7
r,	20

Masses (sec^2 lb/in.)	
m_c,	2.48
m_t,	1.24
m_1-m_6,	0.155

Mass Moments of Inertia (in lb sec^2)	
I_c (roll)	739
I_c^* (pitch)	1831
I_t (roll)	346
I_t^* (pitch)	174

The mass moments of inertia listed above include the sprung masses plus suspensions. In addition to the above values, the following were also used:

- o Moment of inertia of flexible frame, $I = 0.0115 \text{ in}^4$
- o Torsional rate of flexible frame, Q = 16,900 in. lb./rad.

The suspension spring characteristics considered are shown in Figure 5.5.20. The spring characteristics of the wire frame wheel are shown in Figure 5.5.21.

5.5.15 Optimization of Suspension Springs

27 computer runs were conducted at various spring rates and vehicle speeds (see Figure 5.5.22) in order to find the rate associated with the 'best' vehicle ride. The 'best' vehicle ride was considered to be a ride with low accelerations of the forward unit (ride comfort) and a small percentage of wheel lift-offs

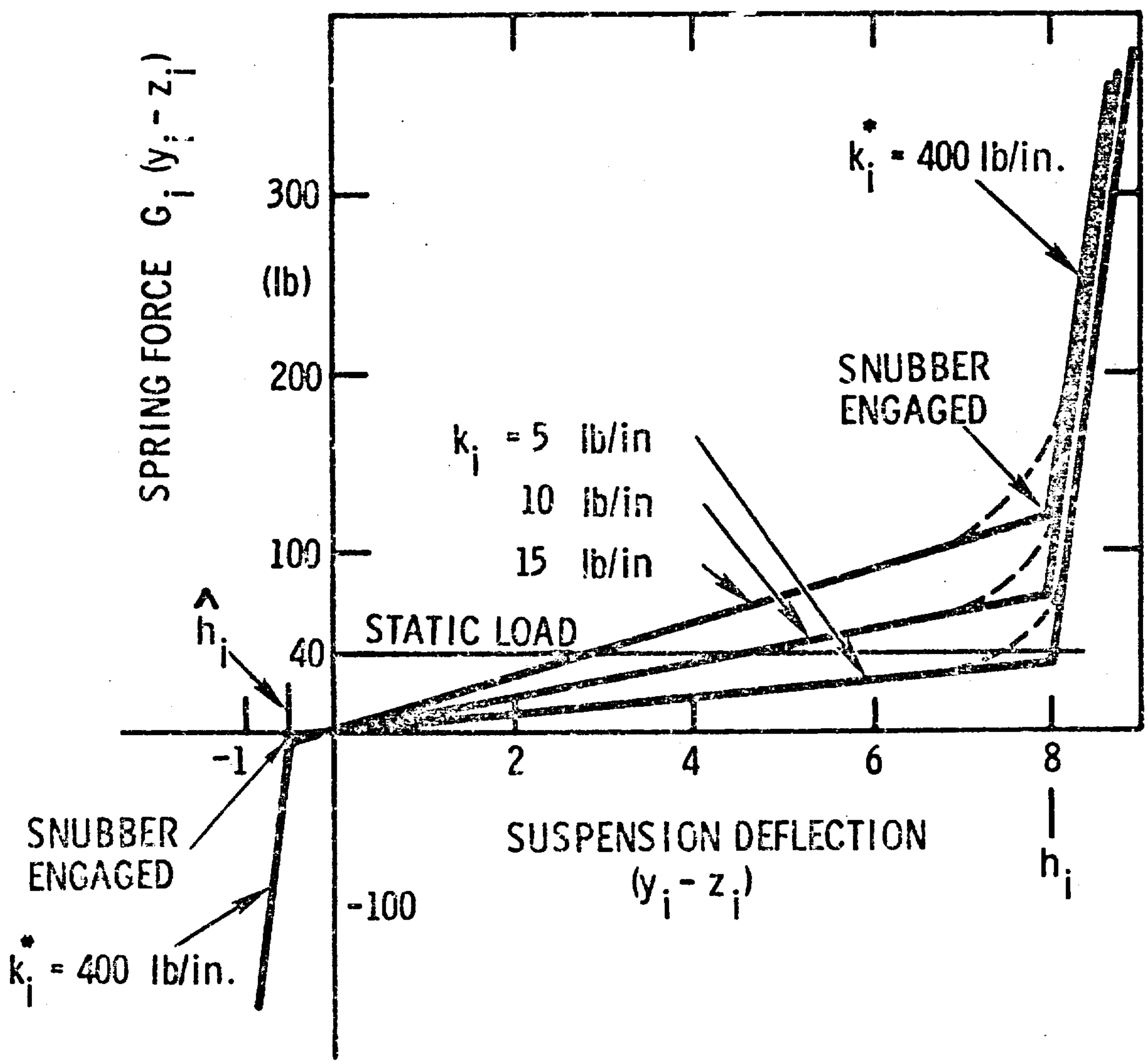

Figure 5.5.20 - Spring Characteristic of Wheel Suspension

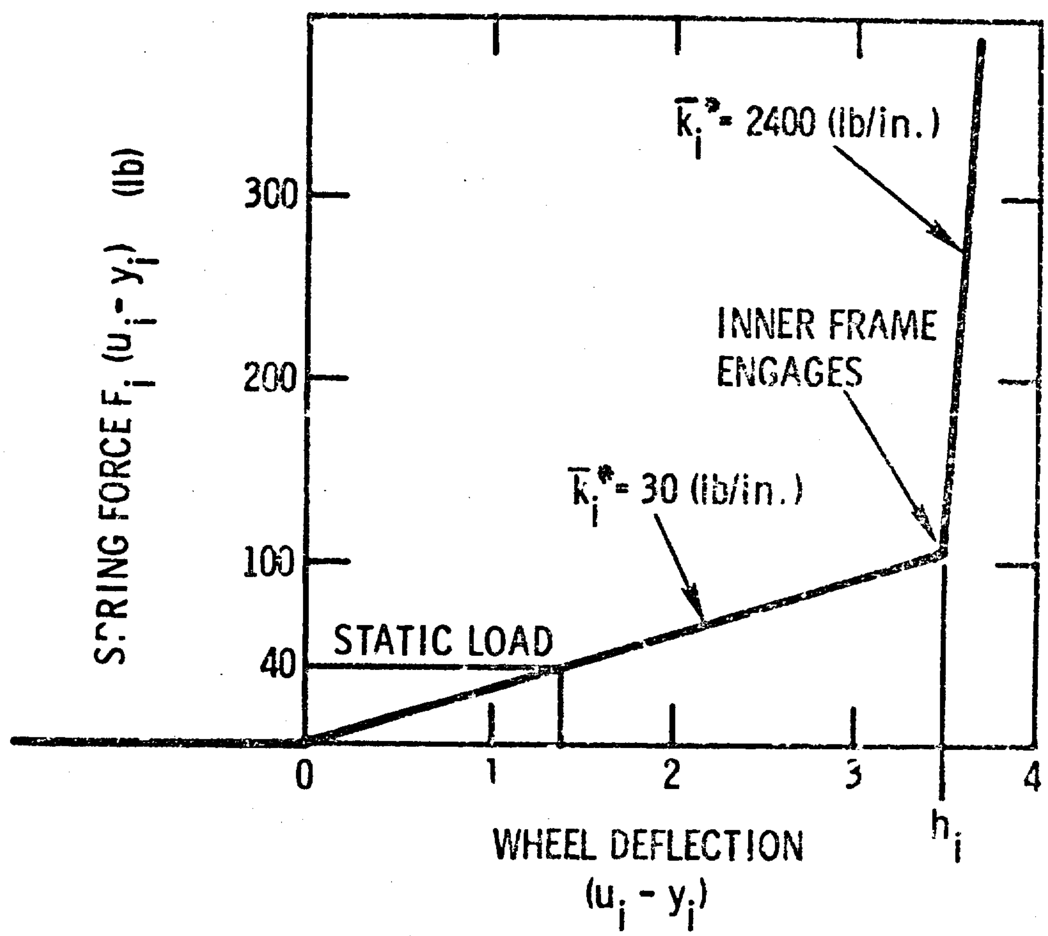

Figure 5.5.21 - Spring Characteristic of Wheel Frame

Spring rate forward unit (lb/in.)	Spring rate aft unit (lb/in.)	Velocity (ft/sec) 5	10	15
5	5	1	10	19
	10	2	11	20
	15	3	12	21
10	5	4	13	22
	10	5	14	23
	15	6	15	24
15	5	7	16	25
	10	8	17	26
	15	9	18	27

Figure 5.5.22 - Computer Run Schedule for Optimization of Suspension Spring Rates

(controllability). The spring rates of the forward unit and the aft unit were varied independently. The terrain used for all runs was the 1-ft terrain, which approximates the Mare Cognitum profile and, therefore, was considered to be most meaningful for the optimization process. During all runs the level of suspension damping rate was fixed arbitrarily at 4 lb sec/in which later turned out to be close to the optimum damping rate.

The results were plotted in a condensed form as averaged, normalized, and combined vertical, pitch and roll accelerations and wheel lift-offs versus the spring rate. Figures 5.5.23 and 5.5.24 show the results for the forward and aft units respectively. The "optimum" spring rate appears to be in the vicinity of 10 lb/in. for both cases. However, due to the relative flatness of the curves, somewhat stiffer springs would not noticeably degrade performance.

5.5.16 Optimization of Suspension Dampers

The optimization of the suspension dampers followed a procedure similar to that for the springs. Again the 1-ft terrain was used for all runs. The suspension damping rate of both forward and the aft units was varied over the range between 0.5 and 10 lb sec/in. Vehicle speeds used were 5.0 and 10.0 ft/sec. During all runs the suspension spring rate was fixed at 10 lb/in. The results are plotted in Figures 5.5.25 and 26. For both units, a flat optimum lies between 3 and 5 lb sec/in.

5.5.17 Vehicle Response as a Function of Speed and Terrain

Having optimized the spring and damping rates of the vehicle suspensions, it was now possible to estimate vehicle dynamic performance on different terrains at various speeds.

Vehicle runs were simulated over random terrain with two degrees of roughness (1 ft and 0.5 ft rms) and over two obstacle terrains (heights 1 in. and .5 in). Runs were conducted at three velocities: 5 ft/sec; 10 ft/sec; and 15 ft/sec.

Additional runs were made using rigid wheels on both the random and the obstacle

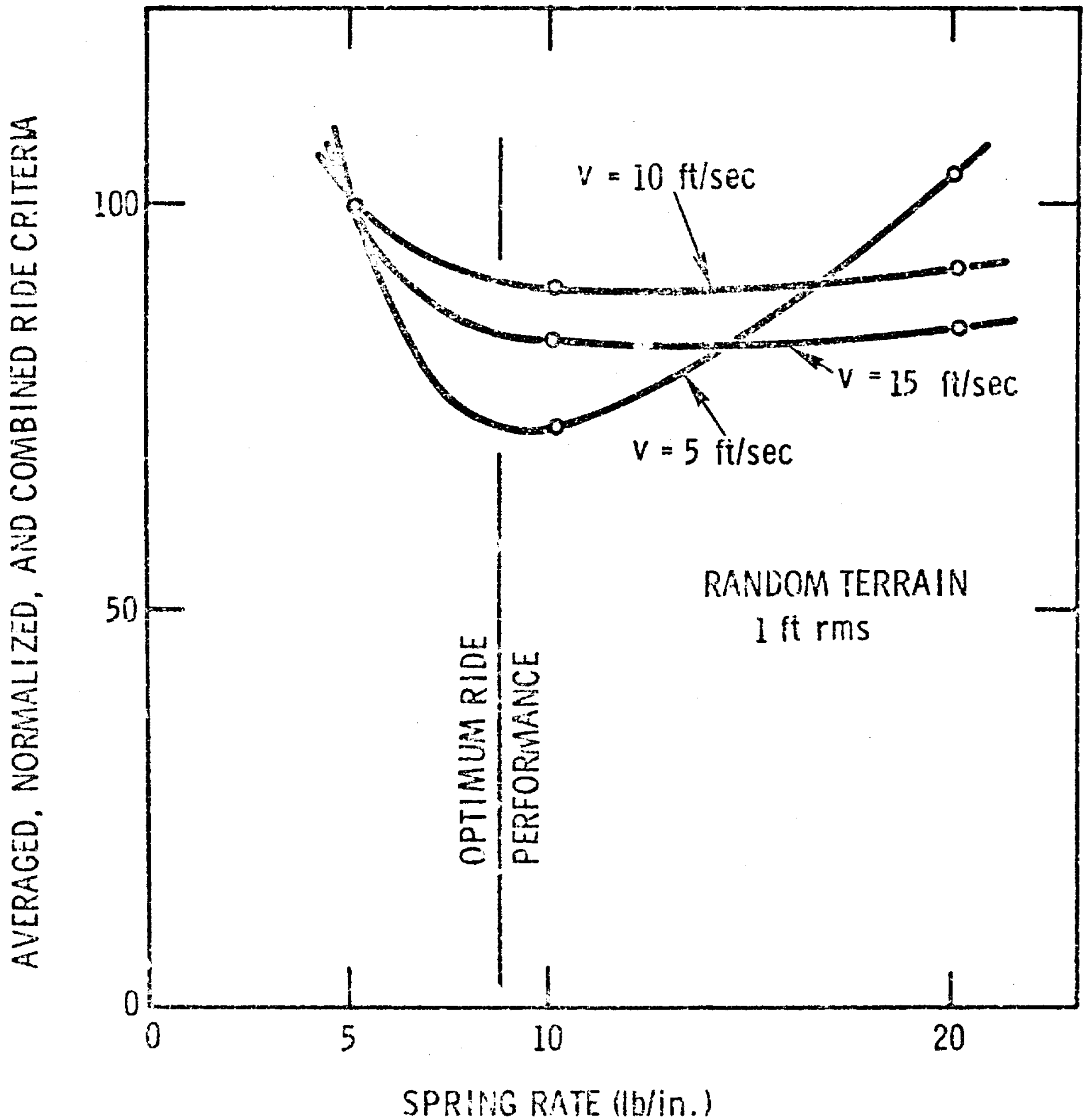

Figure 5.5.23 - Spring Optimization of Suspension Forward Unit

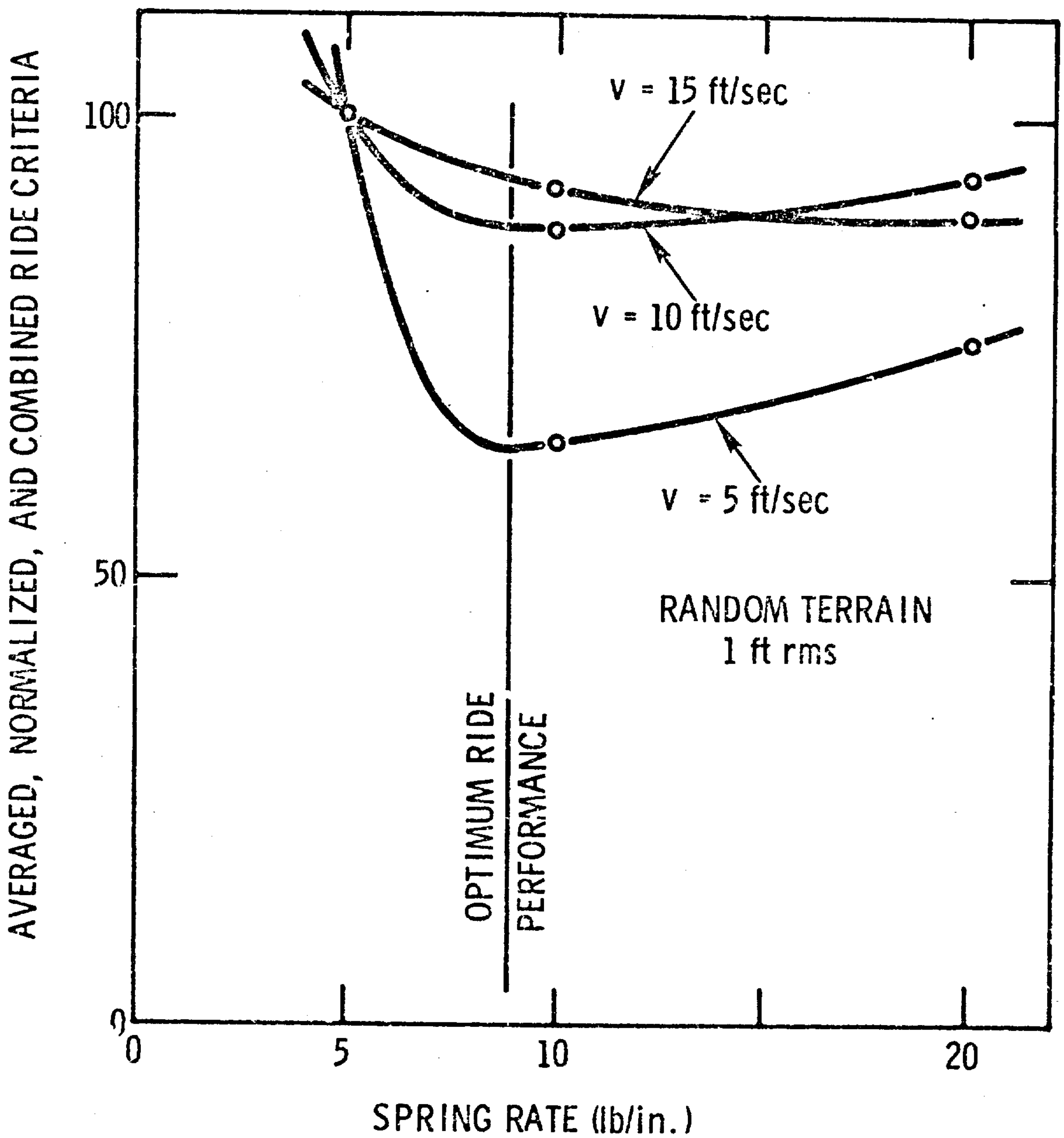

Figure 5.5.24 - Spring Optimization of Suspension Aft Unit

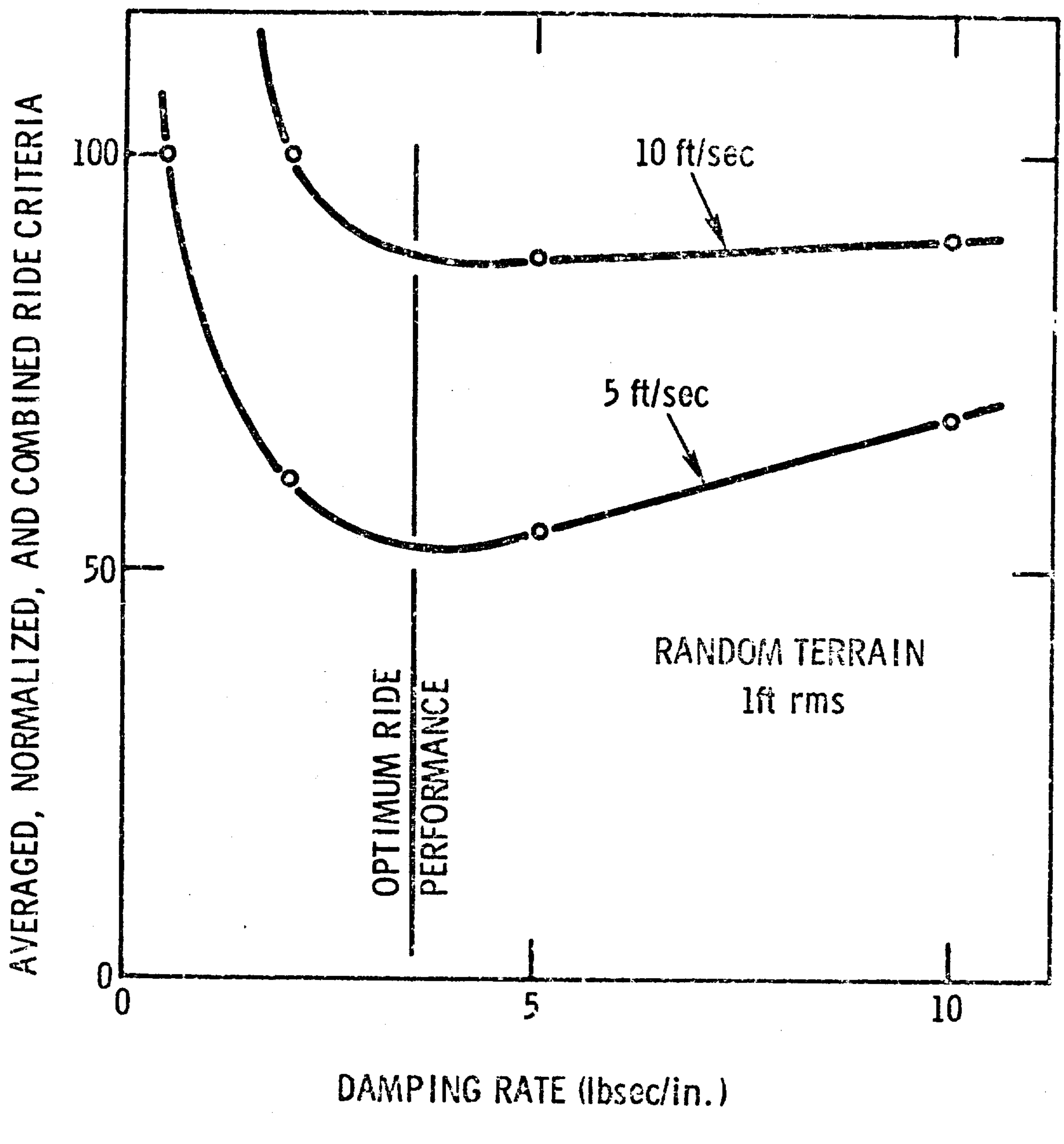

Figure 5. 5. 25 - Damper Optimization of Forward Unit

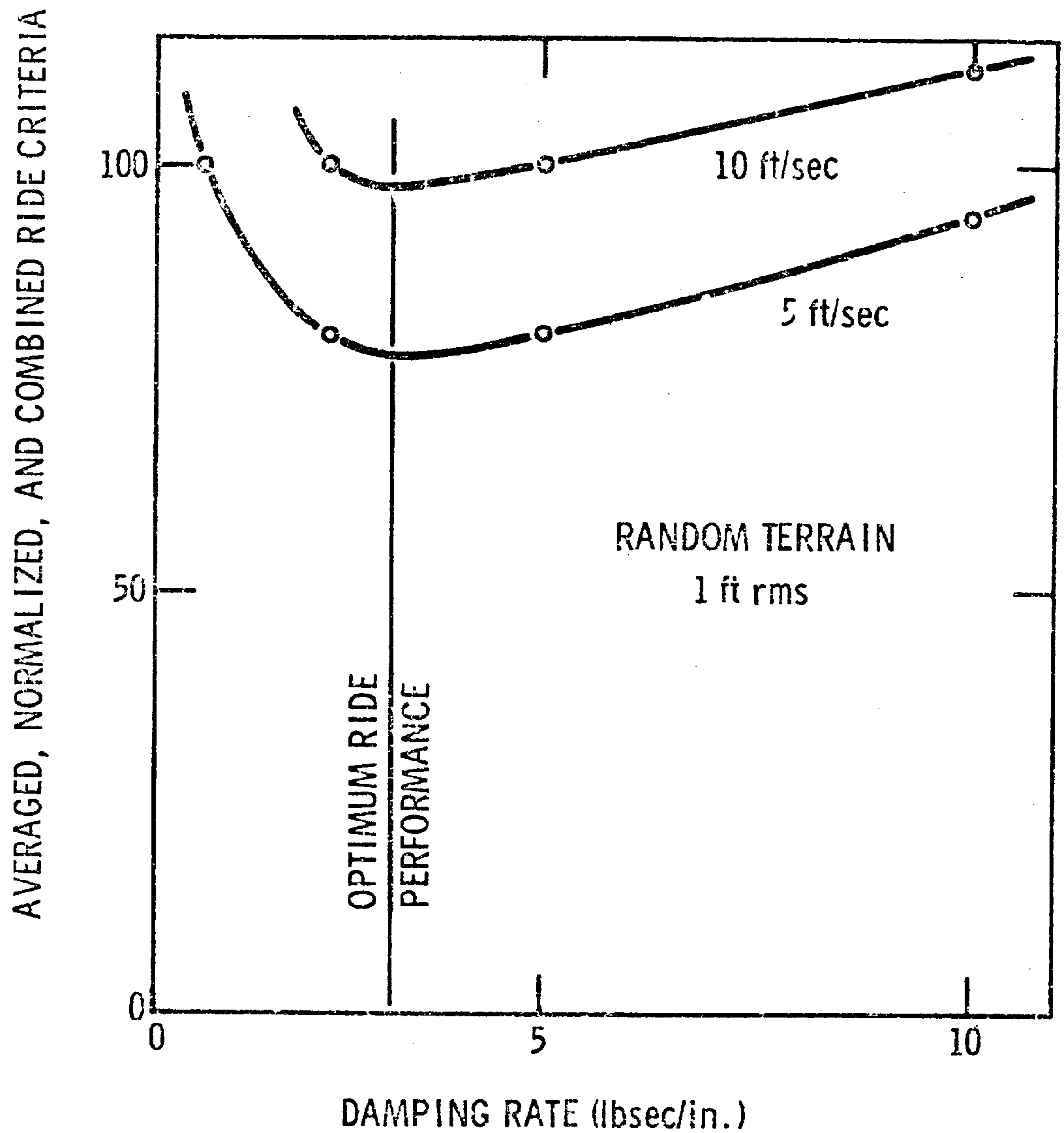

Figure 5.5.26 - Damper Optimization of Aft Unit

terrains to study the effect of terrain-wheel impact as a function of wheel flexibility. A few runs were also made with the vehicle stripped of all suspensions.

Figures 5.5.27 to 5.5.33 illustrate the performance characteristics of the forward and aft units of the vehicle with suspension and flexible wheels over the 1.0 ft rms random terrain.

Figure 5.5.27: Percent of time either one front wheel of the forward unit or both front wheels of the forward unit are off-the-ground, as a function of speed. Percent of time either one wheel of the aft unit or both wheels of the aft unit are off-the-ground, as a function of speed. The wheels of the forward unit are loosing contact with the ground a little more often than the wheels of the aft unit. At a speed of 10 ft/sec the two front wheels of the forward unit and the two wheels of the aft unit are off-the-ground about 10% of the travel time. This may signify the limit of effective controllability of the vehicle.

Figure 5.5.28: rms of vertical accelerations of the c.g. of the forward and aft units, as a function of time. The accelerations do not reach the human tolerance level on earth of approximately 100 in/sec^2 (rms), even at the maximum speed of 15 ft/sec.

Figure 5.5.29: rms of pitch accelerations of forward and aft unit, as a function of speed. The human tolerance level on earth is reached at a speed of about 13 ft/sec.

Figure 5.5.30: rms of roll accelerations of both units as a function of speed. The human tolerance level on earth is never reached.

Figure 5.5.31: Maximum angle between the two units as a function of speed. If the maximum allowable angle between the two units is, for instance, 15°, it is reached at a speed of 9 ft/sec. This is for the case where no pitch limiter is incorporated. If higher speeds are desirable, a pitch limiter should be provided.

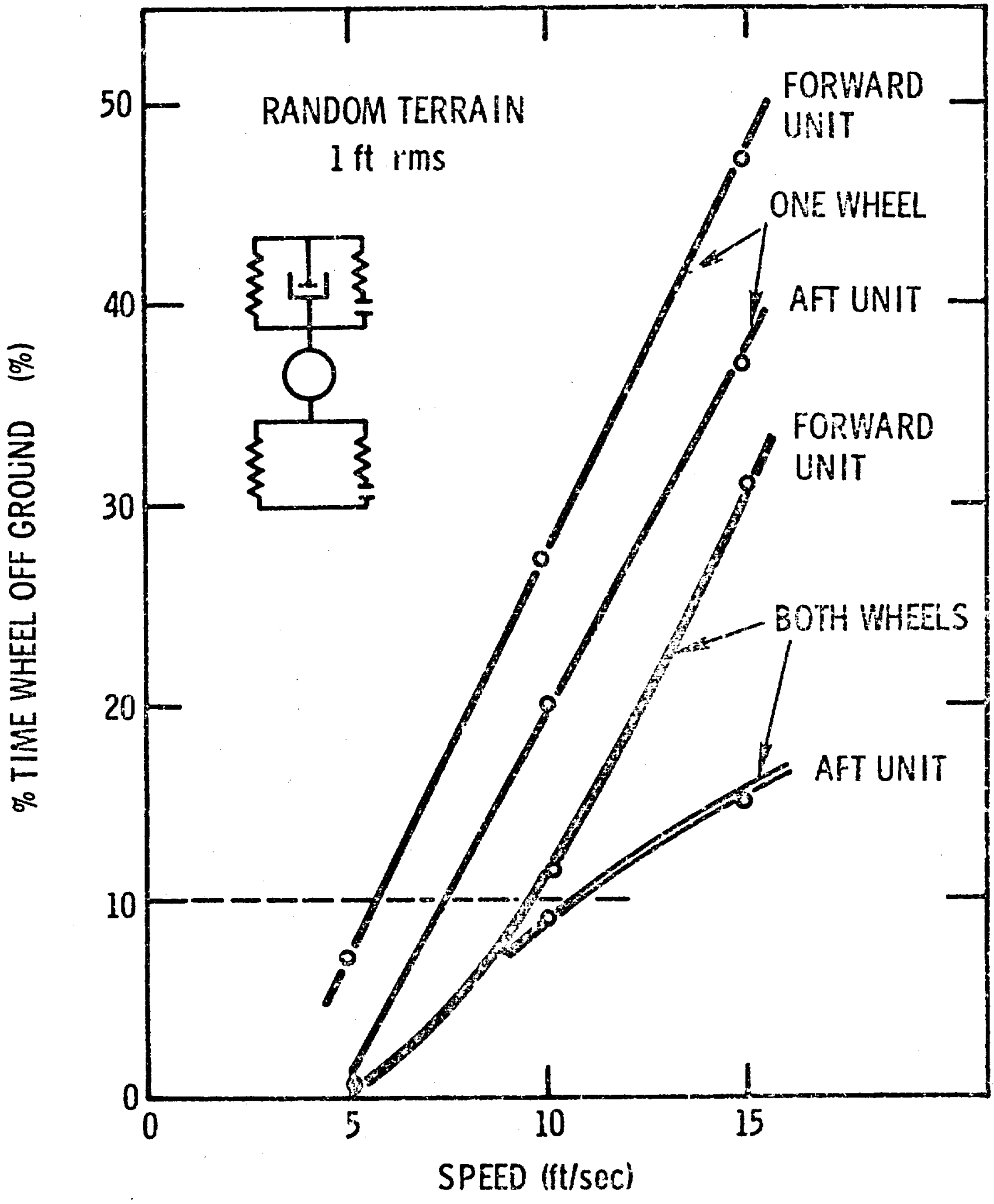

Figure 5.5.27 - Ride Performance of Optimized Vehicle On Random Terrain: Wheel Lift-Offs

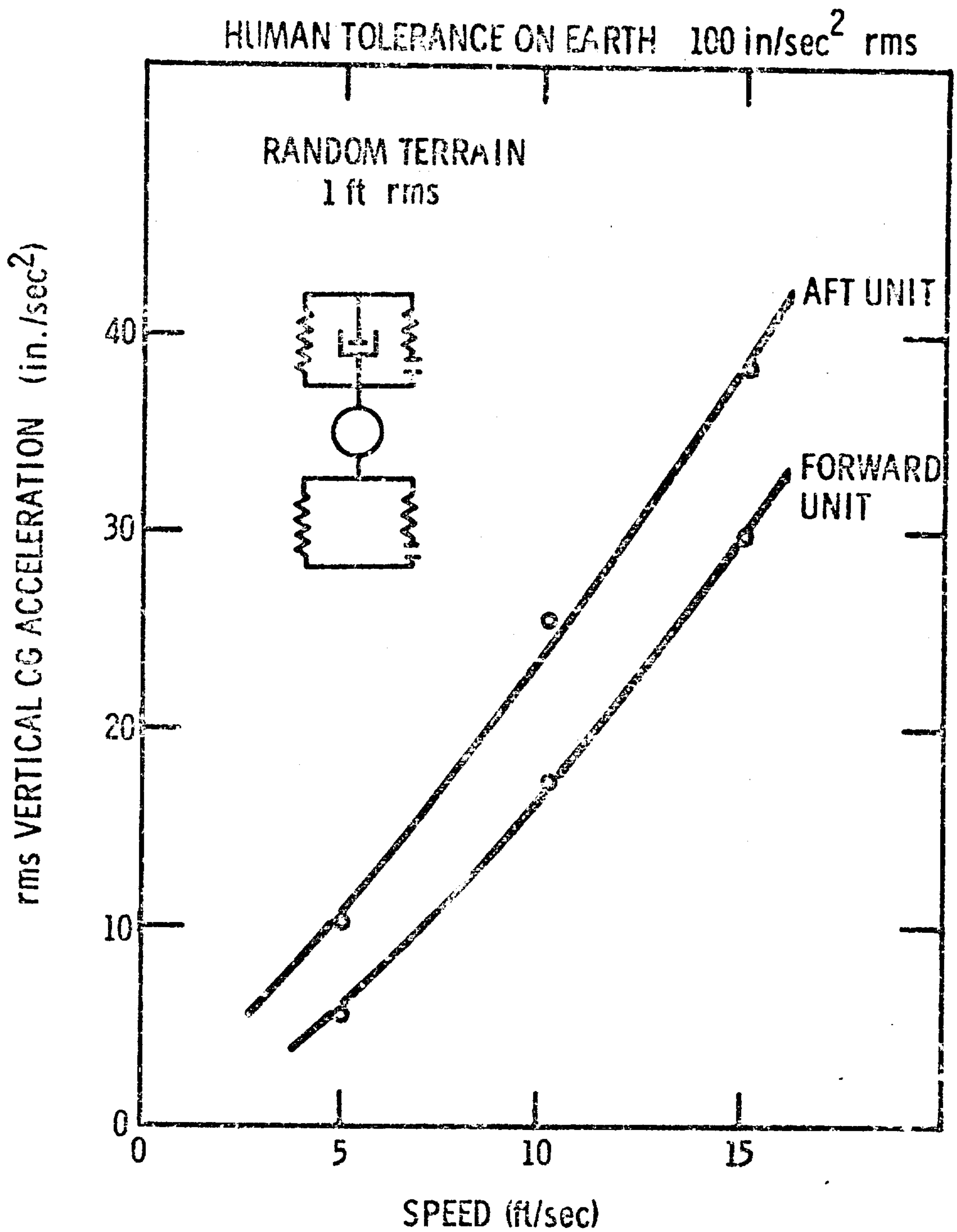

Figure 5.5.28 - Ride Performance of Optimized Vehicle On Random Terrain: Vertical Accelerations

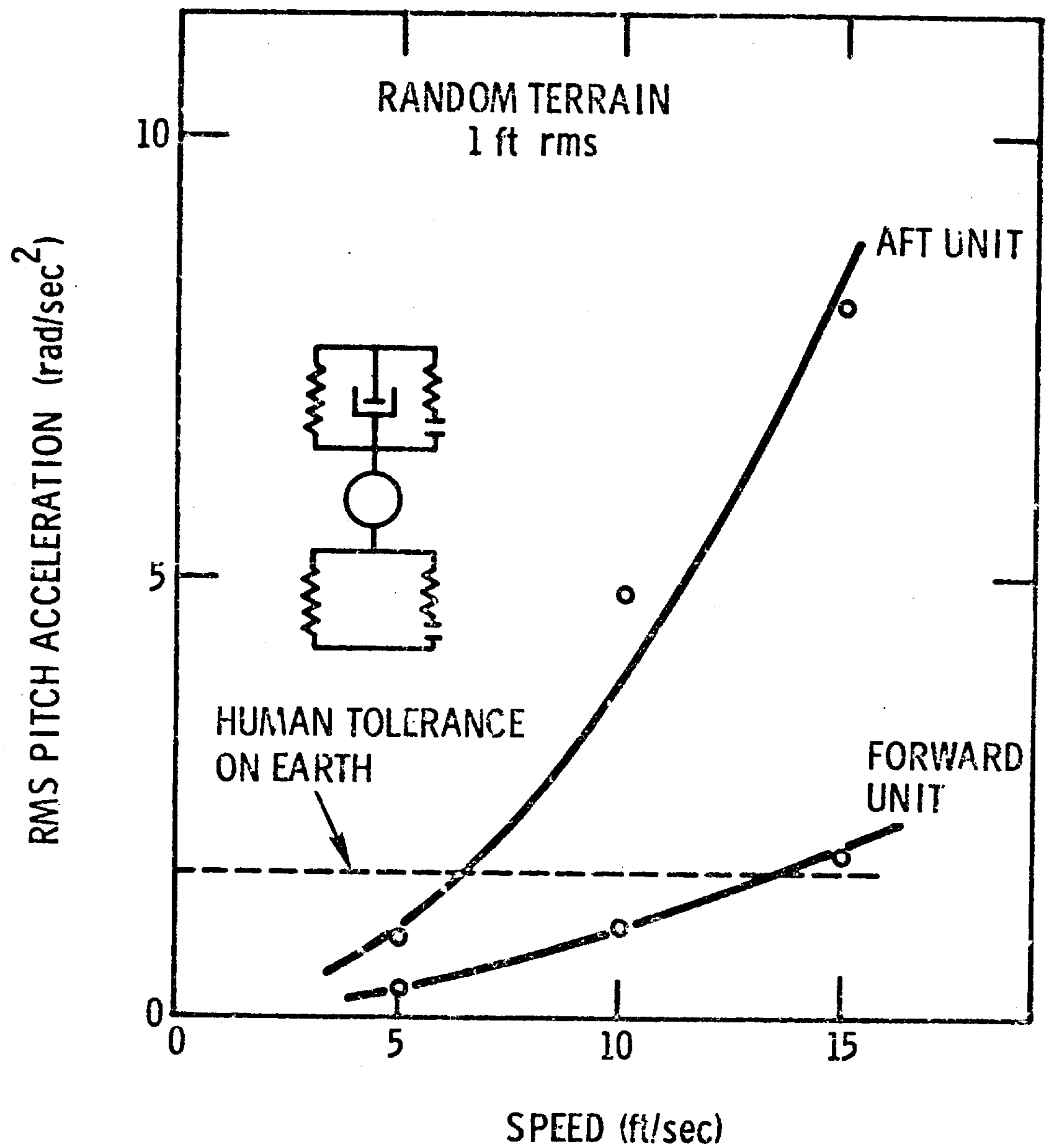

Figure 5.5.29 - Ride Performance of Optimized Vehicle On Random Terrain: Pitch Acceleration

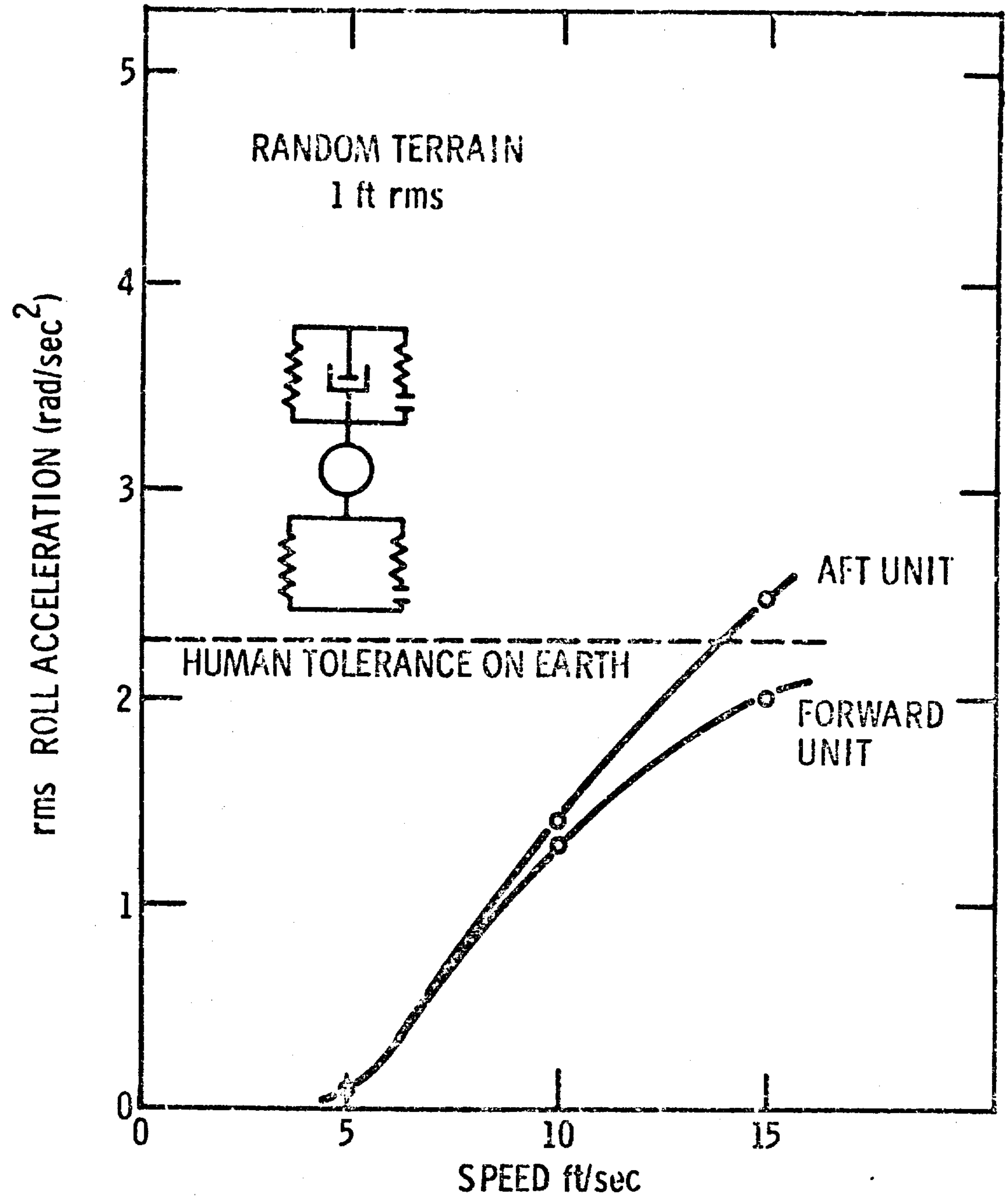

Figure 5.5.30 - Ride Performance of Optimized Vehicle On Random Terrain: Roll Acceleration

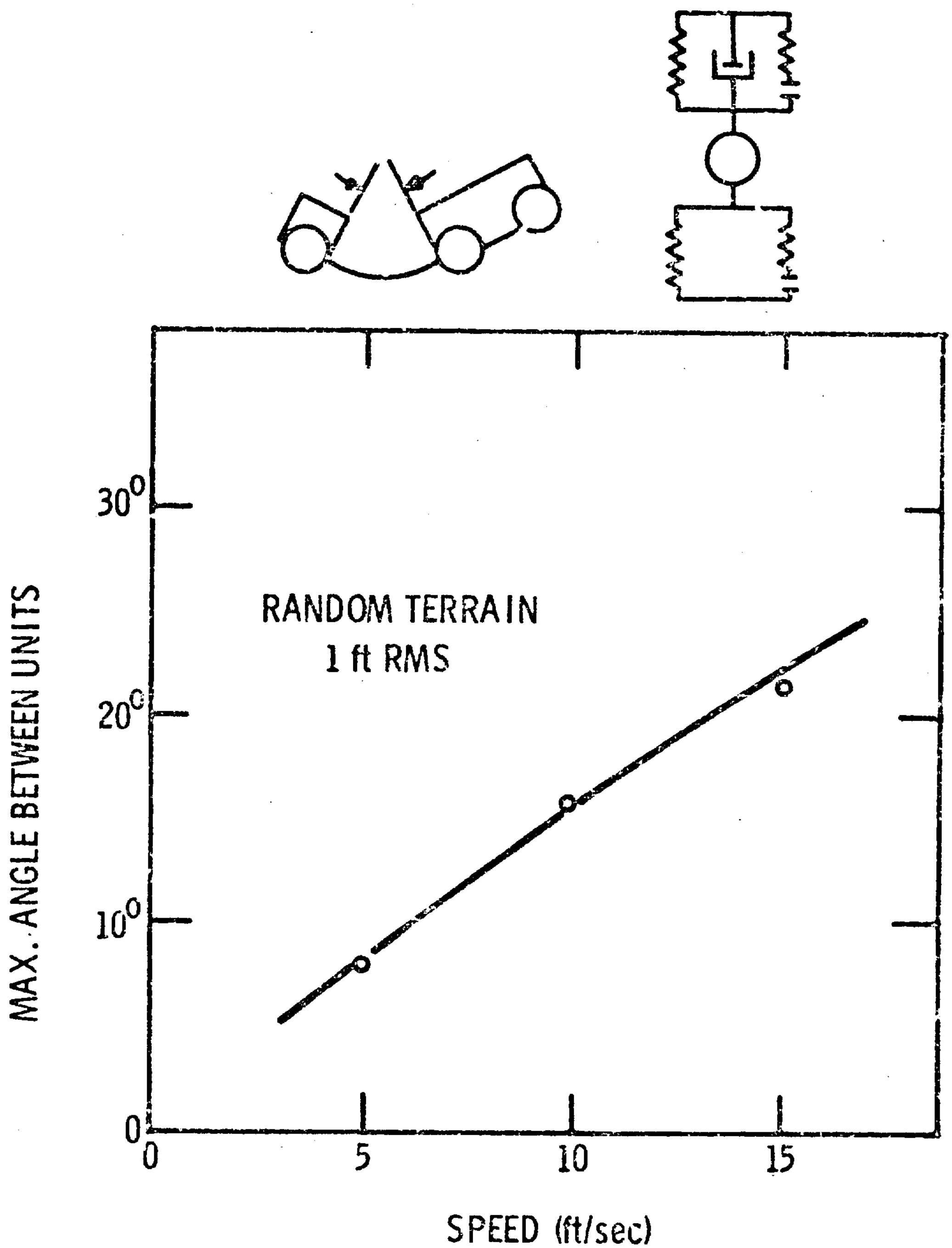

Figure 5.5.31 - Ride Performance of Optimized Vehicle On Random Terrain: Maximum Angle Between Units

Figure 5.5.32: dissipated damping power at one front wheel as a function of speed. This information was utilized to help determine total energy required for locomotion.

Figure 5.5.33: The percentage of time the force between wheel and the ground is greater than a certain force depends on the speed of the vehicle. At a force of 100 lb, which is roughly the force where the inner frame of the wheel becomes active, we can see that at 5 ft/sec the inner frame is engaged only 3% of the time. At 10 ft/sec it is engaged 30% of the time and at 15 ft/sec 45% of the time. These numbers indicate the difficulties of reconciling low lunar weights and high mass forces (which do not change with gravity).

Summarizing the above results, it appears that the maximum speed on random terrain of the Mare-Cognitum type of the LSSM vehicle with optimized suspension and flexible wheels would be approximately 10 ft/sec. At higher speeds the wheels leave the ground more than 10% of the time, the human tolerance level for pitch accelerations is reached, and the angle between the two units surpasses 15°.

Figures 5.5.34 to 5.5.37 compare the response of the forward unit equipped with three different wheel-suspension combinations operating on random terrain (1 ft and 0.5 ft rms). The three combinations are: suspended flexible wheel; suspended rigid wheel; and non-suspended flexible wheel.

Figure 5.5.34: percentage of time one front wheel of the forward unit is off-the-ground as a function of speed, wheel-suspension combination, and terrain roughness. On both terrains the non-suspended wheel performs worst; the suspended, flexible wheel performs best. The same is true for

Figure 5.5.35: percentage of time both front wheels of the forward unit are off-the-ground as a function of speed, wheel type, and terrain roughness. If 10% of the time off-the-ground is the limit of maximum effective controllability, the upper speed limit of the vehicle with unsuspended wheels on random terrain with 1.0 ft rms would be 6 ft/sec, whereas on the same terrain, the vehicle

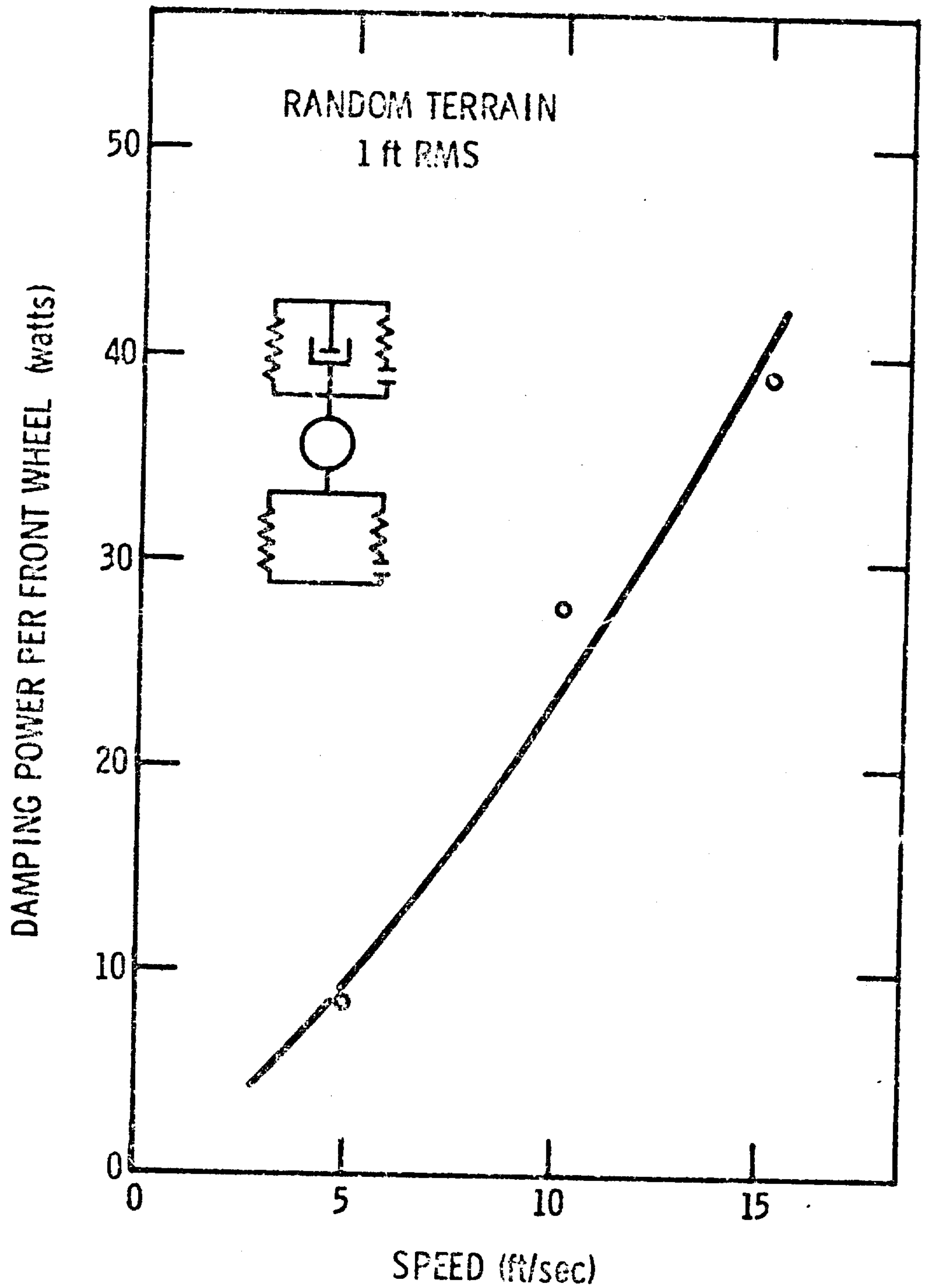

Figure 5.5.32 - Ride Performance of Optimized Vehicle
On Random Terrain: Damping Power

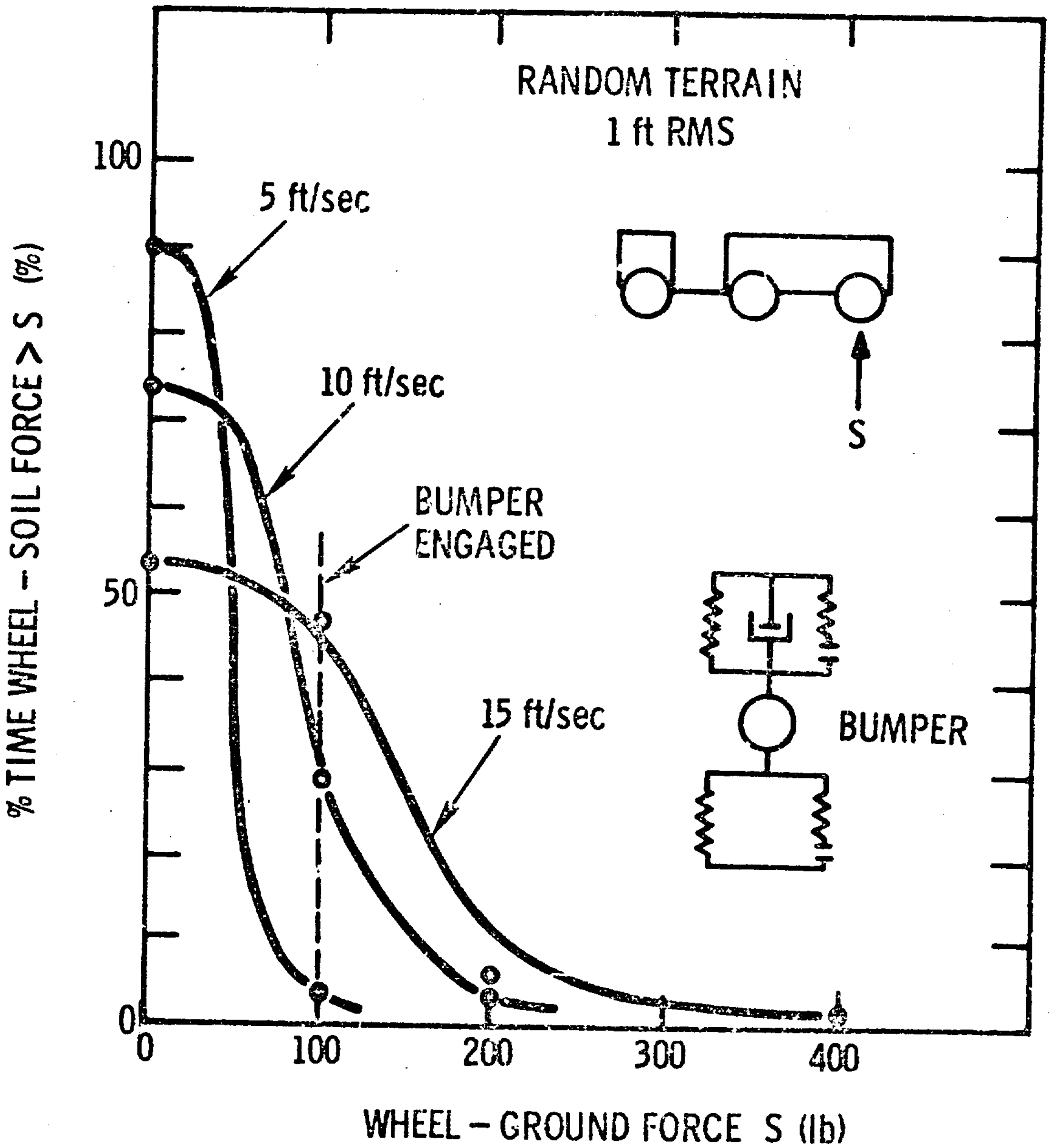

Figure 5.5.33 - Ride Performance of Optimized Vehicle On Random Terrain: Wheel-Ground Force

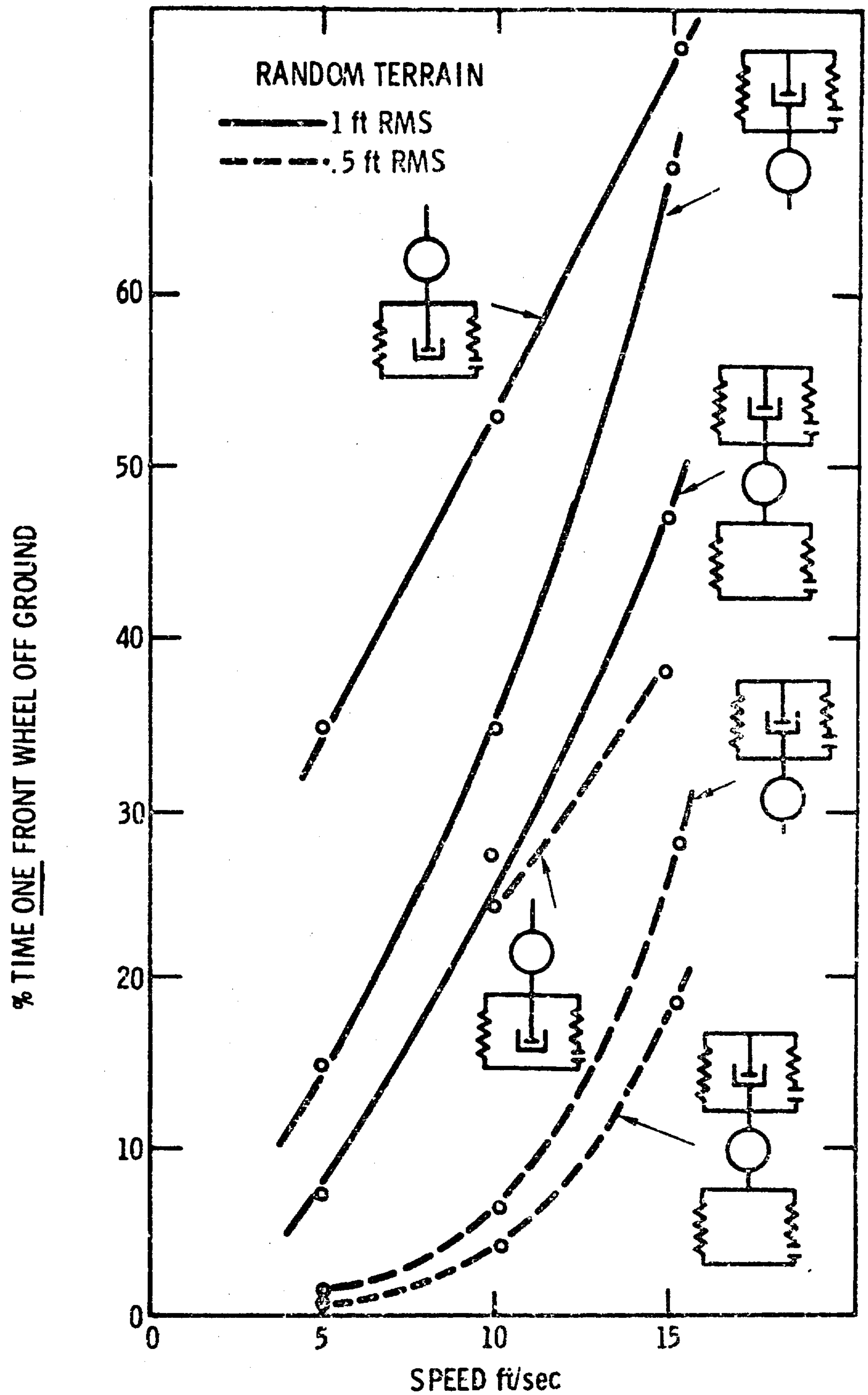

Figure 5.5.34 - Ride Performance of Three Wheel Types On Random Terrain: Wheel Lift-Offs

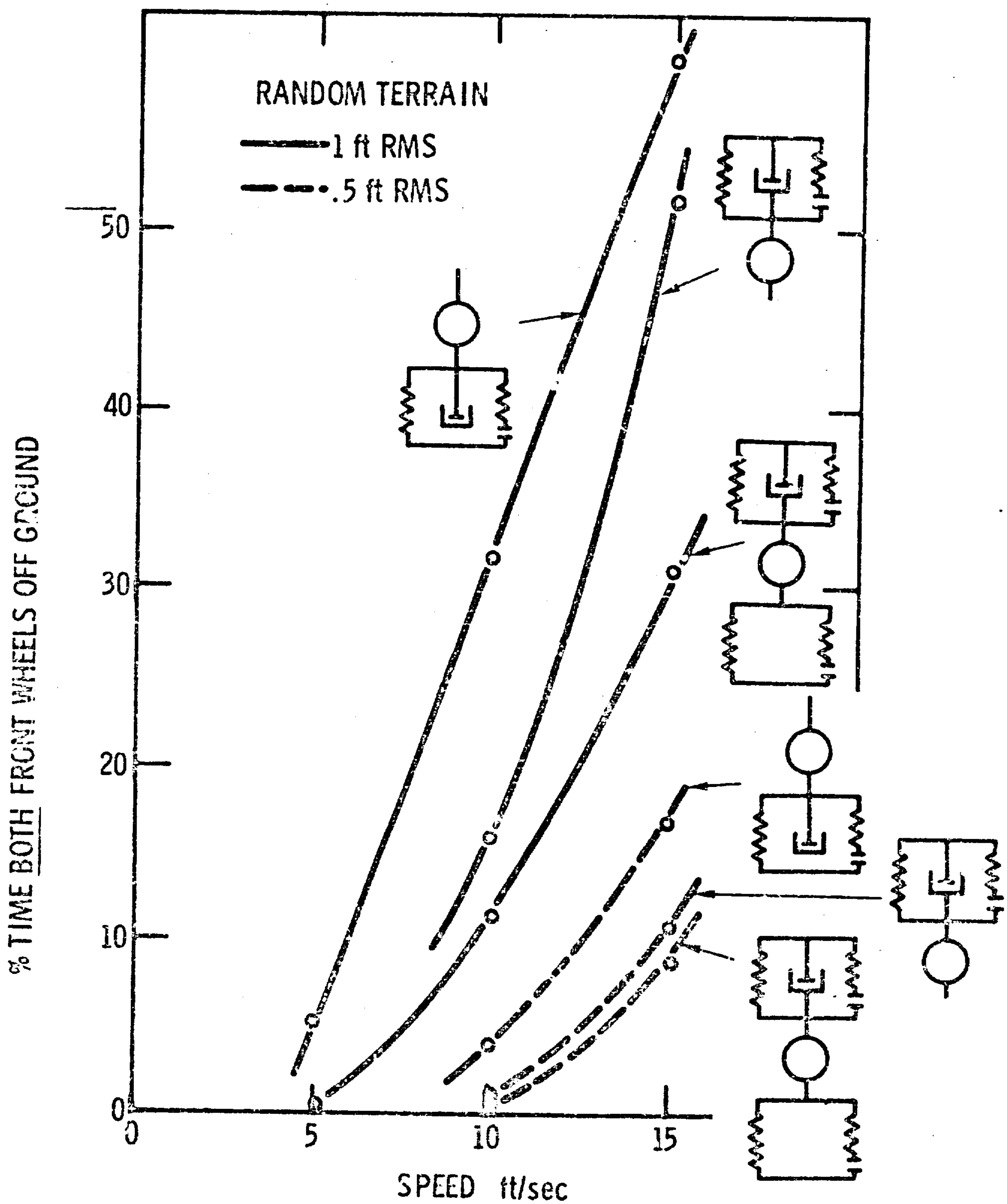

Figure 5.5.35 - Ride Performance of Three Wheel Types on Random Terrain: Wheel Lift-Offs

with suspended, flexible wheels could go at 10 ft/sec.

Figure 5.5.36: rms of vertical acceleration of the forward unit as a function of speed, wheel type, and terrain roughness. The figure indicates clearly the superiority of the suspended wheel over the unsuspended wheel.

Figure 5.5.37: rms of pitch acceleration of the forward unit as a function of speed, wheel type, and terrain roughness. On both terrains the vehicle with suspended wheels performs better than one with non-suspended wheels. On the 1-ft terrain, in the case of the non-suspended wheel, the human tolerance level is surpassed at a speed of 6 ft/sec, whereas for the suspended wheel, be it rigid or flexible, the tolerance level is reached at 14 ft/sec.

Based on the above results, it can be concluded that a suspended wheel allows higher speeds and gives a smoother ride than the non-suspended wheel. The performance differences between the rigid and flexible wheel, both suspended, are small. This is not surprising because the random terrain wavelengths are much larger than the wheel footprint. The difference in performance between these two wheels can be assessed more distinctly on terrain with obstacles smaller in size than the footprint. In this latter case the flexible wheel would tend to envelop the obstacle whereas the rigid wheel would follow the terrain contour, thus developing rather high accelerations and forces.

The comparison between rigid and flexible wheels is demonstrated in Figures 5.5.38 to 41. The vehicle was operated over terrain with periodic, small triangular obstacles (1 in. and 0.5 in. high). Again with the suspended flexible wheel, the suspended rigid wheel, and the non-suspended flexible wheel were compared.

Figure 5.5.38: percent of time both front wheels of the forward unit are off-the-ground, as a function of speed, obstacle height, and wheel type. The rigid wheel is off-the-ground most of the time whereas the soft wheel never loses contact, even at the maximum speed of 15 ft/sec.

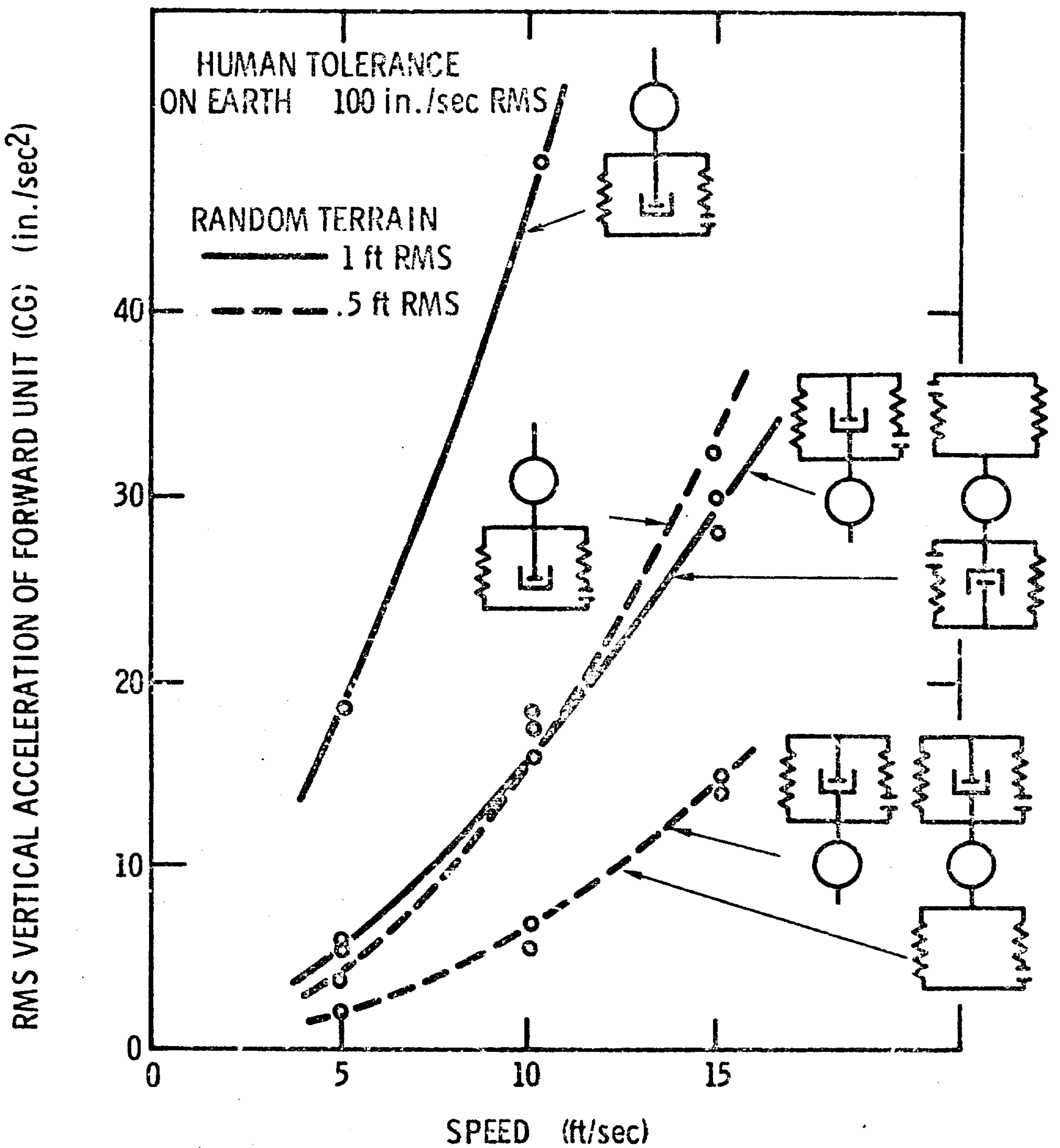

Figure 5.5.36 - Ride Performance of Three Wheel Types on Random Terrain: Vertical Acceleration

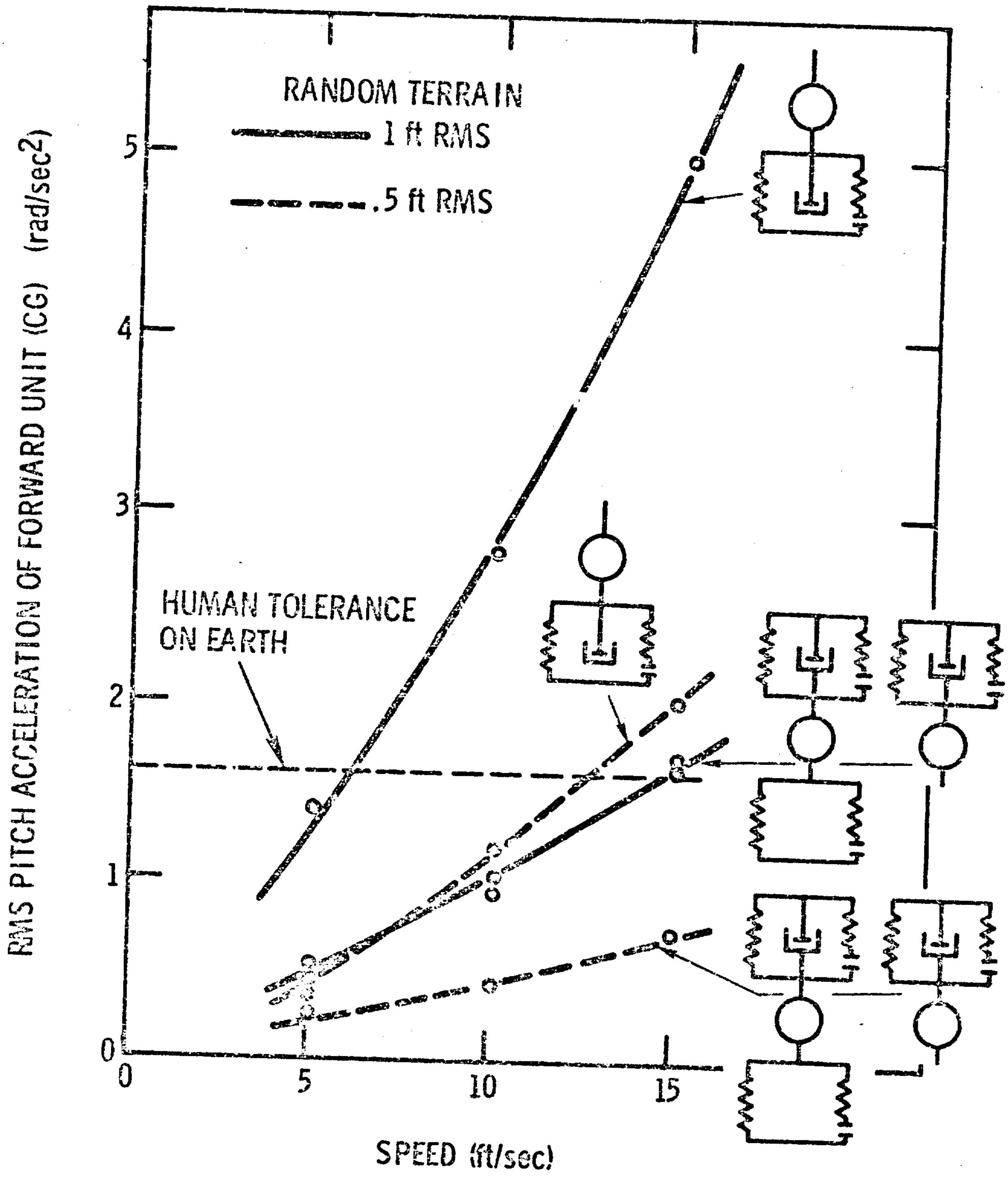

Figure 5.5.37 - Ride Performance of Three Wheel Types on Random Terrain: Pitch Acceleration

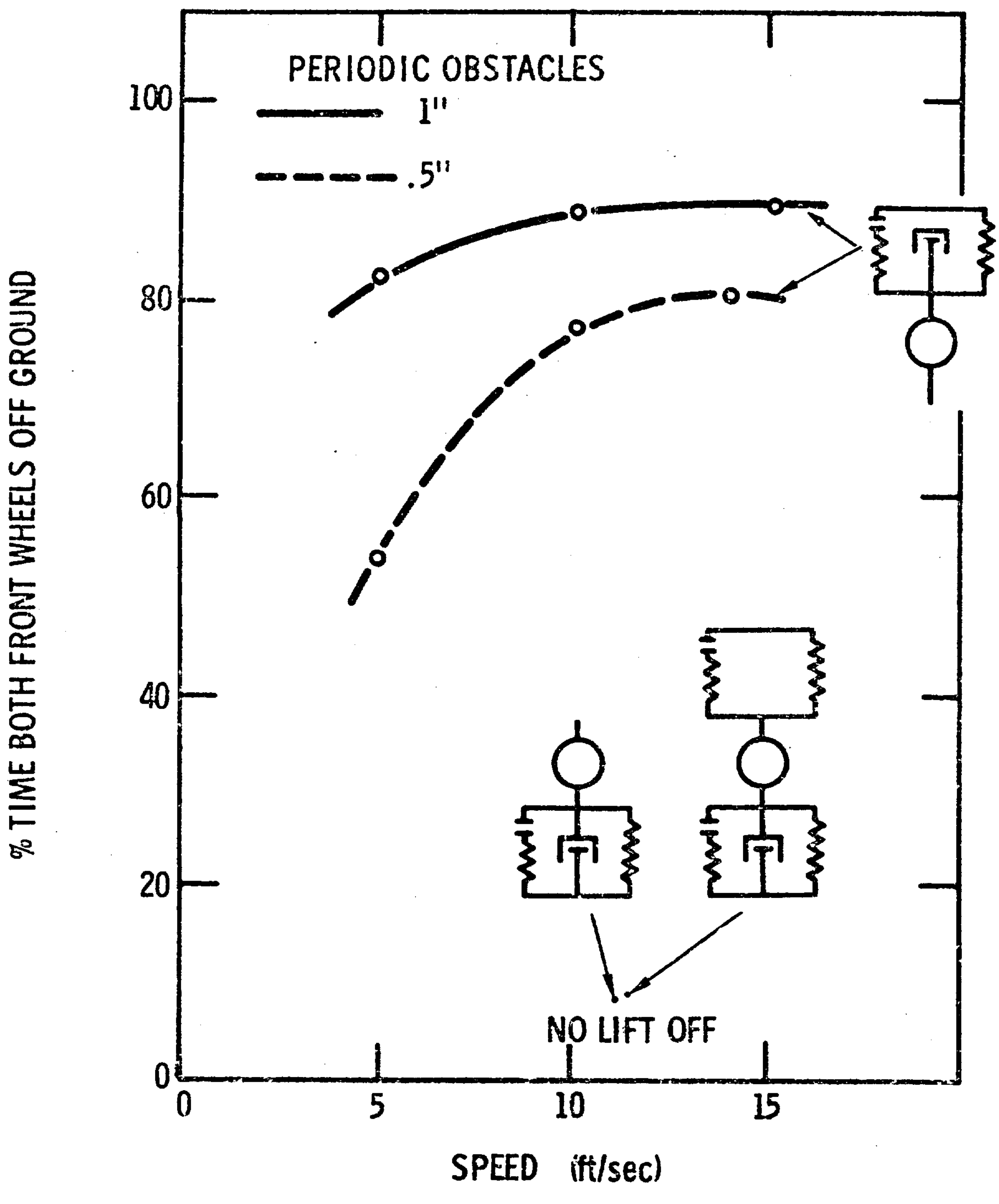

Figure 5.5.38 - Ride Performance of Three Wheel Types on Obstacle Terrain: Wheel Lift-Offs

Figure 5.5.39: rms of vertical acceleration of the cg of the forward unit as a function of speed, obstacle height, and wheel type. The vertical acceleration in the case of the rigid wheel is an order-of-magnitude higher than vertical acceleration for the soft suspended wheel. The flexible, non-suspended wheel also results in rather high accelerations.

Figure 5.5.40: rms of pitch acceleration of the cg of the forward unit as a function of speed, obstacle height, and wheel type. The acceleration for the rigid wheel exceeds the human tolerance level at all speeds, whereas the flexible suspended wheel develops very small accelerations. The performance of the flexible wheel without suspension is also unsatisfactory.

Figure 5.5.41: peak forces between the front wheels of the forward unit and the ground as a function of speed, obstacle height, and wheel type. This figure demonstrates the excessively high peak forces for the rigid wheel, caused by continuously impacting the ground.

Thus, it can be concluded that the suspended flexible soft wheel out performs both the rigid wheel and the non-suspended wheel by far. On a random terrain of the Mare-Cognitum type a suspended wheel permits 4 to 8 ft/sec. higher speeds than an non-suspended wheel; on a terrain with obstacles smaller than the footprint, rigid wheels would bounce continously and develop very high impact forces.

5.5.18: Dynamic Stability on Slopes

On the moon, weight forces are one-sixth as large as on earth. Consequently, mass forces, spring forces and damping forces dominate vehicle performance on the moon. The interplay between these forces determines the smoothness of the ride and the controllability of the vehicle, as has been demonstrated in this study.

Besides smoothness of ride and controllability, another dynamic criterion should be considered as vital for safe and satisfactory vehicle performance; that is,

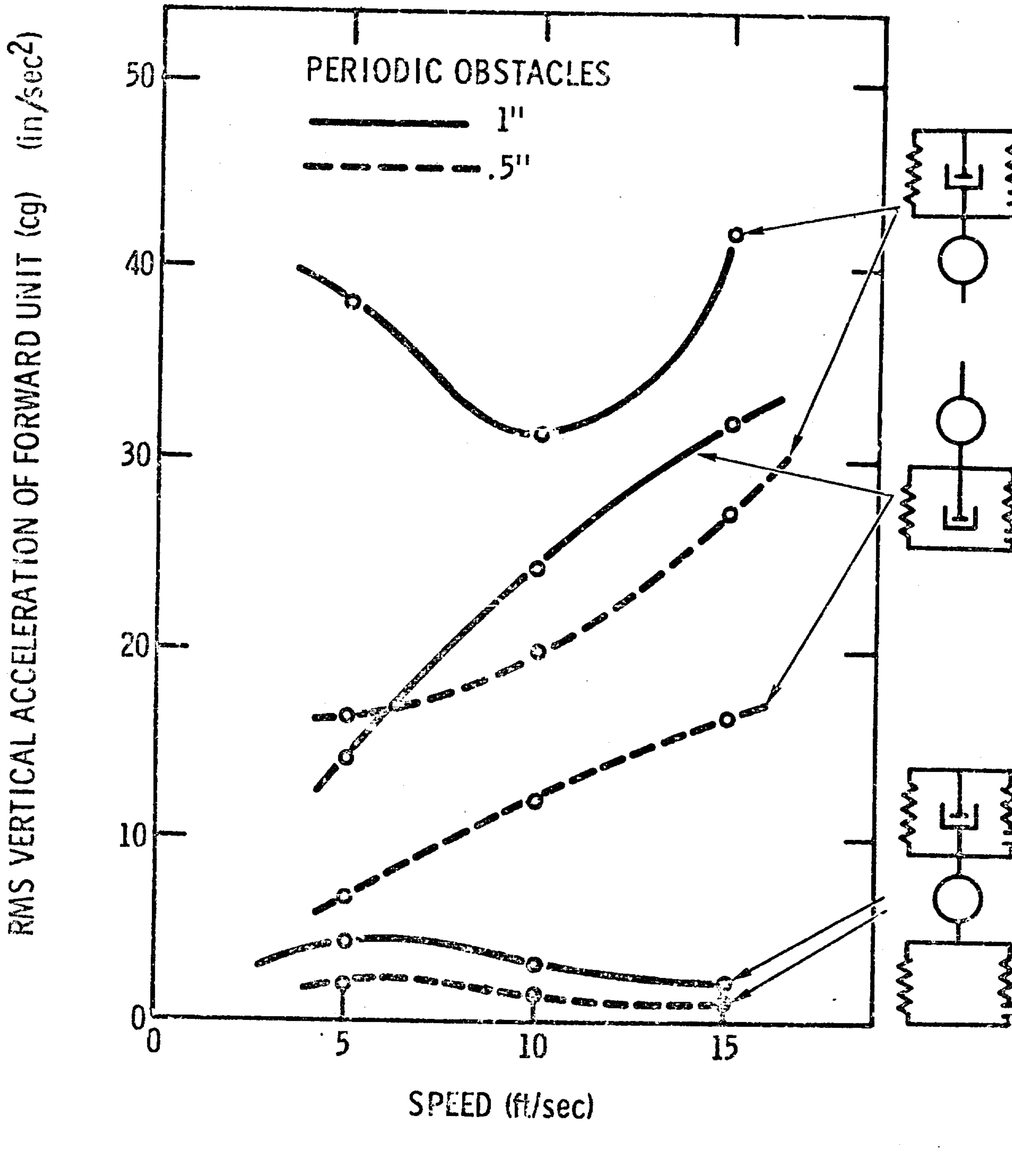

Figure 5.5.39 - Ride Performance of Three Wheel Types on Obstacle Terrain: Vertical Acceleration

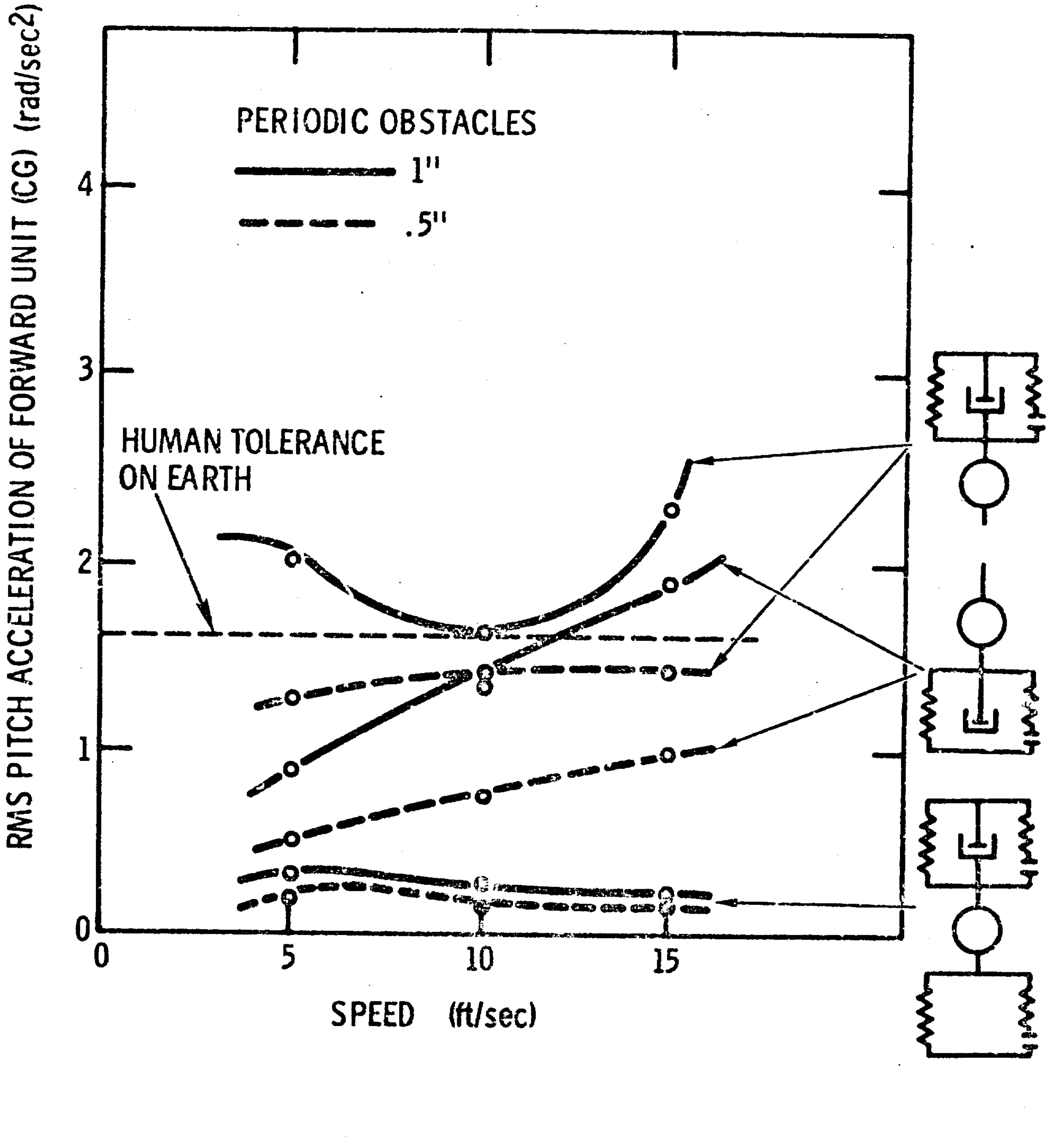

Figure 5.5.40 - Ride Performance of Three Wheel Types on Obstacle Terrain: Pitch Acceleration

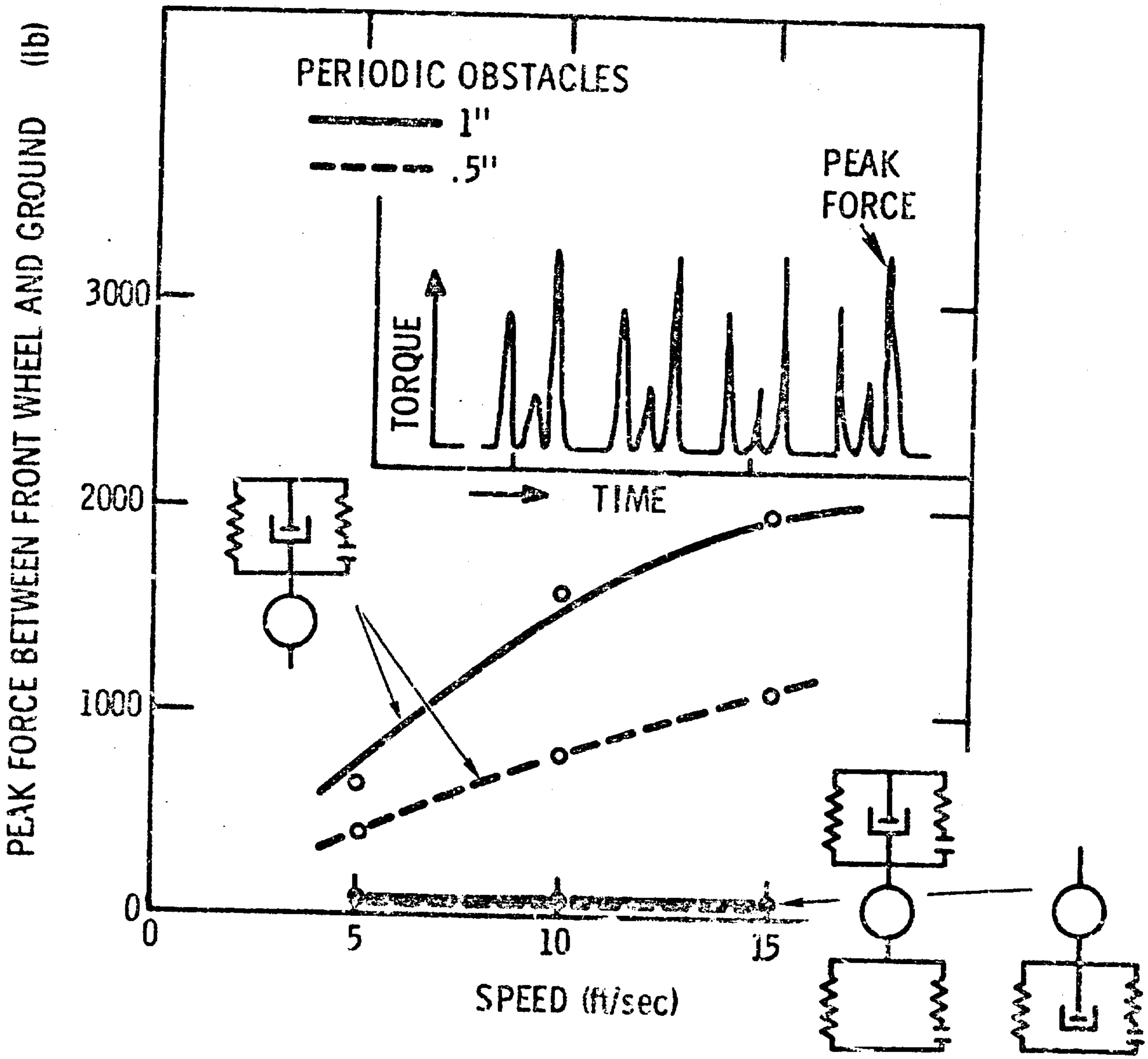

Figure 5.5.41 - Ride Performance of Three Wheel Types on Obstacle Terrain: Wheel-Ground Force

dynamic stability. Because mass, spring, and damping forces on the moon are counteracted only by small weight forces, a lunar vehicle is subject to greater instability than a terrestrial vehicle.

The stability of the vehicle has not been dealt with thoroughly in this study because it requires a mathematical model based on real angles and not on small angles. At small angles, the vehicle is supposedly always stable; instability, however, can be studied even if the vehicle model is based on the small-angle assumption by initiating a transition stage for the vehicle and observing the wheel lift-offs. It can be assumed that if the wheels leave the ground during the transition for a long period of time, the vehicle may be considered to be in an unstable condition. This, of course, is a crude procedure and cannot replace a serious computation based on real angles; however it will indicate the range in which instabilities may occur, and possibly, form a basis for a more exact study.

The following estimate of vehicle stability is based on a transition time of 10 to 20 seconds; if within this time period the wheels lose contact for more than 2 to 3 seconds, we consider the vehicle to be in a state of instability.

To affect a transition time of 10 to 20 seconds, the vehicle was assumed to be traveling on a slope and hitting a bump as was pictured in Figure 5.5.4. Two cases were considered: a front slope with a bump contacting both wheels of an axle simultaneously, and a side slope with a bump contacting the upper wheels of the vehicle.

Computer runs were conducted at two vehicle speeds (4 ft/sec and 15 ft/sec), three slope inclinations (0°, 15°, 30°), and two bump heights (1 ft, 2 ft).

The computer results presented in Figures 5.5.42 to 47 are not immediately applicable to LSSM performance because they were obtained for a lunar vehicle three times heavier than the LSSM (MOLAB - with a lunar weight of 1,200 lbs). However, dimensional analysis, based on the use of Froude and Cauchy numbers, indicated that the stability of the LSSM will be about the same as that of MOLAB.

Figures 5.5.42 to 5.5.45: Wheel lift-off and wheel-ground force for the forward and aft units for two step heights and two speeds, as a function of time. These figures are traces of computer records selected as typical specimens of the changing wheel-ground forces during the transition stage. After hitting the bump the wheel-ground force first increases to a maximum, and then decreases to a minimum which is zero when the wheel leaves the ground. If the wheel leaves the ground for longer than two seconds the vehicle is assumed to be in a state of instability. A striking example of instability is shown in Figure 5.5.45, where the vehicle on a front slope hits a bump 2 ft high with a speed of 15 ft/sec.

Figures 5.5.46 and 5.5.47: These figures are an attempt to find stability limits as a function of speed, bump height, and slope angle. Fox example, if the vehicle hits a bump 2 ft high with one wheel on the horizontal plane ($\beta = 0^{\circ}$), it may become unstable at speeds greater than 10 ft/sec. If it hits the same bump with two wheels simultaneously ($\alpha = 0^{\circ}$), it becomes unstable at a lower speed, that is at 6 ft/sec. The same bump on a side slope, tilted only 15° reduces the speed to 6.5 ft sec, whereas the bump on a front slope with $\alpha = 15^{\circ}$ limits the allowable speed to 4 ft/sec.

These may suffice to demonstrate the importance of dynamic stability investigations. Correctly executed they will yield a strong criterion for the evaluation of lunar vehicle performance.

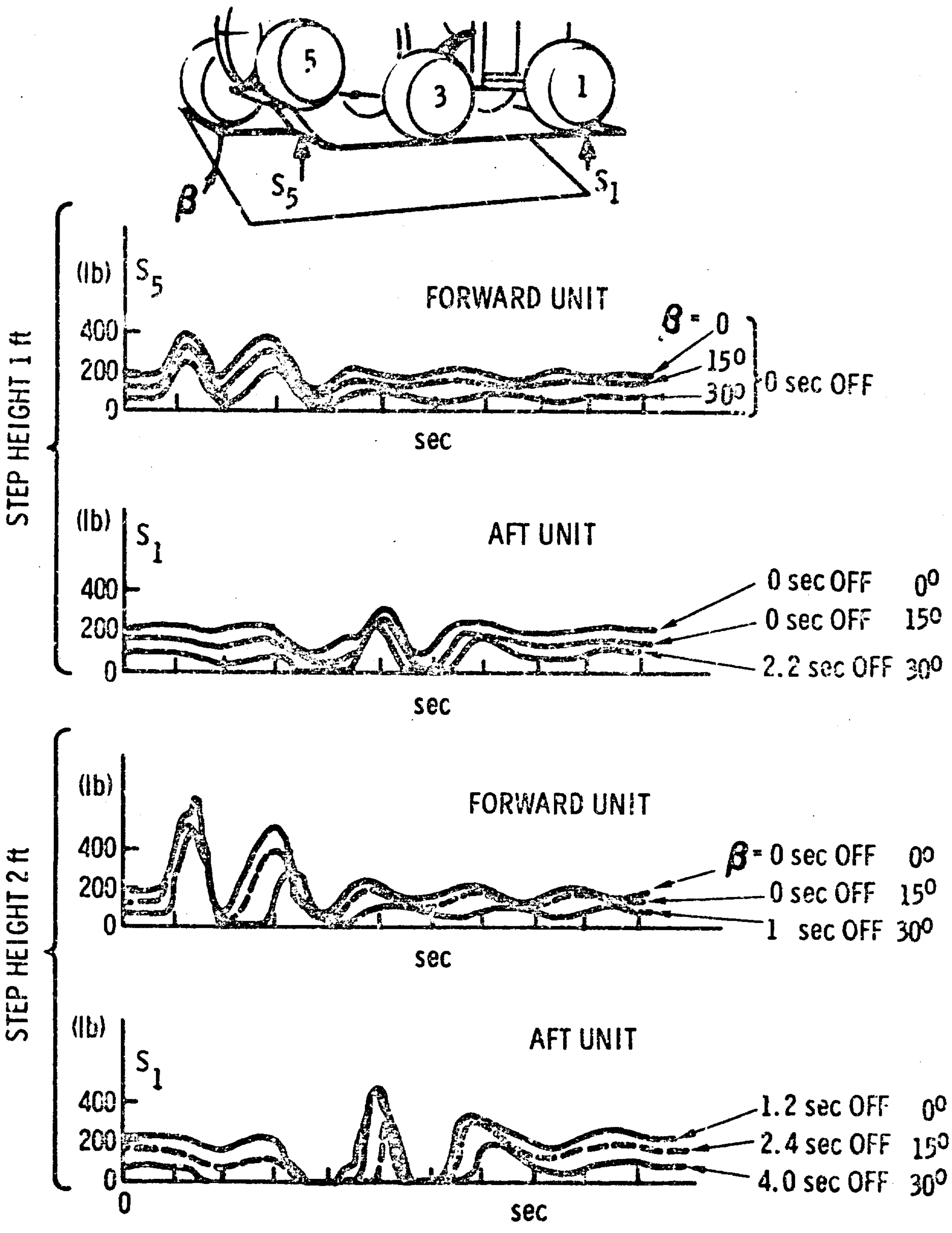

Figure 5.5.42 - Vehicle on a Side Slope: Wheel Lift-Off and Wheel Force - Speed - 4 ft/sec

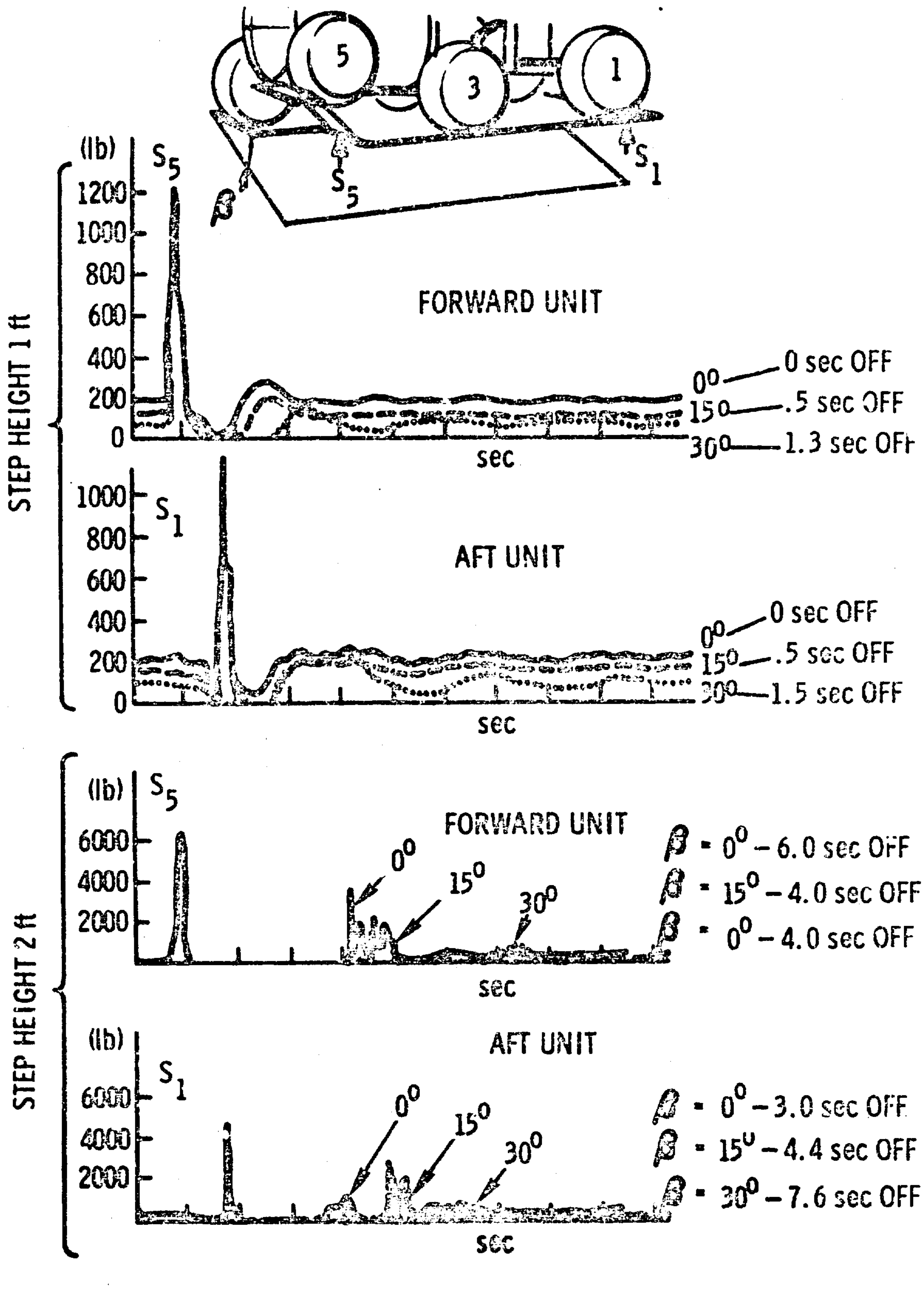

Figure 5.5.43 - Vehicle on a Side Slope: Wheel Lift-Off and Wheel Force - Speed - 15 ft/sec

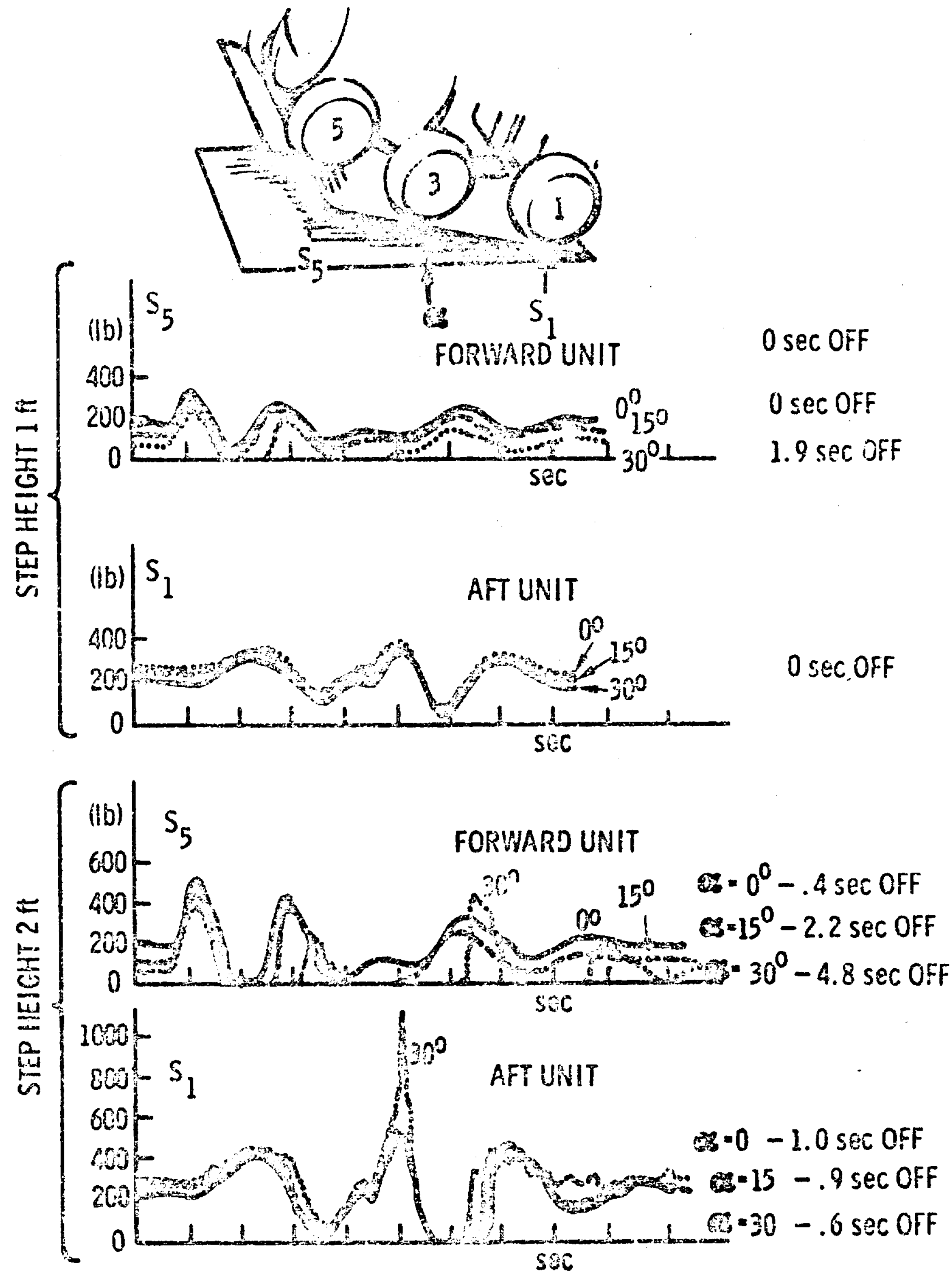

Figure 5.5.44 - Vehicle on a Front Slope: Wheel Lift-Off and Wheel Force - Speed - 4 ft/sec

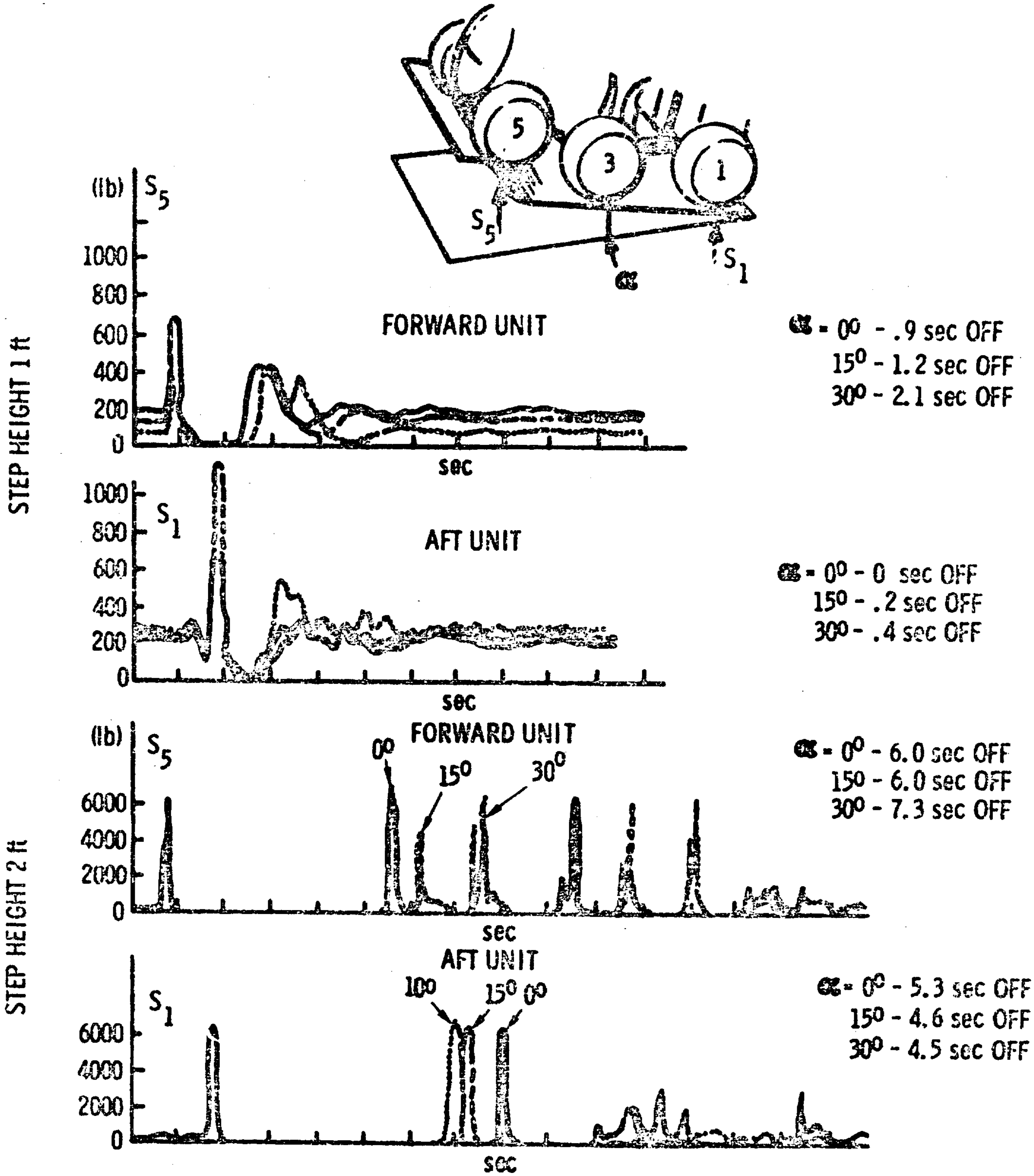

Figure 5.5.45 - Vehicle on Front Slope; Wheel Lift-Off and Wheel Force - Speed - 15 ft/sec

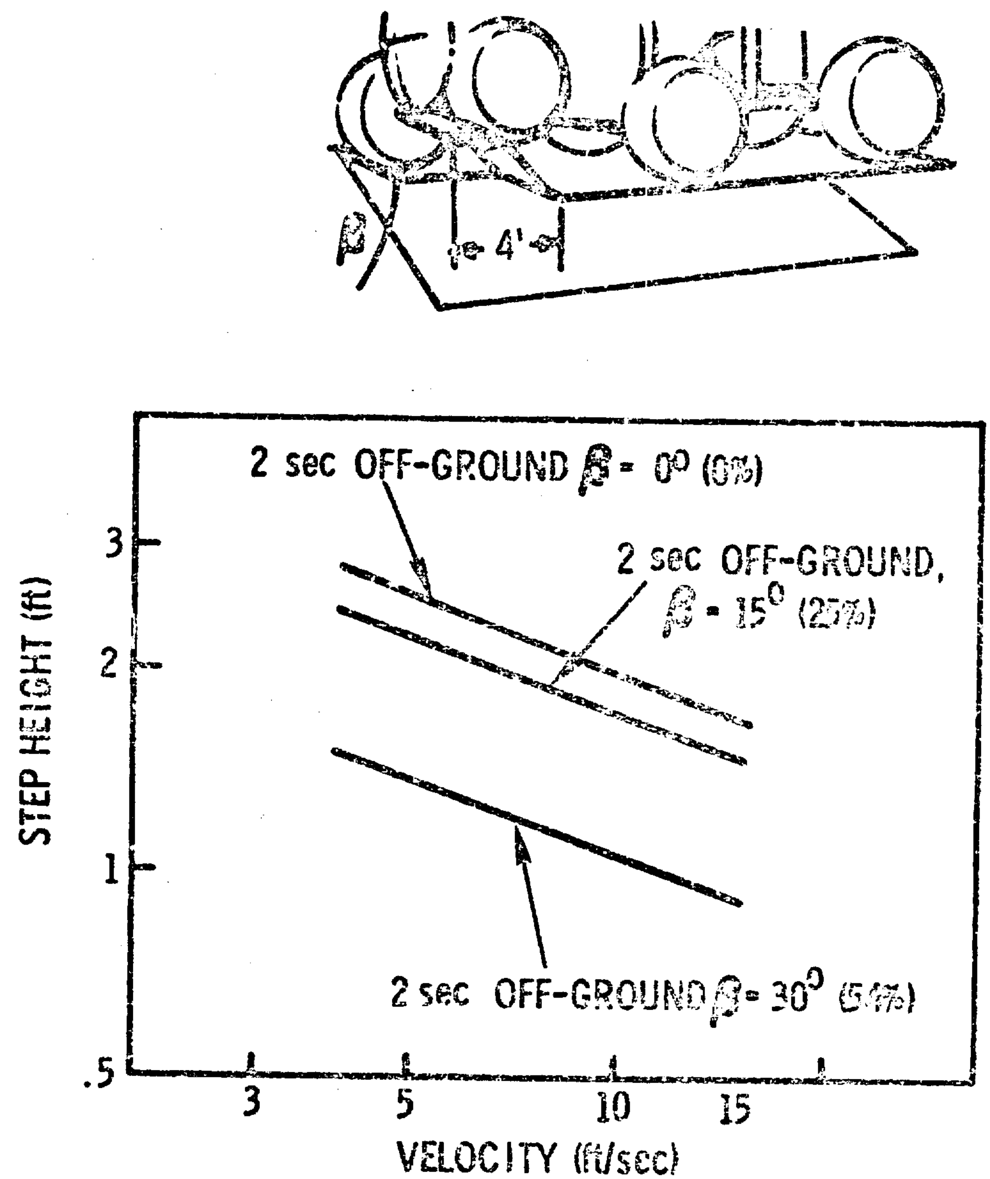

Figure 5.5.46 - Roll Stability on Side Slope

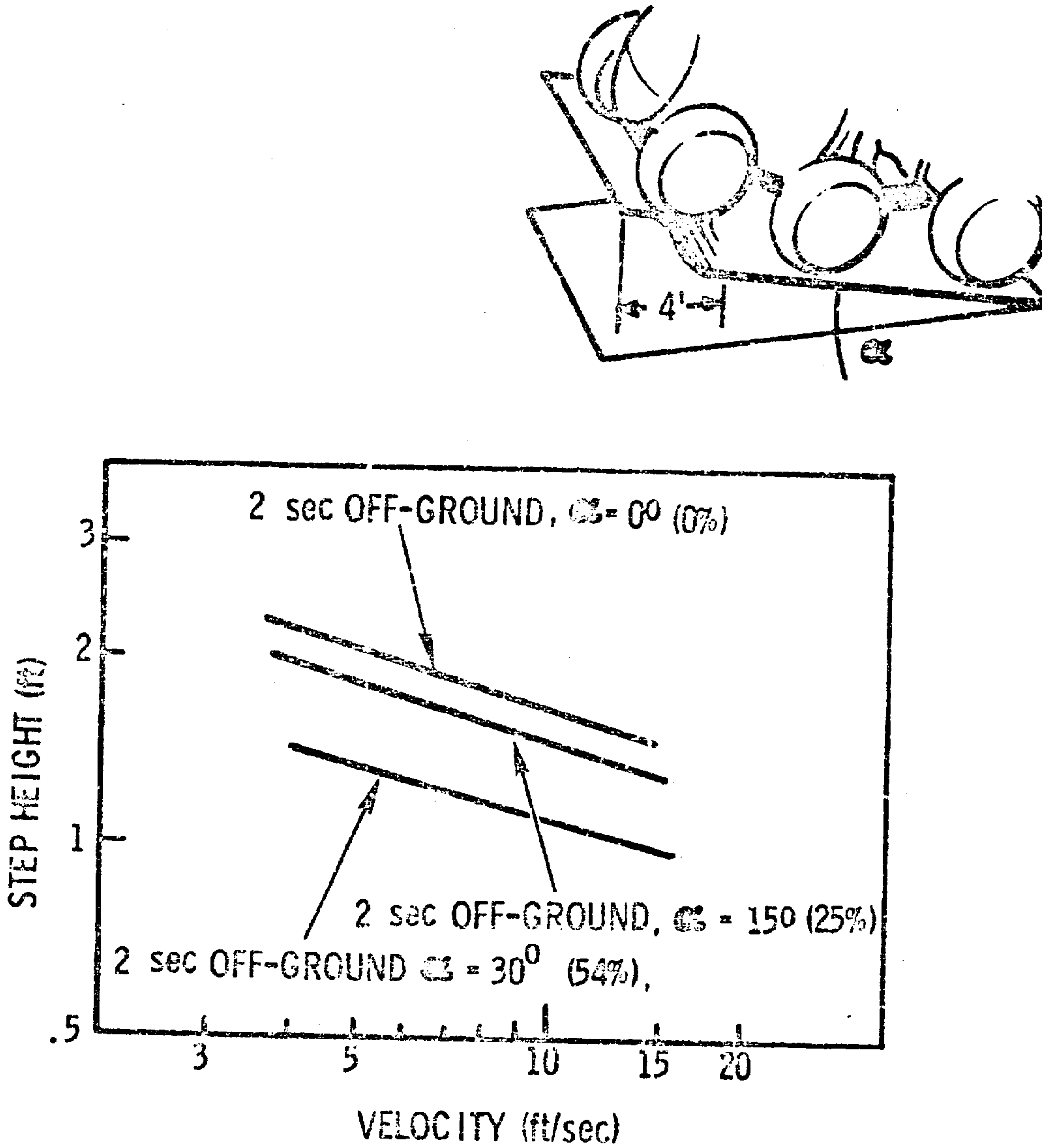

Figure 5.5.47 - Pitch Stability on Front Slope

5.6 LSSM MOBILITY PERFORMANCE SUMMARY

5.6.1 Soft Soil Mobility

The LSSM mobility capabilities over the specified ELMS and Annex G soils are summarized in the following table. It can be seen that the baseline LSSM can negotiate all specified conditions with a comfortable margin of safety.

ELMS MODELS		LSSM PERFORMANCE		
Slope - Degrees	Soil Values	Motion Resistance	DP/W	Slope Capability, Degrees
0° 1 2 3 4	$\phi = 32^\circ$ $k_\phi = 0.5$ $n = 0.5$	31.7 38.1 44.4 50.6 56.9	0.52	27°
5 7.5	$\phi = 32^\circ$ $k_\phi = 1.0$ $n = 0.75$	53.2 68.8	0.55	28°
10 12.5 15 17.5 20	$\phi = 32^\circ$ $k_\phi = 3.0$ $n = 1.0$	80.0 95.3 110.5 125.4 140.2	0.56	29°
25	$\phi = 32^\circ$ $k_\phi = 6.0$, $n = 1.25$	168.0	0.58	30°
30 30 35	hard surface $\mu = 0.8$	193.6 219.6	0.76	37°
ANNEX G SURFACE MODEL				
0°	$\phi = 20^\circ$ $k_\phi = 0.05$, $n = 1$	85	0.13	7.5°

5.6.2 Obstacle Performance

The LSSM has a high degree of capability over all types of obstacles specified in Annex G. Step height capability is 51 inches (130 cm) as compared to the wheel diameter of 40 inches; crevice crossing capability is 56 inches (142 cm).

These values are appreciably greater than conventional rigid frame vehicles are capable of.

5.6.3 Maneuverability

Steering: The minimum wall-to-wall turning radius for LSSM is 18.9 ft (6.1 meters) as compared to an overall vehicle length of 13.3 ft (4.1 meters). This provides extremely good maneuvering capability. The amount of off-tracking of the outside wheels at the minimum turn radius was only 9 inches (23 cm), less than the width of a wheel.

Braking: Minimum stopping distances were calculated as functions of speed and surface conditions. It was shown that in deformable soils, the stopping distance greatly depends on the soil shearing characteristics; that is, the lower the shear strength the greater the distance required. In any case, vehicle velocity must be limited on the moon due to the face that stopping distances will be six times greater than on earth for equivalent surface conditions.

Vehicle Stability: Calculations indicate that the LSSM will be stable under all reasonable conditions. From the static stability point-of-view, the vehicle will not overturn in roll unless slope angles exceed 52°; for overturning in pitch this value in 62°. For the more critical case of maneuvering on continuous slide slopes, it was determined that for all conditions specified in ELMS, the vehicle will slide rather than overturn. In either the roll or pitch modes, the LSSM will not become unstable while maneuvering unless the coefficient of friction is significantly greater than 1.0.

5.6.4 Dynamic Performance

Results of a computer program ride analysis were used to help determine the design ranges of suspension spring and damping rates. Rates established were 15 lb/in (26 N/cm) for the springs and 50 lb sec/ft (730 N sec/cm) for the damper. Results of studies performed for random terrain with a power spectral density distribution similar to that deduced from Ranger 7 photographs, and over small discrete bumps, indicated that from the ride point-of-view flexible wheels are greatly superior to rigid wheels, and that it is important that suspensions be incorporated in the LSSM design.

5.6.5 Summary

A summary of the salient LSSM performance characteristics is given in the chart of Figure 5.6.1.

GROSS VEHICLE MASS (INCLUDING CREW)	984 KG (2170 LBM)
DRAWBAR PULL/WEIGHT RATIO	
$k_\phi = 0.05$ $n = 1.0$, $\phi = 20^0$	0.13
$k_\phi = 0.5$, $n = 0.5$, $\phi = 32^0$	0.52
$k_\phi = 3.0$, $n = 1.0$, $\phi = 32^0$	0.56
STEP OBSTACLE CAPABILITY	130 CM (51 IN.)
CREVICE CROSSING CAPABILITY	142 CM (56 IN.)
TURNING RADIUS (MINIMUM)	6.1 M (18.9FT)
ROLL STABILITY (STATIC)	52°
PITCH STABILITY (STATIC)	62°
*LOCOMOTION ENERGY – MARIA	124.1 W-HRS/KM
– UPLANDS	133.5 W-HRS/KM
** AVERAGE VELOCITY CAPABILITY – MARIA	7.2 KM/HR (4.5 MPH)
– UPLANDS	5.6 KM/HR (3.5 MPH)
DESIGN SPEED (MAXIMUM)	16.1 KM/HR (10 MPH)

* BASED ON: 35% CONTINGENCY ALLOWANCE

** POSSIBLE LIMITATIONS DUE TO RIDE PERFORMANCE NOT TAKEN INTO ACCOUNT

Figure 5.6.1 - Baseline LSSM Performance Characteristics (For Typical Sortie Without ESS)

6.0 CONCEPTUAL DESIGN OF BASELINE LSSM MOBILITY SYSTEM

This section of the report discusses and describes the baseline LSSM mobility system and its major subsystems. These include:

- o Wheel assemblies
- o Wheel drive mechanisms
- o Suspension systems
- o Steering mechanisms
- o Chassis-Frame assembly
- o Electric drive system

6.1 OVERALL MOBILITY SYSTEM

6.1.1 Introduction

The purpose of the LSSM mobility system is to function as a highly mobile platform capable of negotiating the soils, slopes and obstacles of the lunar surface, while providing maximum probability of crew safety and mission success. Since the characteristics of the lunar surface are still largely unknown (or least open to debate), a major design objective was to provide a system capable of high mobility performance over as wide a range of possible surface conditions as possible.

Another major design objective was to achieve simplicity to reduce development costs, consistent with performance and reliability requirements and mass and envelope restraints.

6.1.2 Requirements

Requirements established for the mobility system design were as follows:

(1) Compatibility with the lunar thermal and vacuum environment.

(2) Ability to withstand loads imposed during launch, transit, landing and operation over the lunar surface. (These are described in

Boeing Document D2-82068, MOLAB Structural Design Criteria)

(3) Wherever feasible, provide redundancy in critical subsystems.

(4) Ability to accommodate an astronaut-driver and any necessary communications, navigation, power and thermal systems, and transport 600 to 700 lbm of scientific equipment. It should also be able to accommodate a second astronaut in place of the cargo.

(5) When fully loaded, the LSSM vehicle should have the speed capability of 16 km/hr (10 mph) over smooth, level, hard ground and at least 5 km/hr (4.1 mph) in level soft soils ($k_\phi = 0.5$, $n = 0.5$).

(6) Ability to negotiate all surface conditions specified in ELMS.

(7) Average speed over the ELMS profiles should be at least 5 km/hr (4.1 mph).

(8) Ability to negotiate a step obstacle at least 40 inches (101 cm) high.

(9) Angles of approach and departure should be at least 90 degrees.

(10) Provide as comfortable a ride as possible for the astronaut.

6.1.3 Mobility System Description

The LSSM mobility system, shown in Figure 6.1.1, incorporates a chassis-frame assembly, essentially identical parallel arm suspensions at all wheels, individual wheel drive mechanisms, identical steering mechanisms for the forward and aft wheels, and flexible wire frame wheels. Control electronics for driving and steering are located in a thermal compartment on the aft unit.

The chassis-frame assembly consists of forward and aft unit frames, and a flexible frame and pitch limiter located between the two units. The frames are box structures on which appropriate fittings are located for suspension, flexible frame, crew station, scientific payload, thermal compartment and stowage attachments. Two main structural members near the center of the boxes provide the main load path, and are also the track support on the forward unit for retracting the flexible frame for stowage. The flexible frame consists of eight thin-walled tubes, connecting the forward and aft units, which permit the units

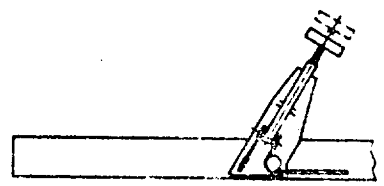

PART SECTION B B

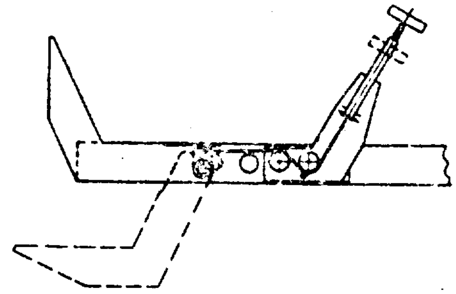

PART SECTION A A

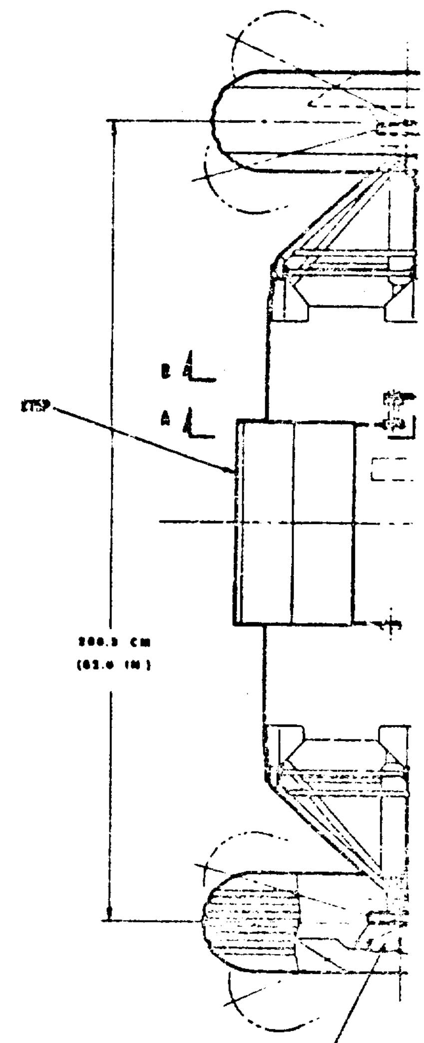

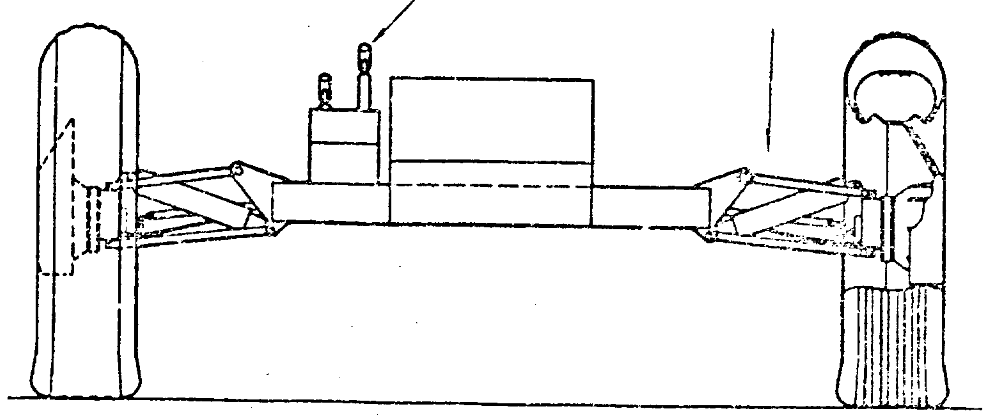

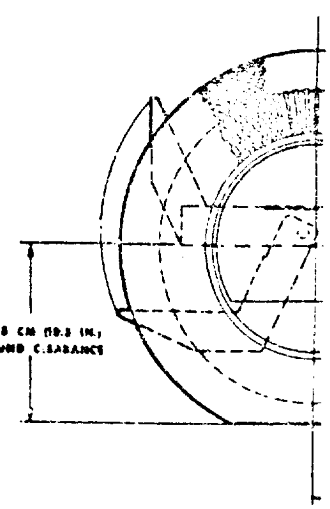

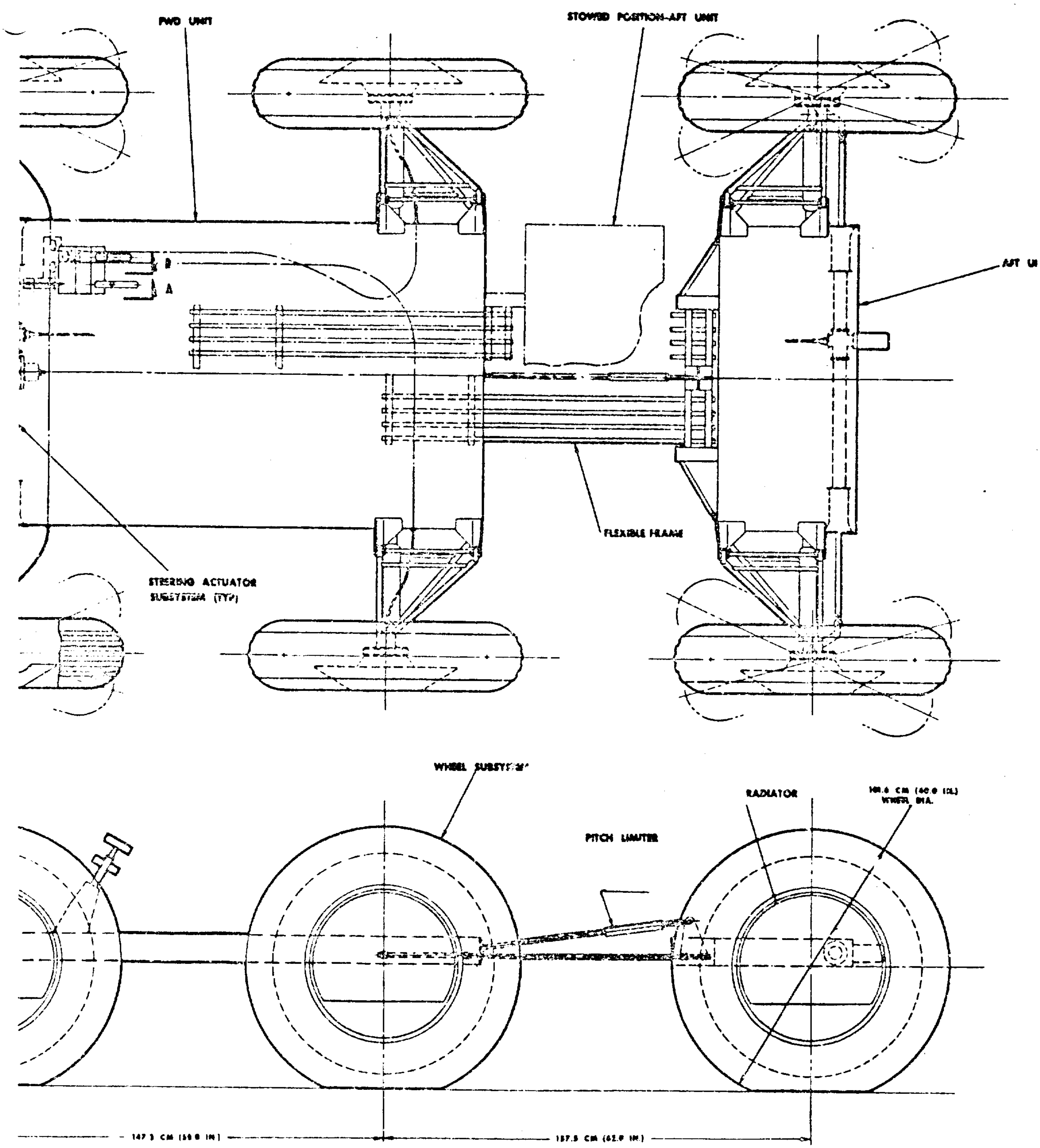

Figure 6.1.1 - Assembly, Mobility Subsystems, LSSM

to roll and pitch relative to each other. The pitch limiter essentially consists of two concentric tubes sliding on each other and is designed to limit relative movement between the forward and aft units, and prevent overstressing of the flexible frame when negotiating severe obstacles.

The parallel arm suspension assemblies are essentially identical at all six wheels. Each consists of welded tubular steel upper and lower arms, damper/stop assembly and torsion bar spring element. The torsion bar is located longitudinally between the chassis attachments for the upper suspension arm. The damper is of the linear dash-pot type with electrical heating elements to maintain necessary fluid temperature, and is located between the lower arm chassis attachment point and upper arm wheel attachment point. The suspension is designed for a total vertical travel of 25.4 cm (10 in.).

The individual wheel drive assemblies are mounted at the wheel hubs and include a harmonic drive, spur gear reduction, brakes, declutching mechanism, electric drive motor and radiator. The harmonic drive provides the major portion of the necessary speed reduction between motor and wheel as well as providing a hermetic seal for the high speed parts. Driving action of the wheel is accomplished through the following sequence: motor output - wave generator - flexspline - circular spline - intermediate pinions - ring gear - wheel hub. Locating the intermediate pinions between the circular spline of the harmonic drive and the ring gear on the wheel hub permits placing the passive radiator outboard of the wheel disc. The service brake is a conventional duo-servo two-shoe brake actuated by a pilot shoe assembly which in turn is actuated by a solenoid. For parking, manual actuation of the solenoid armature is substituted for electrical actuation, through a push-pull cable. For parking purposes it is contemplated that only the brakes of the forward unit wheels will be applied. Declutching of the wheel from the drive emergency operation is also accomplished manually by a release device that disengages the ring gear from the wheel hub.

The electric drive motors are of the three-phase squirrel cage induction type. Torque and speed are varied by controlling motor frequency, slip and current by means of transistorized inverter - modulators. Three motors on one side of the vehicle are controlled by one inverter - modulator. All electronics for the electric drive system are located in the aft unit thermal compartment.

The drive system is capable of producing wheel torques as follows: 89m-N (120 lb-ft) at a wheel speed of 2 rpm (maximum intermittent), 51m-N (69 lb-ft) at 5 rpm (maximum continuous), and 4.5m-N (6 lb-ft) at 92 rpm (maximum vehicle speed of 16 km/hr).

The Ackermann steering actuators for the forward and aft wheels are essentially identical. Each consists of a cross-link assembly, housing, connecting links to the wheels, ball-nut input and an electric motor assembly with a spiroid gear output. The two mechanisms are synchronized by means of a flexible shaft connecting the two. A manual emergency steering capability is provided for the forward actuator.

The wheels consist of the following basic elements: wheel disc, rim, flexible woven wire outer frame, stiff inner frame to limit wheel deflections due to impact loads, and a tread to provide a bearing surface. The wheels are 101.6 cm (40 in.) in diameter with a section width of 25.4 cm (10 in.) and are designed to have a static deflection of about 4.3 cm (1.67 in.) at nominal wheel load.

The general characteristics of the LSSM mobility systems are given in Figure 6.1.2.

The estimated mass breakdown for the mobility system is given in Figure 6.1.3.

OVERALL LENGTH	406 CM (160 IN.)
OVERALL WIDTH	234 CM (92 IN.)
WHEEL DIAMETER	101.6 CM (40 IN.)
WHEEL WIDTH	25.4 CM (10 IN.)
WHEEL DEFLECTION (AT NOMINAL LOAD)	4.3 CM (1.67 IN.)
WHEEL BASE	147/158 CM (58/62 IN.)
WHEEL TREAD	209 CM (82 IN.)
GROUND CLEARANCE	45.7 CM (18 IN)
HANG-UP RADIUS (BETWEEN AXLES) (BETWEEN WHEELS)	35.5/41.9 CM (14/16.5 IN.) 132.1 CM (52 IN.)
ANGLE OF APPROACH	90^{0} +
ANGLE OF DEPARTURE (LESS SNAP 27)	90^{0} +
BASIC PLATFORM AREA – TOTAL FORWARD UNIT AFT UNIT	4.61 M^2 (49.6 FT^2) 3.56 M^2 (38.3 FT^2) 1.05 M^2 (11.3 FT^2)

Figure 6.1.2 - Mobility System General Characteristics

	LBM	KG
Wheel Assembly (6)	180	82
Wheel Drive System (6)	132	60
Suspension System (6)	60	27
Steering Mechanism (2)	34	16
Forward Unit Frame	86.5	39
Flexible Frame (w/Pitch Limiter)	10.5	5
Aft Unit Frame	62.5	28
Electronics for Driving & Steering	37.5	17
	603	274

Figure 6.1.3 - LSSM Mobility System Mass Breakdown

6.2 WHEEL ASSEMBLY

6.2.1 Introduction

The wheel design for LSSM, or for any off-road vehicle, affects mobility over both soft ground and obstacles, energy requirements, stability, and vehicle ride and handling characteristics, as well as drive train and motor design.

Because the character of the lunar surface is largely unknown, it is necessary that the wheels be capable of providing an acceptable degree of performance over a wide range of terrain conditions ranging from deep, loose soils to hard, rough ground and over obstacles and slopes. Rigid wheels, while simple in concept, are considered unacceptable for this application from the viewpoints of both soft and rough terrain performance.

In soft ground, rigid wheels are inferior to flexible wheels from the following points of view:

- They develop considerably higher motion resistance than flexible wheels.
- This means that locomotion energy requirements are considerably higher for rigid wheels.
- Drawbar pull performance (which is a direct measure of the slope climbing capability) of a vehicle equipped with rigid wheels is poor compared to that of one with flexible wheels.

This latter point is illustrated in Figure 6.2.1, where drawbar pull performance for the two types of wheels is compared over a wide range of soil conditions. Rigid wheel performance is clearly inferior, especially in the softer soils.

In rough terrain, rigid wheels transfer high impact forces to the vehicle chassis resulting in possible damage to the vehicle or payload and poor ride performance, as was discussed in Section 5.5 of this report.

In the course of the Lunar Mobile Laboratory (MOLAB) study, six different metallic flexible wheel concepts were evaluated and compared to determine which concept or concepts would best suit the requirements of vehicle operation over the lunar

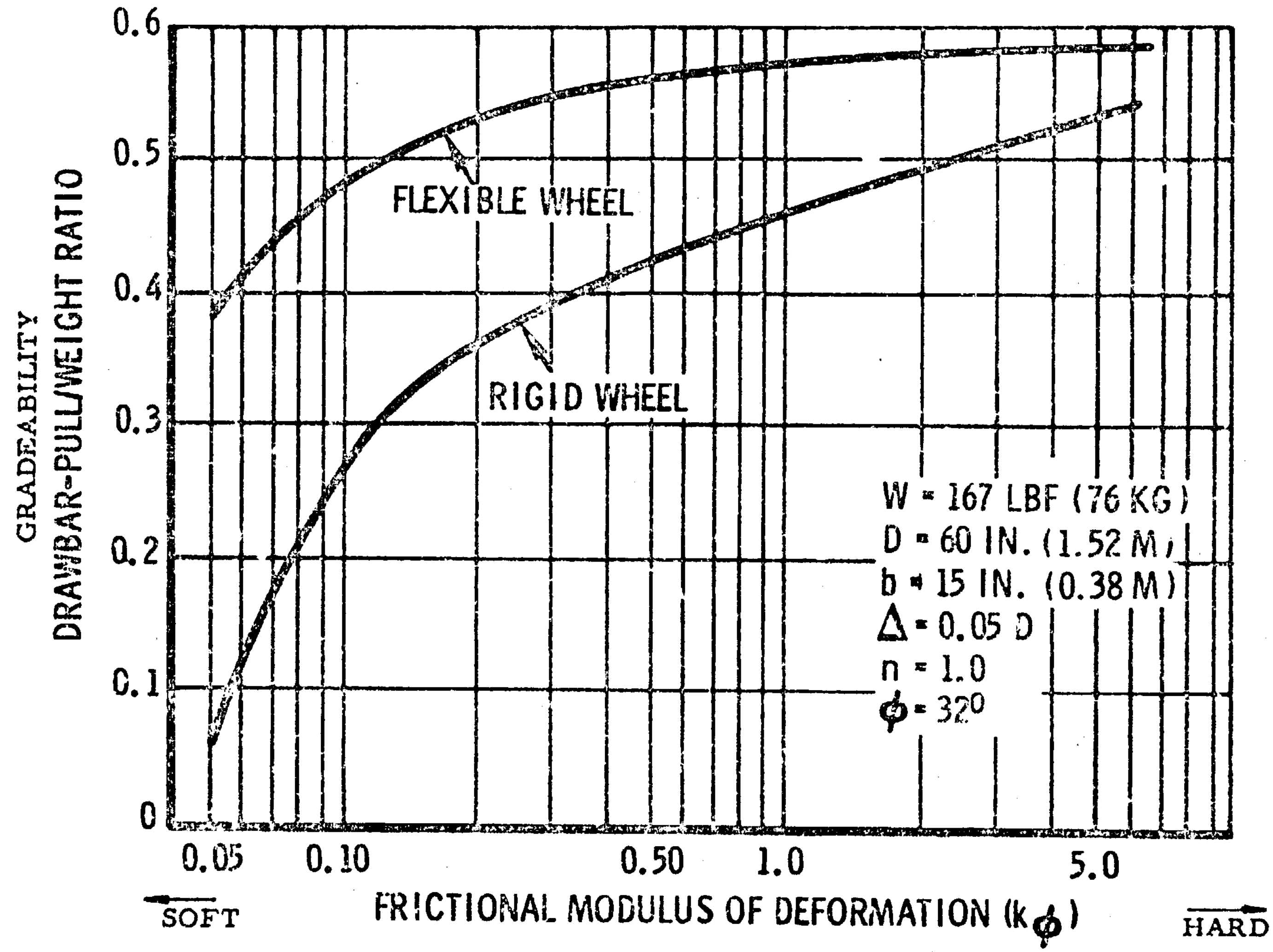

Figure 6.2.1 - Comparison of Rigid and Flexible Wheels

surface. The pneumatic tire and rigid wheel were also included in the evaluation process for comparison purposes.

The eight candidate wheel concepts are illustrated in Figure 6.2.2 and described in Figure 6.2.3. Conceptual design layouts of each were prepared and supporting calculations developed in sufficient detail to provide a basis for comparison of the several concepts from the viewpoints of:

- o Mechanical Reliability
- o Mass
- o Soft Soil Mobility
  - a. Gradeability
  - b. Locomotion efficiency
- o Obstacle Mobility
  - a. Step obstacle
  - b. Crevice
- o Steering Resistance
- o Effect on Ride Comfort
- o Stability
- o Wear Resistance
- o Environmental Compatibility
- o Development Risk and Cost

Results of the evaluation indicated that the wire frame and bi-directional metal-elastic wheels would be the most suitable for lunar application with the wire frame version considered somewhat superior on the basis of importance factors assigned to each of the above criteria. The wire frame wheel was therefore selected as the baseline concept for MOLAB and is presently being used as the basis for LSSM preliminary design. However, both concepts will be tested and re-evaluated in the Lunar Wheel and Drive System Environmental Test Program (AES Payloads), Contract NAS 8-20267, presently being conducted by GM DRL.

It should be noted that at this time, pneumatic tires have been eliminated due to incompatibility with the lunar environment. At present, rubbers and elastomers are in general not considered practical due to their low temperature brittleness and

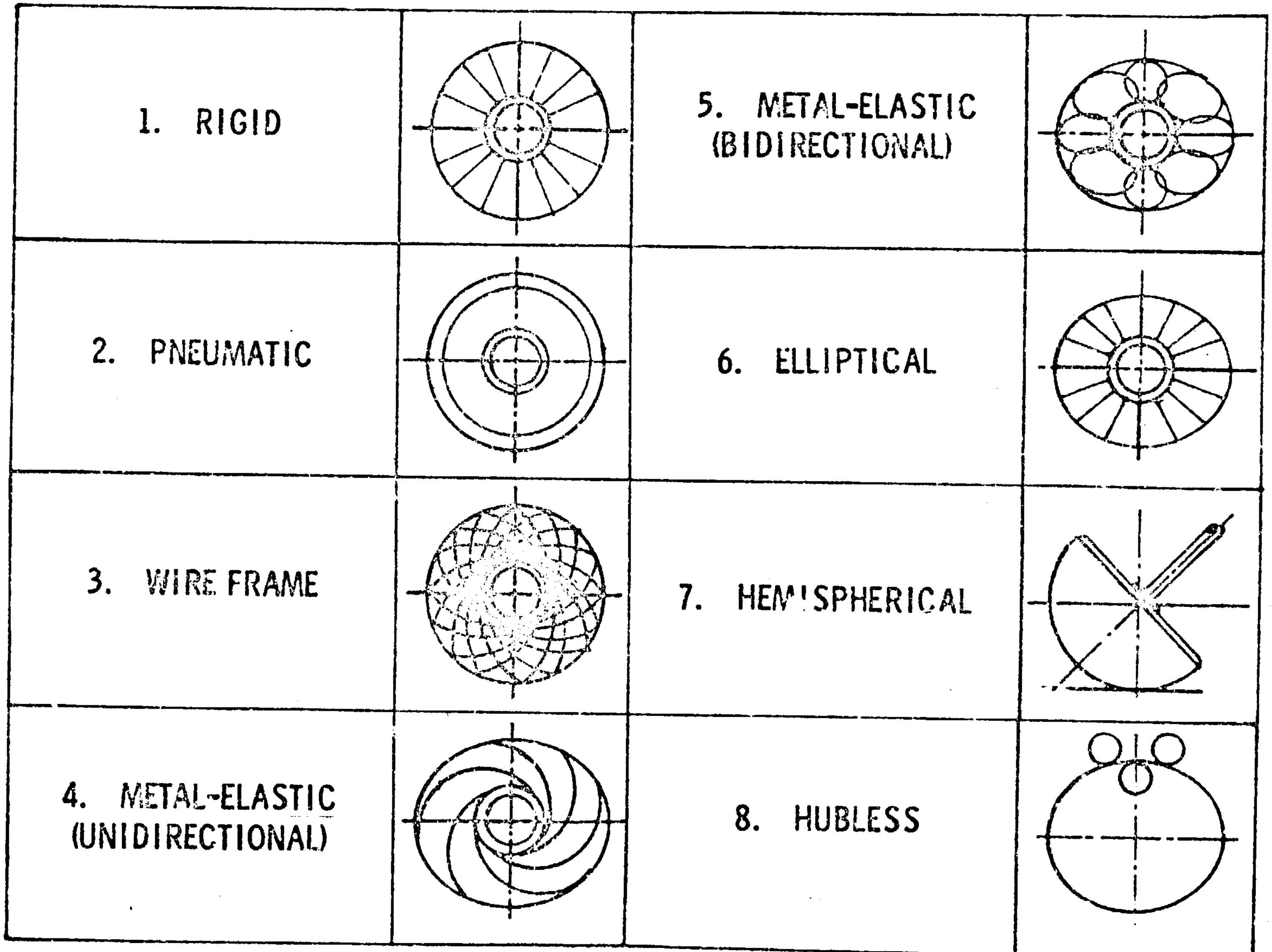

Figure 6.2.2- Candidate Wheel Concepts

CANDIDATE CONCEPT	DESCRIPTION
1. Rigid	Simple, all metal construction. No appreciable deflection under load.
2. Pneumatic	Conventional inflated tire. Highly developed for terrestrial applications.
3. Wire Frame	Steel mesh covering over a pantographing flexible wire frame. Performs somewhat like a pneumatic tire.
4. Metal-Elastic (Unidirectional)	High deflection wheel of open construction. Flexible, semi-circular metal band spokes.
5. Metal-Elastic (Bidirectional)	Same as above with full circular spokes.
6. Elliptical	Metal band wheel of open construction. Canted hubs and pin-ended spokes constrain wheel to elliptical shape.
7. Hemispherical	Canted hub, hemispherical shape, wire frame wheel. Provides increased roll stability.
8. Hubless	Rim-driven flexible band wheel. High deflection, open construction

Figure 6.2.3 Description of Candidate Wheel Concepts

out-gassing characteristics. Other factors such as abrasion and puncture resistance and permeability to gasses must also be considered. If LSSM operations are limited to the lunar day, it may be possible with advances in the state-of-the-art to develop a pneumatic tire for lunar operation. It is doubtful, however, that such a tire would ever be capable of lunar night operations.

6.2.2 Wire Frame Wheel Test Program

A wire frame wheel development program was conducted at GM DRL under the in-house Lunar Roving Vehicle Design Investigation Program (W.O. 20-22108-200) and the Mobility Test Article (MTA) Contract NAS 8-20251.

Primary objectives of this program were to develop design data on the wire frame wheel concept defined under the Lunar Mobile Laboratory (MOLAB) contract and to optimize the design for use on the MTA. In addition, the results of the program would be utilized to help define an LSSM wheel design. A number of 60 in. dia. x 15 in. wide wire frame wheels were tested incorporating various combinations of material, number of wires and fabrication and processing techniques. As a result of this development program, a satisfactory design has been established for use on the MTA and much valuable data has been gathered to aid in the development of a wire frame wheel for surface vehicles capable of operating in the lunar environment.

The tests described herein were conducted on the GM DRL rolling road facility shown in Figure 6.2.4. This facility consists of a variable speed moving belt to which obstacles may be attached for rough surface tests. A parallel-arm attachment structure, to which the wheel with its associated drive system and suspension may be mounted, is rigidly attached to the frame of the rolling road. A loading and counterbalancing platform are also provided. Instrumentation is provided to measure wheel speed, total revolutions, road speed, wheel torque and vertical acceleration. A DC motor drives the wheel through an 80:1 reduction harmonic drive unit. By varying the speed of the wheel drive system and the belt speed of the rolling road, a wide range of speed-torque conditions may be simulated.

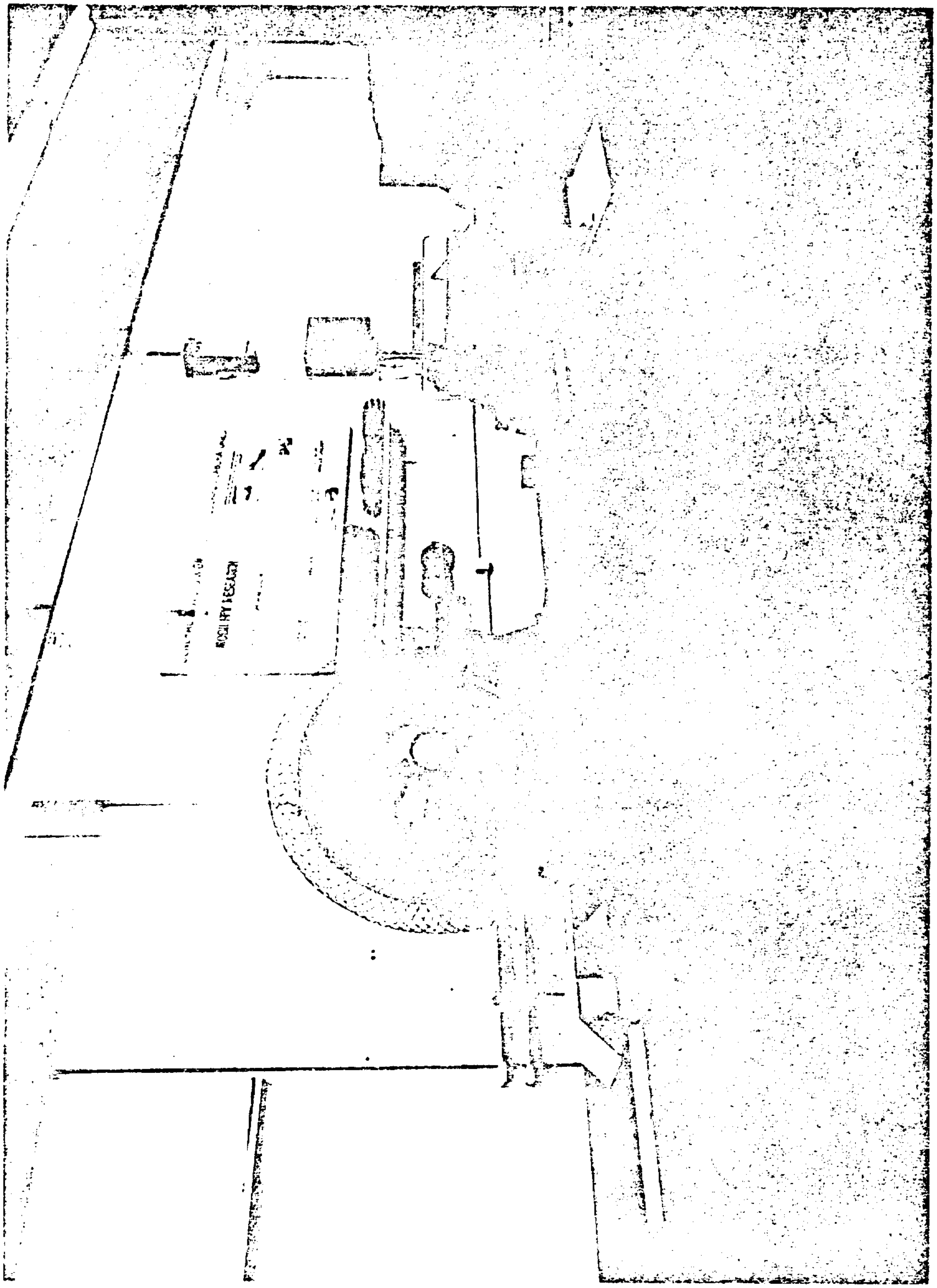

Figure 6.2.4- Rolling Road Wheel Test Set Up

In all, ten test article wheels were subjected to endurance testing on the rolling road. The first test article wheel incorporated all of the critical wheel elements - outerframe, tread, covering, and inner frame. It soon became evident, however, that a major problem existed in obtaining adequate fatigue life. For this reason further testing was restricted to endurance testing of the outerframe only in order to develop a wheel adequate for use on the MTA.

Figure 6.2.5 illustrates four basic variations of the wire frame wheel which were included in the test program. In the looped-joint construction each wire is looped at the intersection resulting in positively interlocked joints. The hand woven construction eliminates the looped joints by simply interweaving intersecting wires. Both versions of the pre-crimped woven construction utilized wires which were crimped at regular intervals to positively locate the wire intersections.

Test Article 1: The first wheel to be tested was a complete system. That is all major elements were represented as follows: Disc and rim - 0.080 thick 6061-T6 aluminum spun construction; outer frame - 0.090 music wire, 90 right hand, 90 left hand wires, 1.5 inch mesh, hand woven; inner frame - 90 SAE 1095 clock, spring steel loops connected by 3 rings; covering - type 304 CRES wire cloth, 24 x 24 mesh, 0.010 wire diameter; tread - plastic-coated chain link fencing, 1.5 inch mesh. Preliminary testing indicated that the cover and tread design required more development. The most serious problem, however, appeared to be the wire outer frame. Operating at a speed of 60 rpm and loaded to a deflection of 2.5 inches the first wire in the frame failed at 20,000 cycles and at approximately 34,000 cycles 5% of the wires had failed. It was, therefore, decided to defer further testing of other wheel elements until such time as the wire frame achieved satisfactory fatigue life and subsequent tests were conducted on uncovered wheels (basic wire frame only). All subsequent endurance tests were run at a speed of 60 rpm and a torque of 25 lb-ft with the wheels loaded to a nominal deflection of 2.5 inches. Failure of five percent of the total number of wires in the wheel was arbitrarily established as the comparison point for fatigue life.

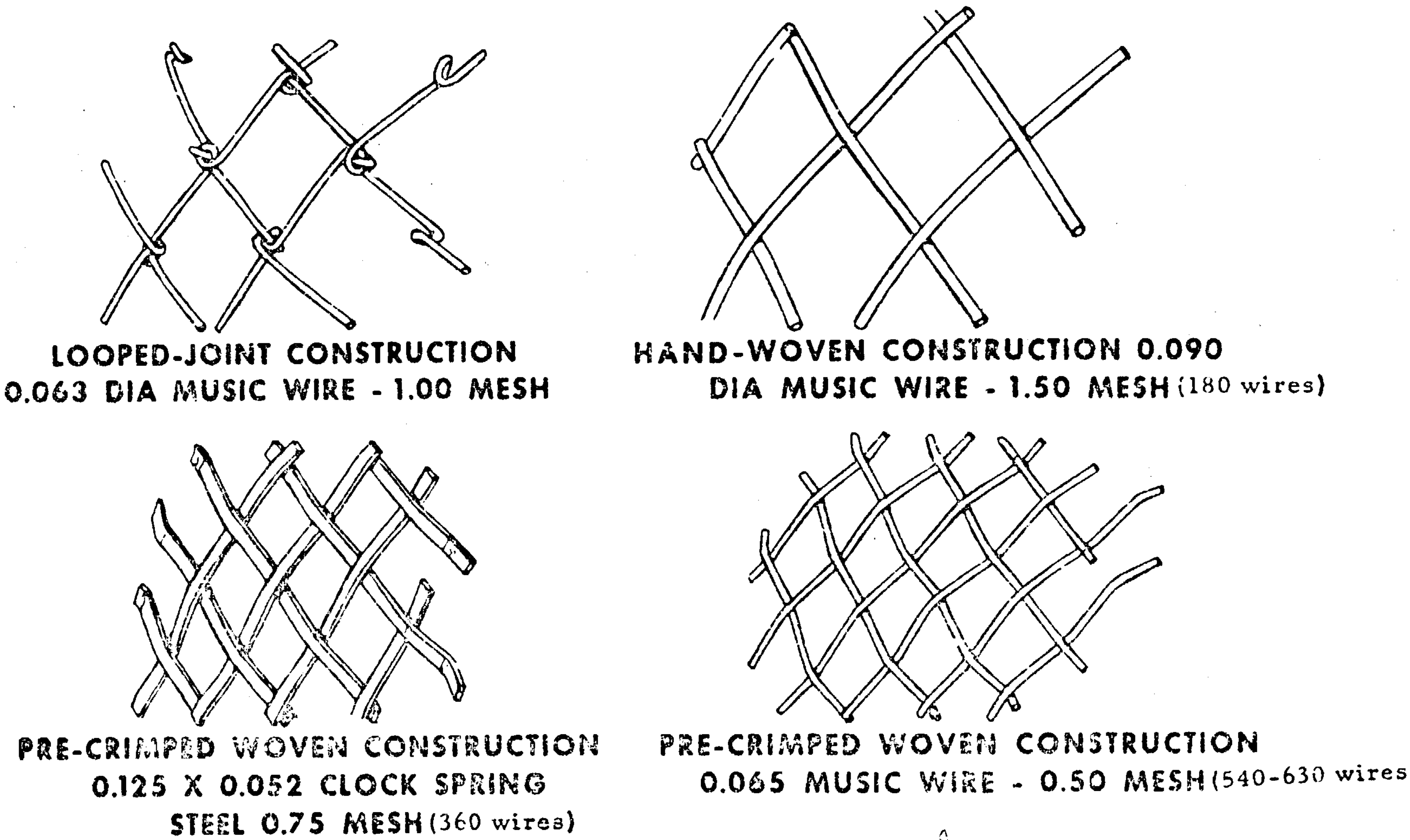

Figure 6.2.5 - Alternate Construction Techniques, Wire Frame Wheel

Test Article 2: Test Article 2, supplied by the Goodyear Tire and Rubber Company, utilized the looped joint method of construction. The wires failed rapidly at the points of intersection, reaching the 5 percent failure level after only 6000 cycles.

Test Articles 3 and 4: The first test series indicated that a design must be designed to provide positive location of the wires at each intersection without introducing the high local stresses associated with the looped-joint mode of construction. The wire frames of the third and fourth wheel constructed were woven as continuous cylinders with the individual wires crimped at each intersection to locate them positively. The number of wires was doubled from 180 (1.5 in. mesh) to 360 (0.75 in. mesh) and the wire size was reduced to 0.072 inch diameaer in order to lower stresses. Wheel No. 3 was woven from type 304 CRES wire while wheel 4 was woven from music wire. Both wheels survived approximately 28,000 cycles of operation before 5 percent of the wires had broken.

Test Article 5: This wheel was constructed using 0.063 inch music wire in order to reduce stress levels still further. The number of wires was maintained at 360 since the 0.75 inch mesh was readily available. Extra care was taken in the crimping process to avoid nicking the wires which causes local stresses. The wheel survived 48,000 cycles before reaching the 5% fatigue failure level.

Test Article 6: Examination of test results and analysis of the wire frame indicated that stresses induced by forming the wheel from a cylinder into a torus were in the order of 100,000 psi. This stress, together with operating stresses, resulting in net working stress levels of 180,000 to 200,000 psi. To attain a fatigue life of at least 100,000 cycles, stresses must be kept at 150,000 psi or lower. Test Article 6 was therefore stress-relieved by forming the flexible wire cylinder into a torus on a fixture and relieving the stresses at 500°F for one hour. This wheel survived approximately 60,000 cycles, indicating some improvement

Test Article 7: Inability to reach the target life of 100,000 cycles with the first six wire frame wheels to be tested prompted the investigation of an alternative concept which did not use interwoven wires. A radial strip wheel, shown in Figure 6.2.6, was fabricated from 90 0.050 inch x 0.50 inch preformed clock spring steel

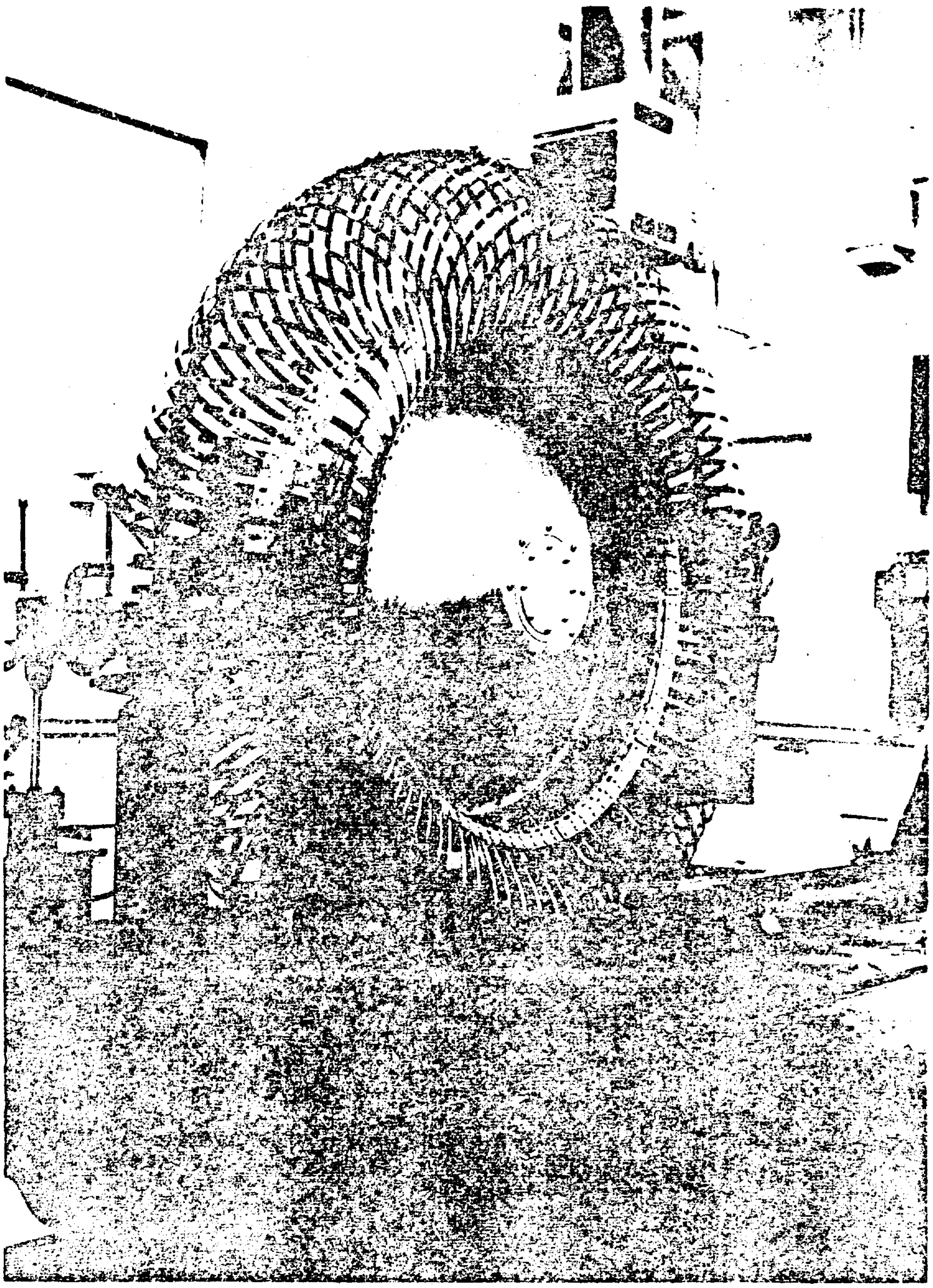

Figure 6. 2. 6- Radial Strip Wheel

loops interconnected by a 1 inch x 0.050 inch circumferential ring of the same material. This wheel survived 90,000 cycles and showed promise as a back-up configuration to the wire frame wheel.

Test Article 8: A test wheel was fabricated from 360 0.125 inch x 0.032 inch clock spring steel strips woven on a 0.75 inch mesh. This wheel proved very difficult to fabricate and lasted less than 20,000 cycles before reaching the 5% failure point.

Test Article 9: Test Article 9 may be considered a pre-prototype of the MTA wheel. It was fabricated from 540 pieces of 0.065 inch music wire woven in a 0.5 inch mesh. Operating stresses were minimized by "over-wrapping" the flexible wire frame during stress-relief and by utilizing a large number of small diameter wires. This wheel has completed approximately 160,000 cycles at the 5% failure point. The results of this test indicate that, with minor modifications, the 0.5 inch mesh would be suitable for use on the Mobility Test Article (MTA).

Test Articles 10 and 11: Test Article 10 was a duplicate of Test Article 9 with the exception that approximately one-third of the wires were plated to evaluate electroless nickel as a corrosion and abrasion-resistant coating. The nickel plated area failed rapidly, indicating that the plating had a delitereous effect on the fatigue life of the wire. Test Article 10 was also used to determine the circumfrential spring rate of an MTA type wheel. This was necessary in order to determine the required load-deformation characteristics of the neathane tread strips to be used on the MTA wheel.

Test Article 11, a prototype of the MTA wheel, was woven from 630 wires of 0.063 inch diameter. This wheel was used to verify fabrication and assembly techniques and to confirm proper fit of the tread strips.

6.2.3 Test Program Summary

In summary it may be concluded that:

- The looped-joint method of construction is not acceptable.
- Hand-woven construction is not acceptable.

- o Pre-crimped construction is an acceptable solution if care is taken in the crimping process
- o Stress-relieving is necessary
- o A wire material is required with fatigue properties comparable to those of music wire
- o A configuration has been developed suitable for operation in the terrestrial environment for MTA.

While a significant amount of progress has been made in the development of the wire frame wheel, a great deal of effort still remains in advancing the development from a functionally acceptable design to the status of fully qualified lunar hardware. Remaining problems include:

- o Selection of suitable wire materials for the flexible outer frame to prevent cold-welding.
- o Design and material selection for the inner frame
- o Design and material selection for the tread

In any event, the information gained during the course of this test program has proven useful in the preparation of the present preliminary design for the LSSM wheel.

6.2.1 LSSM Wheel Design Criteria

The criteria used for LSSM wheel design are listed in Figure 6.2.7. Wheel dimensions are set by LEM/Shelter stowage requirements at 102 cm (40 in.) diameter by 25 cm (10 in.) wide.

The loaded mass of the baseline LSSM ranges approximately from 976 kg (2170 lbm) to 1035 kg (2300 lbm) depending upon the mission profile. As a baseline, the nominal wheel load was normalized at 289 N (65 lbf) which represents the mean between the two extremes. The nominal wheel torque has been normalized to the maximum continuous duty torque required to climb a 35° slope. The limit radial load has been normalized at 5204 N (1170 lbf) which represents a 3 g (earth) input; this is the dynamic load commonly specified for slow-moving, off-road terrestrial vehicles.

1.	Nominal Diameter	101.6 cm (40 in.)
2.	Nominal Width	25.4 cm (10 in.)
3.	Nominal Load	289 N (65 lbf)
4.	Nominal Torque	92 N-m (68 lbf-ft)
5.	Limit Radial Load	5204 N (1170 lbf)
6.	Limit Lateral Load	578 N (130 lbf)
7.	Maximum Torque	165 N-m (120 lbf-ft)
8.	Deflection at Nominal Load	4.3 cm (1.7 in.) Wire Frame
9.	Nominal Spring Rate	66 N/cm (38 lbf/in.) Wire Frame
10.	Maximum Wheel Speed	92 rpm
11.	Life	100,000 Rev.

Figure 6.2.7 Wheel Design Criteria

The maximum torque represents the intermittent duty torque required for obstacle climbing. The wheel deflection at nominal load is set as 17% of the section width. The maximum wheel speed of 92 rpm represents a vehicle speed of approximately 16 km/hr (10 mph) and the life criteria of 100,000 revolutions allows for 200 km (125 mi.) of travel with a safety factor of 1.6.

6.2.5 LSSM Wheel Preliminary Design

The LSSM wheels illustrated in Figure 6.2.8 and 6.2.9 consist of the following basic elements: wheel disc, rim, woven wire outer frame, inner frame, and tread. The wheel design shown in Figure 6.2.8 is that evolved during the course of the present LSSM study. That shown in Figure 6.2.9 is the design under consideration for use in the Wheel and Drive System Environmental Test Program. The two concepts are similar except for the number of wires and inner frame design. The latter concept is the one that appears most promising at this time and is now considered the baseline LSSM wheel and is therefore discussed below.

The wheel disc is a formed or spun conical frustrum which attaches to the wheel drive hub and the rim. 7075-T6 aluminum alloy and 6Al-4V titanium alloy are currently considered promising material for this component.

The rim will be fabricated from the same material as the wheel disc. Fasteners through the rim will secure the wire frame between the rim and the inner frame.

The woven wire outer frame consists of 540 interwoven wires in a 0.375-in. mesh. Some materials under consideration include Rene' 41, L605, A286, 17-7PH, and Beta alloy titanium (13V-11Cr-2Al). The wires will be precrimped and woven into a cylinder and then preformed to a toroidal shape by stress-relieving on a fixture. Design computations were made for the woven wire outer frame based on the analytical method developed in the MOLAB study and subsequently modified by results of tests performed on various breadboard and MTA wheels. The choice of 540 wires was based on the results of the previously discussed wheel development tests and material fatigue life data which indicated that normal operating

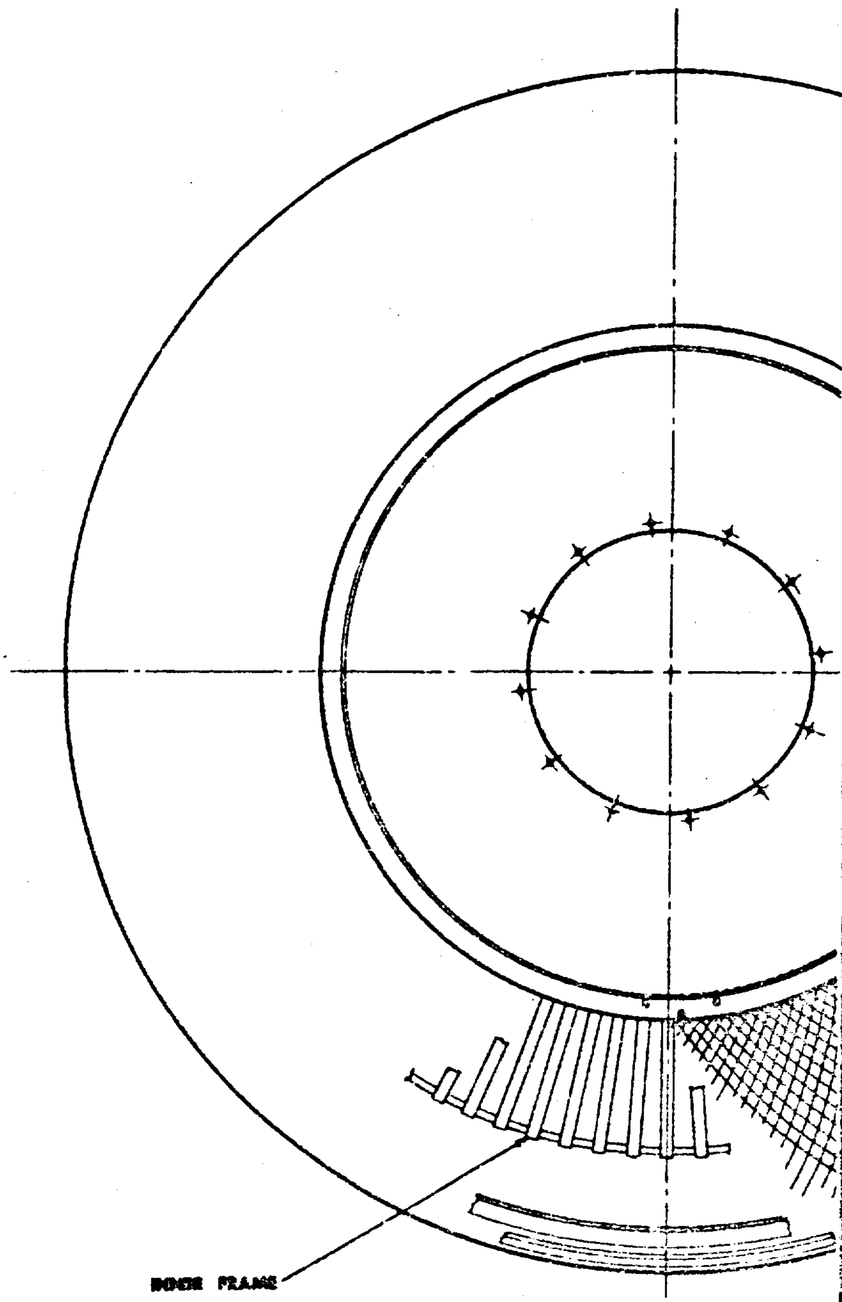
FRAME

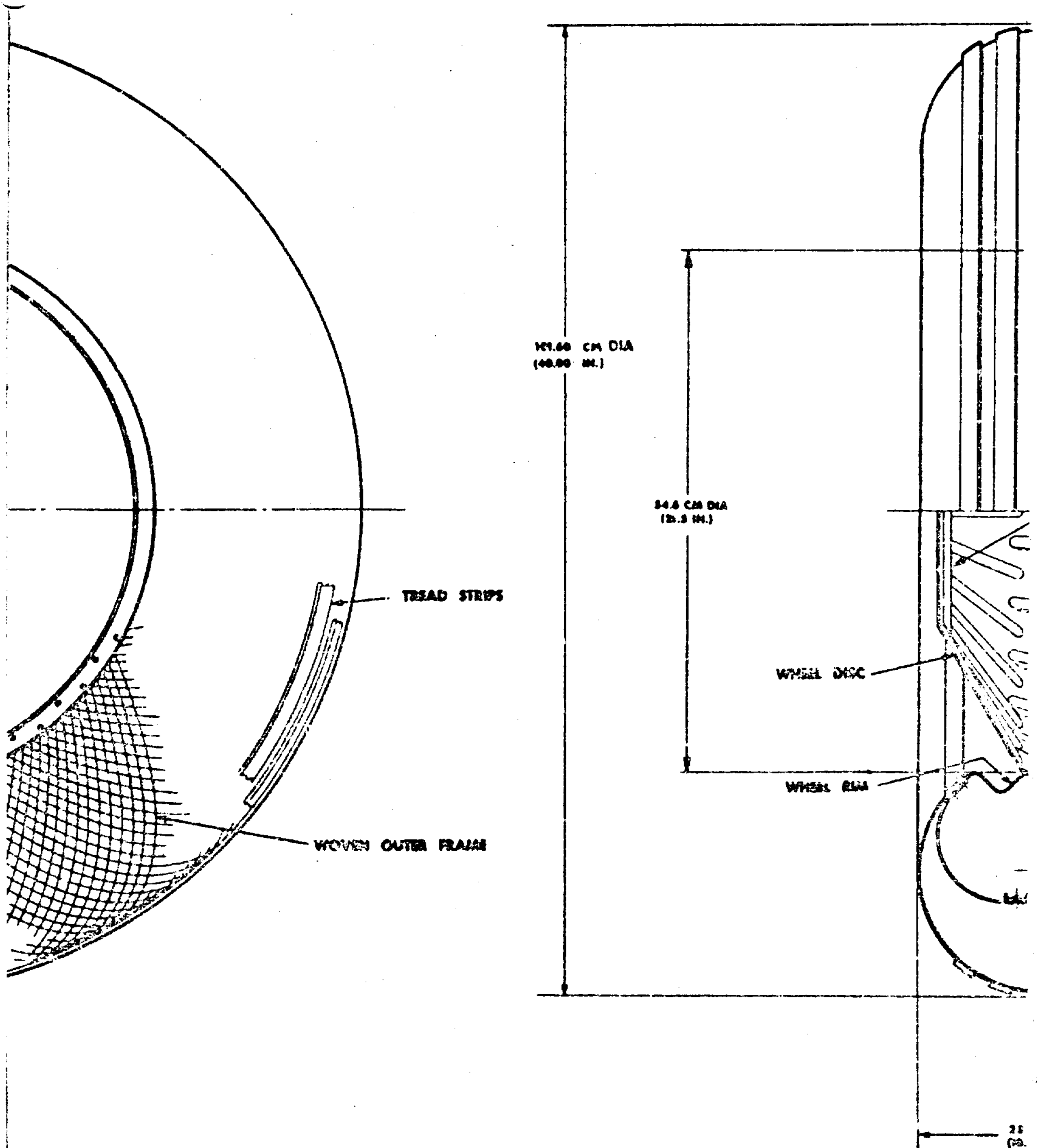

6-23-2

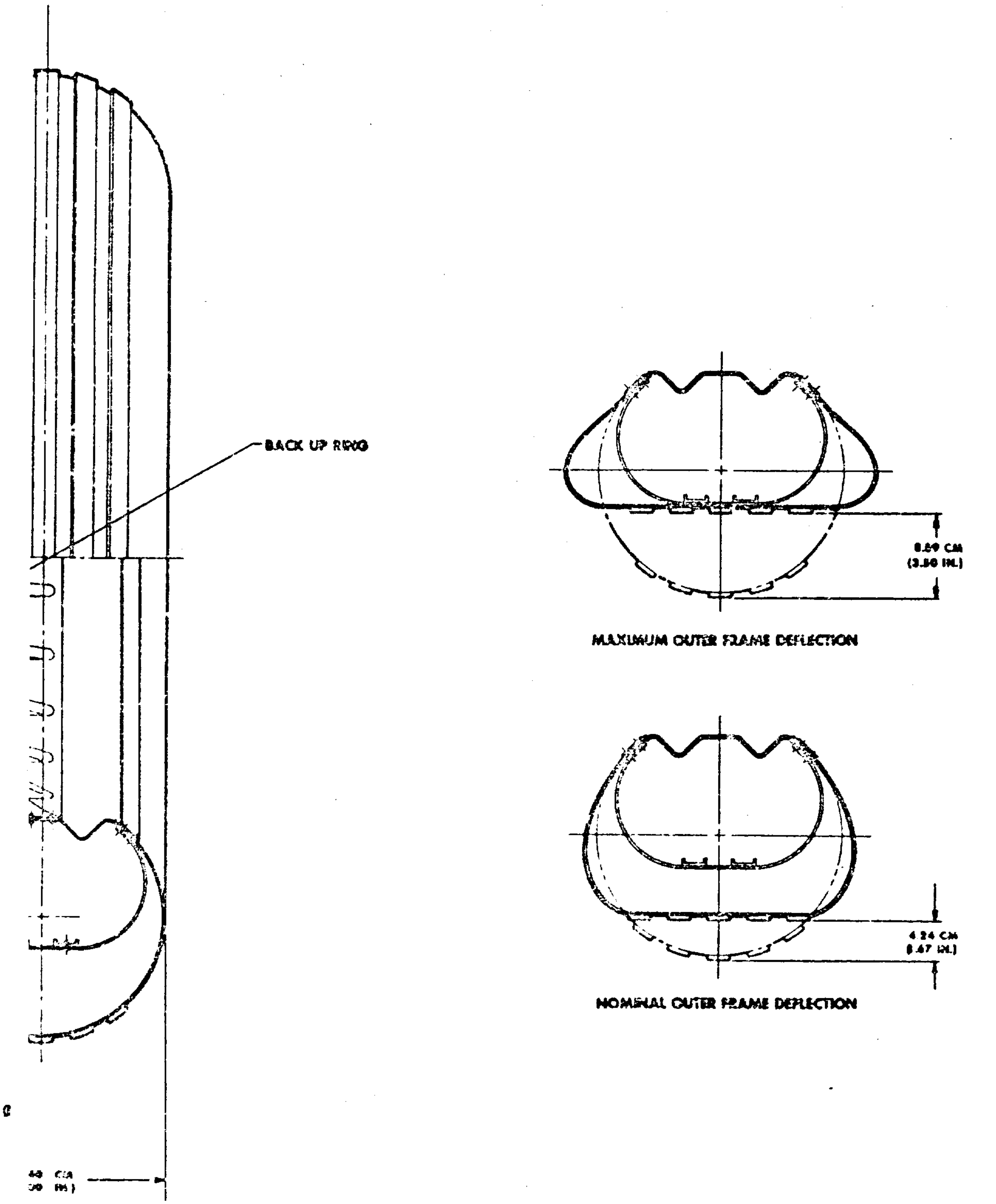

Figure 6.2.8 - Wheel, Wire Frame, Mobility Subsystem, LSSM

3

WIRE FRAME WHEEL CONCEPT

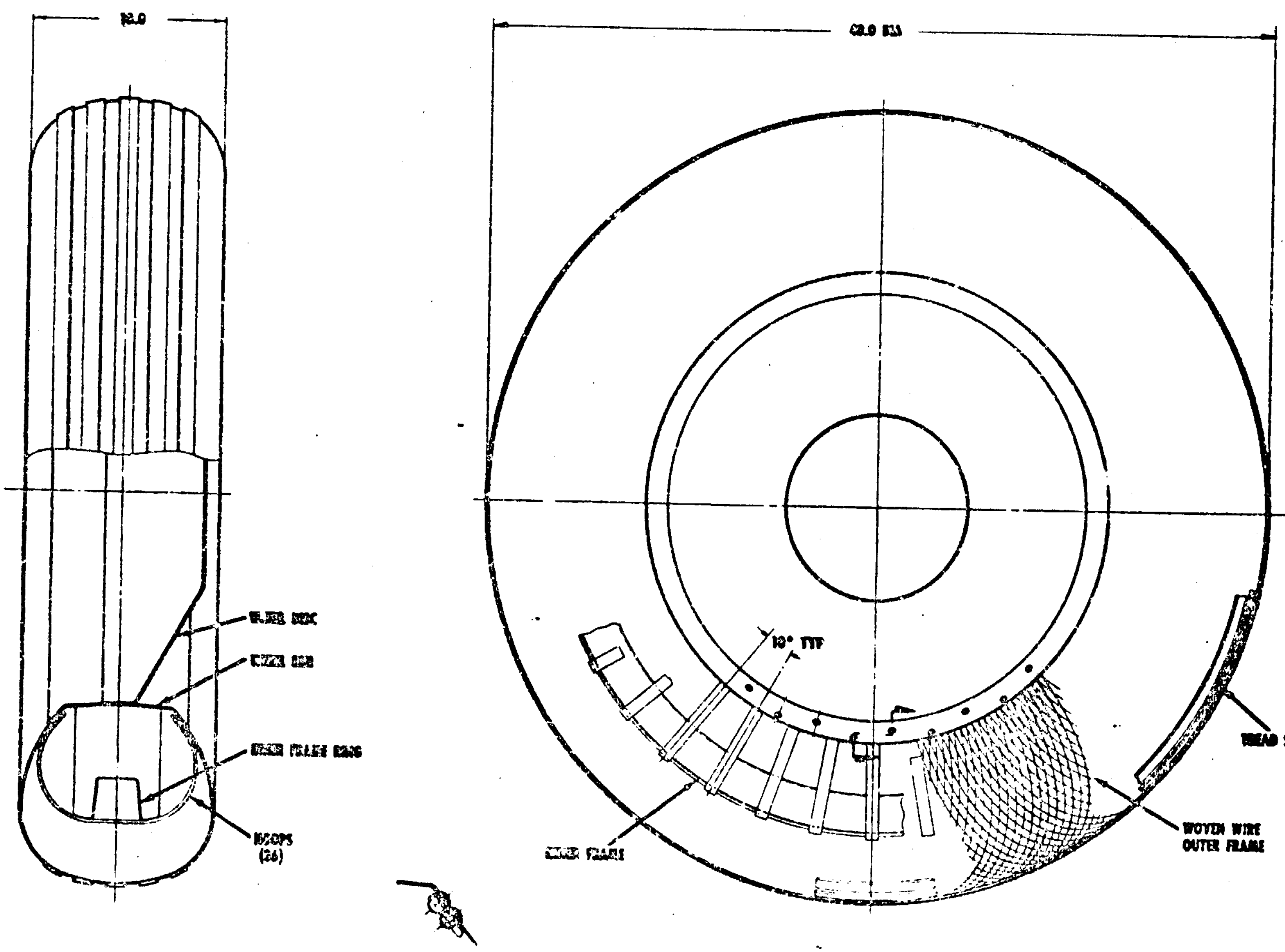

Figure 6.2.9- Wire Frame Wheel Concept, Test Article

stresses should be kept at or below 150,000 psi for materials with fatigue properties comparable to those of music wire and 100,000 psi for titanium alloy wire. The computations established the stress levels as 151,000 psi for the materials having a modulus of approximately 30 x 10^6 psi and as 96,000 psi for the titanium alloys. The wire diameters were established as 0.127 cm (0.050 in) for the 13V-11Cr-2Al titanium alloy and approximately 0.107 cm (0.042 in) for the other materials. Peak stresses in the wire frame are expected to be up to 50% higher than the normal operating stress. However, the high tensile strengths of the alloys being considered (225 to 375 ksi) will prevent any overstressing of the wire at maximum deflections.

The inner frame limits vertical and lateral deflection of the outer frame and absorbs impact loads. It consists of 36 hoop elements interconnected by a hat-section ring. Two clamp rings at the ends of the hoop elements carry clinch nuts used to clamp the outer frame. A welded construction of 6Al-4V titanium alloy is currently being considered for the inner frame because of its high strength-to-weight ratio.

The assumption was made that the flexible wire outer frame will deflect 7.62 cm (3 in.) before encountering the inner frame. Since it had been determined that maximum wheel deflection must be limited to 8.89 cm (3.5 in.) to prevent overstressing of the wire frame, design calculations for the inner frame were based on 1.27 cm (0.5 in.) deflection at the limit radial load of 5204 N (1170 lbf). The number of hoop elements was established as 36 based on the trade-off of minimizing the number of hoop elements to save weight while locating the hoops close enough to each other to evenly distribute the load. The shape of the hoops was scaled from the MOLAB inner frame and a rectangular cross-section was assumed. In order to maximize themoment of inertia of the circumferential ring while keeping weight to a minimum, a stable hat cross section was assumed. Computations established the hat section dimensions as 3.81 cm (1.5 in) high x 2.54 cm (1.0 in) wide x 0.11 cm (0.043 in) thick and the radial hoop section as 0.82 cm (0.322 in) wide x 0.31 cm (0.123 in) thick. Stresses at the limit load were calculated as 38,000 psi in the ring and 100,000 psi in the hoop elements. These stresses are well within the capabilities of the alloys under consideration.

The tread provides a bearing surface for the wheel. The design of a tread which will be capable of the elastic deformations required to conform to the wheel circumference as the wheel rolls under load will be developed in the Wheel and Drive Experimental Test Program. A woven wire braid material or separate metal lugs are currently under consideration.

6.2.6 Wheel Mass Summary

The results of the mass analysis for the baseline LSSM wheel are presented in Figure 6.2.10. The estimated mass shown represents a reduction of about 5 lb. per wheel as compared to the previous wheel concept shown in Figure 6.2.8.

Item	Mass (kg)	Mass (lbm)
1. Outer Frame	2.6	5.8
2. Inner Frame	3.9	8.6
3. Rim	0.8	1.7
4. Disc	1.1	2.5
5. Tread	2.0	4.5
6. Fasteners and Weldments	0.7	1.5
Total	11.1	24.6

Figure 6.2.10 Wheel Mass Summary

6.3 WHEEL DRIVE MECHANISM

6.3.1 Introduction

The conceptual design of the LSSM wheel drive mechanism was guided by the following general considerations:

- Mechanical simplicity
- Compatibility with the lunar thermal and vacuum environment
- Ease of integration into the LSSM mobility system

Earlier studies performed during the MOLAB and MTA programs had resulted in the conclusion that, for lunar operation, the harmonic drive system was the preferred mechanism for a wheel drive. This conclusion has been carried over into this study.

6.3.2 Requirements

General requirements for the wheel drive mechanisms were set forth as follows:

(1) Each wheel shall be independently powered by a separate drive assembly mounted in the wheel hub.

(2) Each wheel drive assembly shall consist of a drive motor, gear reducer, brake system and declutching mechanism.

(3) The entire drive assembly shall be hermetically sealed to the maximum extent possible.

(4) The wheel drive shall be capable of operating in either direction.

(5) Ability to declutch each wheel from its drive mechanism is required to allow vehicle operation without skidding a wheel should failure of a wheel drive mechanism occur, or if only some of the wheels are to be driven, as in the case of smooth hard ground.

(6) Independent passive thermal control (radiator) shall be provided for each wheel drive system.

(7) High reliability, high efficiency, low weight, and small size are primary design objectives.

Operational requirements were established as follows:

o	Output Torque	
	@ 92 rpm (maximum speed)	6 lb-ft
	@ 5 rpm (maximum continuous duty)	68 lb-ft
	@ 2 rpm (intermittent)	120 lb-ft
o	Overall Speed Reduction	130:1
o	Maximum System Temperature	$400^{\circ}F$ ($477^{\circ}K$)
o	Maximum Brake Torque	120 lb-ft
o	Maximum Continuous Brake Dissipation	45 watts

The intermittent duty torque point is that required for the LSSM to climb a step obstacle 40 inches high. This value was determined from scale-model tests. The maximum continuous duty point corresponds to the requirement for climbing a 35 degree hard surface slope. The maximum speed torque is derived from the requirement for a maximum vehicle speed of 16 km/hr (10 mph) over a level, hard surface.

The overall speed reduction of approximately 130:1 converts the 12,000 rpm input to the drive from the integrally mounted electric motor to a maximum wheel speed of 92 rpm.

Maximum brake torque was established to match maximum drive torque requirements and the continuous brake heat dissipation is designed to permit continuous downhill braking at speeds equal to the maximum driving speed uphill. In addition there are requirements for manual operation of the brakes for both emergency and parking modes, and for emergency manual declutching of the wheel in case of wheel drive malfunction.

6.3.3 Drive Mechanism Description

The design evolved to meet these requirements is shown in Figure 6.3.1. It consists of the following major elements:

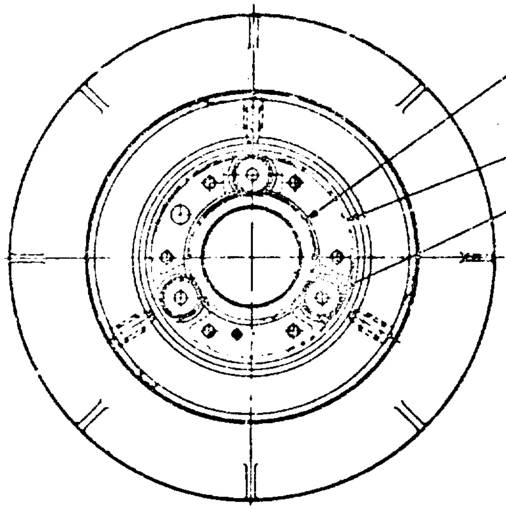

SECTION A A

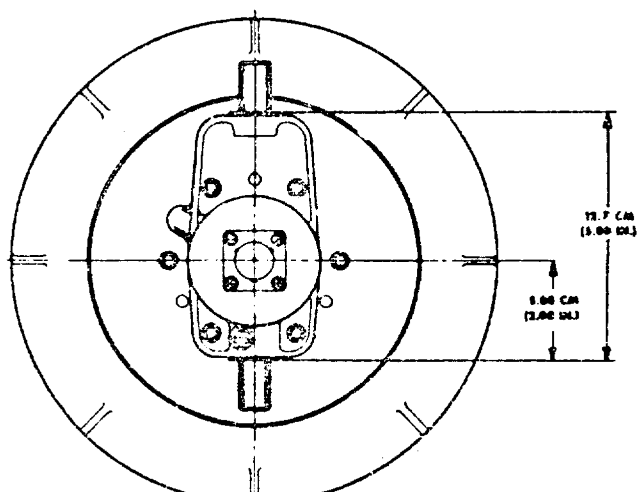

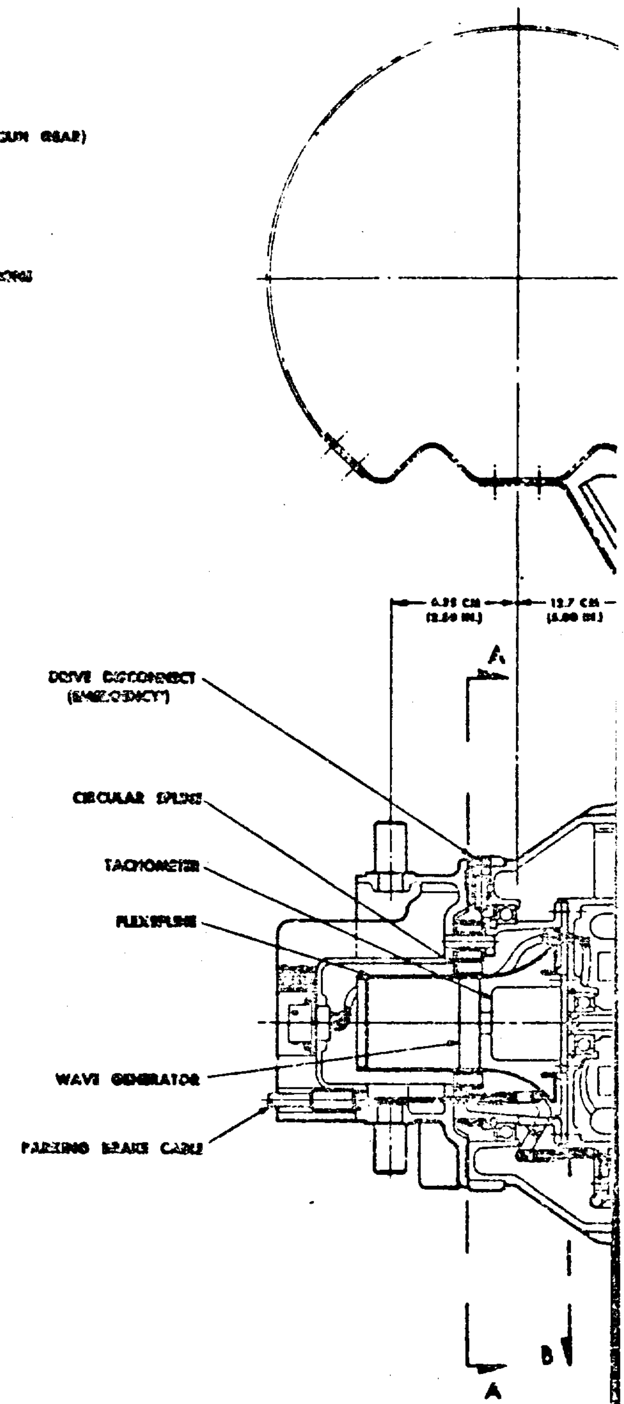

6-29-1

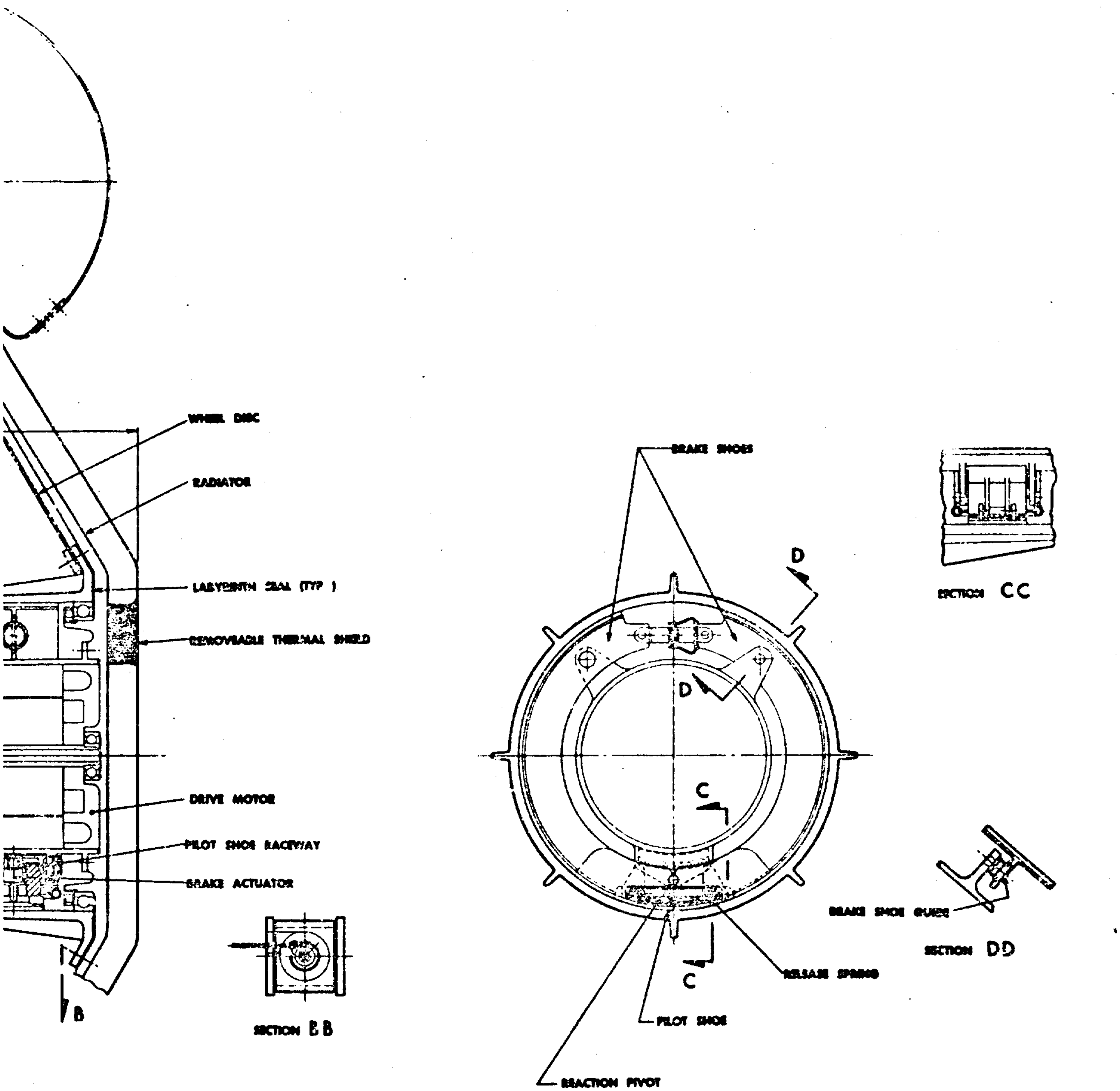

Figure 6.3.1 - Wheel Drive Mechanism Subsystem

-2

- o Electric drive motor
- o Gear train
- o Brake system
- o Lubrication system
- o Wheel drive disconnect
- o Radiator

The drive motor is of the squirrel cage induction type, and is directly coupled to the wave generator of the harmonic drive. (The motor is discussed in detail in Section 6. 7 of this report, under Electric Drive System.) The harmonic drive provides the major speed reduction and a hermetic seal that permits high speed components to be operated in a pressurized atmosphere. The output of the harmonic drive is the circular spline which has gear teeth on its outer circumference to engage three small pinions which drive a ring gear attached to the wheel hub. The wheel hub contains a brake drum surface against which a duo-servo brake system operates. Dynamic seals between the wheel hub and drive assembly provide a means of controlling pressure in the space where the output gears and brake operate.

The assembly is mounted on the vehicle with the motor outboard. The radiator attached to the motor therefore is located in the best available position for effective radiation to space.

With a maximum harmonic drive input speed of 12, 000 rpm and a wheel speed of 92 rpm, the overall speed reduction is about 130:1. The use of intermediate pinions at the output provide a final output reduction. This reduction, equal to the ratio of the ring gear and circular spline drive gear pitch diameters, is 1. 6:1. A reduction of 82:1 is provided by the harmonic drive.

The efficiency of the drive is not readily determined, however, a reasonable estimate that takes into consideration the operating environment would be 0. 85 for the harmonic drive and 0. 90 for the output gearing, or an overall nominal torque efficiency of about 75%.

The ring gear drives the wheel hub through a set of spring loaded pins that transmit the torque between the two members. A collar normally retains these pins in engagement. When this collar is rotated relative to the wheel hub to a second position, these pins are released and the drive is disconnected from the wheel hub. An alternate system could use a split collar retained by explosive bolts that could be fired electrically to disconnect the drive.

The LSSM brake is based on a conventional duo-servo two-shoe brake assembly actuated by a pilot shoe assembly controlled by a small short stroke solenoid. This means of actuation is similar to that of commercial electric trailer brakes, where a solenoid forces a friction pad against the rotating brake drum to obtain actuation forces.

The decision to have the brake react against the wheel hub eliminates the need for a second emergency brake such as was required for the MOLAB wheel drive, where declutching the drive system disconnected the service brake. The LSSM design also makes the wheel hub, disc and wheel available as heat sinks and radiating surfaces to dissipate braking energy.

This location of the brake placed a requirement on it for a high torque capability and led to a brake configuration with a high degree of self-energization to minimize brake actuator forces. The detailed design of the brake system will be sensitive to the brake lining material and its friction coefficient in the LSSM environment. The main effect of this variable is in the actuator force requirement. Considerable study of actuator systems resulted in the system shown.

In this system, a small friction shoe with a certain amount of self-energization is essentially always in contact with the drum and free to rotate with the drum and react against the brake shoes. Such an arrangement results in requirements for an actuator for this pilot shoe of essentially zero travel and minimum force--requirements that can be met with a low power solenoid. To develop full braking torque of 120 lb-ft it is estimated only 15 lbf is required from the solenoid.

The parking brake is operated by a manual push-pull cable actuating a small cam device in parallel with the armature of the solenoid. These manual forces required are small, largely determined by return spring forces required to overcome friction. A tension equalizing system of pulleys is tied to a single operating lever to apply the parking brakes on the four wheels of the forward unit.

With respect to lubrication, the following principles were generally followed:

- o To the extent necessary or feasible, mechanisms should be hermetically sealed from the vacuum.
- o Mechanisms or parts of mechanisms that cannot be hermetically sealed will be closed-off from the vacuum by mechanical or molecular seals to achieve an ambient pressure higher than the lunar vacuum.

Aside from the obvious benefits of avoiding vacuum material problems by hermetically sealing -- several other justifications exist:

- o The presence of an atmosphere assures convective currents to help in the thermal control of the mechanism.
- o A controlled pressure alleviates problems that could arise because of the presence of electrical potentials in the mechanism at ionization pressures.
- o The presence of controlled and predictable pressures reduces the development and test effort for elements and materials enclosed by the hermetic seal.

The use of molecular or mechanical seals on all other mechanisms is dictated by the fact that such seals in conjunction with a suitable outgassing material can maintain an ambient pressure for mechanisms substantially in excess of that of lunar ambient with the following advantages:

- Material problems are substantially reduced.
- Pressures are of a magnitude that can be readily achieved with ordinary vacuum equipment, simplifying development testing.

Application of these principles is, of course, not simple. They will be strongly dependent on considerations of temperature, which varies over an extremely wide range, and materials problems that even for a hermetically sealed mechanism will require considerable investigation and testing.

The proposed LSSM wheel drive design is concerned, therefore, not with a specific solution to the lubrication problem, but in reflecting a mechanical design that will permit the development of an acceptable lubrication system when the detailed environmental parameters are firmly established.

Instrumentation at the wheel drive mechanism will be limited to measurement of temperature at the motor case and of pressure in the hermetically sealed section. This latter measurement would be used to obtain operational status data and provide a means of checking the condition of the seal after final assembly.

Based on MOLAB data and assuming similarity of thermal models, a 2 ft^2 hub-mounted radiator would dissipate enough heat on a continuous basis to maintain maximum temperatures in the wheel drive assembly under 400 ^{o}F. This assumes full solar load, maximum lunar surface temperature, and an average heat input of 70 watts. This, therefore, is considered a conservative estimate of radiator size.

For night-time operation, the low temperatures are a problem. There are material, structural and development considerations that dictate that the minimum operating temperature of the drive be maintained reasonably high. For this reason, it is proposed that electrical energy be used to pre-heat or condition the drive for operation. To minimize the amount of energy used to heat the drive and conserve waste heat from the drive, a shield over the radiator is proposed as shown on the drawing for night-time operation.

The mass of a complete drive system is estimated at 22.0 lbm (10 kg) with the breakdown as shown in Figure 6.3.2.

		lbm	kg
Drive Motor & Electrical		8.3	3.8
Gear Train & Lubrication		3.5	1.6
Housing		1.6	0.7
Wheel Hub & Brake Drum		4.5	2.0
Radiator		2.4	1.1
Brake Assembly		1.7	0.8
	Total	22.0	10.0

Figure 6.3.2 Wheel Drive Mechanism Mass Summary

6.4 SUSPENSION SYSTEM

6.4.1 Introduction

A choice of suspension systems is strongly dependent on the specific vehicle configuration under consideration, as well as the desired performance characteristics. For example, in the case of MOLAB, which utilized Ackermann-type steering of the front wheels and articulated pivot steering of the aft unit, it was concluded that to minimize problems associated with incorporating steering mechanisms and to minimize interference with the cabin structure, parallel arm type suspensions would be used on the forward unit. Since these problems did not exist with respect to the aft unit, a trailing arm type suspension was considered to be most suitable for that application.

In the case of LSSM, the configuration originally selected for baseline design (see "Preliminary Design Study of a Lunar Local Scientific Survey Module (LSSM)", First Interim Report, Boeing Document D2-36072-4, September 1965) was similar to that of MOLAB. The suspension system for this concept consisted of parallel arm type suspensions at the front wheels, and trailing arm suspensions for the center axle and aft unit. In this case, trailing arms were chosen for the center and aft axles because they were readily adaptable to the basically flat chassis-frame structure.

As LSSM design progressed, however, the baseline configuration was altered to utilize Ackermann steering at both the front and aft unit wheels. This in turn led to the conclusion that all the steered wheels should incorporate parallel arm suspensions. Although the center axle wheels could still use a trailing arm suspension, it was decided that in the interest of commonality and in the hope of reducing development time and costs, parallel arm suspensions with torsion bar spring element would be used throughout.

6.4.2 Requirements

General requirements established for the suspension system design are summarized as follows:

1) Essentially the same suspension shall be used at each wheel to achieve the greatest commonality of parts.

2) Each suspension assembly shall be of the parallel arm type, incorporating a torsion bar spring element.

3) A linear dash pot damper shall be used at each suspension. Travel stops shall be incorporated in the damper.

4) The suspension shall be designed to maximize ground clearance and resistance to damage from ground surface obstructions.

5) Reliability, minimum weight and simplicity shall be design objectives.

Functional design requirements were established as follows:

1) Total vertical travel	10 in. (25.4) cm
2) Spring rate	15 lb/in (26 N/cm)
3) Damping rate	50 lb sec/ft (730 N sec/cm)
4) Ability to react wheel torque of	120 lb - ft)162 N-m)
5) Ability to withstand longitudinal impact load (applied at wheel centerline)	2300 lbf (10,400 N)
6) Ability to withstand lateral wheel load	130 lbf (578 N)

6.4.3 Description

The parallel arm suspension assembly for the LSSM is essentially identical at all six wheels. It consists of welded tubular steel upper and lower arms, the damper/stop assembly and torsion bar spring element as shown in Figure 6.4.1. Fittings at the upper and lower edges of chassis provide the mount for the inner suspension while the drive mechanism provides the attachment for the outboard ends of the suspension. Glass filled teflon sleeve bearings are used at the suspension bearing points.

The two arms for the suspension are fabricated from 150,000 - 170,000 psi heat treated 4130 steel tubing 0.75 inch O.D. with 0.065 inch walls, with forged steel end fittings. Tubing size was determined from the design condition of 2,300 lbf wheel impact load.

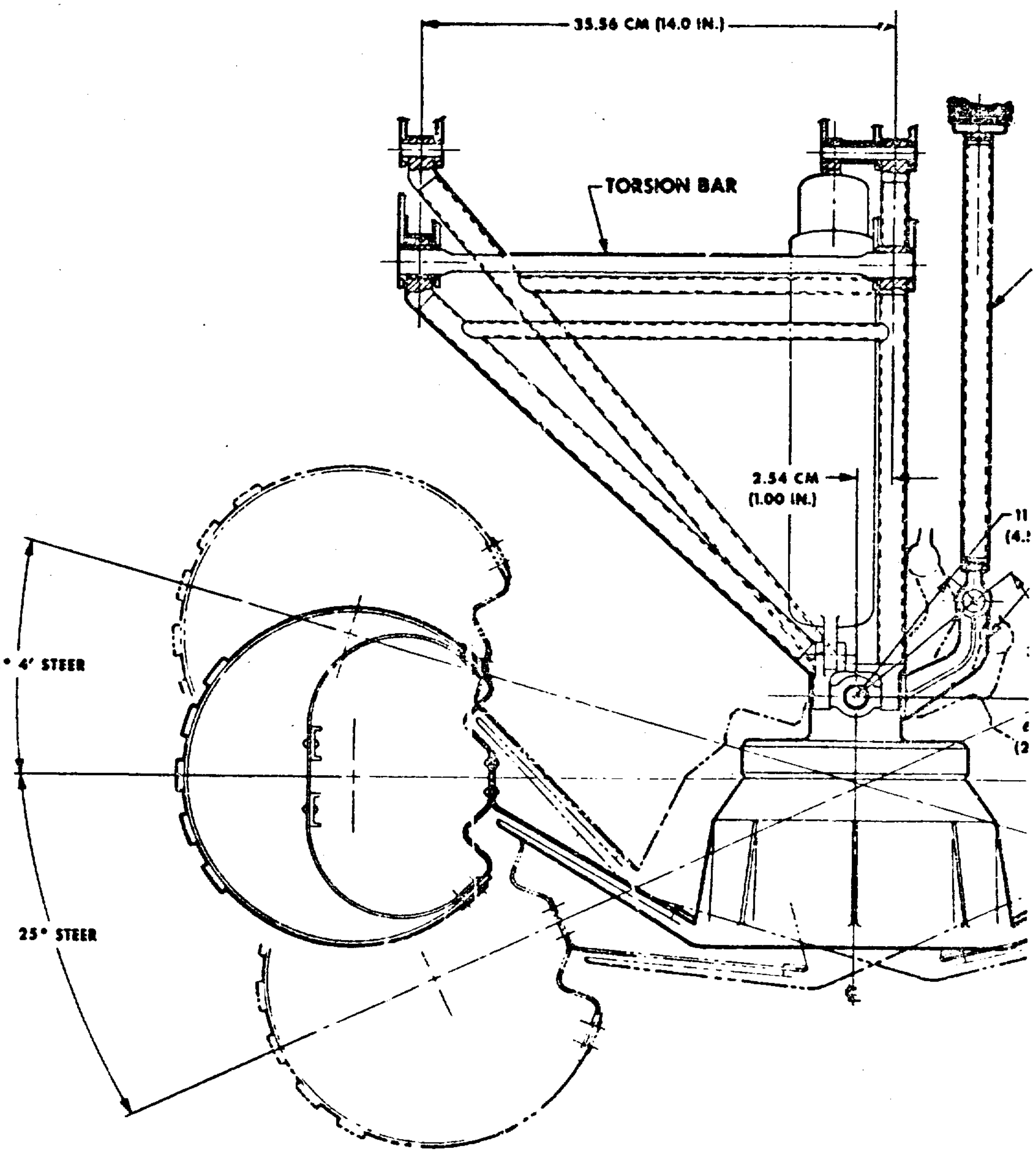

6-37-1

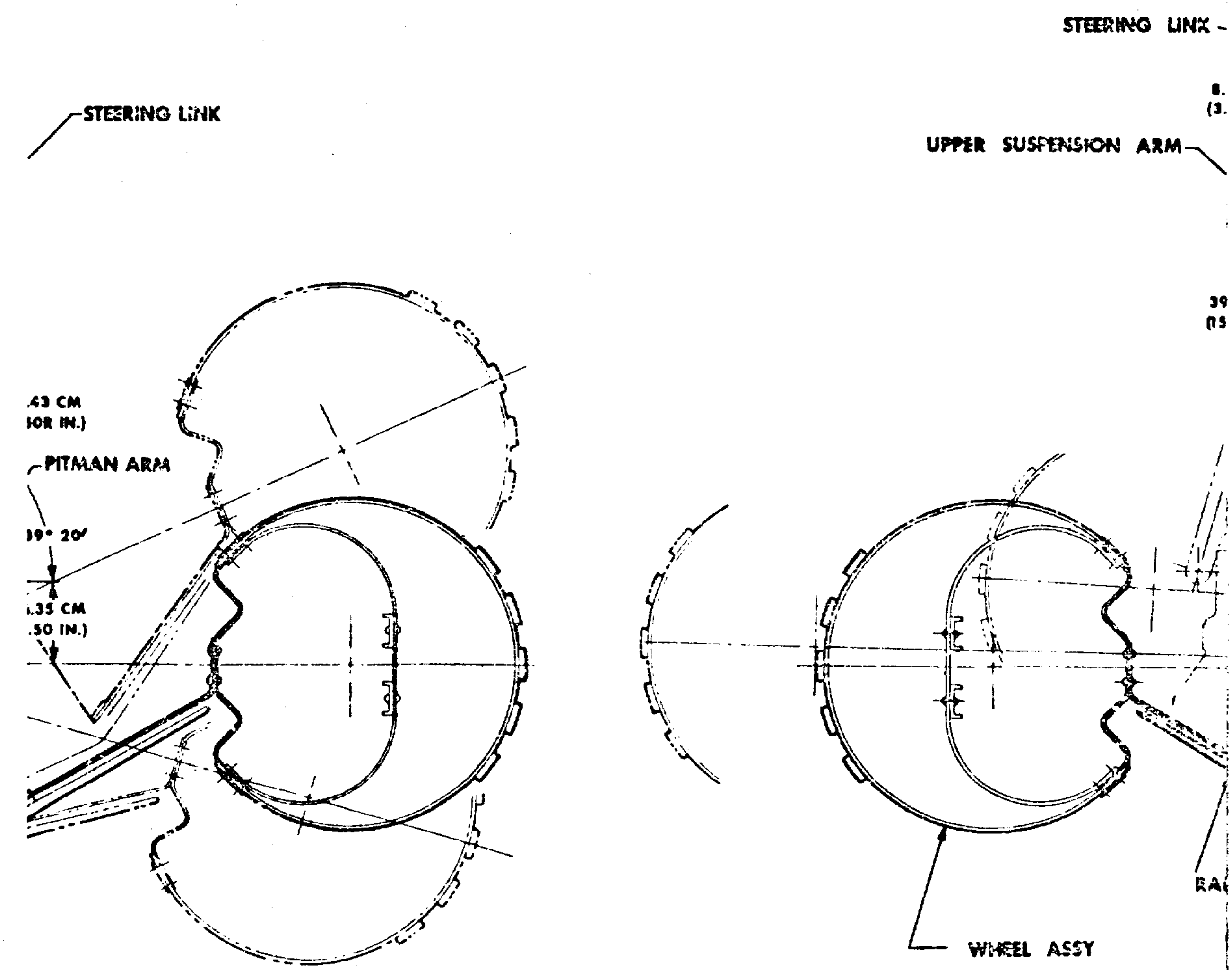
STEERING LINK -
8.
(3.
UPPER SUSPENSION ARM
39
(15
STEERING LINK
.43 CM
.50R IN.)
PITMAN ARM
39° 20'
.35 CM
.50 IN.)
RA
WHEEL ASSY

6-37-2

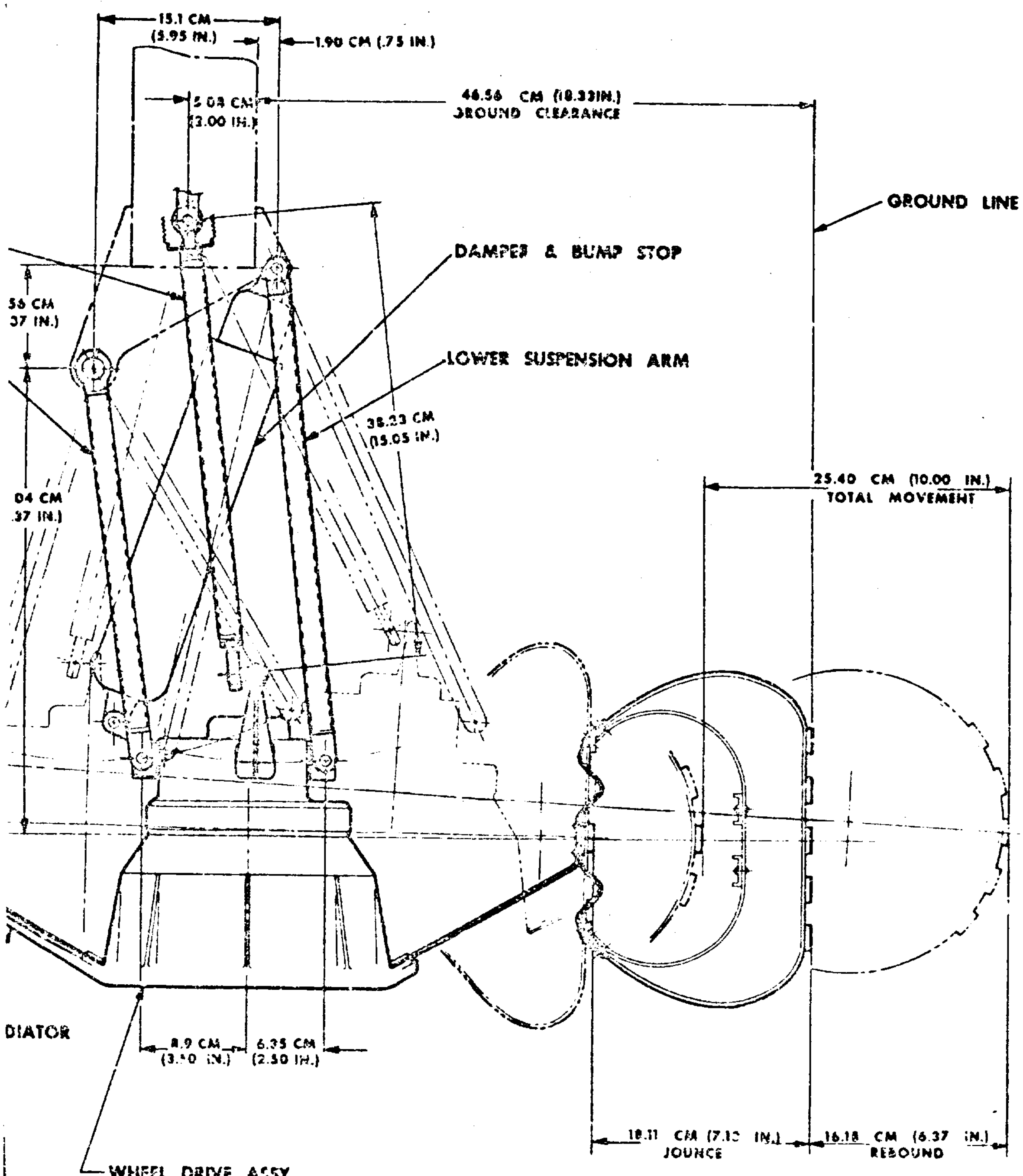

Figure 6.4.1 - Suspension Subsystem, LSSM

The torsion bar is fitted between the two chassis fittings of the upper suspension arms and is of conventional design. The damper is a linear dash-pot type using electrical heating elements to raise damper fluid temperature to the required operating level.

The suspension is designed for a total vertical travel of 25.4 cm (10 in) of which 3.3 cm (1.3 in) is the upper bump stop travel and 1.27 cm (0.5 in) the rebound bump stop travel. Total jounce is 5.3 in (13.5 cm); rebound is 4.7 in. (11.9 cm). The relative travel between the vehicle and the ground contact point is 18.1 cm (7.13 in) of jounce and 16.2 cm (6.37 in) of rebound. The estimated mass per suspension assembly is 10 lbm (4.5 kg).

6.5 STEERING SYSTEM

6.5.1 Introduction

As in the case of the suspension system, the selection of a steering system depends on the specific configuration and performance and functional requirements of the vehicle under consideration.

The baseline LSSM originally selected for preliminary design incorporated Ackermann steering of the front wheels and articulated pivot steering of the aft unit. This scheme was utilized because the required size of the aft unit platform was not well-defined at that time, and articulated steering permitted a wider platform by eliminating encroachment of the wheels on the platform area. Furthermore, two methods of steering the front wheels were also considered at that time:

1) Individual hermetically sealed mechanisms at each of the front wheels consisting of an electric motor driven harmonic drive assembly (similar to the Boeing-GM DRL MOLAB).
2) An electric motor driven cross-link assembly connected to pitman arms at the wheels. This method provided positive mechanical synchronization of the wheel turning angles.

The choice would ultimately depend on problems of integration with the suspension, wheel drive and chassis assemblies.

As preliminary design of the mobility system progressed and system requirement became better defined, the decision was made to Ackermann steer both the front and aft unit wheels. In addition, it was determined that it was feasible to incorporate the mechanical cross-link assembly both on the forward and aft units. This resulted in two essentially identical steering mechanisms, thereby potentially reducing development time and costs. Furthermore, by interconnecting the two units with a flexible shaft, problems associated with the synchronization of individual mechanisms would be eliminated. Another important consideration was the fact that this type of system lent itself to incorporation of a manually actuated emergency steering capability.

6.5.2 Design Requirements

Torque-Speed Characteristics: Torque-speed characteristics for the outputs of the steering mechanisms were derived for four assumed steering conditions. All calculations were made for an assumed static coefficient of friction of 1.0 between wheels and ground, which is the worst possible case to envision.

Condition 1: The vehicle is stationary or moving very slowly, all wheels are in contact with the ground, and one wheel encounters an obstacle it cannot negotiate. The assumption is made that the vehicle will pivot ab out its center of gravity when sufficient torque is generated at the steered wheel to overcome the total resisting force of the vehicle.

For this condition it was determined that the steering torque required at the wheel would be 260 lb-ft (352 N-m) at 0.6 degrees/sec (0.1 rpm).

Condition 2: The vehicle is stationary and all wheels are in contact on level ground. In this case the torque is that required to rotate a deflected wheel.

Steering torque was determined to be 20 lb-ft. (27 N-m) at a steering rate of 6 degrees/sec (1.0 rpm).

Condition 3: This condition is the same as (2) above, except that the torque was determined for a steering speed of 15 degrees/sec (2.5 rpm). Furthermore, an assumed equivalent sliding coefficient of friction of 0.63 was used in place of the static coefficient of 1.0.

The torque requirement for this case was calculated to be 12 lb-ft. (16 N-m).

Condition 4: This condition was established to determine the maximum resisting torque which the steering mechanism must be able to develop.

This was determined to be 407 lb-ft. (552 N-m) for an assumed dynamic longitudinal load input through the wheel centerline.

Geometric Characteristics: Other important requirements established for the steering system were minimum turning radius consistent with vehicle geometry, and synchronization of steered wheel angles to maintain a common center of rotation at all times. The maximum angle was determined to be 25 degrees, which would result in a wall-to-wall turning radius of about 19.0 ft. (6.1 m). The required angular relationships between the steered wheels are shown in Figures 6.5.1 and 6.5.2.

6.5.3 Steering System Description

Steering Mechanism: The proposed design is shown in the drawing of Figure 6.5.3. The system consists of two electric motor-powered units, one steering the forward set of wheels, the other steering the wheels of the aft unit. The concept is similar to that of conventional automotive Ackermann steering.

Each steering actuator assembly consists of a cross-link assembly, housing, connecting links to the wheels, ball-nut input, motor assembly with a spiroid gear output and a flexible drive shaft interconnecting and synchronizing forward and aft steering actuators. The short stroke of these linear actuators makes hermetic sealing with conventional bellows feasible with no significant weight penalty. In addition, there is provision for a manual emergency steering input for the forward unit actuator. Overall reduction of the mechanism is approximately 1250:1; 33:1 at the ball screw and 38:1 from the spiroid gear and pinion.

Each actuator can develop a maximum thrust of 7,450 N (1675 lbf), a maximum rate of travel of 2.7 cm/sec (1.08 inches/sec) and total stroke of 5.6 cm (2.2 inches). The complete steering system weighs approximately 15.5 kg (34.0 lbm) of which 2.2 kg (4.8 lbm) is associated with the emergency steering mode.

The emergency mode of operation is designed to operate independently of the actuator mechanism and thereby remain operative in case of complete freeze-up of the internal parts of the actuator. This is accomplished by releasing the locks that retain the housing so that the housing becomes the cross-link regardless of the position the internal cross-link is in when it becomes inoperative.

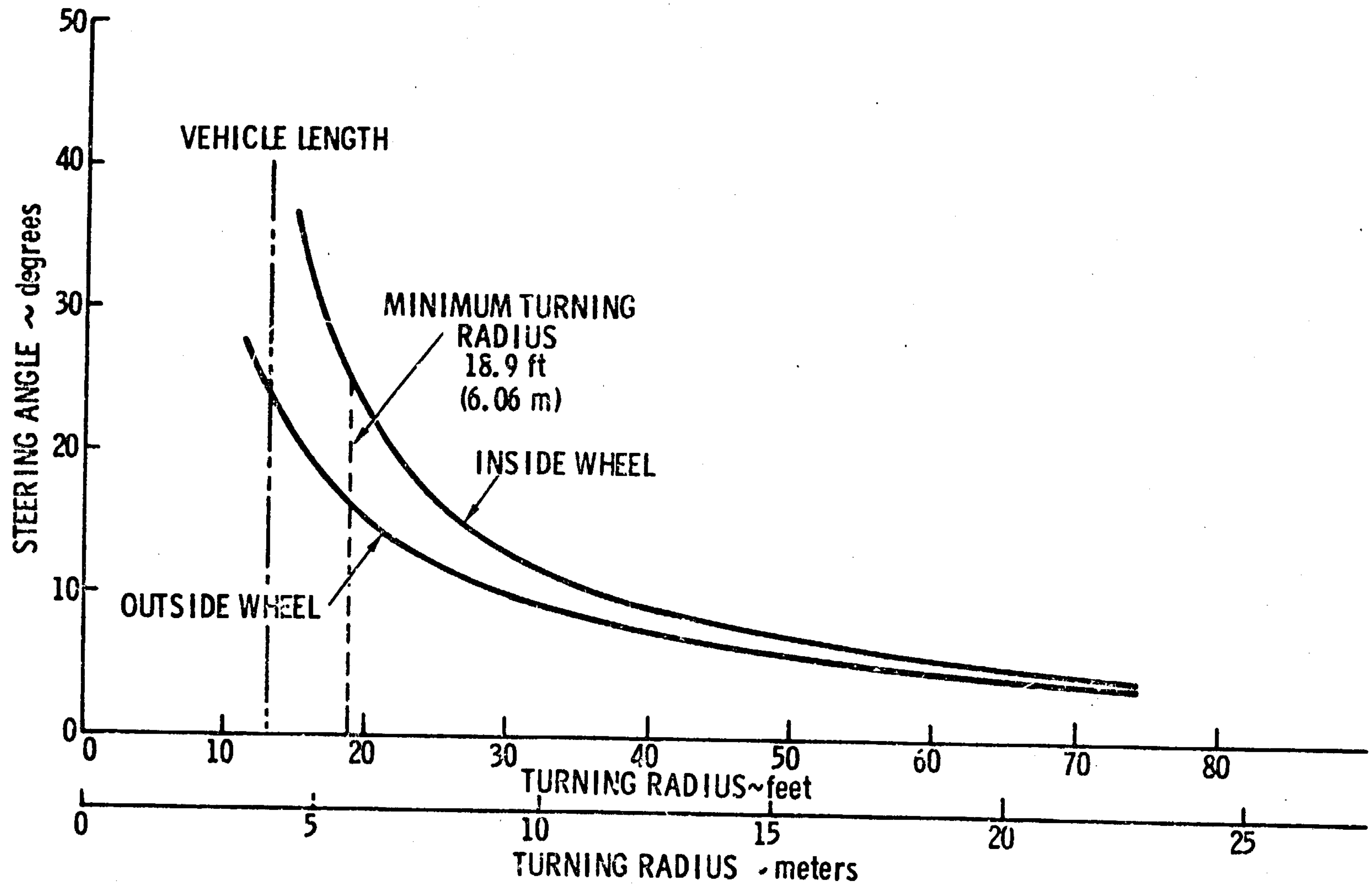

Figure 6.5.1 - LSSM Steering Angle vs Turning Radius - Rear Axle Wheels

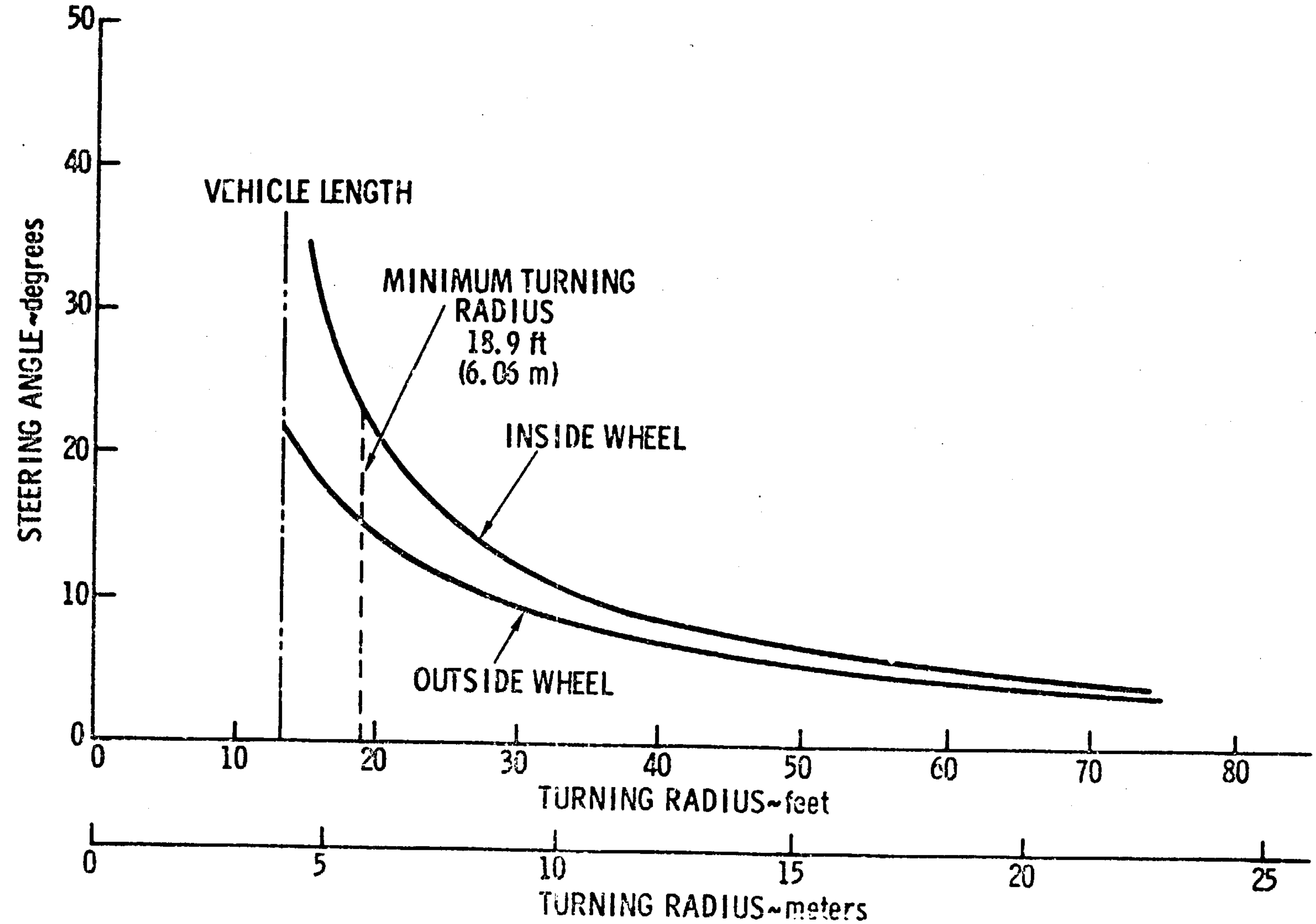

Figure 6.5.2 - LSSM Steering Angle vs Turning Radius - Front Axle Wheels

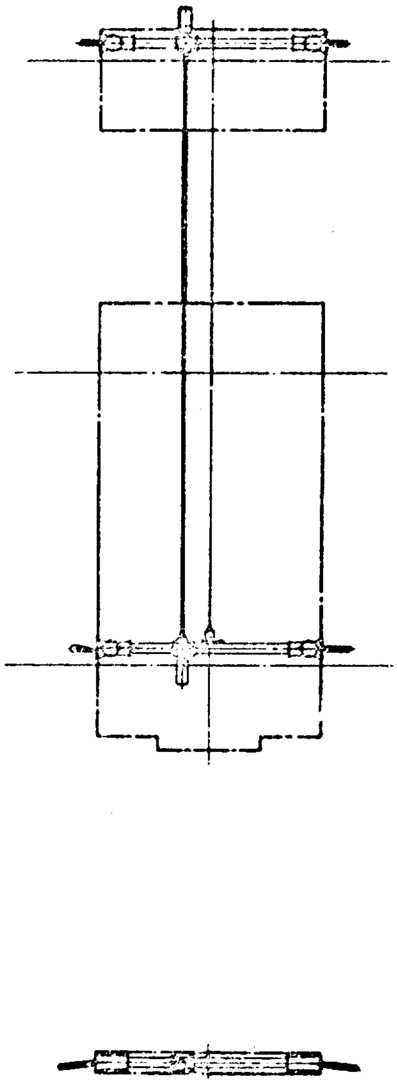

STEERING ACTUATOR SUBSYSTEM ASSY LAYOUT

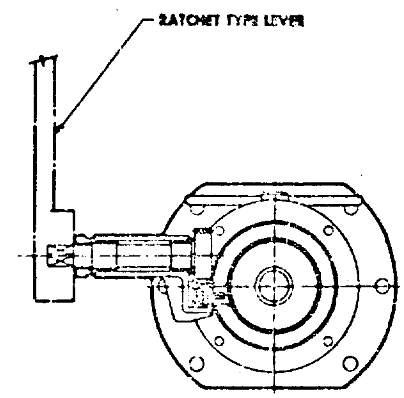

SECTION B B

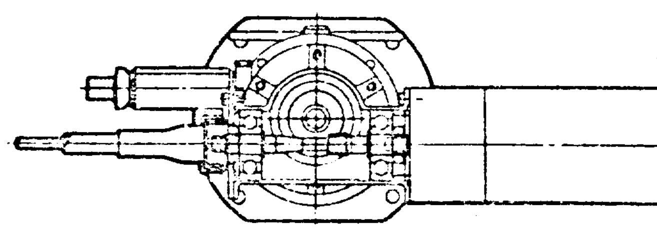

SECTION A A

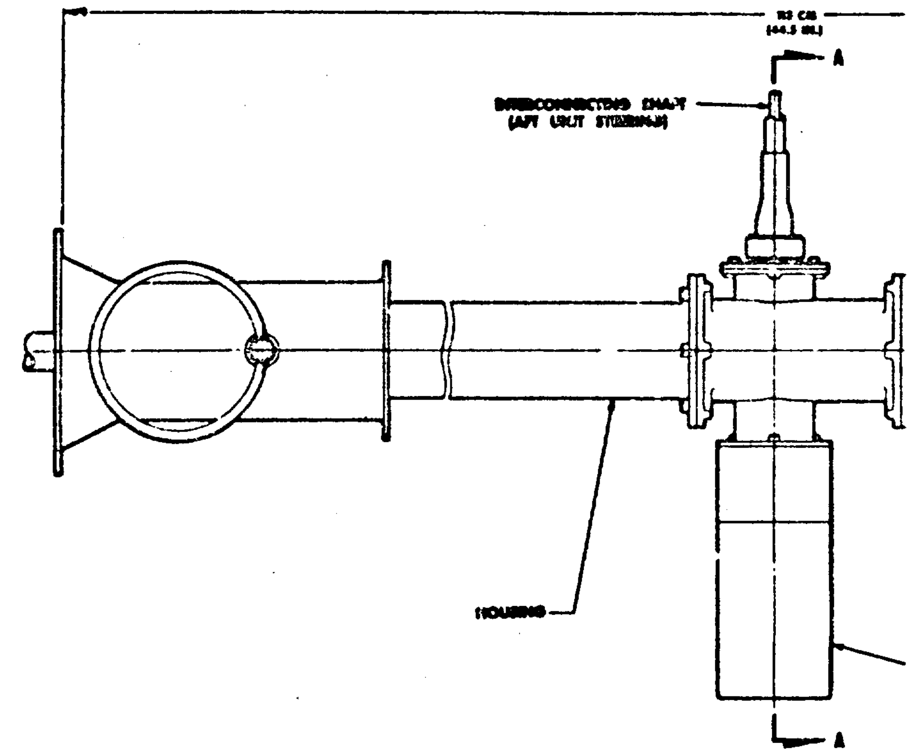

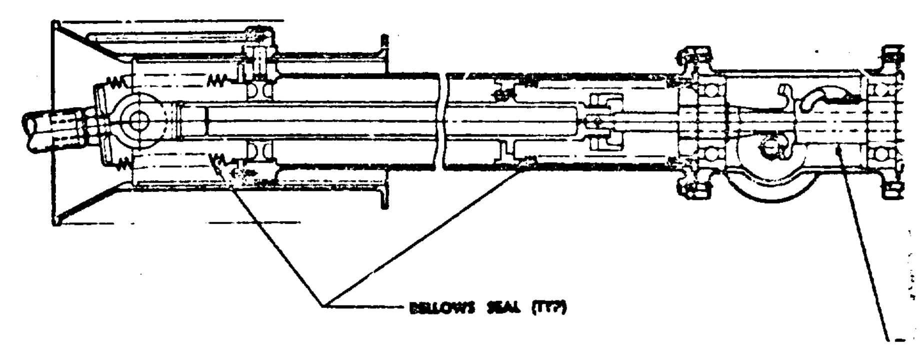

6-44-2

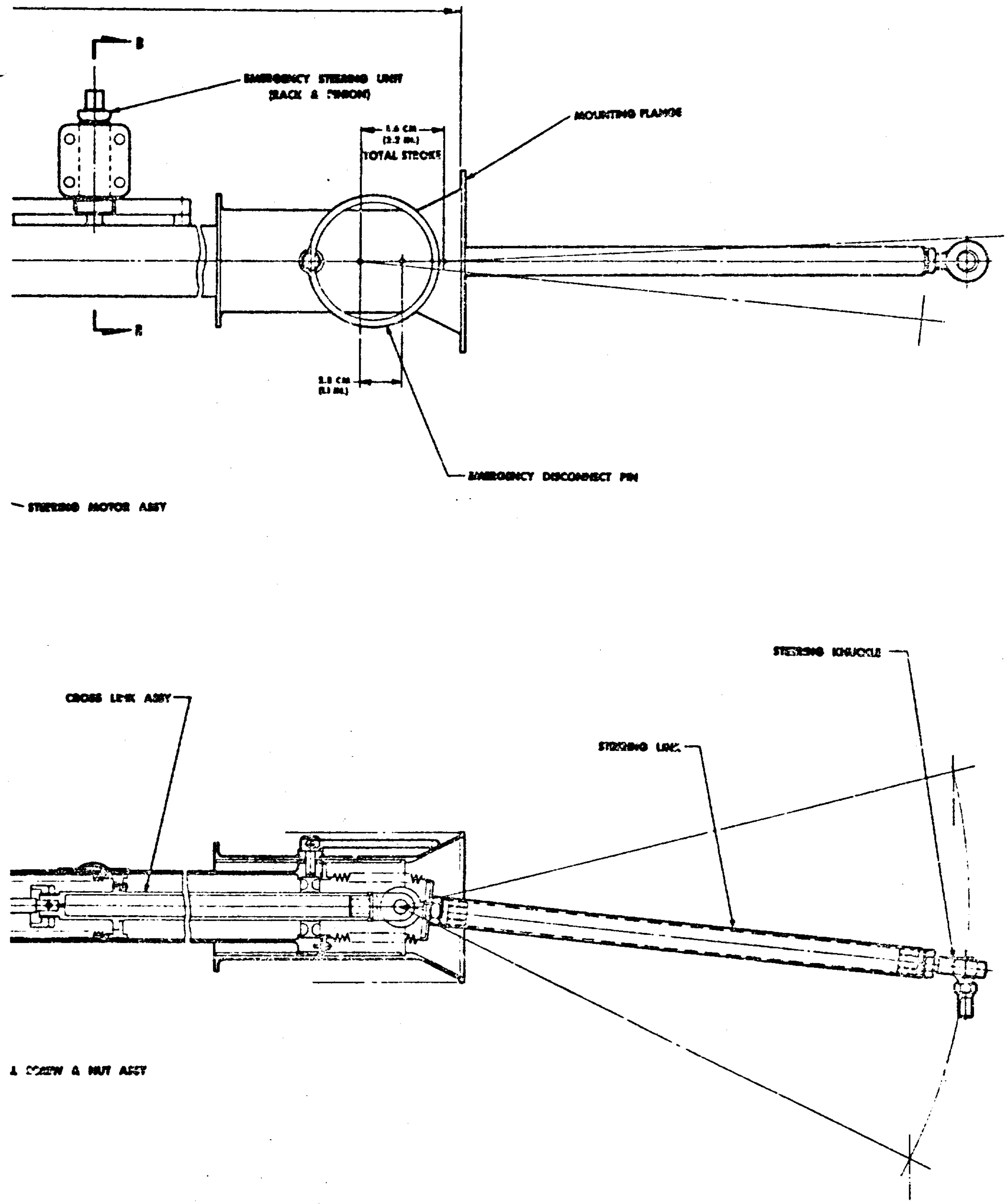

Figure 6.5.3 - Steering Actuator Subsystem, LSSM

Steering Motor and Controls: The electric motor for each actuator is rated at about 30 watts output. The motor output characteristics are shown in Figure 6.5.4. These characteristics are representative of a Globe Industries type BL dc motor or equivalent.

Steering control could be either by an open or closed loop system. The open loop system is simpler in terms of circuitry, but steering control is more precise for the closed loop method. The choice of system might depend on human factors considerations or the requirement for remote operation of the vehicle.

An example of an open loop steering system is shown in Figure 6.5.5. Two permanent magnet motors are used to provide simple reversing and dynamic braking operation. A turn is made by moving the steering control handle in the direction of the desired turn. A clock-wise tilt closes switch S_1 and relay K_1 becomes energized. Current flows thru speed control rheostat R_1 into the motor armature and the motors turn to produce a clockwise turn. When the desired turning angle is achieved the steering control lever is returned to its neutral position and the steering mechanism remains turned in the desired angle. The tilt angle of the control lever determines the turning rate by adjusting the speed rheostats.

Synchronization of the two motors is maintained by a flexible shaft which mechanically couples the motor shafts (thru reduction gears) to each other. Mechanical coupling also provides for sharing the steering load between the two motors.

The steering mechanism can be either directly coupled to motor shafts or thru clutches. Use of clutches, such as magnetic particle clutches, would reduce the motor starting currents considerably by delaying application of the load until the motors are up to speed.

Figure 6.5.6 shows the circuit for a closed loop system employing series field motors and magnetic particle clutches for coupling the motors to the steering mechanism. In this system movement of the steering mechanism follows the

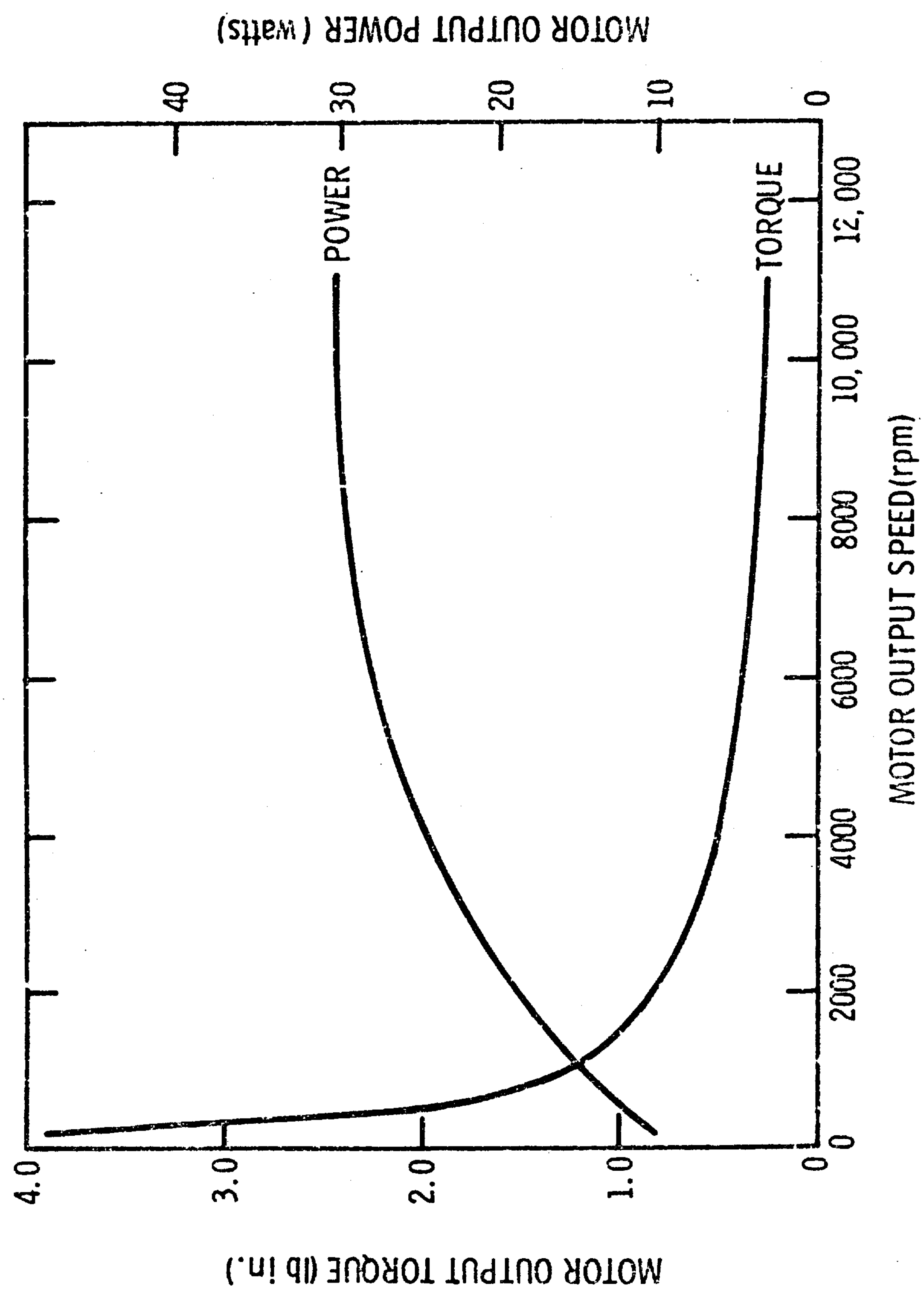

Figure 6.3.4 - LSSM Steering Motor Output Characteristics

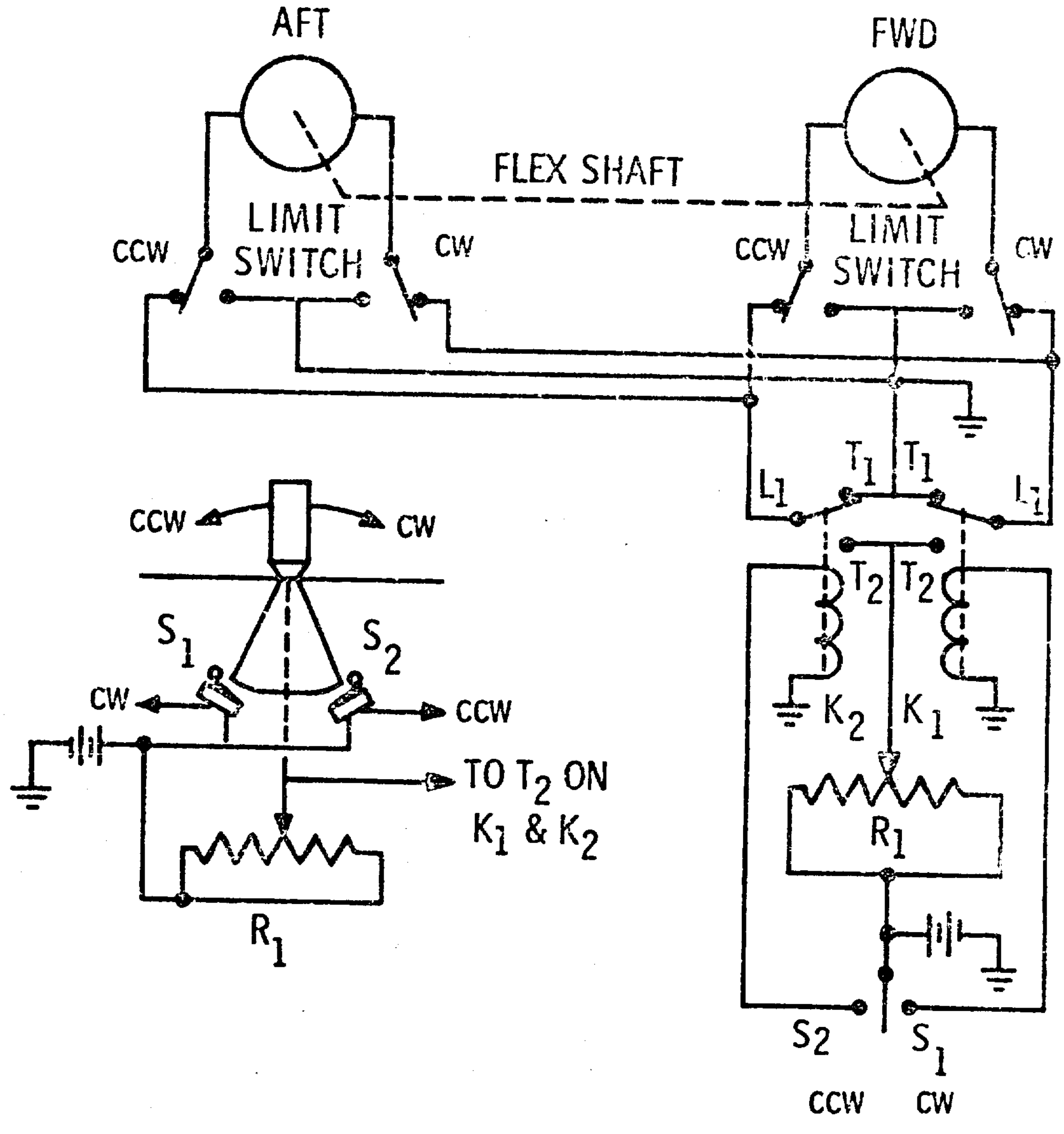

Figure 6.5.5 - LSSM Steering - Open Loop

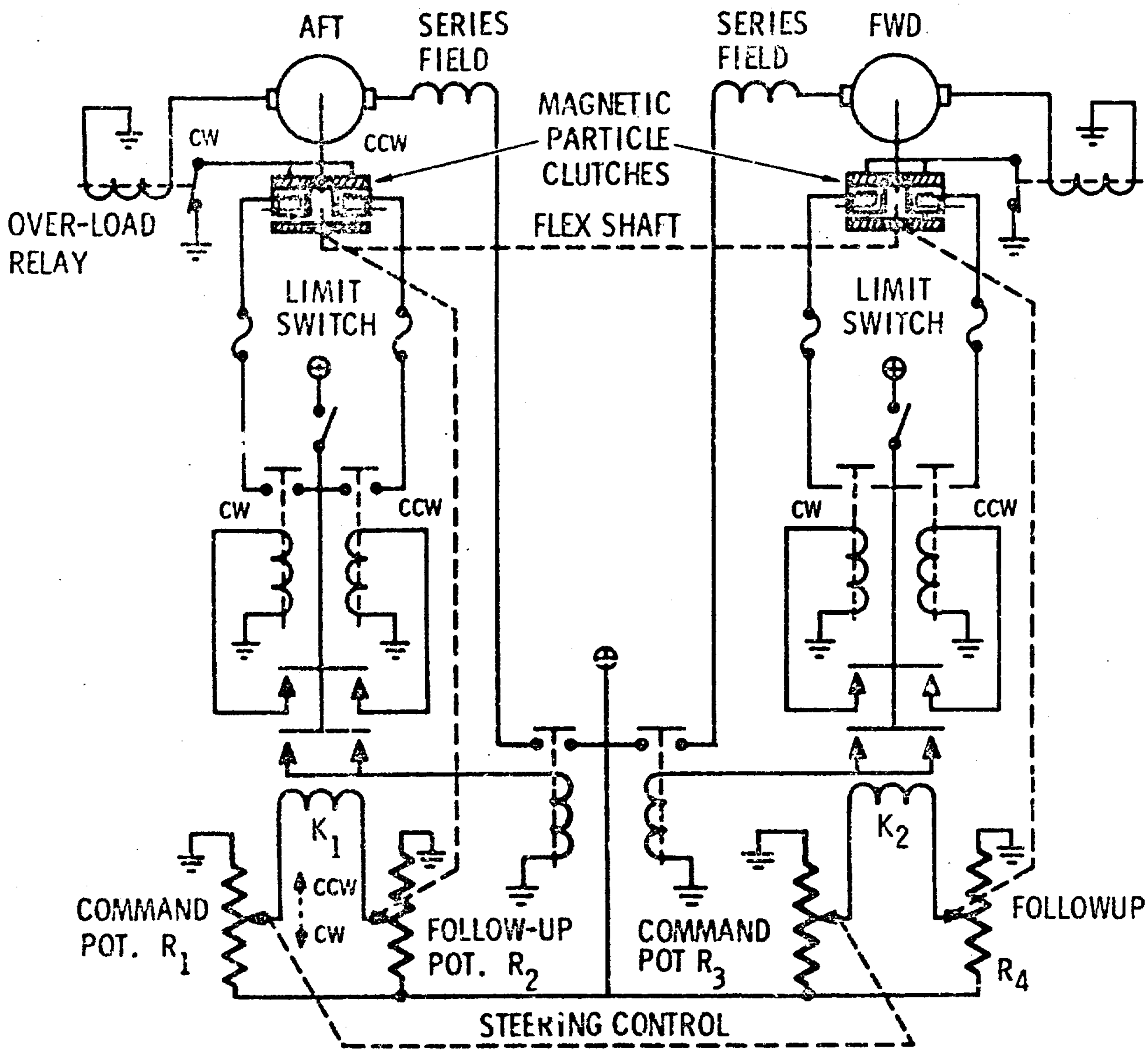

Figure 6.5.6- LSSM Steering - Closed Loop

This emergency input is a rack and pinion driven by a rachet handle.

A detailed analysis was made of the steering mechanism from the points-of-view of loads, velocities and speed - torque requirements. The major results are summarized in the paragraphs following.

It was determined that the ball screw must be capable of handling a maximum static load of 1700 lbf and operational loads up to 2200 lbf. For the method of loading employed, the ball screw which meets the sizing requirements is type 0375-1875. The minimum required nut length is determined by the static load per turn of balls and the lead of tread. In this case the static limit per ball turn for the screw is 720 lbf. Assuming the ball nut has five complete turns, the maximum static capacity of the ball nut would be 3600 lbf which provides a safety factor of 2.2. For an operating load of 2200 lbf the expected life of the screw is 60,000 cycles. The minimum length of the ball nut to carry the operational and static loads is 1.5 inches. It should also be noted that the screw speed falls well within the maximum safe speed.

The selection of the spiroid gear for this application was based upon its reduction ratio and capability to meet the torque requirements. The spiroid selected has the following characteristics:

o Reduction ratio	38:1
o Center distance	0.5 inches
o Pinion O.D.	0.456 inches
o Full depth	0.075 inches
o Nominal torque	100 lb-in.
o HP out at 1750 rpm	0.038 HP
o HP in at 1750 rpm	0.067 HP

Based on spiroid gear tables, the above power characteristics provide a factor of safety of 1.4 for the maximum output torque condition, and 2.4 at the maximum input speed condition. The efficiency of this gear pass is estimated at 58%.

movement of the steering control lever. The steering control lever is directly coupled to the command pots R_1 and R_2 while the steering mechanisms are coupled to the follow-up pots R_3 and R_4. Two Wheatstone bridges are formed by pots R_1 and R_2 and by pots R_3 and R_4. Movement of the steering control causes an unbalance in the bridge. The unbalance is detected by polar relays K_1 and K_2 which energize the magnetic particle clutches to cause the steering mechanism to move in the direction which will electrically balance the bridge.

Synchronization is maintained by coupling the command pots together. An optional flexible shaft provides for sharing the load.

A current relay in the motor armature circui prevents application of the load until the motors are up to speed and also disengages the motor if an overload develops. Limit switches are placed in the clutch circuits. The dual control circuitry permits independent operation of either the aft or forward steering mechanism.

6.6 CHASSIS FRAME ASSEMBLY

6.6.1 Introduction

The conceptual design of the LSSM chassis-frame assembly was guided by the following general considerations:

- o Structural simplicity consistent with the semi-flexible frame concept.
- o Provide an integrated mobility subsystem to minimize interface problems with other vehicle systems.
- o Provide maximum flexibility for adaptation to other vehicle systems such as crew station, scientific equipment, etc.

While space frames and other chassis types were studied conceptually, the above considerations led to a chassis-frame concept based on flat box structures.

6.6.2 Requirements

The general requirements established for the chassis-frame assembly are summarized as follows:

1) A flat top surface shall be maintained.
2) Load paths for the stowage and deployment modes shall be integrated into the structure.
3) Superficial or secondary structure shall be used to provide additional payload platform area or mounting points for equipment.
4) Extension of the aft unit and flexible frame shall require minimum effort on the part of the astronaut.
5) The chassis shall provide a basis for a complete integrated mobility system.
6) High reliability, low weight and simplicity shall be primary design objectives.

6.6.3 Description

The LSSM chassis-frame assembly consists of the following major components (see Figure 6.6.1):

- o Forward unit frame assembly
- o Aft unit frame assembly
- o Flexible frame assembly

Chassis-Frame: Both the forward and aft chassis-frame units are load carrying box structures on which appropriate fittings are located for the suspension, flexible frame assembly, crew station, thermal compartment and stowage attachments.

Two main structural members near the center of both boxes provide the main load path. These two members also provide the track support for retracting the flexible frame for stowage on the LEM/Shelter. For all practical purposes, the stowage loads determined the size and weight of the chassis members. Attached to this prime chassis structure will be secondary structure configured as required to support the scientific payload.

The two units are fabricated from extruded angles and tees, skin covered into a box beam configuration. The material of the box beam consists of 7075-T6 aluminum alloy sheet and extrusions. The forward unit, 113 cm (44.5 in) wide, 218 cm (86 in) long and 10.2 cm (4 in) deep, has continuous longitudinal cap members and vertical webs. Lateral members are spaced at approximately 14 inch intervals. The upper and lower skins are .127 cm (.050 in) thick and all vertical webs are .102 cm (.040 in). The aft unit, 113 cm (44.5 in) wide, 50.8 cm (20 in) long and 10.2 cm (4 in) deep, has continuous lateral and longitudinal cap members. The upper and low skins are 0.127 cm (.050 in) thick, as are the internal vertical webs. The external vertical webs are 0.102 cm (.040 in) thick.

In the stowed position the forward and aft units are attached together at the longitudinal vertical webs by fittings which carry the bending moments due

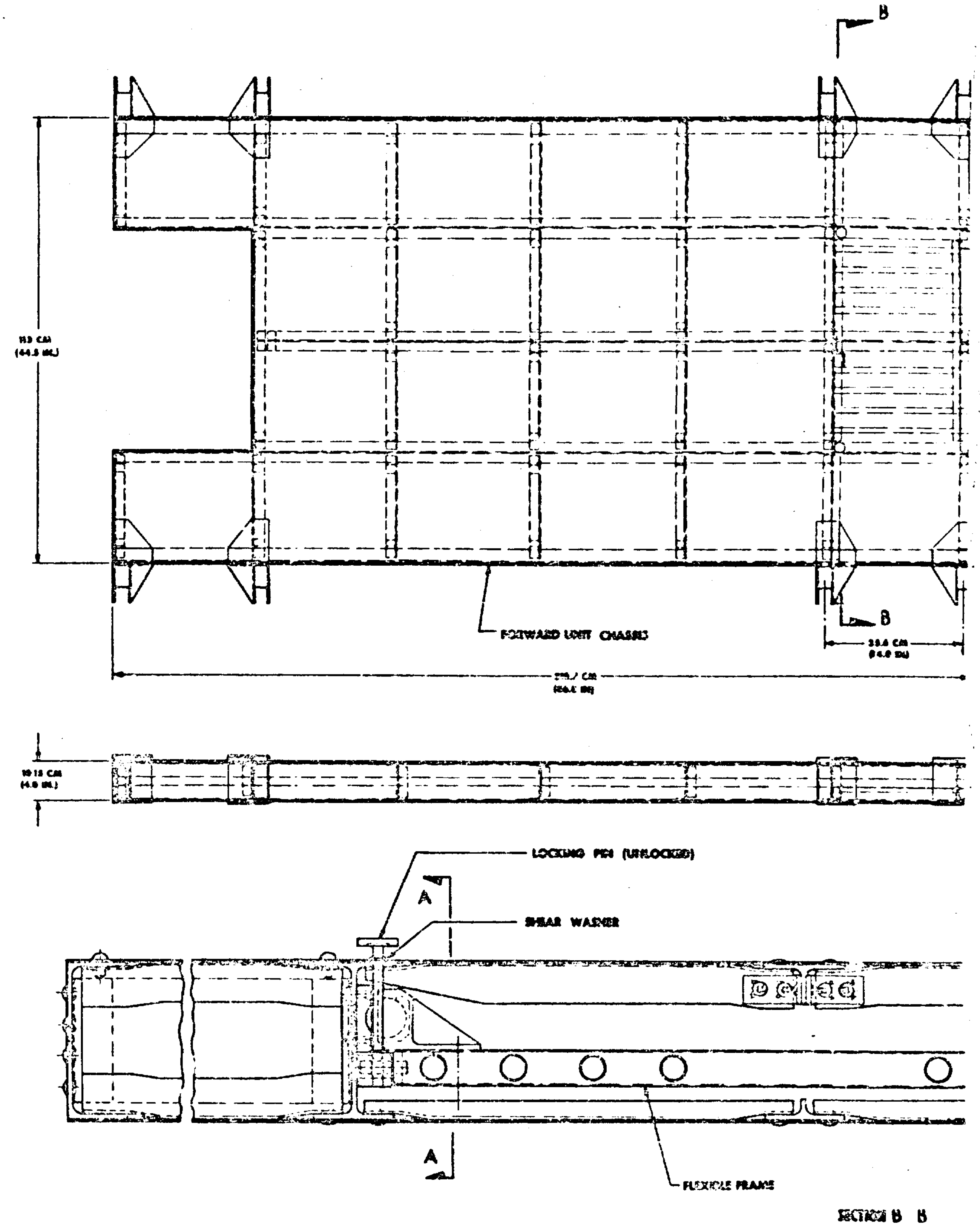

B
FORWARD UNIT CHASSIS
LOCKING PIN (UNLOCKED)
A
SHEAR WASHER
FLEXIBLE FRAME
SECTION B B

6-53-1

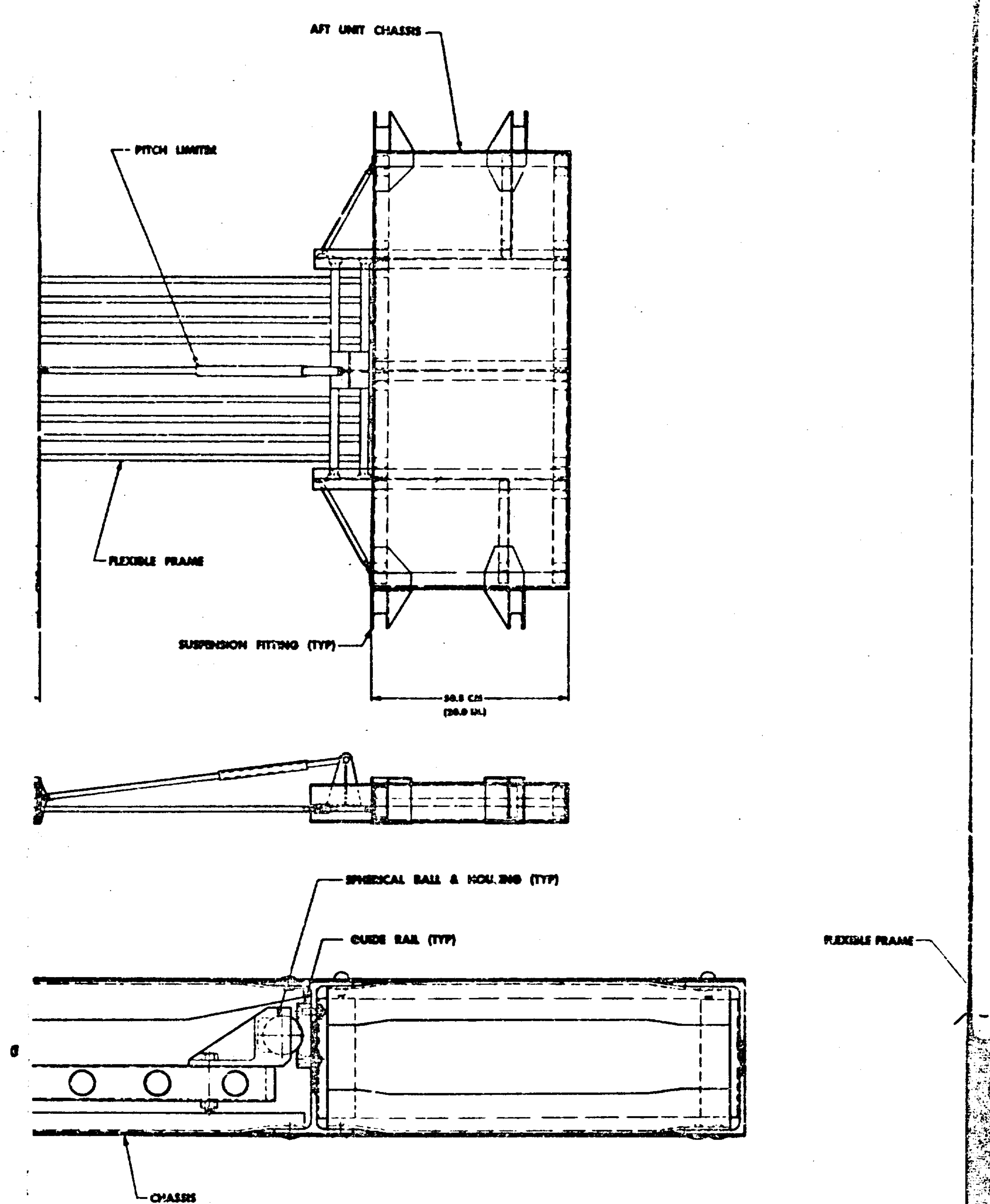
AFT UNIT CHASSIS
PITCH LIMITER
FLEXIBLE FRAME
SUSPENSION FITTING (TYP)
SPHERICAL BALL & HOUSING (TYP)
GUIDE RAIL (TYP)
FLEXIBLE FRAME
CHASSIS

6-53-2

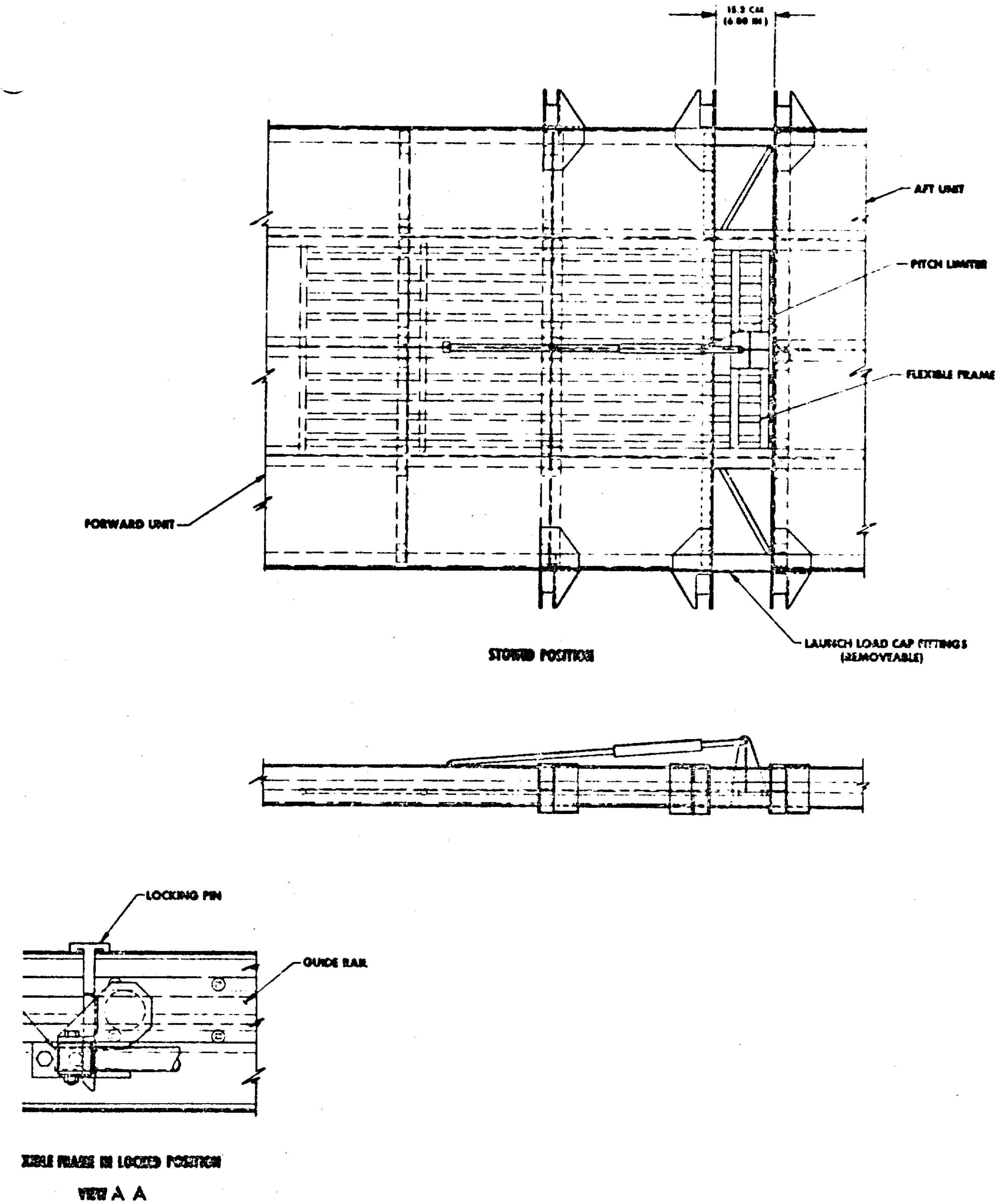

Figure 6.6.1 - Chassis Assembly, Forward and Aft Structure

to Load Condition 6, as defined in Boeing letter 2-4466-00-115, "LSSM Tie-Down Requirements", dated 23 December 1965. This condition imposes an acceleration vector in the Y-Z plane of $\pm$ 258 ft/sec^2 and a rotation acceleration about any axis in the Y-Z plane of $\pm$ 14 rad/sec^2. If these attached fittings were only used at the internal longitudinal cap members, they would increase in size appreciably, therefore, a weight saving is realized by providing fittings at four locations.

Flexible Frame Assembly: The flexible frame installation consists of the flexible frame, pitch limiter, and the retraction mechanisms.

The spring members of the flexible frame are eight 6AL4V2Co Titanium tubes, 0.625 inch O.D. with a 0.40 inch wall. The tubes are welded to sheet metal box structure cross members at either end. The flexible frame provides for relative displacement between forward and aft units of $\pm$ 30 degrees in roll and $\pm$ 15 degrees in pitch (limited by a pitch limiter).

The pitch limiter is a telescoping cylinder with $\pm$ 12.7 cm ($\pm$ 5 in) of travel. It incorporates springs to cushion the travel against the stops and is expected to provide a certain degree of damping through use of a high viscosity silicone grease (NASA Technical Brief #65-10144).

For stowage on the LEM/Shelter, the overall length of the LSSM is reduced by sliding the flexible frame into the forward unit structure. For deployment on the lunar surface, the flexible frame is moved aft and secured in place.

The flexible frame rides on rollers in a track fitted to the two main chassis members of the forward unit. Upon release of the fastening devices that lock the forward and aft units together for stowage, vehicle power can be used to separate the two units. As the frame travels aft, pins in the ends of cross members of the flexible frame engage a ramp into a blind slot to stop frame travel. These pins in the frame are then trapped in the slot by applying a force on the enlarged head of the locking pin (this may be done by the astronaut's foot). This force shears a low strength retraining washer. The end of the pin that locks the elastic frame in place is tapered to wedge the frame into its seat.

Estimated Mass: The estimated mass breakdown for the complete chassis-frame assembly is given in Figure 6.6.2.

	Kg	Lbm
Forward Unit	39.3	86.5
Aft Unit	28.2	62.1
Pitch Limiter	1.7	3.9
Flexible Frame	2.9	6.5
Total	72.1	159.0

Figure 6.6.2 Chassis-Frame Breakdown

6.7 ELECTRIC DRIVE SYSTEM

6.7.1 Introduction

This section describes the preliminary design of an electric drive system for LSSM propulsion. Based on information gathered and results of the MOLAB study, laboratory tests, and design analyses, an electric drive system has been defined that will perform the LSSM propulsion functions. The basic system is one that can benefit from advances in materials and circuit technology and can be scaled up or down for various size lunar vehicles.

Figure 6.7.1 depicts the major elements of the LSSM electric drive system. The blocks indicated by dotted lines are not considered part of the electric drive system for purposes of this study. Power handling elements are the distribution cables and circuit breakers, the power conditioner semiconductor switches, and the drive motors. The information handling elements are the motor speed sensors, signal cables and power conditioner control circuits.

Squirrel-cage induction motors are used to supply propulsion power to the wheels. Torque and speed are varied by controlling motor frequency, slip and current by means of transistor current control inverters.

6.7.2 System Requirements

The following define the requirements for the LSSM drive system:

- o Capable of day or night operation in the lunar environment.
- o High system reliability (including voltage controllers, inverters, brakes, cables, circuit breakers, and motors)
- o Maximum locomotion efficiency. In terms of wheel control this means that:
    1. Each wheel should be individually powered.
    2. For constant input voltage the torque of each drive motor should increase as wheel speed decreases.
    3. The speed of an individual wheel should remain close to the average speed of the other wheels when contact with the ground is lost.

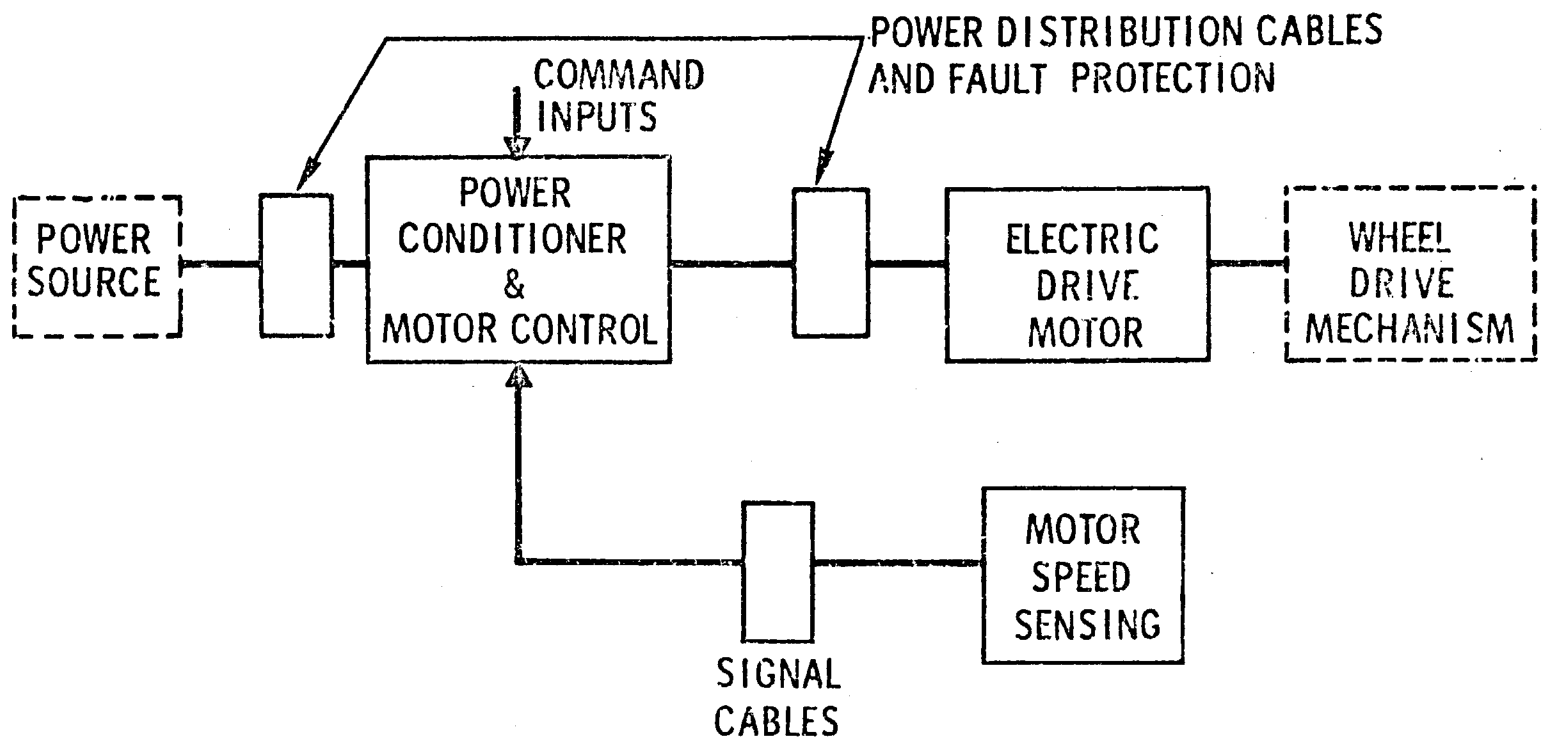

Figure 6.7.1 - Major Elements of an Electric Drive System

4. Torques at the outside wheels should equal the torques at the inside wheels when the vehicle is turning.
5. Average torque of the wheels on each side of the vehicle should not be significantly reduced because of differences in wheel speeds due to terrain slope variations, unequal wheel diameters, or unequal wheel loadings.

- Capable of reversing.
- Failure of a single major component or system should not abort the mission.
- Maintenance capability preferred.
- Ability to electrically and mechanically isolate any drive motor and to skid steer the vehicle for emergency modes of operation.
- Gear shifting not desirable.
- Dynamic braking not necessary.
- Peak electric drive efficiency of 70% or greater (excluding gear box).
- Maximum steady state power demand 1 kw or lower.

In addition, it is preferred that the drive motors be cooled by direct radiation to space rather than by circulating fluids. Temperature control for the logic circuits and power switches should be accomplished by transferring heat from the semi-conductors to phase-change materials or circulating fluids.

Required motor torque as a function of shaft speed is plotted in Figure 6.7.2. Motor output power versus shaft speed is shown in Figure 6.7.3. A plot of wheel velocity correction factors versus outside Ackermann steering angle for the LSSM is shown in Figure 6.7.4. Wheel differential speed information is required so that the proper voltages can be supplied to the inside - and outside - wheel motors to maintain equal wheel torques when the vehicle is turning.

A 56 VDC battery system will provide energy for the electric drive system.

6.7.3 Drive System Configurations Considered

Preliminary conceptual designs of candidate electric drive systems were prepared in sufficient detail to enable estimates to be made of weight, size, efficiency,

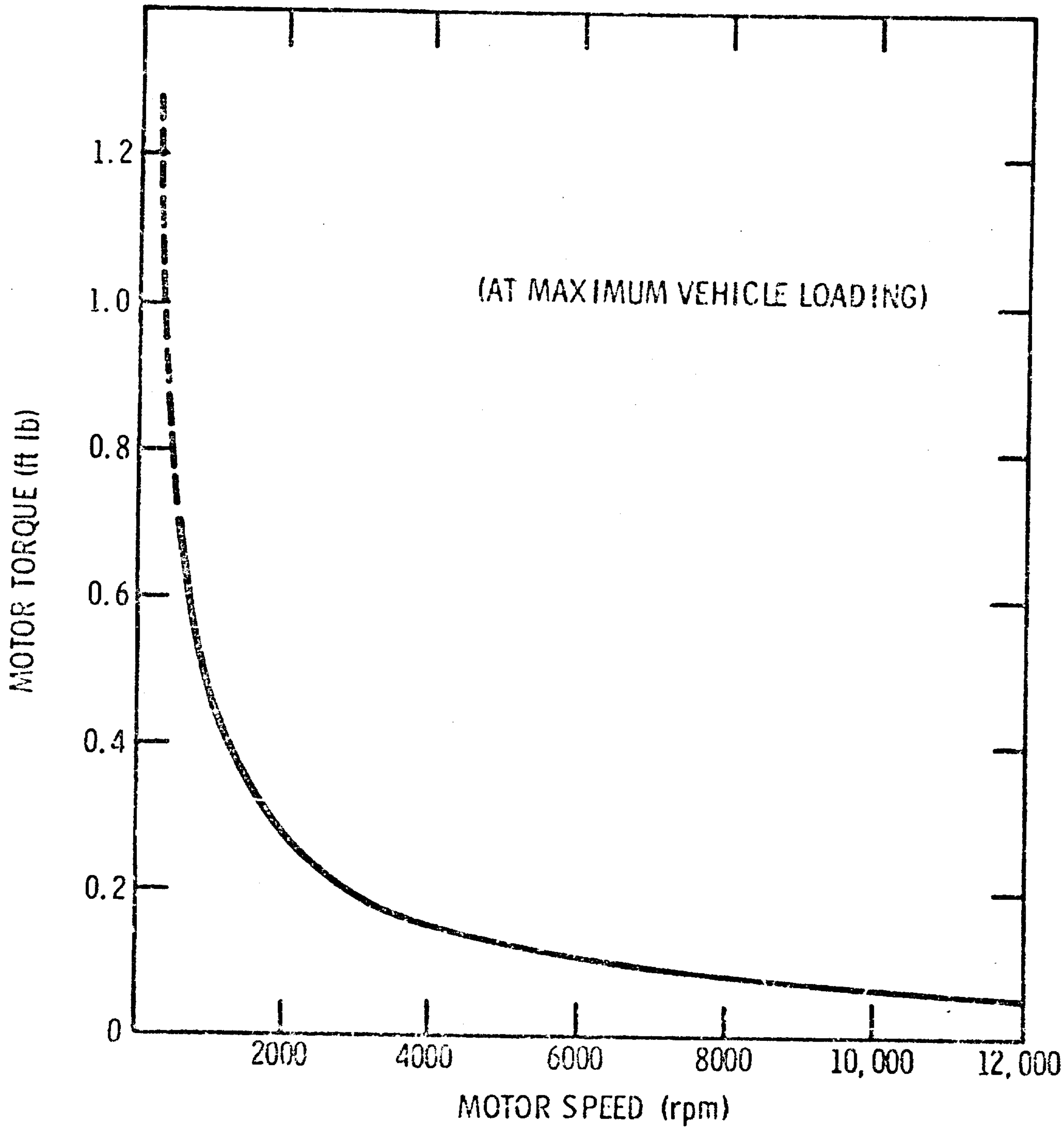

Figure 6.7.2- LSSM Drive Motor Torque vs Speed

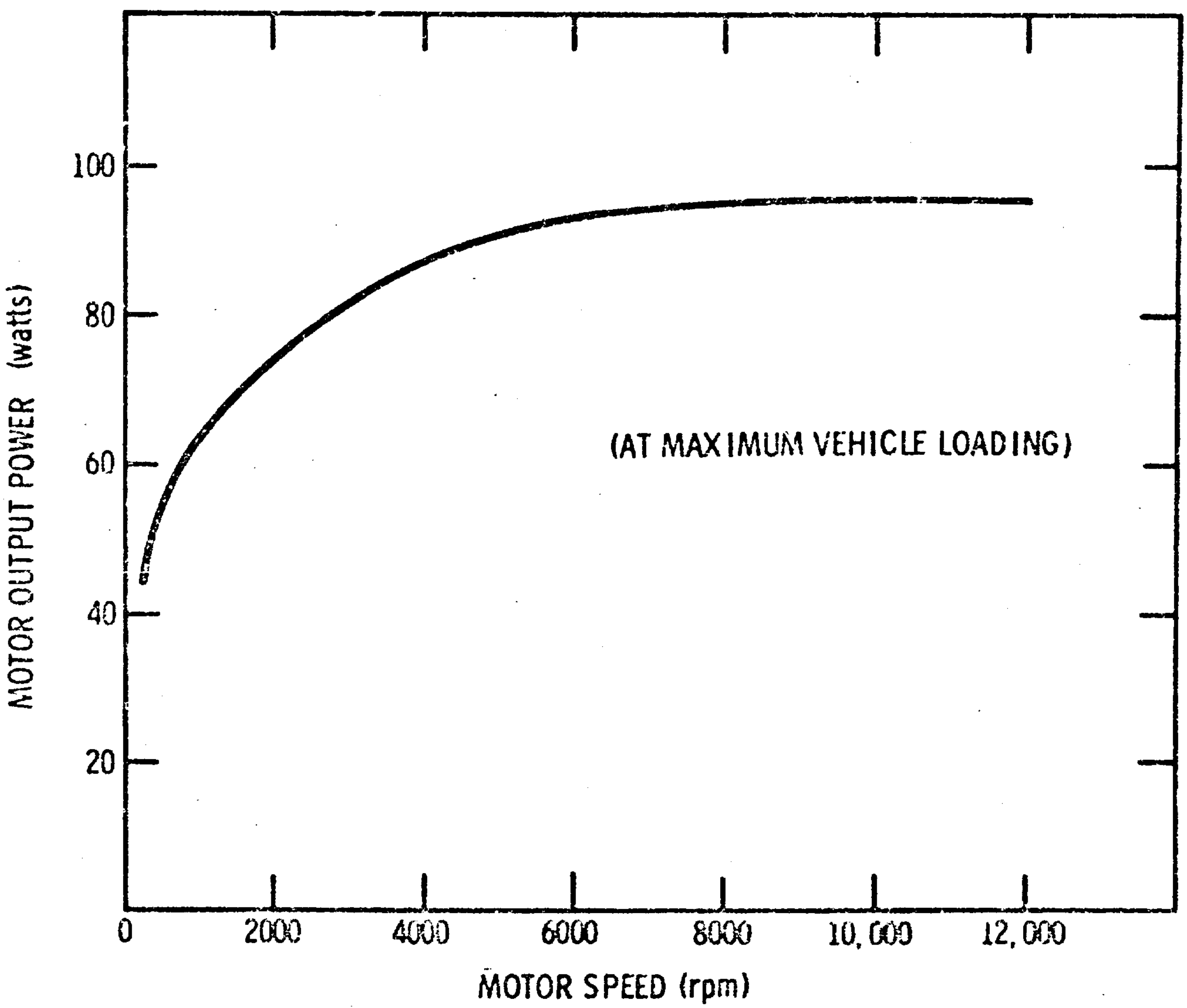

Figure 6.7.3- LSSM Drive Motor Output Power vs Speed

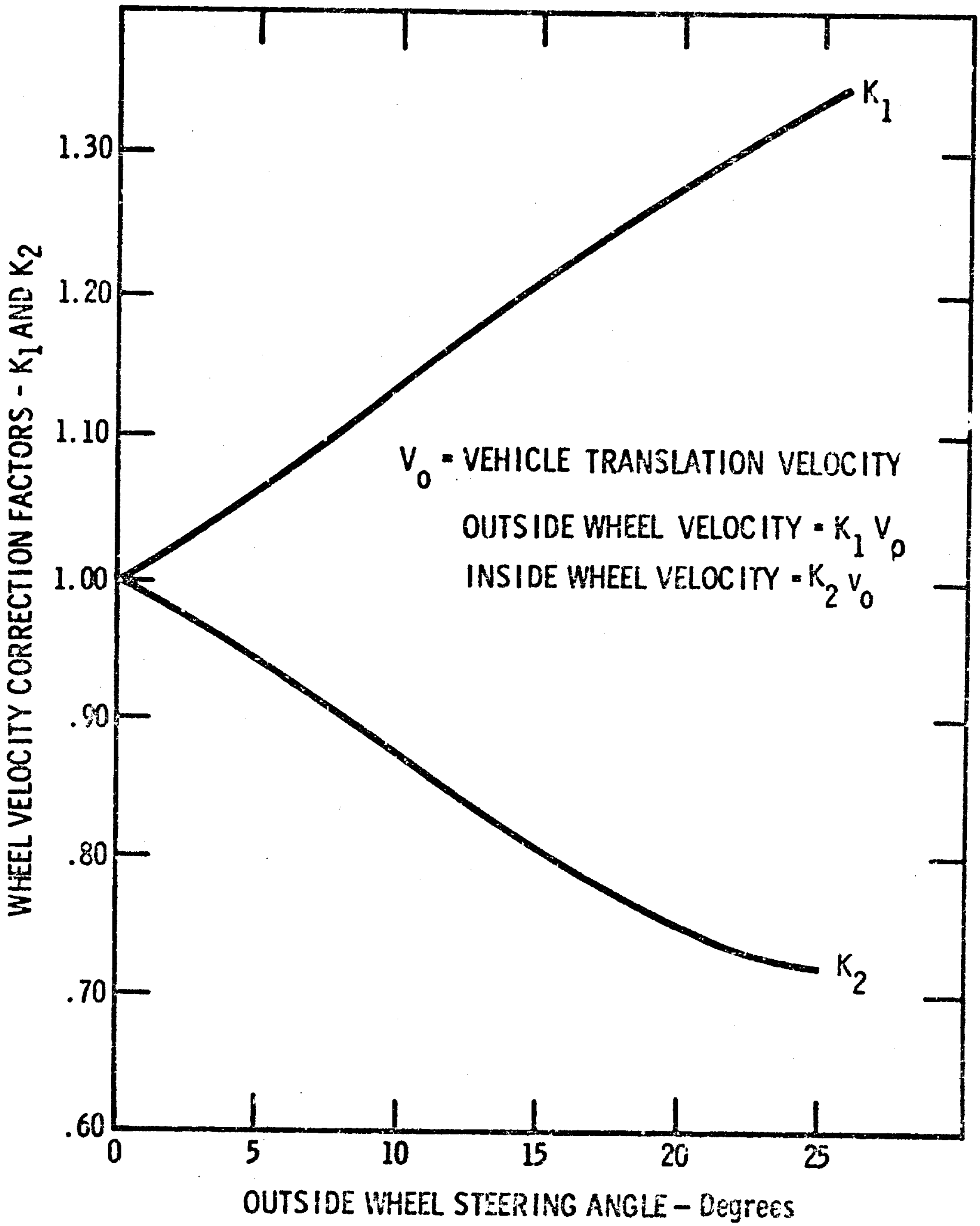

Figure 6.7.4- Wheel Velocity Correction Factors for Various Steering Angles

performance characteristics, development time, and reliability.

Three types of electric drive designs -- d-c series motor, induction motor, and synchronous motor -- were evaluated and compared. This analysis resulted in the selection of the induction motor system as most suitable for LSSM application.

In addition, trade-off analyses were made to permit optimizing the selected drive system. A preliminary design of the selected LSSM electric drive system was then performed and functional specifications prepared.

During the course of the study a thermal analysis was made for several motor configurations. The conclusions reached were that the motor for the selected drive system would not require major technological advances. Motor temperatures will be low enough to permit the use of state-of-the-art magnetic materials, conductors, insultion systems, bearings, and motor design practice. If it is desired to have the motor operate unsealed in the vacuum environment for long periods of time, a program will be required for the development of low friction lubricants that will insure long bearing life at pressures of 10^{-13} mm Hg.

Conclusions of the reliability study were that a-c electric drive systems can be developed that have greater reliabilities than d-c drive systems. In a d-c system, failure is most likely to occur in the commutator, with a resultant loss of wheel traction. In an a-c system, failure is most likely to occur in the static inverter. Since inverters can be maintained or made redundant, reliability can be increased to a value not achievable by in-wheel commutators.

A block diagram of an induction motor drive system is shown in Figure 6.7.5. The power train components are the d-c power source, the inverter-modulator, and the three-phase induction motor. The sensing and control components are the motor shaft digital tachometers, the frequency control circuits, and the current control circuits.

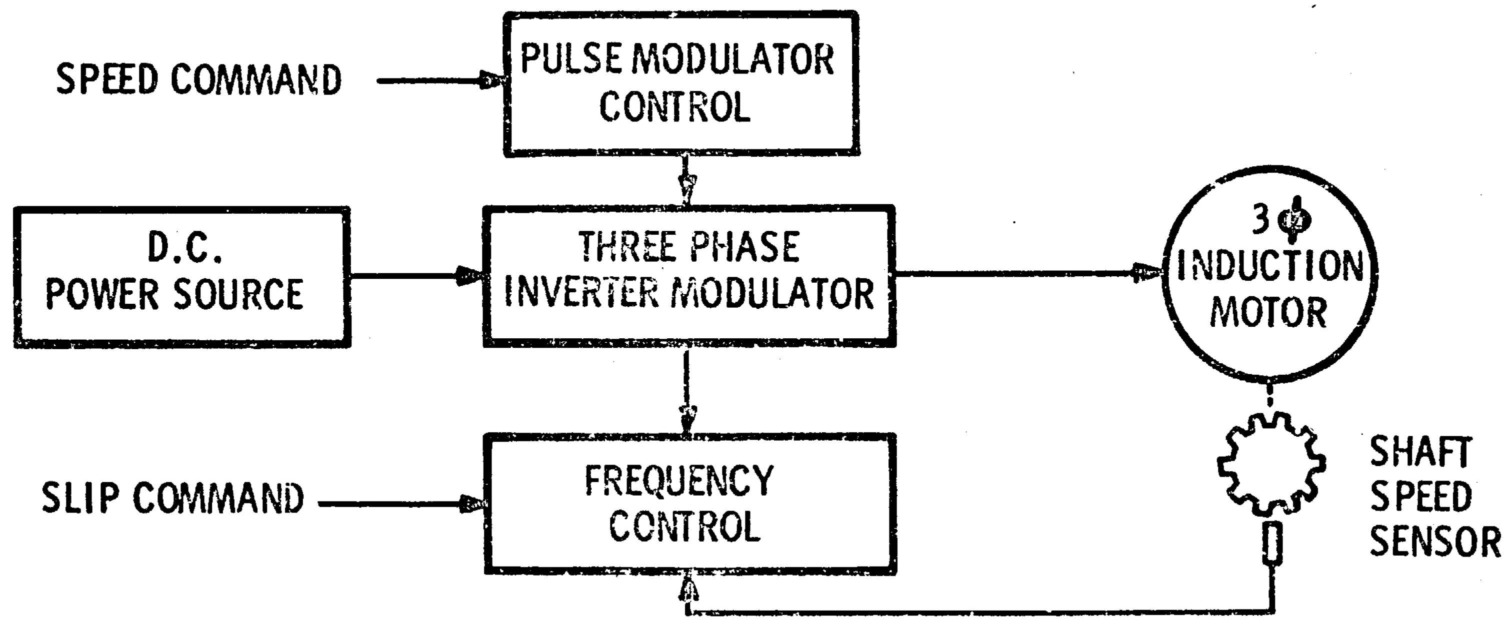

Figure 6.7.5- LSSM Electric Drive System

By substituting a three-phase synchronous motor for the induction motor and operating at zero slip, one could achieve an adequate drive system that may offer somewhat different functional capabilities than the induction motor system. As an example, dynamic braking can be achieved with less complexity with a synchronous motor than with an induction motor.

Inverter-driven synchronous motor systems were eliminated from final consideration in this study primarily because of insufficient design information that would permit a meaningful comparison with induction motor designs.

Preliminary examination indicated that a double air gap synchronous motor would be heavier and less efficient than a squirrel-cage induction motor for the LSSM application. A synchronous motor drive system requires six inverter-modulator controllers (one per wheel). For an induction motor drive system two control schemes can be considered: either a two - or a six-inverter system.

Figure 6.7.6 illustrates a LSSM electric drive configuration in which two inverters are used, each energizing three induction motors on one side of the vehicle. There are basically two separate drive systems operating from a common power source. The left and right power trains are each controlled by the driver command signals. When the vehicle is turning, torque of the outside wheels can be made equal to the torque of the inside wheels by increasing the voltage of the outside motors relative to the inside motor voltages. Skid steering as an emergency mode of steering can be accomplished by reversing the motors on one side of the vehicle.

In the two-inverter drive system the average wheel speed on each side can be used to determine the inverter frequency. With this system large differences in wheel speed can cause one of the motors to "pull out" and thereby reduce the total output torque of the drive system. The curves shown in Figure 6.7.7 indicate maximum wheel speed differences allowed as a function of vehicle speed for two values of induction motor slip frequency. For example, at 2 mph the curves show that the wheel speed difference number can be 0.225 at a motor electrical slip of 10 cps.

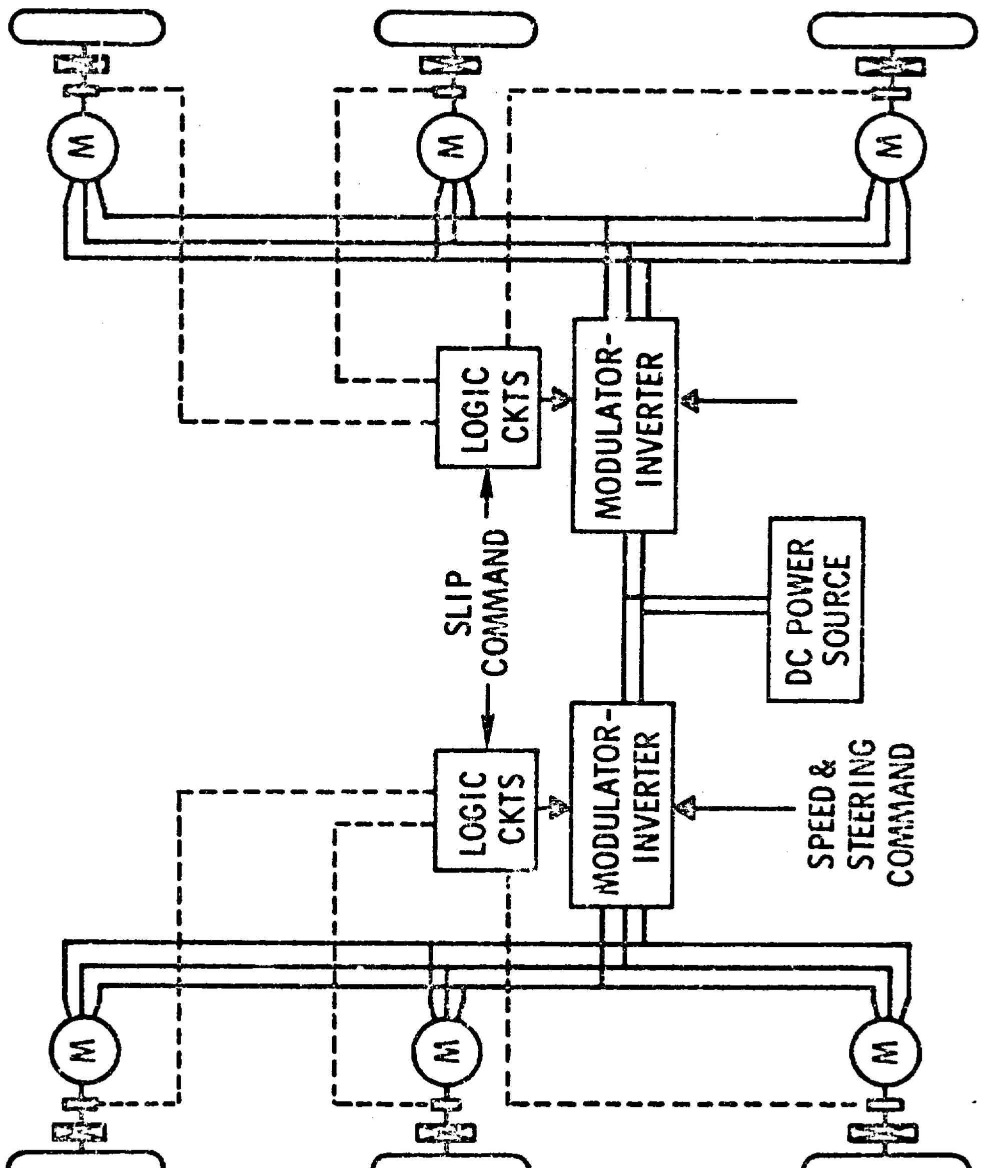

Figure 6.7.6- Two-Inverter Drive System

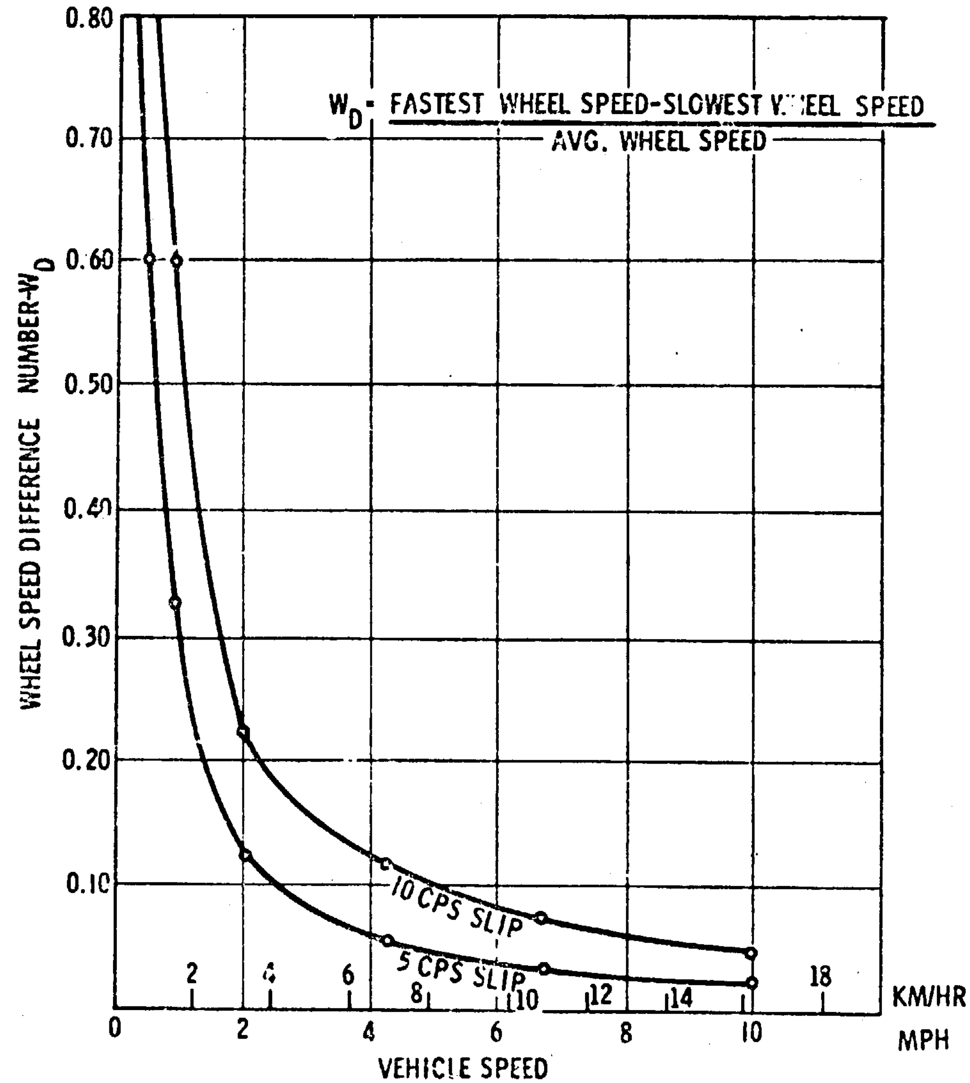

Figure 6.7.7- Wheel Speed Difference Number vs Vehicle Speed

As long as the wheel speed difference number is less than 0.225, the vehicle will be able to develop maximum tractive effort. If this value is exceeded, the available tractive effort will be reduced to some extent.

The wheel speed difference number is defined as:

$$W_D = \frac{\text{fastest wheel speed - slowest wheel speed}}{\text{average wheel speed}}$$

It appears that two inverter drive systems can be designed in which vehicle mobility is not significantly compromised. In a six inverter drive system, wheel speed differences are less restricted and vehicle mobility may be somewhat greater under some conditions, but actual tests of the two systems on a common vehicle would be required before the superiority of one system over the other could be established quantitatively. A schematic drawing of a six-inverter drive system is shown in Figure 6.7.8.

The two-inverter system is preferred for LSSM for the following reasons:

(1) Less complexity
(2) Lighter weight

However, system reliability and mobility requirements might dictate the use of a six-inverter system. This system appears to offer:

(1) Somewhat higher mobility capabilities.
(2) Higher reliability. (In the two-inverter system, if a redundant inverter is not provided, system reliability is less than that of a six-inverter system.)

6.7.4 LSSM Drive Motor Discussion

Every dynamo-electric machine has two electric circuits linked with a magnetic circuit. The function of one of the electric circuits is to serve as a source of magnetomotive force whereby magnetic flux is produced in the magnetic circuit.

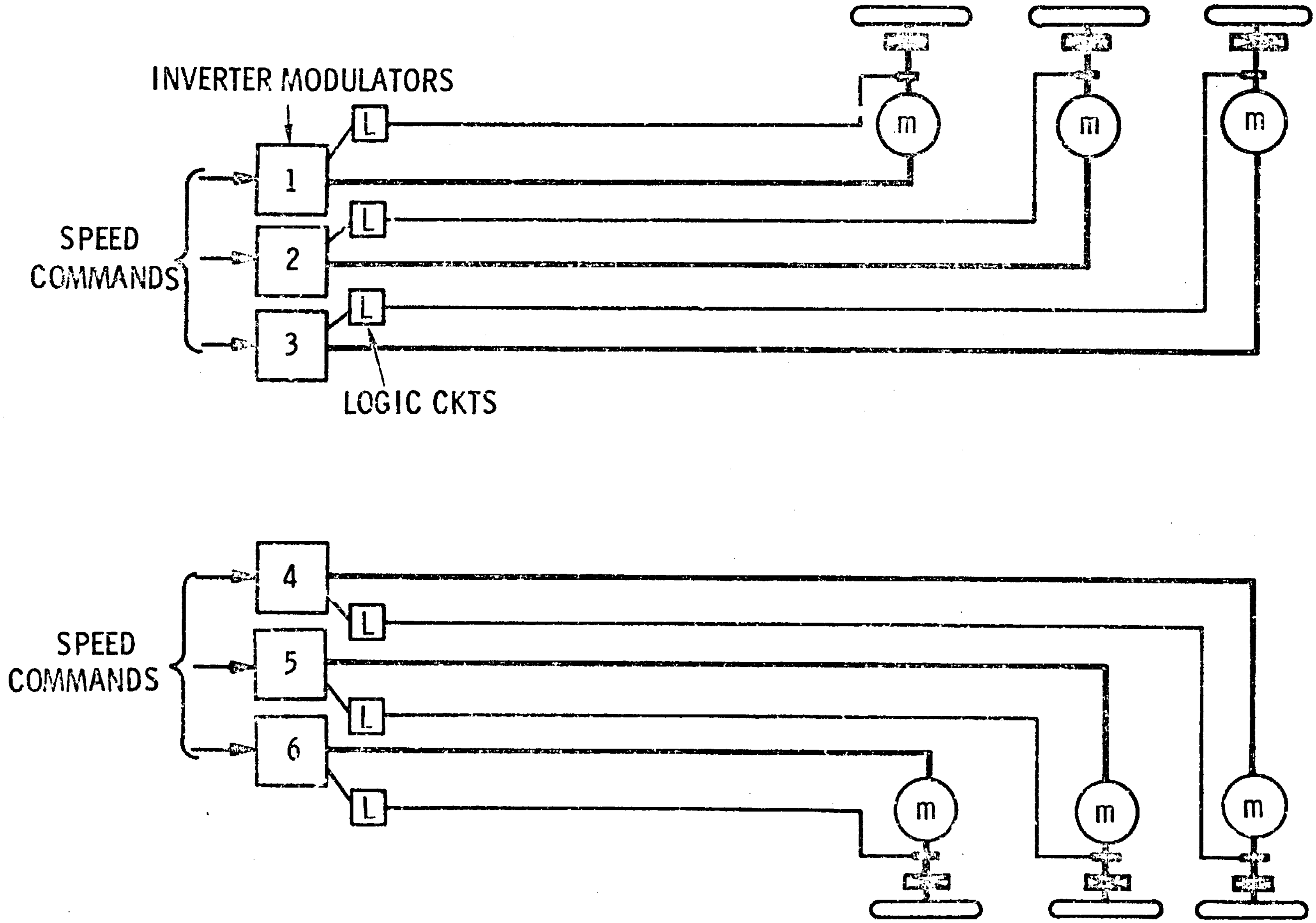

Figure 6.7.8 - Six Inverter Drive System

The function of the other circuit is to serve as a seat of energy exchange between mechanical and electrical energy. A synchronous motor has a direct current in the field winding and alternating current in the armature winding. An induction motor has alternating current in both windings.

Output power of an induction motor depends upon the volume of iron and copper in the motor. The volume can be expressed as D^2L where D is the outside diameter of the stator laminations and L is the length of the lamination stack. For a given voltage, frequency, and slip, the torque that a motor can produce is approximately equal to a constant times D^2L.

The required efficiency and cooling method, in addition to the required torque, will directly affect the weight of the motor. For traction applications, the torque requirement is generally defined by a torque versus speed curve and a problem arises in matching the inherent torque-speed characteristics of the motor to the requirements.

The torque capabilities of an induction motor under three conditions are of interest: starting torque, maximum torque, and running torque.

The starting torque of an induction motor can be expressed as follows:

$$T_{start} = \left[\frac{kE_2^2}{f}\right]\left[\frac{r_2}{r_2^2 + x_2^2}\right]$$

where E_2 = rotor induced voltage at standstill (volts)

r_2 = rotor winding resistance (ohms)

x_2 = rotor winding reactance at standstill (ohms)

f = stator frequency

k = constant

Examination of this expression reveals how starting torque varies as a function of frequency. Assume that the stator current is held constant as frequency f is varied.

When $f = 0$, no secondary voltage is induced and torque is zero. As frequency is increased, E_2 increases and torque increases until a peak is reached. After peaking, torque varies approximately inversely with frequency until rotor reactance becomes significant. Curves of starting torque vs. frequency are shown in Figure 6.7.9 (a) for various values of stator current.

The maximum torque of an induction motor $T_{max} = \left[\frac{k' E_2^2}{f^2} \right]$. For a constant applied motor voltage, the maximum torque varies approximately inversely with the square of the frequency. Variations in r_2, the rotor resistance, do not change the value of the maximum torque, but do affect the slip frequen cy at which it occurs. This fact is important when one inverter is used to energize more than one motor in the LSSM system. Maximum torque is independent of rotor resistance and slip. Figure 6.7.9 (b) shows curves of maximum torque vs. motor speed. Curve 1 results when E_2 is held constant at a high value; a motor capable of producing these high torques would be oversized but still just capable of producing the required torque at maximum speed. Curve 2 is obtained by increasing E_2 as speed is increased; a lighter weight motor could be designed to do this job and still exceed the vehicle requirements indicated by Curve 3.

Figure 6.7.9 (c) shows motor torque versus slip for constant input voltage and frequency. The curve shows clearly that the amount of running torque is dependent upon the slip s. Slip s is defined as $\frac{\Delta f}{f}$. The term Δf is called the slip frequency and is equal to the difference between f, the stator frequency, and f_r, the rotor rotational frequency. Frequency of the current flowing through the rotor bars of the squirrel cage motor is Δf. When slip is very small

$$T = \left[\frac{k'' E_2^2}{f} \right] \left[\frac{s}{r_2} \right]$$

and torque varies directly with slip and inversely as secondary resistance.

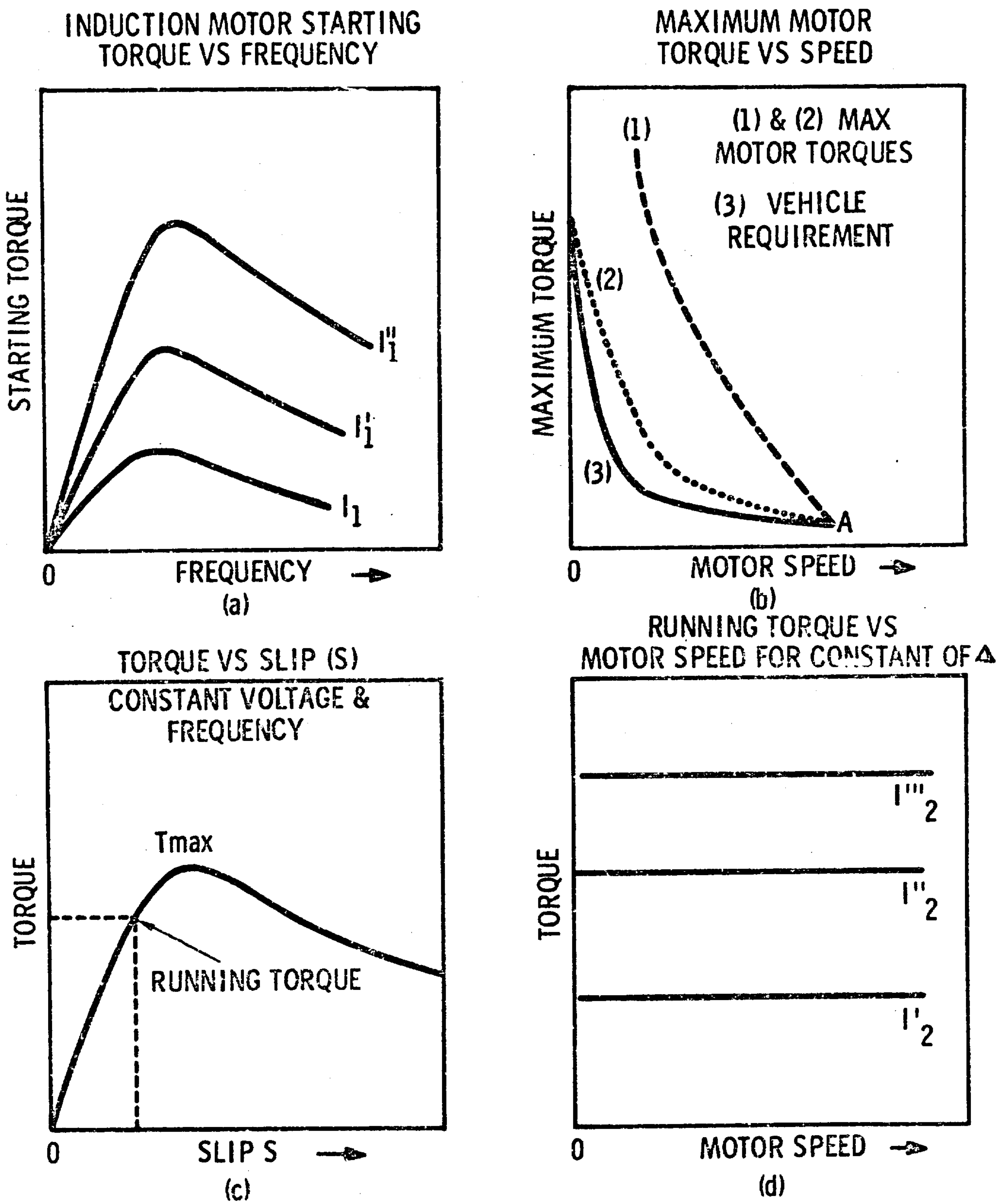

Figure 6.7.9- Induction Motor Characteristics

Substituting $s = \frac{\Delta f}{f}$ changes the expression for running torque to

$$T = \frac{k'' E_2^{\,2} \, \Delta f}{f^2 \; r_2}$$

If Δf and E_2 are constant, the running torque varies inversely with the square of the frequency. However, the following expression for running torque in terms of rotor current can be derived.

$$T = \frac{k_o \, I_2^{\,2}}{\Delta f}$$

If I_2 and Δf are kept constant then the running torque is constant and independent of frequency or shaft speed as shown in Figure 6.7.9 (d). Changing the rotor slip frequency not only varies the rotor torque but also varies the heat dissipated in the conductors of the rotor.

The copper power loss of the rotor

$$I_2^{\,2} \, r_2 = P_2 \left[\frac{s}{1 - s} \right]$$

$$= P_2 \left[\frac{\Delta f}{f - \Delta f} \right]$$

where P_2 is the mechanical power output of the motor shaft. For small values of slip the heat generated by the rotor bars is approximately proporational to the slip frequency.

Heat generated in the rotor of lunar vehicle traction motors must be carefully considered because the primary mode of heat transfer will be by conduction through the shaft and bearings into the housing. The magnitude of the heat generated in an LSSM drive motor as a function of speed is shown in Figure 6.7.10.

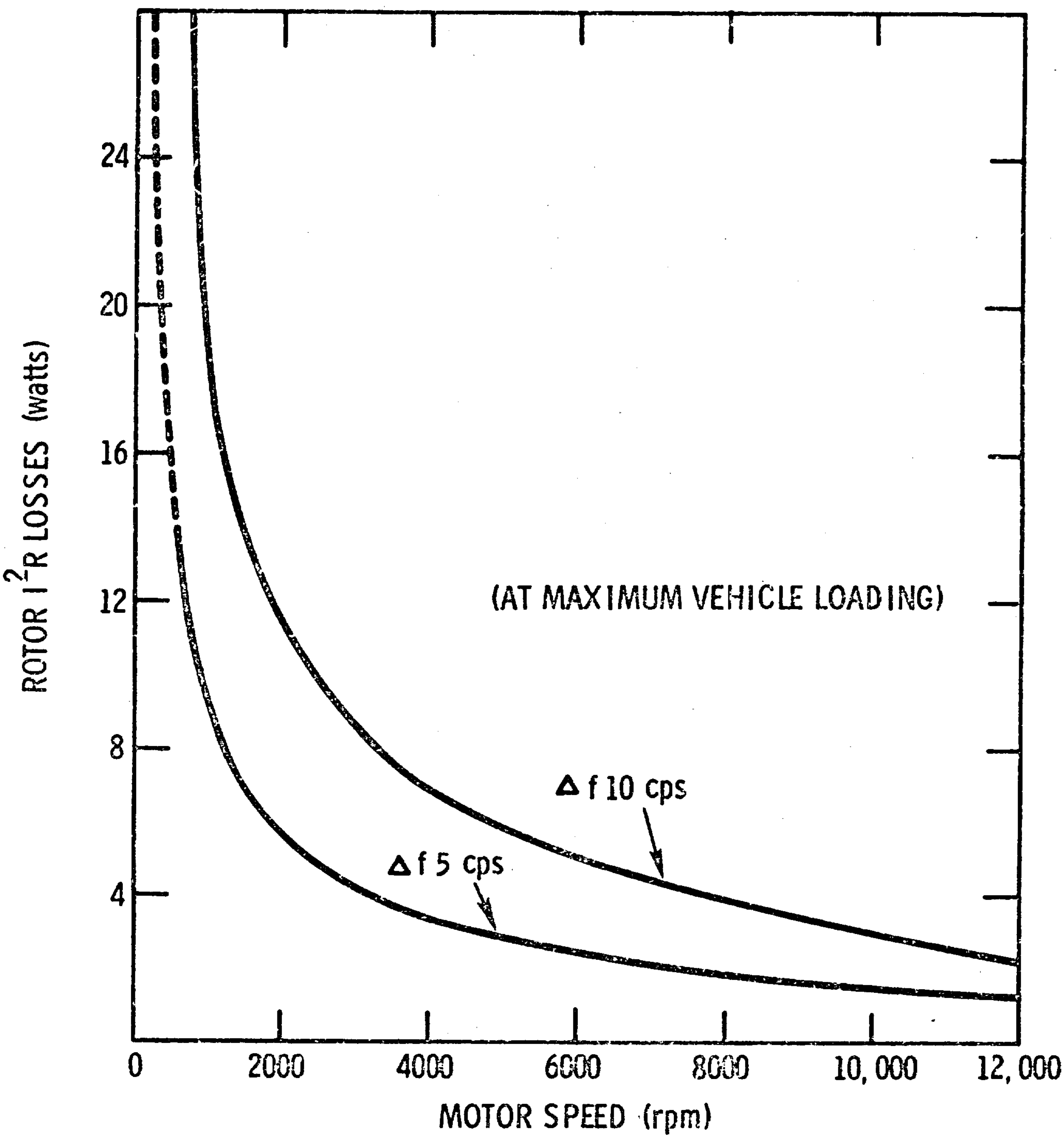

Figure 6.7.10- LSSM Drive Motor I^2R Rotor Losses

Calculations were made for maximum vehicle loading and for two values of slip frequency: 5 and 10 cps. For 5 cps slip, maximum steady state $I_2^2 r_2$ losses are about 13 watts at a speed of 650 rpm. At the same speed the losses at 10 cps slip frequency would reach about 33 watts.

6.7.5 Preliminary Motor Design

The experience gained with MOLAB and MTA facilitated the preliminary design of the LSSM drive motors. The design was subject to the following ground rules:

- The torque-speed requirements of the motor are as shown in Figure 6.7.2. For a maximum motor speed of 12,000 rpm, a gear reduction of about 130:1 is required. A gear reduction efficiency of 75% is assumed. The maximum continuous duty torque is 0.69 ft. lb. at 650 motor rpm, and the maximum intermittent duty torque is 1.22 ft. lb. at 260 rpm.

- The vehicle is powered by six variable-speed squirrel-cage induction-type motors with controlled slip frequency. The volume of each motor must be contained within a diameter of 5 inches and a length of 4 inches. The motors are passively cooled. The motor case design temperature shall not exceed 440°K.

- The voltage source is 56 vdc.

The basic dimensions of the LSSM motor were determined from the D^2L of the motor used for the GM DRL MTA. For a given flux and ampere loading, which are determined by the magnetic saturation and cooling capability of the machine, the value D^2L essentially defines the torque rating of the motor at a given applied frequency. Figure 6.7.11 lists the pertinent scaling informa. on.

Figure 6.7.11 - Motor Scaling Factor D^2L for LSSM, MTA

	Maximum Continuous Duty Torque		D^2L
	(ft. lb.)	@ cps	(in^3)
MTA	2.00	20.0	18.4
LSSM	0.69	25.0	5.2

To determine the sensitivity of motor efficiency and performance on weight and size, three basic designs were considered with D^2L values of 5.76, 5.10 and 4.20, respectively. The designs were designated A, B and C and dimensions and weights determined

Motor Designation	A	B	C
Stator OD (exclusive of housing) (inches)	4.10	3.70	3.30
Stack Length (inches)	1.0	1.15	1.15
Weight (active material only) (lbs.)	4.0	3.70	2.95

Performance calculations were programmed on a digital computer, taking into account all first order effects such as stray losses, magnetizing iron losses, magnetic saturation, etc. Results of the computer analysis indicate the performance of the motors at any required operating point.

Motor performance for various torque-speed points over the entire speed range are shown in Figures 6.7.12 to 6.7.14. Figures 6.7.12 and 6.7.13 show the required input voltages and currents of the three motor designs as a function of motor speed. The calculations were made for maximum vehicle loading. Motor design A, the largest, requires the highest line current and lowest line to neutral voltage because it offers the lowest impedance to the power source. If a higher motor voltage and lower current is desirable higher motor impedance can be obtained by increasing the stator turns.

COMPARISON OF THREE MOTOR DESIGNS

DESIGN		STATOR	
		O.D.	LENGTH
A	o	4.10	1.0
B	Δ	3.70	1.15
C	□	3.30	1.15

MOTORS LOADED AS FOLLOWS:

105 watts AT 12,000 rpm
97 watts AT 5,200 rpm
71 watts AT 1,300 rpm
57 watts AT 585 rpm

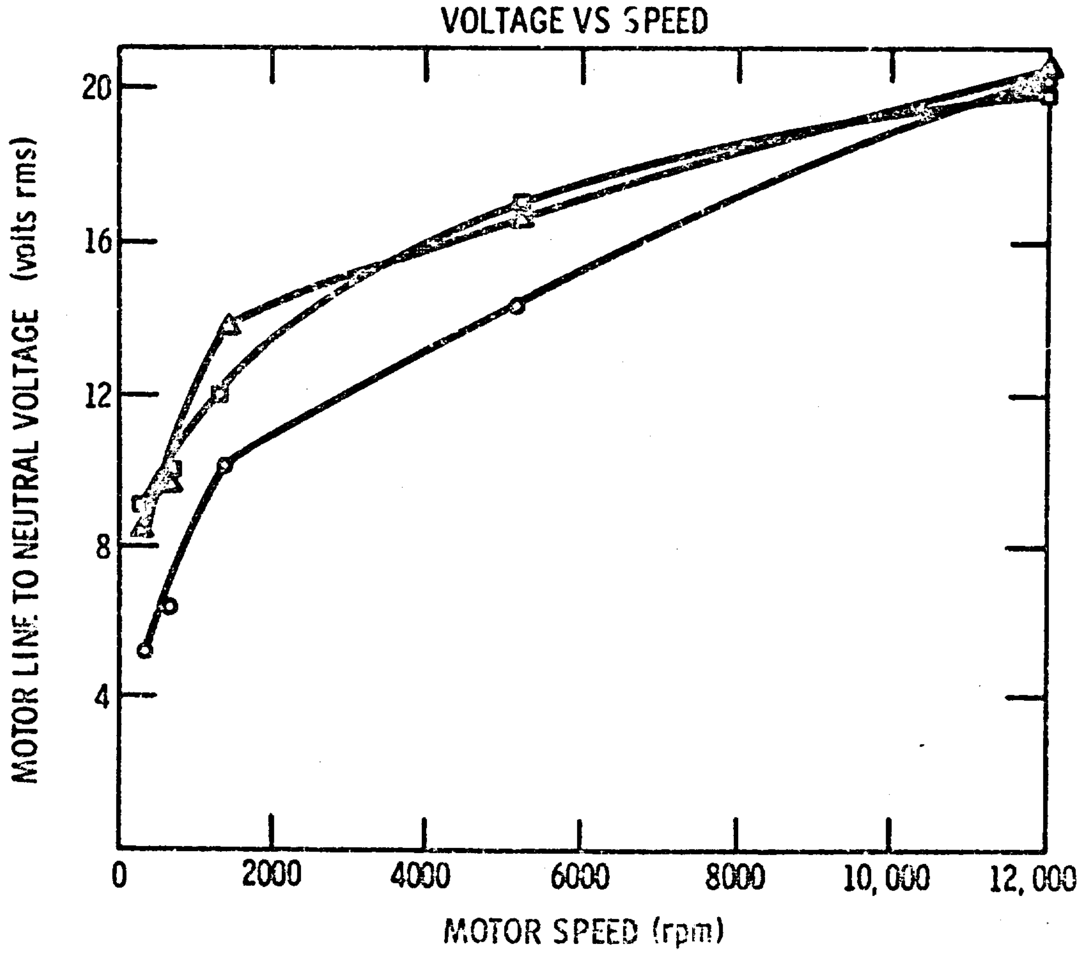

Figure 6.7.12- Motor Voltage vs Speed

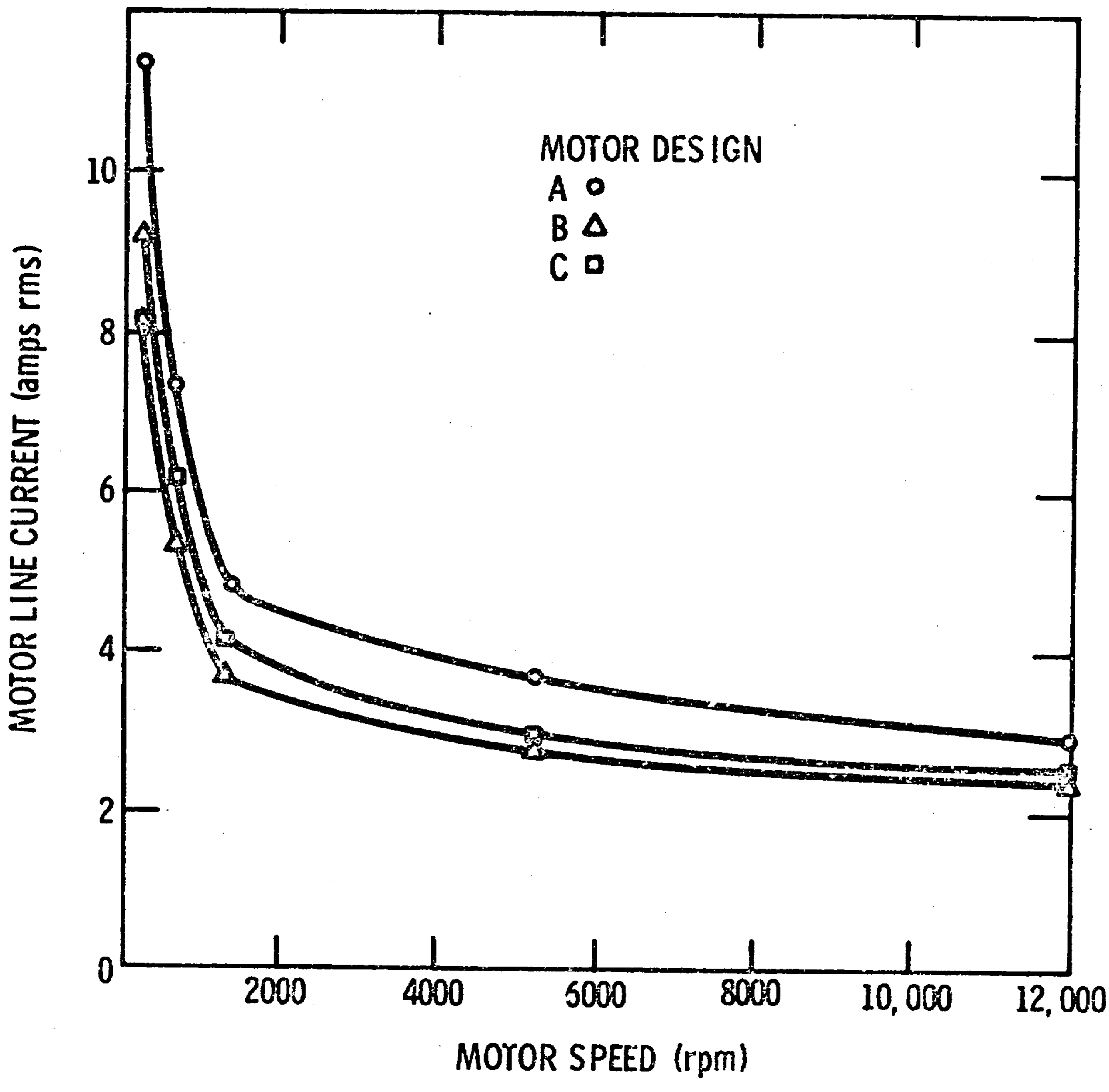

Figure 6.7.13- Line Current vs Motor Speed

However, motor design A is 20% higher in efficiency than design C at low speeds as shown by the curves of efficiency vs. speed in Figure 6.7.14a. These curves will help establish the motor weight, fuel consumption, and system weight relationships for planned vehicle missions.

In the LSSM application, programming the slip frequency is required to permit operation of the induction motors at optimum efficiency at various vehicle speeds. Figure 6.7.14b shows the desired slip frequencies for designs A, B and C as a function of motor speed.

At maximum torque the motors draw the highest currents. However, since torque is equal to a constant times $\frac{I_2^2}{\Delta f}$, for a given torque motor current can be varied by changing the slip frequency. Figure 6.7.15 indicates the sensitivity of motor line current to changes in slip frequency for the three motor designs with a load torque of 1.22 ft-lb. Motor design A produces this torque at a minimum current of 11.4 amps rms and a slip frequency of 4.7 cps. It is important to minimize the motor line current for this operating condition to minimize the required rating of the modulator-inverter power transistors.

For the peak torque condition, Figure 6.7.16 indicates how motor efficiency varies as a function of slip frequency.

Figure 6.7.17 indicates efficiency and power losses for the three motor designs for various load conditions. The maximum losses were used to determine the required cooling radiator weight as shown in Figure 6.7.18. Motor design A requires the lightest radiator to maintain the case at a maximum temperature of 440°K. (The following assumptions were made in determining the radiator weight: lunar surface temperature 406°K; radiator emissivity 0.7; absorptivity 0.3; view factor to the moon 0.5.)

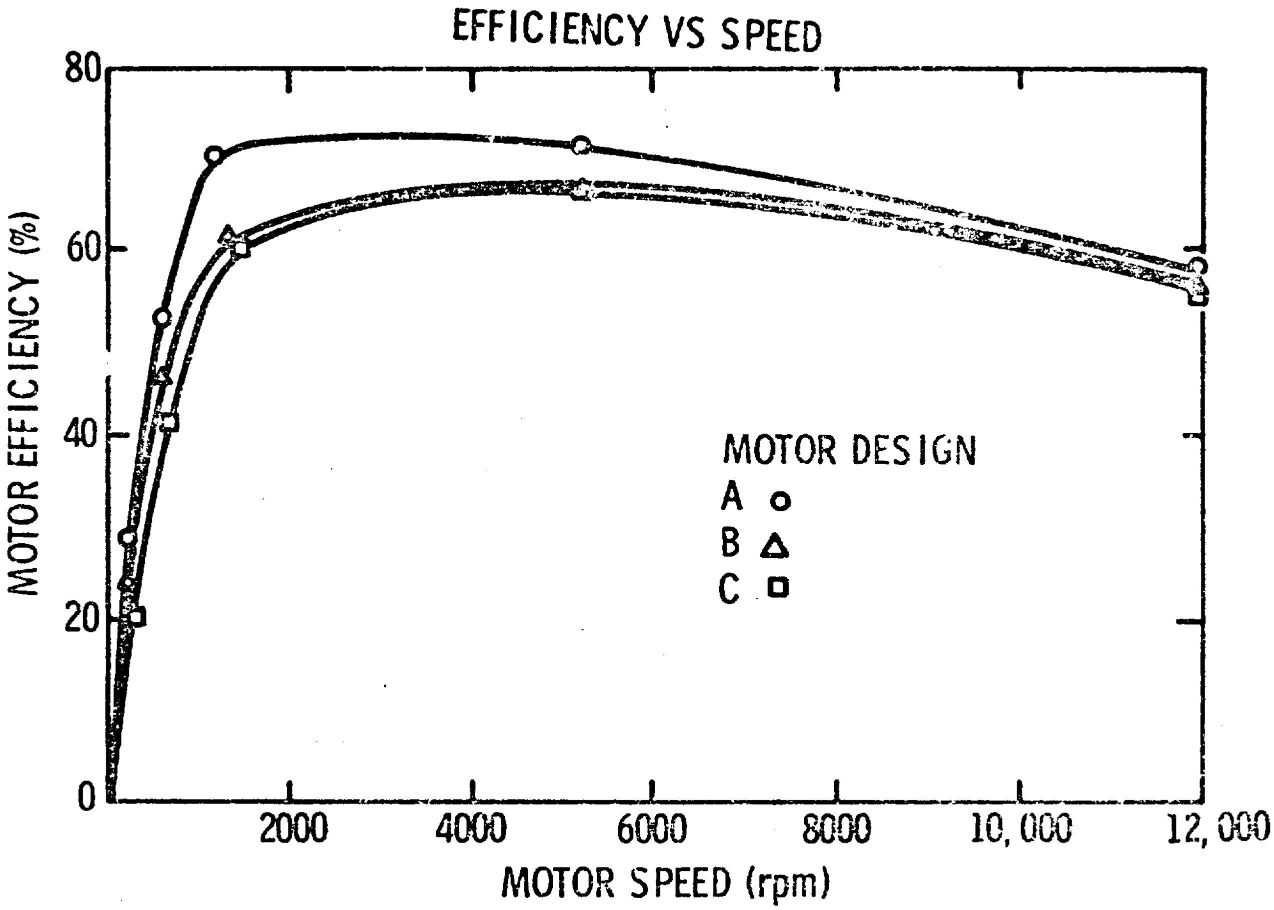

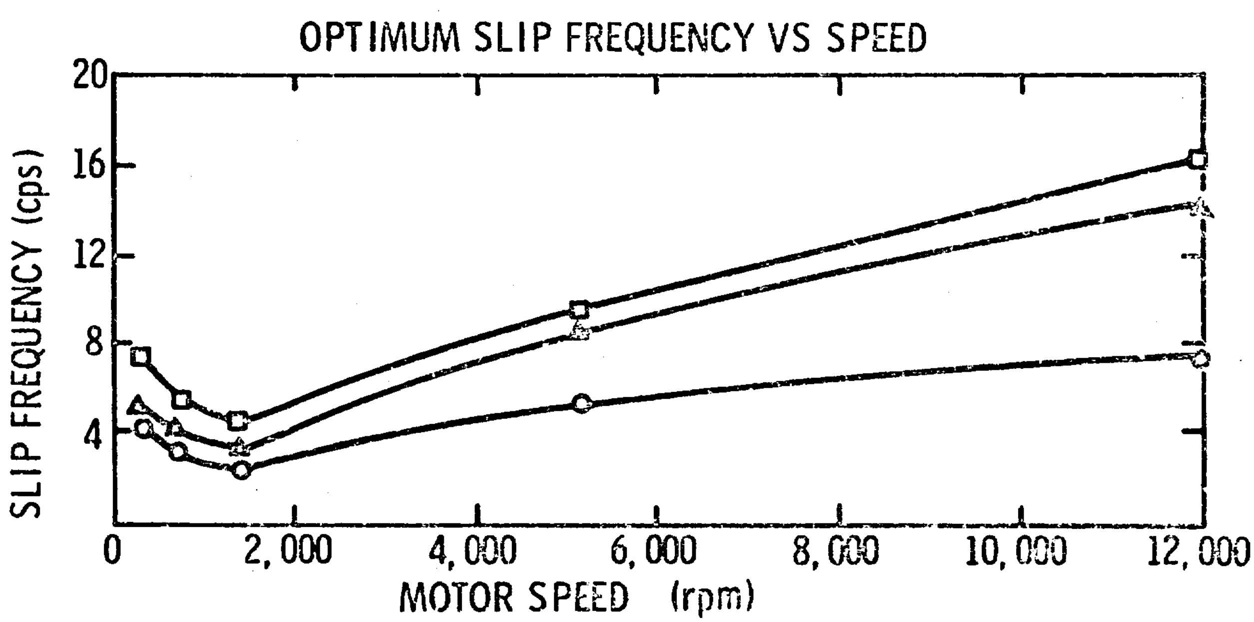

Figure 6.7.14- Efficiency and Optimum Frequency vs Motor Speed

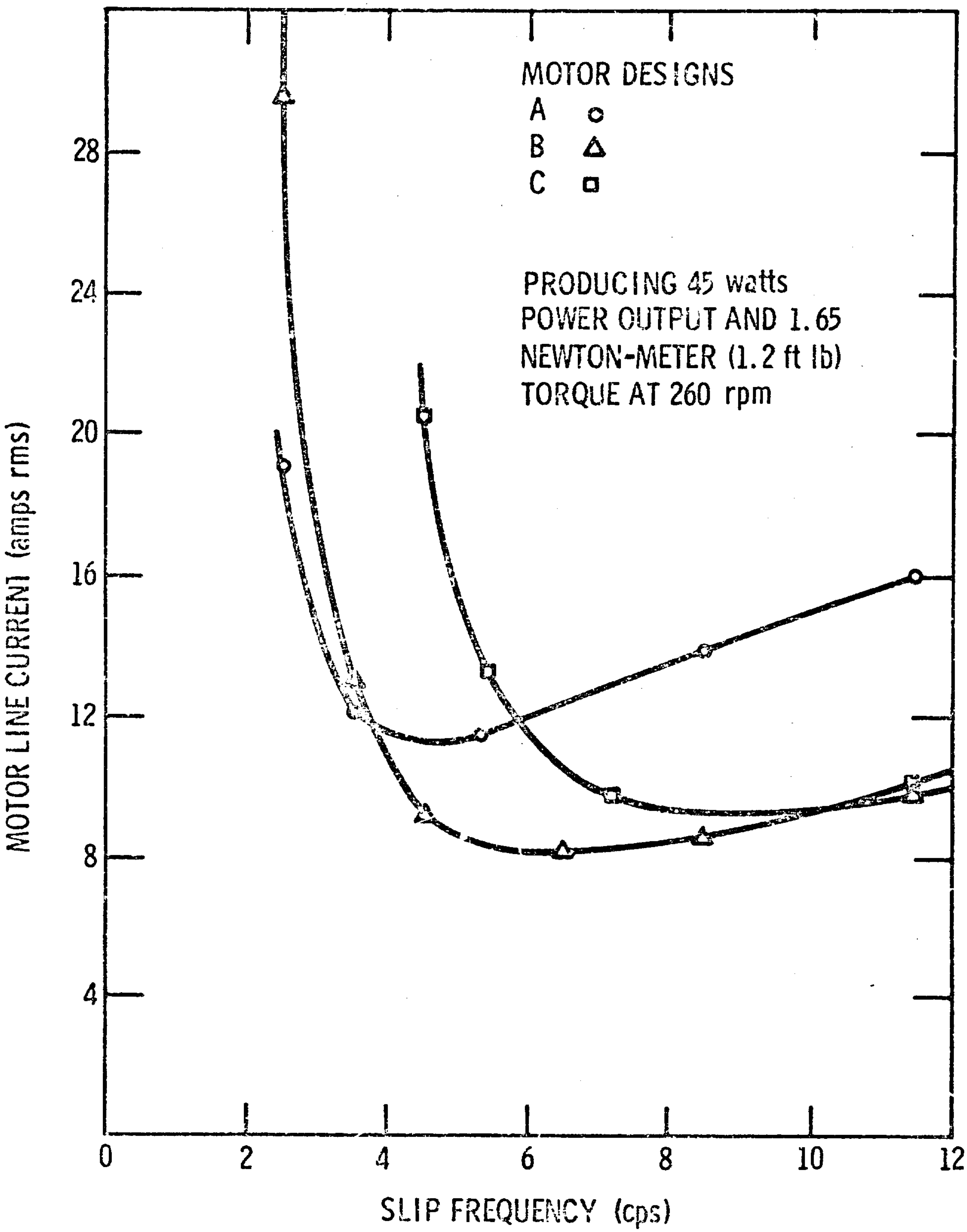

Figure 6.7.15- Motor Current vs Slip Frequency

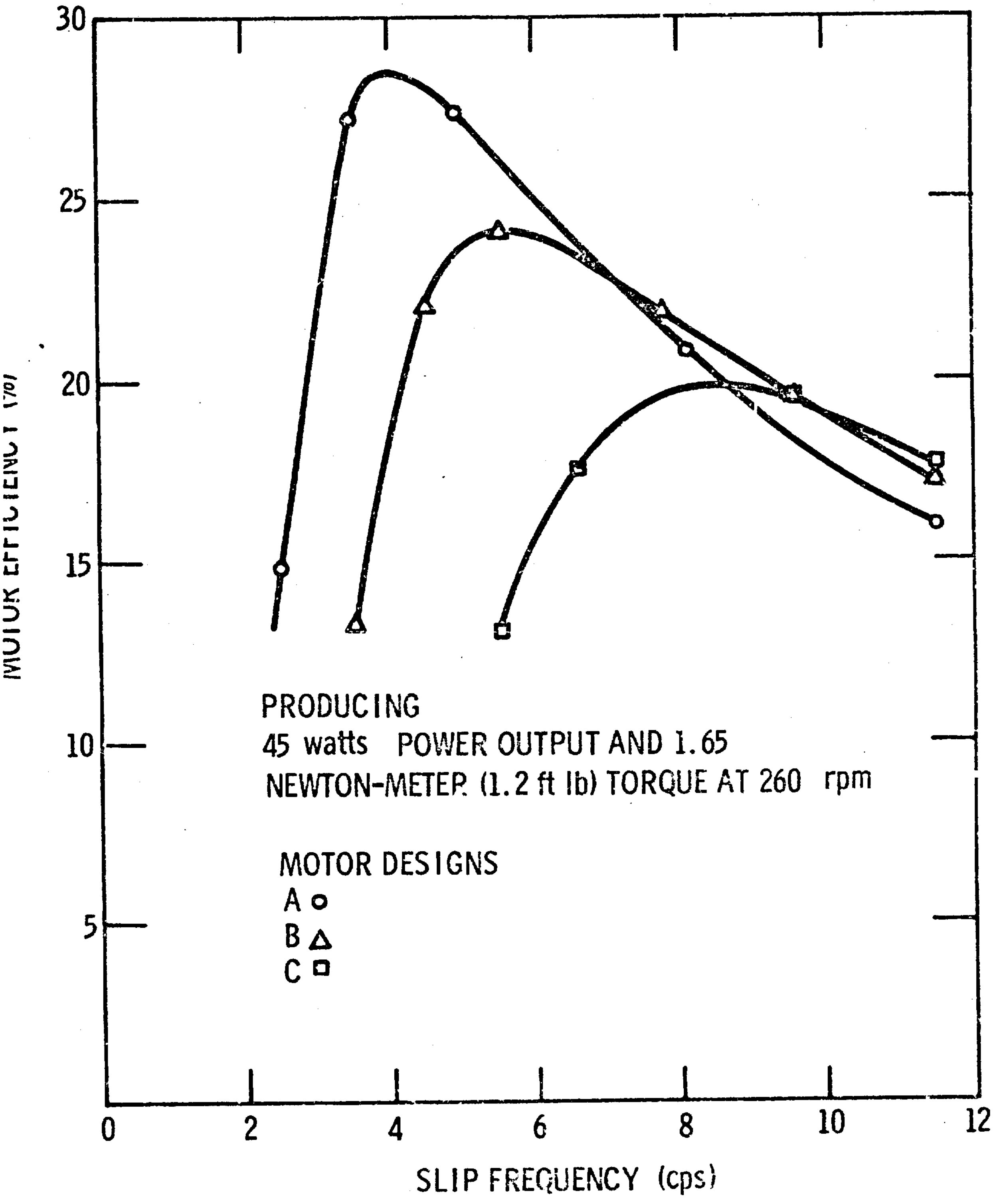

Figure 6.7.16-Motor Efficiency vs Slip Frequency

MOTOR SPEED (RPM)	MOTOR POWER OUTPUT (WATTS)	DESIGN A EFF. (%)	DESIGN A LOSS (WATTS)	DESIGN B EFF. (%)	DESIGN B LOSS (WATTS	DESIGN C EFF. (%)	DESIGN C LOSS (WATTS
12,000	105	57.6	77	55.3	85	55.4	85
5,200	87	71.4	39	66.1	49	65.8	51
1,300	71	71.2	29	62.8	42	60.6	46
585	57	53.3	49	46.8	65	41.9	79

Figure 6.7.17- Three Motor Designs, Efficiency and Power Loss

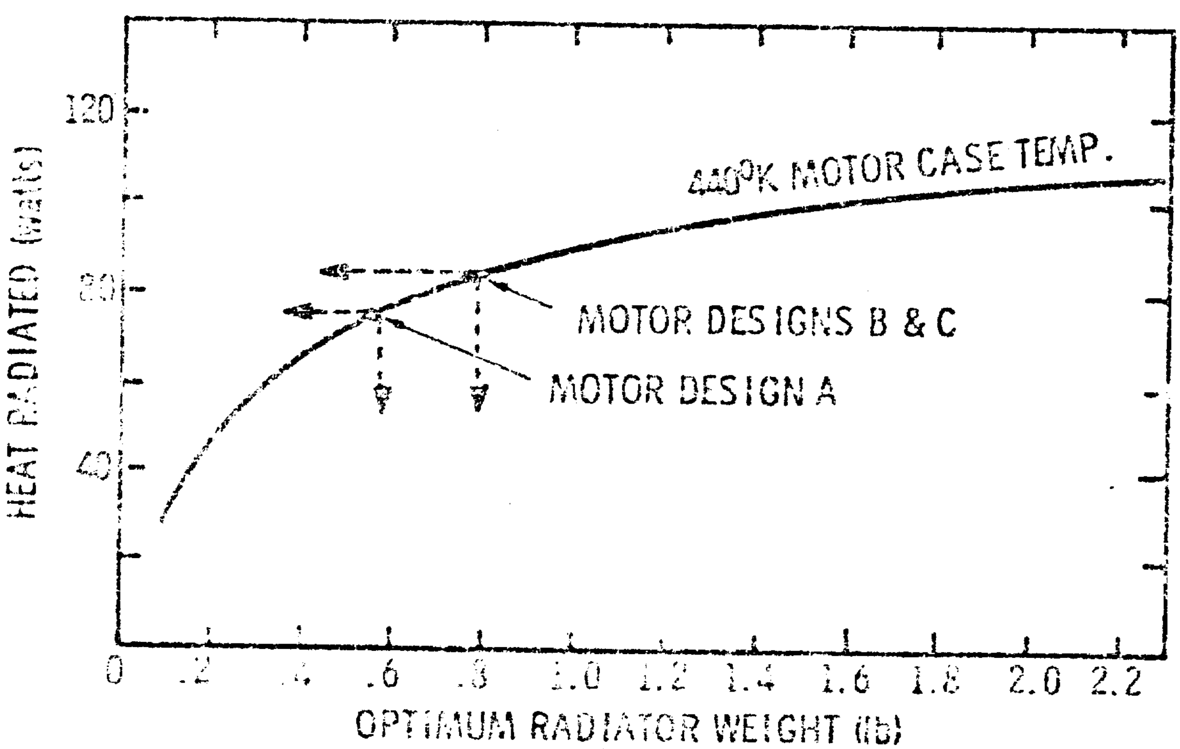

Figure 6.7.18- Motor Heat Dissipation

On the basis of efficiency and radiator size motor design A was selected for the LSSM traction application. Total motor weight including radiator will be approximately 3.6 kg (8 lb.). Maximum motor efficiency will be about 73%. Figure 6.7.19 shows approximate dimensions of the motor.

6.7.6 Power Conditioning Circuit

The power switch portion of the LSSM electric drive system consists of a relatively simple three-phase transistor inverter that also functions as the current controller for the motors. Figure 6.7.20 shows a schematic diagram of the inverter-modulator, a motor load, and blocks indicating the logic and driving circuits. In the LSSM drive it is preferred that three motors on one side be energized by one inverter-modulator. The present status of the solid state control art indicates that this scheme is less complex and lighter in weight than using individual inverters for each motor. However, new control concepts and changes in methods of fabricating transistor power switches could result in a preference for a six inverter drive system.

All transistors in the inverter-modulator function as programmed switches to convert the d-c battery power to three-phase a-c power. Conduction times of the transistors are determined by the output of the ring counter circuit. Current control is accomplished by pulsing the conducting transistor Q'_a or Q'_b or Q'_c through the appropriate AND circuit. The diodes connected across the power transistors serve to maintain motor current flow due to energy stored in the inductances of the motors between transistor conduction pulses.

Motor torque is controlled by turning a potentiometer that controls the pulse width of a simple pulse modulator circuit. Motion of the vehicle is reversed simply by interchanging two of the three output leads to the inverter.

The power switch transistors must be capable of supporting the highest possible system voltage and of switching the highest required motor currents. High derating factors will insure high reliability. For example: The propulsion power source voltage will be 56 vdc; the transistors might be rated at 200 volts across the collector and emitter or higher. The highest expected peak current may be 24 amperes; the transistors might be rated at 70 amperes or higher.

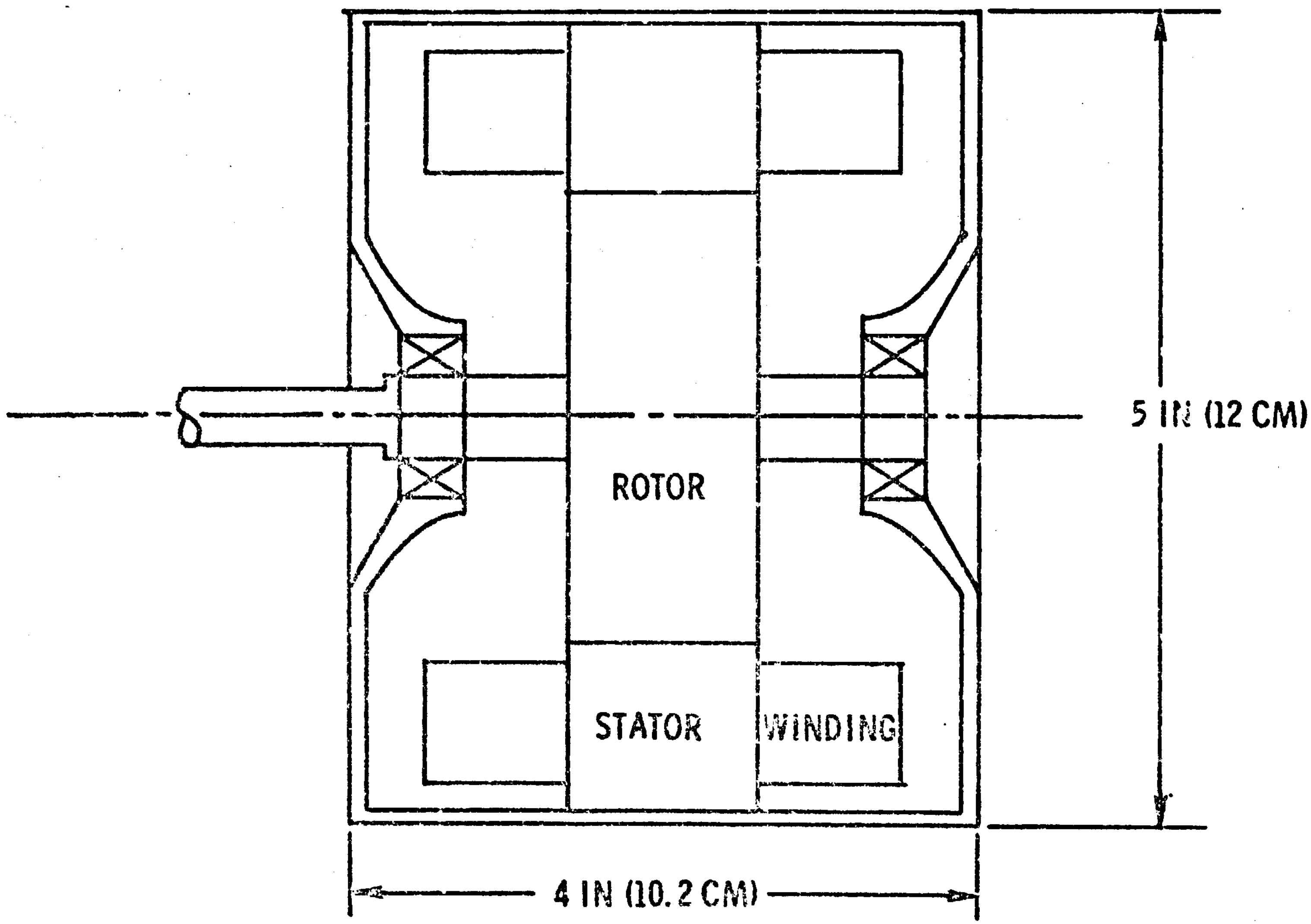

Figure 6.7.19- LSSM Three Phase Traction Motor

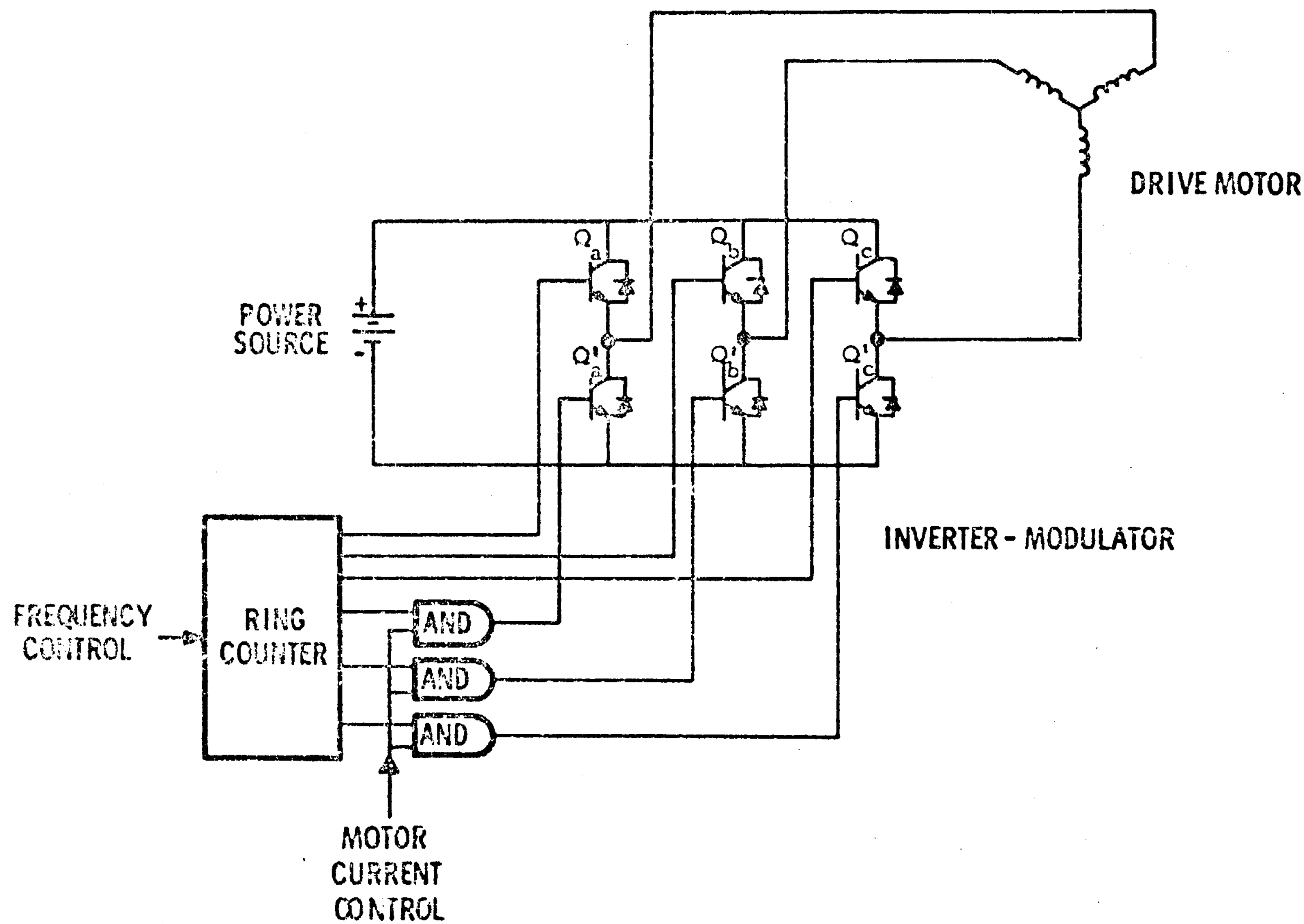

Figure 6.7.20- LSSM Electric Drive Power Conditioning Circuit

Figure 6.7.21 illustrates the input and output current waveforms of the power conditioner circuits. The d-c input current I_{dc} consists of a series of pulses, the magnetude of which is a function of motor speed and the width of which depends upon the required motor torque. The a-c output current I_l is a stepped waveform with saw tooth tops and bottoms. Frequency of the output current is determined b y the motor speed and magnitude is determined by the required motor torque.

If an average reading ammeter were inserted in the d-c current line of Figure 6.7.21, it would read the average battery current drawn by the electric drive. Figure 6.7.22 illustrates the average battery current drawn per LSSM drive motor as a function of motor speed for maximum vehicle loading. An a-c ammeter inserted in one of the motor lines would read rms line current. A plot of line current vs motor speed for maximum vehicle loading is shown in Figure 6.7.13.

In addition to derating, operating the transistors and diodes of the power conditioning circuits at low junction temperatures will also enhance the drive system reliability. Heat generated in the transistors and shunting diodes is primarily due to conduction losses. A plot of inverter-modulator losses per motor is shown in Figure 6.7.23. Maximum non-intermittent power losses in the inverter are about 12 watts per motor or 36 watts for three motors; this condition occurs when a fully loaded LSSM is climbing a 35^{o} slope. Temperature rise of the semiconductor junctions will be maximum for this condition - which will occur during less than one percent of the mission life of the vehicle.

Heat from the power semiconductors will be conducted to a phase-change material heat exchanger that may utilize Technical Eicosan or polyethylene glycol. Power dissipation of each transistor for the above conditions will be about 5 watts. If the junction to case thermal resistance is 1^{o}K/watt the junction temperature will be about 5^{o}K above the temperature of the phase-change material. A possible packaging arrangement for the inverter-modulator is shown in Figure 6.7.24.

6.7.8 System Power Consumption and Efficiency

LSSM electric drive power consumption per motor as a function of motor speed is shown in Figure 6.7.25. Since the vehicle has six motorized wheels, total power

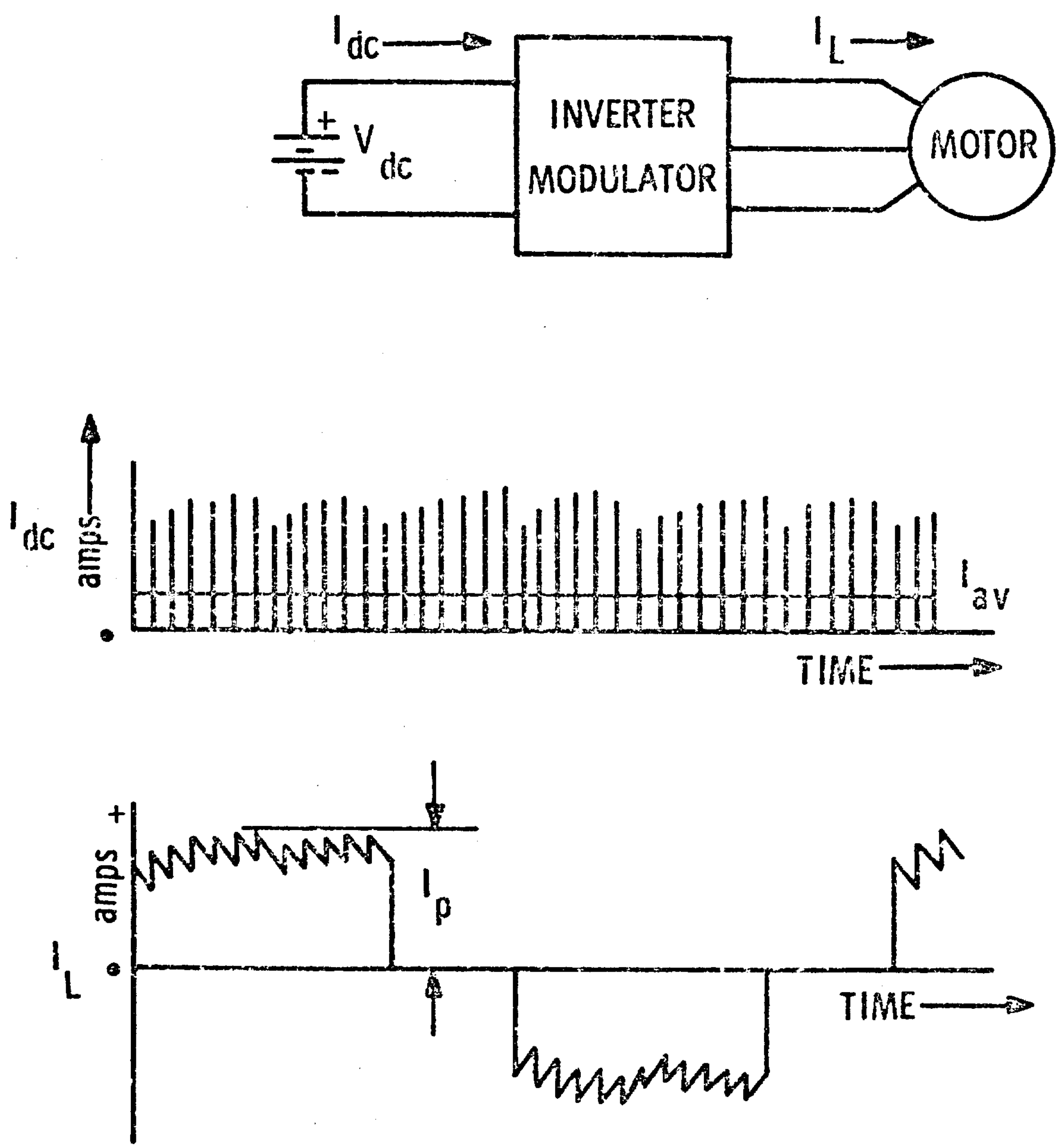

Figure 6.7.21 - Power Conditioning Circuit Input and Output Waveforms

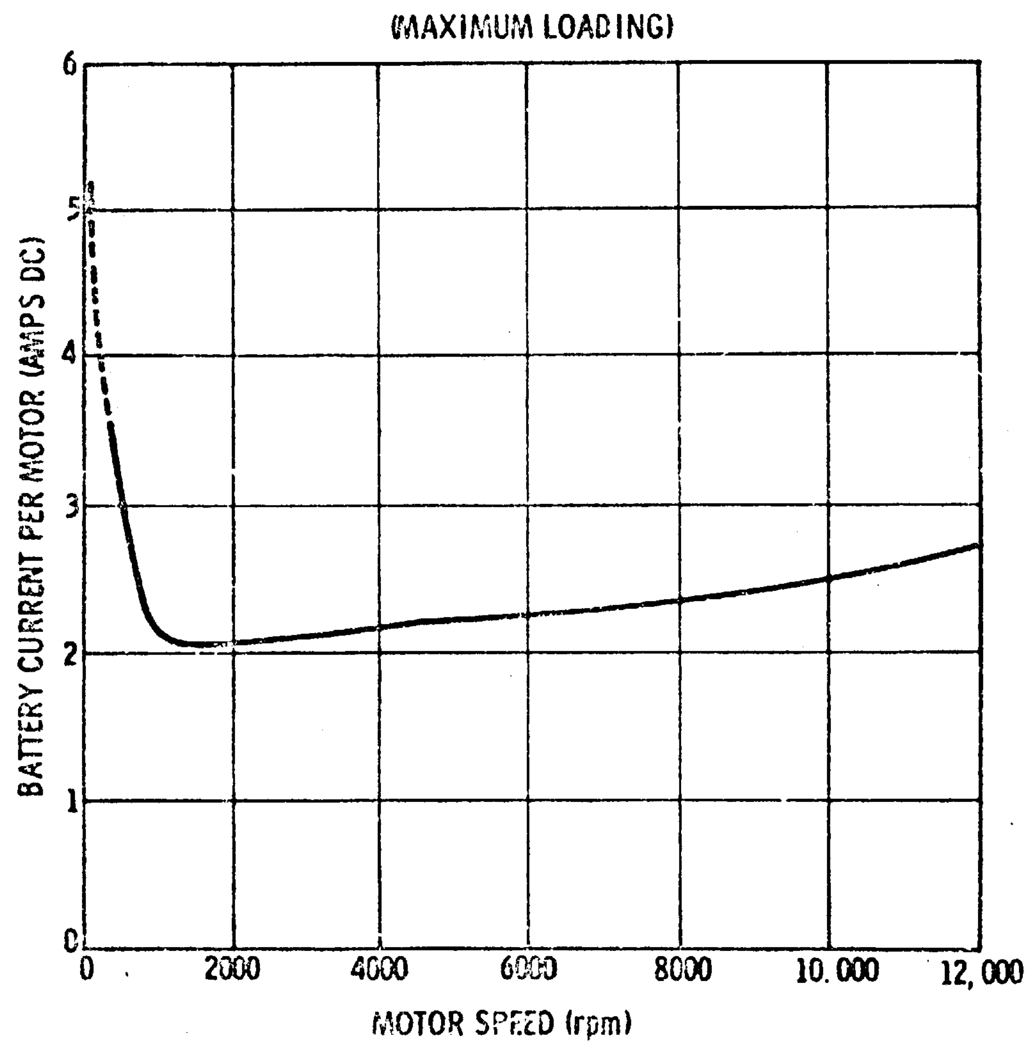

Figure 6.7.22- Battery Current vs Speed

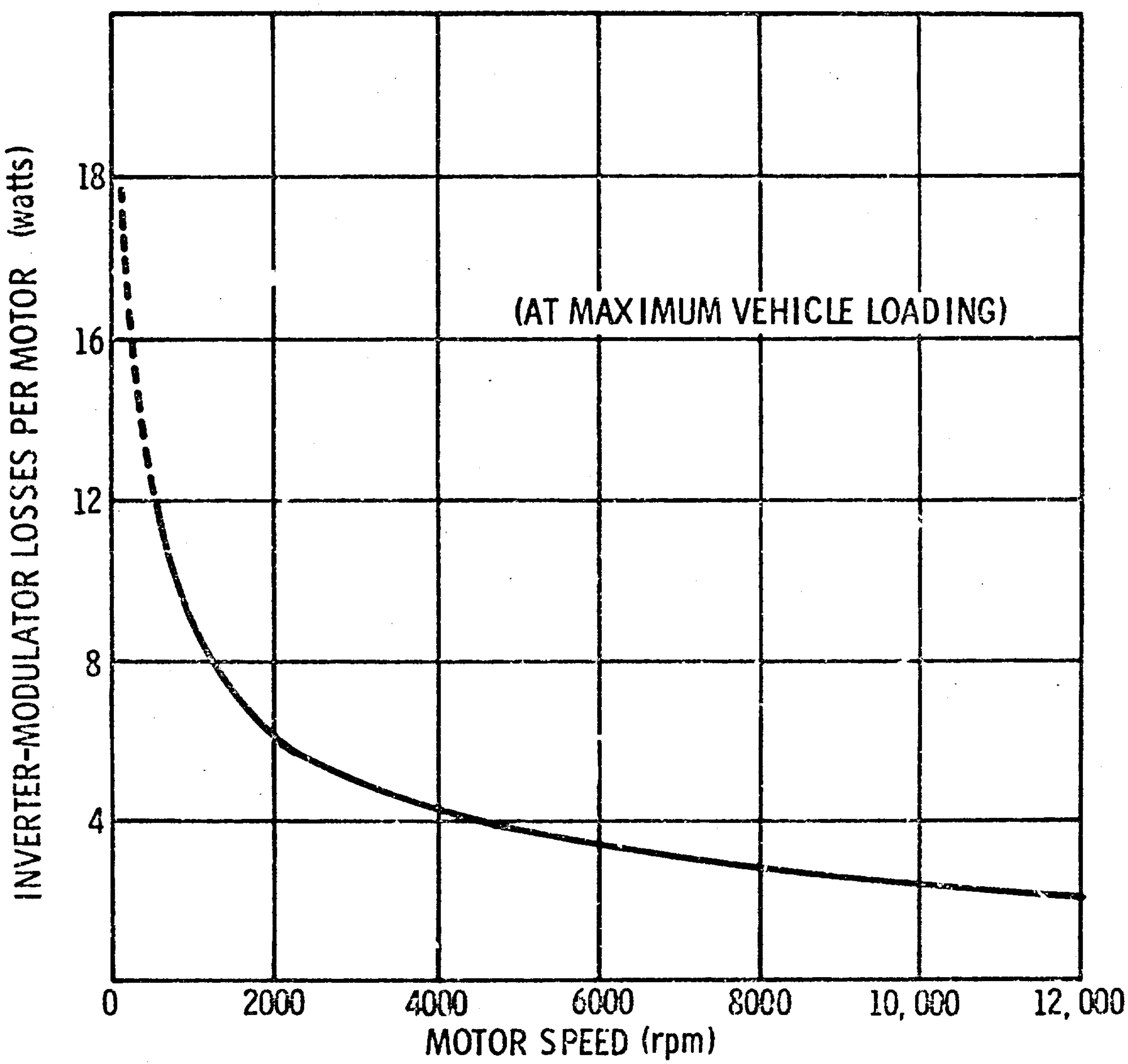

Figure 6.7.23- Inverter-Modulator Power Losses vs Speed

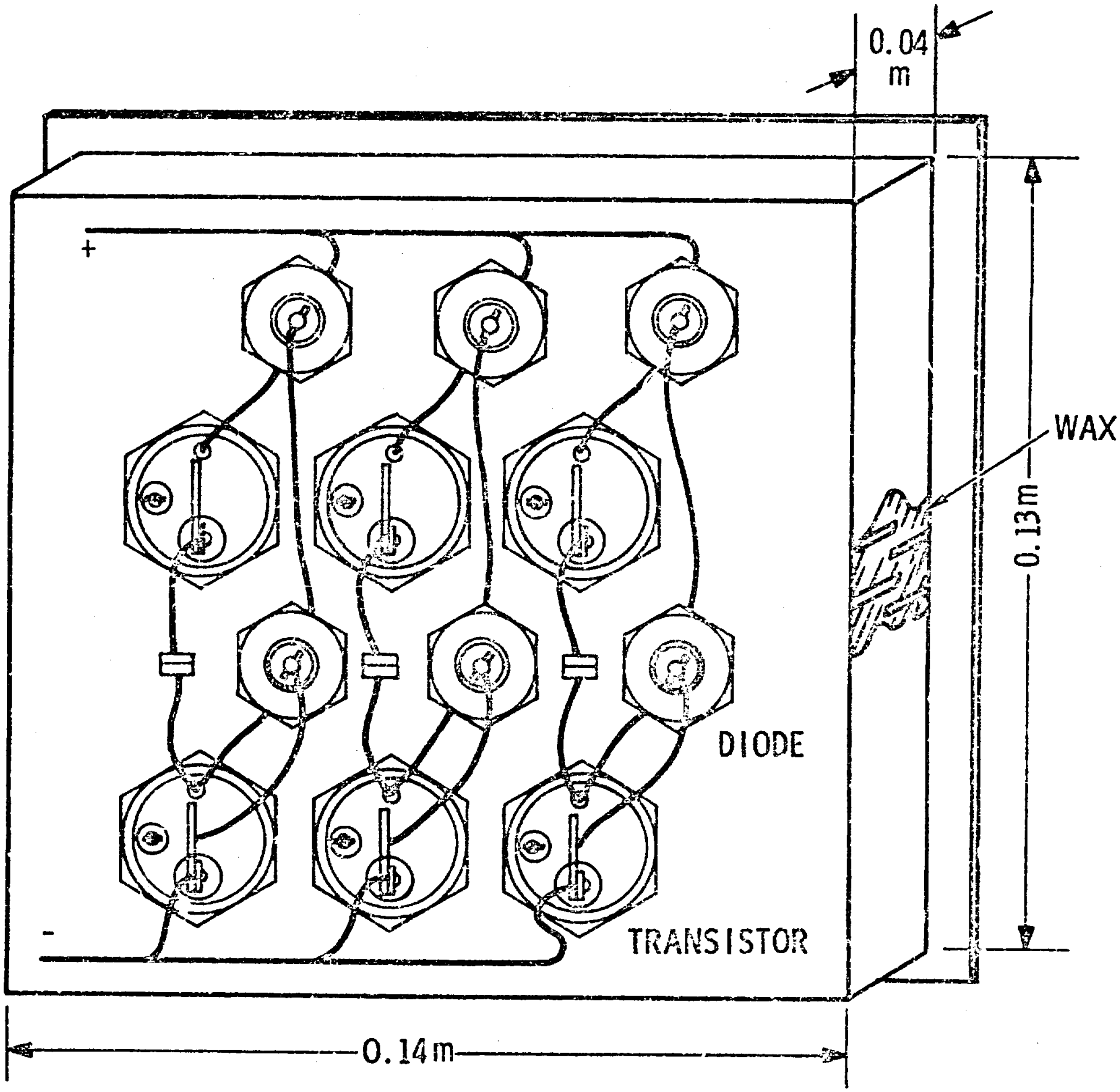

Figure 6.7.24- Inverter-Modulator Packaging Arrangement

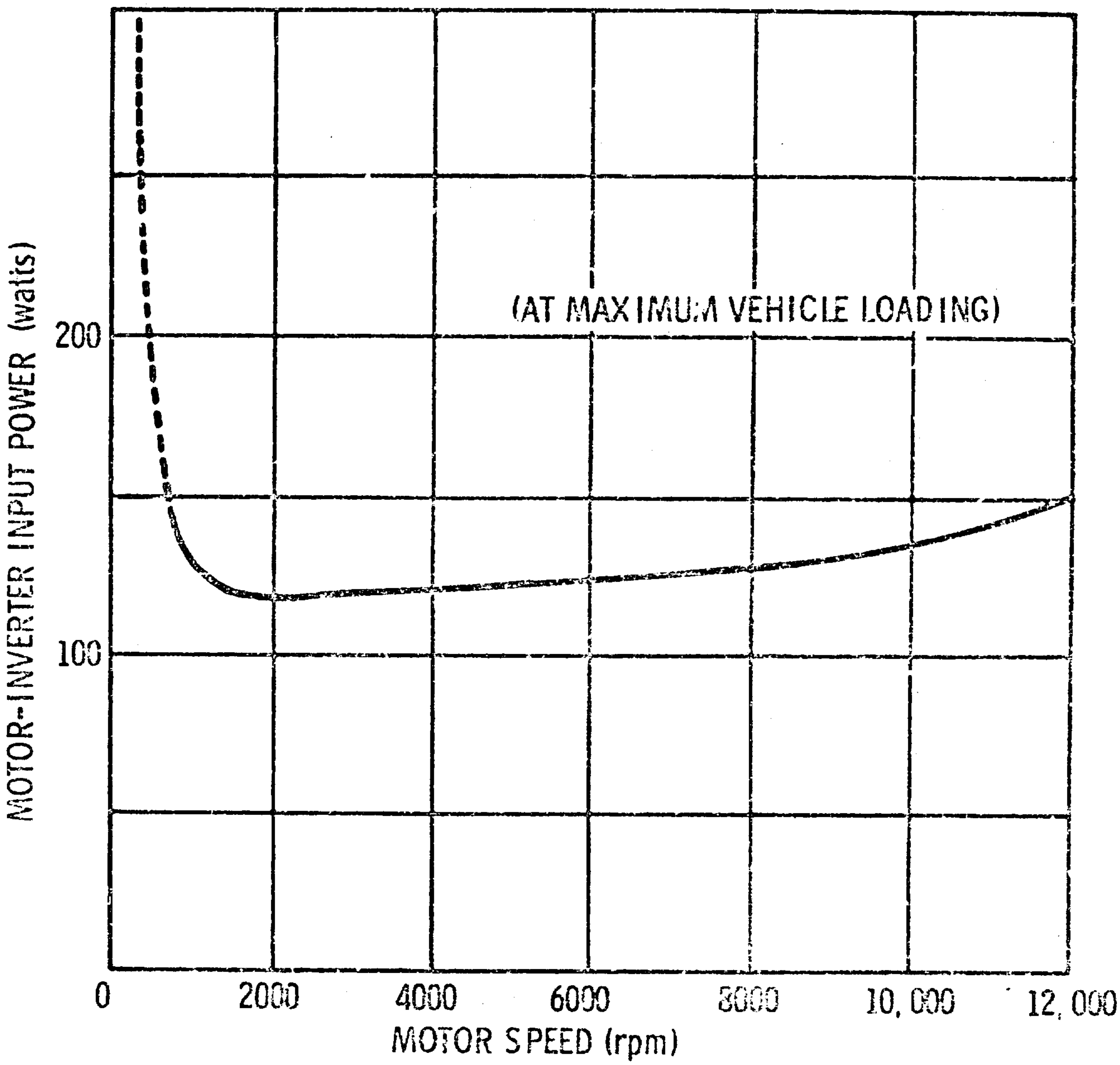

Figure 6.7.25- Motor-Inverter Input Power vs Speed

consumption will be six times that shown on the curve. Maximum steady state power of about 900 watts will be required at speeds of 650 rpm and 12,000 rpm for maximum vehicle loading.

The efficiency of the LSSM electric drive system as a function of motor speed is shown in Figure 6.7.26. Conditions for which the efficiency was calculated are a 56 volt dc power source and maximum vehicle loading.

Total inverter and motor losses were included in the calculations. The drop in efficiency at the high speeds is due primarily to bearing friction losses. Measurements of the efficiency of the MTA drive system closely approximate the calculated efficiency of the LSSM electric drive.

6.7.9 Reliability Discussion

Analysis of the failure modes of an electric drive wheel operating on the lunar surface indicates that a wheel assembly utilizing an a-c motor will be more reliable than one using a d-c motor. The commutator of a d-c motor requires a gaseous environment at a pressure greater than 5 mm Hg, must be operated at temperatures below 470°K, limits the maximum speed of the armature to several thousand rpm below induction motor speeds and generates heat due to mechanical friction and electrical resistance. Scant information is available on commutator reliability when operated at relatively high temperatures in sealed enclosures. Because of the large effort going into making semiconductor switches reliable devices, much more data and experience that enables one to predict the probable reliability of a well designed inverter system.

Failure rate studies of electric machines conducted in the past indicate that for all possible uses, operating conditions, and abuses, the failure rate of d-c machines is two to three times the failure rate of a-c machines. If attempts are made to design equivalent weight d-c or a-c machines, there appears to be an inherent failure rate penalty associated with d-c machines. Reliability studies have indicated that an a-c drive system can be designed with a reliability equal to or higher than that of a d-c system. Of major importance is the fact that the a-c motor power wheel will have a much greater reliability than the d-c motor powered

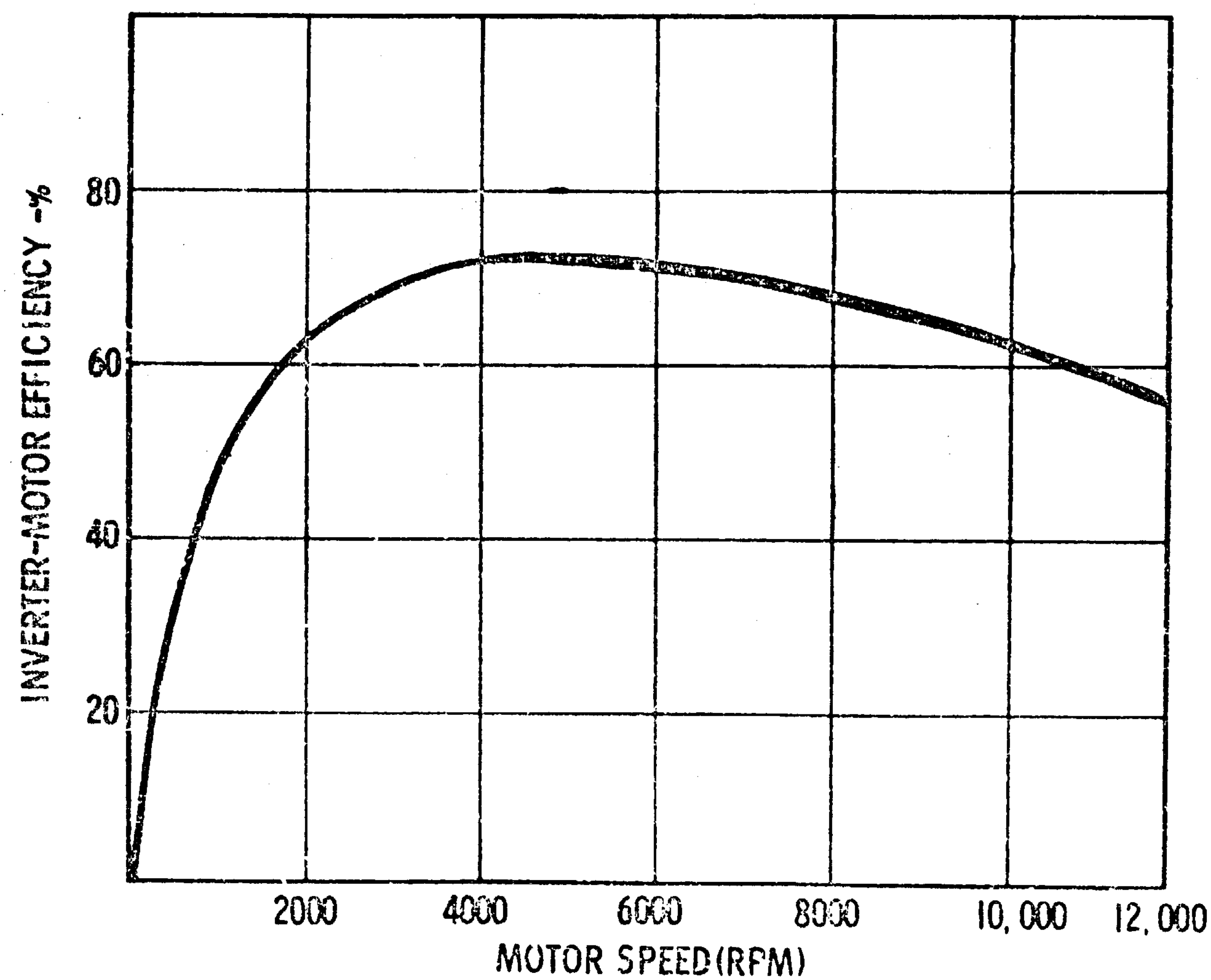

Figure 6.7.26- LSSM Electric Drive Inverter-Motor Efficiency

wheel. The reasons are as follows:

(1) Heat dissipation caused by commutation is eliminated from the wheel.

(2) The rotor of the a-c machine can be a nearly solid structure compared to a wire wound d-c rotor.

(3) Wheel assembly weight is less because of the higher a-c motor speeds and removal of commutator and brushes.

(4) The a-c motor can continue to operate even though the motor enclosure is broken and the gaseous environment is lose. Heat transfer analysis shows an a-c drive motor mounted in the LSSM wheel will operate even in the vacuum environment. Life of the drive mechanism will be limited by the bearing and gear lubricants. But since dry lubricants can be used, 100 to 200 hours operation may be obtainable after the bearing seal is broken.

(5) A d-c drive motor system will require a one-or two-step gear shift if the efficiency of an a-c drive system is to be approached. This gear shift would be located in the wheel and would reduce drive mechanism reliability.

Therefore, the actual reliability of the wheel assembly of the a-c system is significantly superior to that of the d-c system. A failure in the d-c drive system is most likely to occur in the commutator-brush assembly, a place where maintenance is difficult to perform and where redundancy cannot easily be provided. A failure in the a-c drive system is most likely to occur in the inverter. The inverter can be located where maintenance tasks can be performed. Redundant inverters can also be used.

Highest transistor current stress occurs at wheel speeds of from 2 to 5 rpm when the vehicle is obstacle climbing or climbing 35° slopes. Highest junction temperatures occur at nearly the same speeds. An analysis of the LSSM probable mission indicates that peak currents are required less than 1 percent of the time. For about 45 percent of the mission time current demand per motor will range from 2 to 4 amperes. No current is required for almost 24 percent of the time due to vehicle movement from higher to lower elevations.

6.7.10 LSSM Electric Drive System Summary

Electric drive system performance characteristics, power losses and major component weights have been discussed. In addition, methods of drive motor control have been presented. Motor and power switch specifications were given.

In brief: The electric drive system will produce a peak torque of 1.22 ft-lb (1.65 N-m) at a wheel speed of 2 rpm, a maximum continuous duty torque of 0.69 ft-lb (0.93 N-m) at 5 rpm, and 0.06 ft-lb. (0.08N-m) at the maximum wheel speed of 92 rpm. This latter speed represents a vehicle velocity of approximately 16 km/hr (10 mph).

Maximum steady-state input power will be approximately 900 watts at a wheel speed of 5 pm and at a vehicle speed of 16 km/hr for maximum vehicle loading. Maximum drive efficiency will be about 75% at 10 km/hr. Each drive motor will weigh about 3.6 kg (8 lb) including the heat radiator. Total weight of the power conditioning equipment and electronic control circuitry will be approximately 14 kg (30.8 lb) exclusing the phase-change heat exchanger, circuit breakers and connecting cables.

7.0 LSSM MOBILITY SYSTEM SPECIFICATIONS

7.1 SCOPE

These specifications provide the functional and performance requirements for the baseline LSSM mobility system. The mobility system encompasses the following subsystems:

- Wheel Assembly
- Wheel Drive Mechanism
- Suspension System
- Steering System
- Chassis - Frame Assembly
- Electric Drive System

7.2 APPLICABLE DOCUMENTS

o "ALSS Payload Design Criteria; Structural Design Criteria", Prepared by Hayes International Corporation for R-P & VE-AL, NASA MSFC, Under Contract NAS 8-5307, June 29, 1964.

o "MOLAB Structural Design Criteria", Boeing Document D2-82068, Prepared Under Contract NAS 8-11411, August 1964.

o GM DRL Drawing Nos. PD-00810, PD-00813, PD-00816, PD-00820, PD-00821, PD-00822, PD-00823.

o Engineering Lunar Surface Model (ELMS), KS C TR-83-D

7.3 REQUIREMENTS

7.3.1 Overall Mobility System

The purpose of the mobility system is to function as a mobile platform, day or night, capable of negotiating the soils, slopes and obstacles of the lunar surface, while providing maximum probability of crew safety and mission success. It shall have the capability of accommodating an astronaut-driver and approximately 700 lbm of scientific equipment, as well as the necessary power, thermal, navigation and communications systems.

It shall be capable of negotiating the surface profiles specified in ELMS at a minimum average speed of 5 km/hr, and maintain speeds of at least 16 km/hr over level hard ground and 5 km/hr over level soft ground with soil characteristics $k_\phi = 0.5$ and $n = 0.5$. The minimum mission range will be 200 km over a 14 (earth) day period.

7.3.2 Wheel Assembly

The wheel assembly shall consist of the following major components:

- wheel disc
- stiff inner frame
- rim
- tread
- woven wire outer frame

The design of the wheel shall conform to the configuration of GM DRL drawing PD-00821, and the functional capabilities and limitations as specified herein.

Emphasis shall be placed on reliability, minimum weight, performance, and compatibility with the lunar environment. Six wheel assemblies shall be used to support the LSSM vehicle and to transmit driving torque to the lunar surface. The wheel disc, which shall be attached to the drive mechanism wheel hub, shall be a spun conical frustrum. The rim shall be flanged to provide stiffness and shall be rigidly attached to the wheel disc. The spring wire outer frame shall consist of 540 interwoven wires in a 0.375 mesh. Suitable materials shall be utilized for the right-hand and left-hand wires to reduce the possibility of vacuum cold-welding at the points of intersection. The ends of the spring wire outer frame loops shall be rigidly attached to the rim. The stiff inner frame shall be rigidly attached to the rim and shall consist of 36 loops interconnected by hat section circumferential rings.

The tread shall cover the normal running surface of the wheel, and shall consist of a specially woven wire braid, or separate metal lugs.

The wheel sub-assembly shall be capable of reacting the following dynamic forces:

- limit radial wheel load — 5204 N (1170 lbf)
- limit lateral wheel load — 578 N (130 lbf)

The wheel sub-assembly shall be capable of reacting or transmitting 165 N-m (120 ft-lb) of torque. The wheel shall be capable of a maximum speed of 92 rpm. The wheel shall be capable of completing 100,000 revolutions without significant deterioration of performance. The wheel disc shall provide for attachment of the wheel assembly to the wheel drive mechanism wheel hub. The rim shall provide for attachment of the stiff inner frame and flexible wire outer frame. The spring wire outer frame shall be the primary load supporting structure of the wheel assembly. It shall deflect 4.30 cm (1.70 in) at the nominal wheel load of 289 N (65 lbf). That is, the outer frame shall have a spring rate of 66 N/cm (38 lbf/in).

The stiff inner frame shall prevent excessive deflection of the spring wire outer frame and shall absorb maximum dynamic loads. It shall have a spring rate of 3620 N/cm (2074 lbf/in).

The tread shall protect the wheel covering from abrasion and provide a gripping tread for traction.

7.3.3 Wheel Drive Mechanism

The wheel drive mechanism (WDM) shall consist of the following major elements:

- o wheel hub
- o harmonic drive
- o spur gear reduction
- o electric drive motor
- o brake system
- o wheel drive housing
- o wheel drive disconnect
- o radiator

The design of the WDM shall conform to the configuration of GM DRL drawing PD-00813, and to the functional capabilities and limitations set forth herein. Emphasis shall be on reliability, performance, minimum weight and compatability with the lunar environment.

The WDM shall drive the wheel assembly of the LSSM vehicle. The wheel hub which supports the wheel shall be the driven member of the mechanical drive. The WDM shall be supported by the steering pivots of the Ackermann steering actuators at the forward and aft axle wheels; and by the suspension system at the center axle wheels.

The WDM shall be capable of operating in either direction or braking the vehicle when the drive is not energized. All electrical and high-speed mechanical components shall be enclosed in a hermetically sealed chamber. A manually operated wheel drive disconnect shall be incorporated to declutch each wheel from the WDM for emergency operation. Each WDM shall have a passive radiator located outboard of the wheel for cooling, and at a minimum, the four wheels of the forward unit shall be capable of being braked by manual means for purposes of parking. Instrumentation shall include a temperature transducer, pressure switch and odometer.

The WDM shall provide, at a minimum, the output torque-speed characteristics shown in Figure 7.3.1. These are summarized as follows: 6 lb-ft. at 92 rpm, 68 lb-ft. at 5 rpm (maximum continuous duty), and 120 lb-ft. at 2 rpm (intermittent).

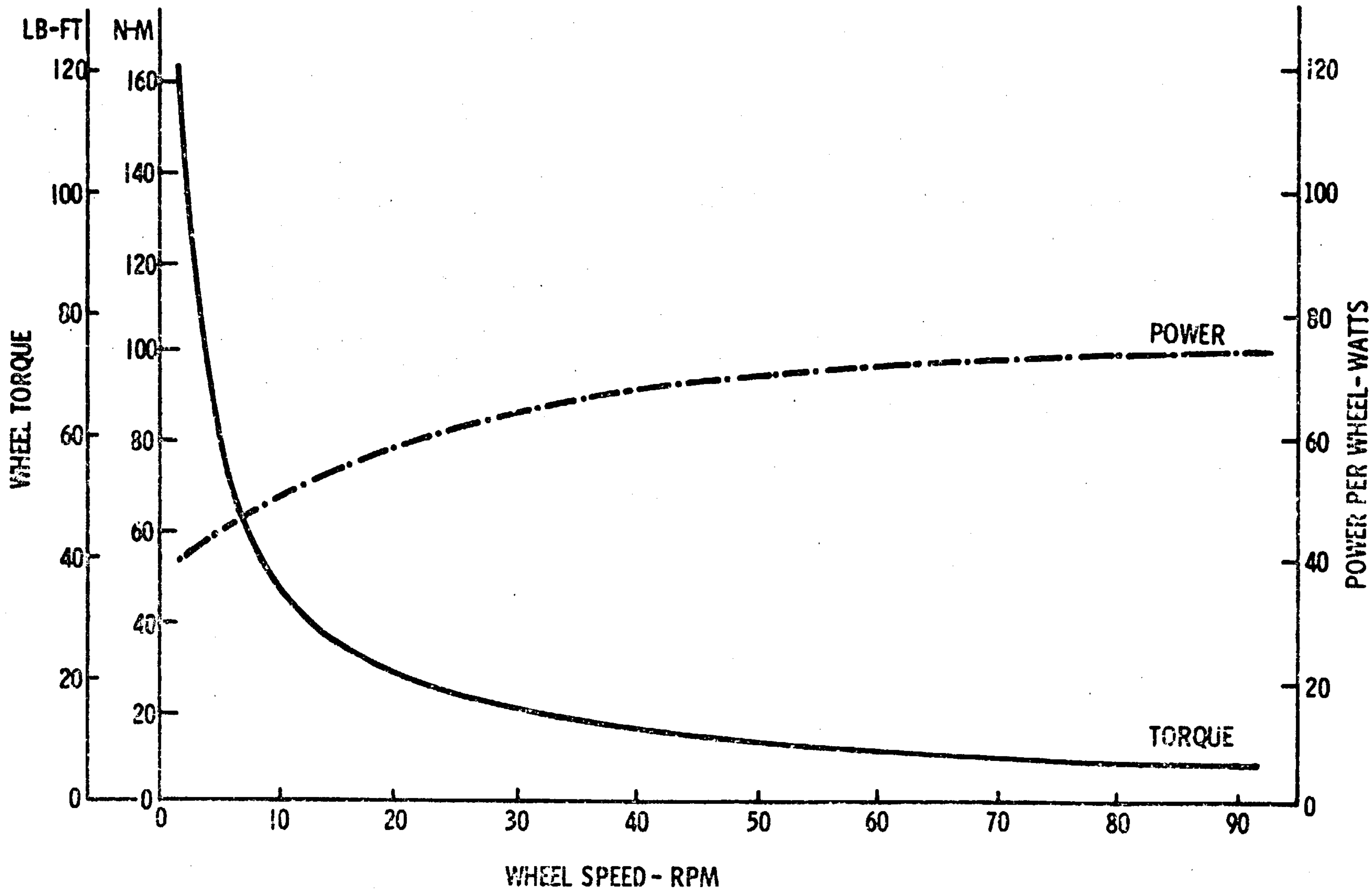

Figure 7.3.1 - Wheel Net Torque and Power Characteristics

A size 25 harmonic drive unit shall provide a gear reduction of 88:1 for the output of the WDM. This unit, coupled with the WDM housing, shall provide the hermetic sealing capability. The wave generator of the harmonic drive shall be coupled directly to the electric drive motor. The flexspline is a thin-walled member in contact with the wave generator. The elliptically shaped wave generator deflects the flexspline in two diametrically opposed areas, and causes the external teeth of the flexspline to engage with the internal teeth of the harmonic drive circular spline. The output of the harmonic drive is the circular spline which shall have gear teeth also on its outer circumference. The outer teeth of the circular spline shall engage three small pinion gears which in turn shall drive a ring gear attached to the wheel drive. This final reduction due to the use of intermediate pinion gears shall be equal to 1.5:1.

Disconnecting of the WDM from the wheel for emergency operation shall be accomplished manually by a single release device that will disengage the ring gear from the wheel hub.

A conventional duo-servo two-shoe brake assembly shall be utilized for the service brake. Actuation shall be by a pilot shoe assembly which is controlled by a small short stroke solenoid. Minimum braking torque shall be such that with the electric drive motor de-energized, there shall be no rotation of the wheel drive mechanism when subjected to an external torque of 120 lb-ft. (165 N-m). The service brake shall be capable of dissipating a peak power load of approximately 560 watts, and an average continuous load of 40 watts. For purposes of parking, the brakes shall be actuated by means of a cam device in parallel with the solenoid armature, controlled by means of a manual push-pull cable.

The wheel hub shall be supported by two main bearings mounted on a circular housing attached to the suspension system. The wheel shall be attached to one end of the wheel hub. The wheel drive mechanism housing, in conjunction with the harmonic drive flexspline, shall provide a hermetically sealed chamber for the mechanism. The electric drive motor, spur gear reduction, service brake, and instrumentation shall be located with the flexspline - housing envelope. The hermetically sealed chamber shall be charged with a suitable gas at a nominal pressure of four psia such that the high speed mechanical and electrical components are protected from the low pressure lunar environment.

A temperature-compensated pressure switch shall be located within the hermetically sealed mechanism. It shall actuate whenever the initial pressure (corrected for temperature) has changed by 25 percent, plus or minus three percent, over a nominal temperature range of minus 250 degrees to 500 degrees F. Two temperature transducers shall be provided to monitor motor winding and motor bearing temperatures. The transducers shall be capable of a range of temperature measurement from -250 to 500 degrees F with a maximum accuracy of plus or minus three percent. Odometer requirements shall be as required by the Navigation System. (See Section 7.3.7 of this report.)

The wheel drive mechanism shall be capable of operation regardless of its orientation. It shall be capable of completing a minimum of 100,000 revolutions of nominal operation without difficulty, malfunction, or repair. The wheel drive mechanism shall be designed and constructed such that, when supplied with voltage and power, the mechanism will meet the performance requirements specified herein.

The electromagnetic service brake shall operate from a source voltage of 28 volts dc and shall have a maximum power drain of 30 watts. The pressure monitoring switch shall operate on an applied voltage of approximately 28 volts dc and 0.2 amperes.

Requirements for the electric motor are given under section 7.3.7 of this specification.

7.3.4 Suspension System

The suspension system assembly shall consist of the following major components:

- o lower suspension arm
- o upper suspension arm
- o torsion bar spring element
- o shock damper
- o wheel drive mounting bracket

The design of the suspension assembly shall conform to the configuration of GM DRL drawing PD-00822, and the functional capabilities and limitations as specified herein. Emphasis shall be placed on reliability, minimum weight, performance, and compatibility with the lunar environment. Six suspension assemblies shall be used to support the LSSM structure, absorb dynamic loads resulting from operation on the lunar surface, and provide suitable spring and damping action for ride comfort and crew and equipment safety.

The lower suspension arm shall be a tubular welded structure, attached to the chassis-frame subsystem.

The upper suspension arm shall complete the parallel arm linkage. It shall also be of tubular welded construction and attached to the chassis-frame subsystem. The longitudinal torsion bar spring element shall be fixed to the upper arm and chassis-frame between the suspension mounting pivots. The shock damper shall be a hydraulic linear damper. A heating element shall be provided for start-up and lunar night operation. Hermetic sealing shall be provided by means of a bellows.

The suspension assembly shall be capable of reacting a wheel torque of 162 N-m (120 ft-lb). The suspension assembly shall provide for 13.5 cm (5.3 in) of jounce at the wheel and 11.9 cm (4.7 in) of rebound. The suspension assembly shall have a spring rate of 26 N/cm (15 lbf/in) and a damping rate of [illegible]10 N sec/cm (50 lb sec/in).

7.3.5 Steering System

The steering system for LSSM shall consist of two essentially identical steering actuators to result in Ackermann-type steering of the front wheels of the forward unit and the aft unit wheels. The two actuators shall be connected by means of a flexible shaft to aid in wheel angle synchronization in turns.

Each actuator shall consist of the following major components:

- Electric Motor
- Gear Box
- Mechanism Housing
- Cross Link
- End Housing

The design of the steering actuator shall conform to the configuration of GM DRL drawing PD-00816, and the functional capabilities and limitations specified herein. Emphasis shall be placed on reliability, performance, minimum weight and compatibility with the lunar environment.

Two actuator assemblies shall be used to position the wheels; one for the front wheels of the forward unit, the other for the aft unit wheels. Each actuator shall be attached to the chassis-frame structure and the steering links connected to the wheel drive mechanism. Each steering actuator shall be capable of positioning the wheels up to 25 degrees from the normal wheel centerline. It shall be capable of maintaining any given position against external nominal loads. Switches shall be provided to prevent exceeding the maximum steering angle by cutting power to the steering motor.

All functioning electrical and high speed mechanical components shall be enclosed in a hermetically sealed housing. The pressure in the housing shall be monitored by a simple temperature compensated pressure switch.

A temperature transducer shall be provided to monitor motor temperature. An emergency release for the mechanism shall be provided. Ingress and egress of electrical wiring at the mechanism shall be accomplished using a hermetically sealed connector.

The steering actuator shall have the following minimum torque-speed characteristics: 260 ft-lb (352 N-m) at a steering speed of 0.1 rpm (0.6 degrees/sec); 20 ft-lb (27 N-m) at 1.0 rpm (6.0 degrees/sec); and 12 ft-lb (16 N-m) at 2.5 rpm (15.0 degrees/sec). In addition, the actuator must be capable of developing a resisting torque of 407 ft-lb (552 N-m) to withstand longitudinal load inputs through a wheel centerline.

Each actuator shall have an overall speed reduction of approximately 1250:1 and be capable of developing a thrust of 1675 lbf (7450 N), a rate of travel of 1.08 in/sec (2.7 cm/sec), and a total stroke of 2.2 inches (5.6 cm).

A drive assembly, consisting of motor, spiroid gear set and ball nut and screw, shall provide the torque-speed requirements described above. The drive motor-gear reducer combination shall drive the spiroid gear set which in turn shall drive the ball nut and screw. The screw is part of the cross-link assembly that positions the wheels.

The actuator shall be driven by a dc permanent magnet motor, operating from a 28 volt dc power source. The motor shall be reversible and capable of withstanding intermittent stall loads for 30 seconds. The motor shall have a rated power output of approximately 30 watts with the torque/ and power/speed characteristics shown in Figure 7.3.2. Efficiency of the motor shall be at least 60% at rated nominal conditions.

The spiroid gear set shall provide a speed reduction of 38:1. It shall have

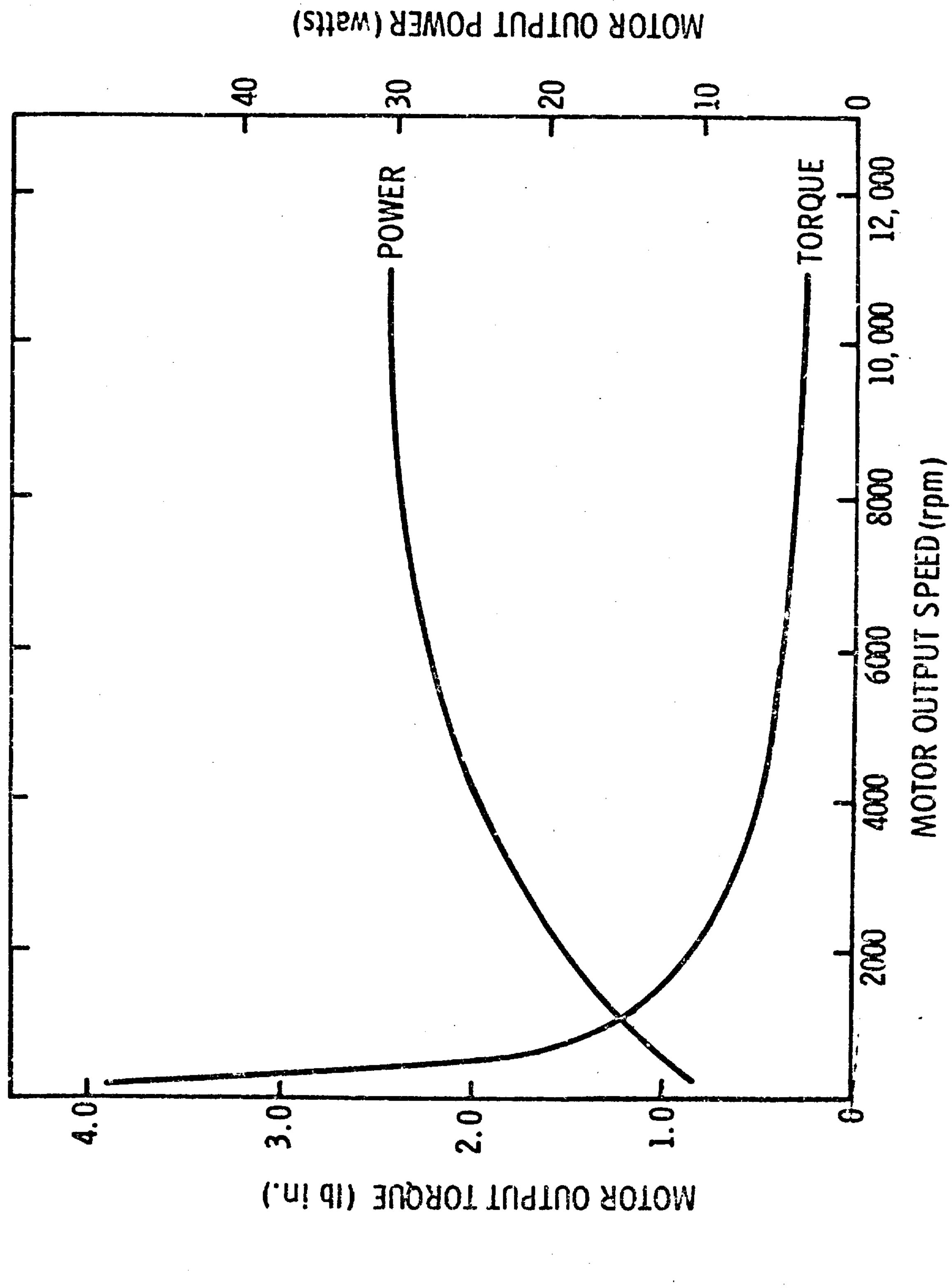

Figure 7.3.2 - LSSM Steering Motor Output Characteristics

nominal ratings of 100 in. lb of torque, 0.067 HP input at 1750 rpm, and 0.038 HP output at 1750 rpm.

The ball nut and screw shall provide a speed reduction of 33:1. It shall be capable of withstanding operational loads up to 2200 lbf.

An emergency shall be provided on the end housing so that the wheels may be steered by means of a manual input. This emergency input shall be by means a rack and pinion on the forward unit actuator driven by a ratchet handle.

Steering control shall be by means of a driver operated sidearm control. The control system can be either an open or closed-loop system.

The entire mechanism shall be hermetically sealed and charged with a suitable gas at a nominal pressure of 4.0 psia such that all high speed mechanical and electrical components of the mechanism are protected from the low pressure lunar environment.

A temperature compensated pressure switch shall be located within the hermetically sealed chamber. It shall actuate whenever the initial pressure (corrected for temperature) has changed by 25 percent, plus or minus 3 percent, over a nominal temperature range of minus 250 degrees to 500 degrees F. This switch shall operate from a 28 volt dc power source. Limit switches shall limit maximum steering position of the mechanisms in either direction. These switches shall operate on an applied voltage of 28 volt dc and have a rating of 0.5 amperes.

Temperature transducers shall be provided to monitor steering motor winding temperature. Range of temperature measurement from -250 to 500 degrees F with a maximum accuracy of plus or minus three percent shall be provided.

Steering actuators shall be capable of completing a minimum of 6,000 cycles of nominal operation without difficulty, malfunction, or repair. The steering actuators shall be capable of operation regardless of its orientation. The mass of a single actuator mechanism shall not exceed 17 lbm (k kg).

7.3.6 Chassis-Frame Assembly

The chassis-frame subsystem shall consist of the following major assemblies:

- o Forward unit frame assembly
- o Aft unit frame assembly
- o Flexible frame assembly

The design of the chassis-frame subsystem shall conform to the configuration of GM DRL drawing PD-00820 and the functional capabilities and limitations specified herein. Emphasis shall be on reliability, minimum weight, performance and compatibility with the lunar environment.

The chassis-frame assembly shall provide the basic support structure for the entire LSSM vehicle. It shall provide attachment points for the suspension system and steering mechanisms, and provide means for accommodating crew system and scientific equipment, as well as the power, navigation, communications and thermal subsystems.

The chassis-frame structure shall be capable of withstanding repeated flexures and shock loads, and shall permit a minimum of 90 degrees for the angels of approach and departure of the assembled vehicle.

The chassis-frame subsystem shall provide for the retraction and extension of the flexible frame permitting in-flight stowage aboard and deployment onto the lunar surface from the LEM/Shelter.

The design of the chassis-frame subsystem shall permit the following relative displacements between the forward and the aft units:

- plus or minus 15 degrees (from reference axis) in pitch
- plus or minus 30 degrees (from reference axis) in roll

The forward unit assembly shall consist of an aluminum box structure with an integral rail structure for flexible frame retraction. The chassis rails shall be capable of withstanding the reactions of the following dynamic loads as well as those specified in D2-82068:

o	Limit vertical wheel load	5, 200 N (1, 170 lbf)
o	Limit lateral wheel load	578 N (130 lbf)
o	Limit longitudinal wheel load	10, 200 N (2, 300 lbf)

Four pairs of mounting brackets for the four forward unit suspension assemblies shall be provided. There shall be guide tracks for operation of the retractable flexible frame. Provisions shall be made to accommodate the flexible frame locking mechanism and for attachment of the steering actuator for the forward wheels.

The aft unit frame structure shall provide attachment points for the rear wheel suspension assemblies and steering actuator, and provide support for a thermal compartment containing power system and navigation, communications and drive electronics. The aft unit shall be able to withstand the loads specified above.

The flexible frame assembly shall control the relative attitudes of the aft and forward units in pitch and roll. The assembly shall consist of the flexible frame, pitch limiter, and pitch limiter bracket, and shall provide an "elastic coupling" of the forward and aft units. During the stowage mode, the flexible frame shall have the capability of being retracted along the guides of the forward unit rails. At deployment the flexible frame shall have the capability of being extended to its operating position. Two locking mechanisms (one for each rail) shall be provided to secure the flexible frame in the locked or extended position.

The flexible frame shall limit freedom of roll between the two units to plus or minus 30 degrees and shall be capable of reacting the loads specified above.

The pitch limiter shall restrict the pitch freedom of the aft unit to plus or minus 15 degrees. A means shall be incorporated into the limiter so that it can be stowed between the forward and aft units. A mechanism shall be provided at the forward unit to lock the pitch limiter into operating position when the vehicle is deployed. The pitch limiter shall incorporate snubber springs to react impact loads. The pitch limiter bracket shall provide for the securing of the aft end of the pitch limiter. It shall serve as a spacer and fixity for the aft end of the flexible frame.

7.3.7 Electric Drive System

The electric drive system shall consist of the following major elements:

- o Motors
- o Power Switching
- o Controls

The electric drive system shall perform the following functions:

- o Convert electric energy produced by the battery system into mechanical energy to drive the LSSM wheels.
- o Control vehicle speed in response to commands from the manned control loops.
- o Supply wheel velocity information for the navigation system.

The design of the electric drive system (EDS) shall conform to the functional capabilities and limitations as specified herein. Emphasis shall be placed on reliability, minimum weight, efficiency, controllability, performance and compatibility with the lunar environment. The EDS shall be capable of propelling the vehicle in either direction at the command of the driver. Cooling of the power switching and control elements shall be accomplished by a phase change material heat exchanger system.

The EDS motor shall be an ac squirrel cage induction motor. It shall be bolted to a flange on the wheel drive mechanism and drive an 88:1 step-down harmonic drive. Heat transfer shall be accomplished by radiation attached to the case. The motor case and radiator are parts of the wheel drive mechanism.

The motor shall be energized by cables running from the wheel mechanism to the aft unit thermal compartment in which the power switching and control elements are mounted. The power switching circuits shall be controlled by control elements which receive signals from the digital tachometers mounted on the motor shafts, and from the astronaut's side-arm controller.

The EDS motor shall be capable of producing an intermittant torque of 1.7 N-meters (1.2 ft-lb) at 0 to 260 rpm and a maximum steady-state torque of 0.84 N-meters (0.7 ft-lb) at 650 rpm. Maximum steady-state power output shall be 95 watts at 12,000 rpm. Maximum motor weight including radiator will be 3.6 kg. Maximum overall motor dimensions shall be 5.0 inches O.D and 40 inches length.

The power switch subsystem shall produce a stepped, alternating, three-phase voltage varying from 0 to a maximum voltage of 56 volts peak. It shall be capable of delivering a maximum current of 25 amperes peak. The power switching equipment is controlled by the control system which will receive signals from digital tachometers mounted on the motor shafts and from the drive console unit. The controls shall be mounted in the aft unit thermal compartment. The control elements shall receive motor speed signals and drive and steering commands, and control the voltages and frequencies applied to the drive motors. They shall control the speed of the vehicle in forward or reverse, and shall enable the vehicle to skid steer in an emergency mode of operation.

To interface with the navigation system, each wheel transducer shall produce a pulse train output specified as follows:

1. Pulse amplitude - Any amplitude between 6 and 28 volts.
2. Pulse width - Between the limits of 1 and 10 milliseconds.
3. Pulse rate - 128 pulses per meter or greater.
4. Pulse spacing accuracy - $\pm$ 3%.
5. Rise and fall time - 0.1% (or less) of pulse width.
6. Load impedance - 50,000 ohm or greater.

The pulse rate specified shall be the minimum acceptable. The rate may be increased to a higher value as long as it is a binary multiple of distance (in meters). A +6 volt dc signal is required for the navigation system interface when the vehicle is going in reverse. This signal will instruct the distance computer to subtract wheel transducer output pulses.

The steering and drive command signals shall be of the analog type varying from 0 to 5 volts dc. Input impedance of the control subsystem shall be 1,000 ohms or higher.

Power switching shall be designed to operate from a battery voltage of 56 volts dc with voltage excursions from 52 to 71 volts dc. The controls shall be designed to operate from a battery voltage of 28 volts dc $\pm$1 volt.

Maximum weight of the electric drive system shall be 38 kg (86 lbm), including inverters, motors, cables and circuit breakers. Average efficiency of the drive system shall be greater than 50 percent.

8.0 FAILURE MODE AND RELIABILITY ANALYSES

8.1 FAILURE MODE AND EFFECT ANALYSIS

8.1.1 Introduction

A failure mode and effect analysis was conducted for the LSSM mobility system consistent with the guidelines of Boeing Company memo 2-5022-66, "LSSM Reliability Prediction and Failure Mode Analysis", dated 20 December 1965. Such an analysis is useful for making system level reliability predictions for the LSSM.

Each major component of the mobility system was reviewed for significant failure modes which would adversely effect the intended function of the component. Significant failure modes were listed with possible causes. Effects of each failure on the component and on the mobility system were also determined. The seriousness of each failure was considered and indicated by a "criticality number". Possible actions to relieve the adverse effects of each failure were listed.

8.1.2 Conclusions

A review of the results, using a conservative approach, suggests the more serious failure modes to be associated with:

(1) loss or excessive dislocation of more than one wheel.

(2) parting of the forward chassis or flexible frame.

(3) total failure of the drive electronics system.

Each of these failure areas involves almost certain abandonment of the vehicle, with loss of life if failure occurs outside the walk-back radius in the traverse.

8.1.3 Discussion

The results of the failure mode and effect analysis are given in the 9-page attachment at the end of this section. Most of the features listed are not critical due to the many redundant design features of the six-wheel configuration. Several of those failures listed as serious would involve a significant time factor before vehicle abandonment would be necessary. This time could be used to minimize the distance to the shelter.

Comments pertinent to the contents of the attachment are as follows:

Component Identification - This column lists each of the major mobility system components.

Function - The function of each component is considered to aid in determining all significant failure modes.

Modes of Failure and Causes - Modes of failure are listed consistent with component functions. Potential causes were determined from review of the component drawings.

Effects on Component and Subsystem - Listed are the effect of each failure mode on the performance requirement of the component and on the subsystem performance.

Criticality Number - The number refers to the expected seriousness of the failure under consideration as follows:

(1) High probability of causing loss of life.

(2) High probability of causing disablement of LSSM, but no immediate loss of life.

(3) Seriously degrades the usefulness of LSSM, but does not cause abandonment.

(4) Less serious than (3) but would cause the LSSM to be kept within astronaut's walk back capability.

(5) Least serious and might not cause restrainment of traverse.

Alternates - Alternate modes of operation and other corrective actions that might be used to get the LSSM back to the LEM/Shelter should the failure occur.

LRSM MOBILITY SUBSYSTEM - Failure Mode and Effect Analysis

Component Identification	Function	Modes of Failure and Cause	EFFECTS on component	EFFECTS on subsystem	Criticality Number	Alternates
Drive Mechanism	Provides drive torque to wheel.	Parts fail to transmit torque. Motor shorts out. Wave generator fails. Flexspline housing fails. Gear teeth strip. Disconnect pins shear.	Wheel's drive force lost. Drive load increased on units still operating.	Need for abort after second drive failure. Vehicle disablement with third drive failure depending on terrain.	One failure 4. Two failures 3 Three failures 2	Drive system can continue to function, at a reduced level of capability, with two wheels free wheeling. Six independently functioning units make the system highly redundant. Disconnecting of failed units will minimize drag on drive system.
		Mechanism operates at reduced efficiency. 1. Brake drag: a. actuator won't ... b. shaft linkage stuck 2. Mechanism overheats, reducing drive motor efficiency. a. radiator damaged or obstructed. b. brake dragging. c. increased bearing friction. 3. Friction between bearing surfaces increases. a adverse effect of environment.	Requires more energy for same performance. Operating temperature increases if speed is maintained.	Effects depend on magnitude of additional power consumed and lunar terrain. Could reduce length of traverse if power consumption increased significantly.	3-4	Redundancy of six drive units lessens severity of reduced efficiency. Speed could be reduced to avoid overheating. Drive disconnect would improve 1.(a).

LSSM MOBILITY SUBSYSTEM - Failure Mode and Effect Analysis

Component Identification	Function	Modes of Failure and causes	EFFECTS on component	EFFECTS on subsystem	Criticality Number	Alternates
Drive mechanism (continued)...	Supports wheel and allows rotation of wheel.	Mechanism housing or pivot pin fail: (a) overstress of good part. (b) defective part.	Mechanism ceases to function.	High probability of detachment of wheel.	2 (1 - if outside walk-back radius)	None, but probability of occurrence would be very small.
		Parts seize: (a) motor bearing (b) wave generator bearing (c) gear teeth (d) wheel bearings - from adverse environment	Would cause dragging of wheel if not overridden by drive disconnect mechanism.	High probability of vehicle abandonment with second uncorrectable wheel seizure.	3-4	Redundancy of six drive units lessens severity of failure mode. Disconnect effective against all but wheel bearing failure.
		Brake engages and will not disengage: (a) actuator sticks (b) linkage sticks	Mechanism becomes completely inoperative.	Same as above.	3	None, but probability of occurance would be very small.
	Provides braking force to wheel.	Brake fails to operate (a) electrical connection fails (b) actuator sticks "off" (c) parking linkage or cable brakes. (d) structure fastener(s) fail.	Load increased on remaining brake units.	Effects depend on magnitude of slopes to be traversed downhill and soil characteristics. Could result in alteration of course to be traversed.	2-4	Normal resistance of drive mechanisms to rotation may reduce loss of a brake to a minor event. The parking brake actuation linkage is a backup to the service brake electrical actuator.

LSSM MOBILITY SUBSYSTEM - Failure Mode and Effect Analysis

Component Identification	Function	Modes of Failure and causes	EFFECTS on component	EFFECTS on subsystem	Criticality Number	Alternates
Wheel	Provides traction and minimizes contact pressure.	Loss of tread: (a) worn and damaged from rough terrain.	Degrades capability of wheel.	Degrades capabilities in soft soil, hard surfaces, and obstacle climbing.	4	Six-wheel design provides good redundancy. Wheel structure redundant.
	Provides support and shock absorbing capability.	Spring wire outer frame fails: adjacent wire hoop fail, causing weak area which continues to widen as hoops are stressed. (a) Wire-restraining components fail. (b) Wire(s) overstressed by sharp rock acting as punch with inner frame as backup. (c) Wires wear excessively due to loss of tread.	Wheel integrity significantly degraded.	Significant probability of reducing length of traverse. Operating speed would be adversely effected.	3	Wheel dragging, due to reduced diameter, could be eliminated by operating disconnect mechanism. Wheel inner frame would give "safety tire" redundancy.
		Stiff inner frame fails: (a) overstressed from excessive transient loads. (b) Restraining parts fail. (c) Damaged subsequent to loss of outer frame.	Wheel integrity severely degraded.	Vehicle velocity would be reduced to minimize damage to remaining components. Abandonment would be probable based on subsequent wheel deterioration.	3	Six-wheel redundancy gives some protection against abandonment.

LSSM MOBILITY SUBSYSTEM - Failure Mode and Effect Analysis

Component identification	Function	Modes of Failure and causes	EFFECTS on component	EFFECTS on subsystem	Criticality Number	Alternates
Wheel (continued)...	(continued).....	Wheel collapses or becomes completely detached: 1. Rim and/or wheel disc collapse or separate. (a) Overstressing from excessive transient loads. (b) Damaged due to damage or loss of inner frame. (c) Rim - to-wheel disc fasteners fail. 2. Wheel hub fasteners fail.	Total capability lost.	High probability of vehicle abandonment with second wheel failure.	2 (1- if outside walk-back radius for 2 failures 3 for one failure	Six-wheel design would allow operation subsequent to first failure in all but rough terrain. Second such failure would probably cause abandonment descending on terrain.
Suspension	Supports wheel. Controls wheel. Absorbs shock.	Joints do not pivot: 1. Bearing surfaces damaged. (a) Parts cold weld (b) Damaged due to misalignment. (c) Intrusion of foreign particles. 2. Damper jams.	Suspension will ride stiff.	Length of traverse may be reduced if velocity must be significantly reduced to avoid overstressing of systems and maintain a reasonable level of ride comfort.	4	Number of joints lessens possibility of significant problem.
		Damper fails to restrain action: (a) Structural parts fail (b) Restraining medium lost.	Wheel control degraded. Deflection limits lost if damper parts.	May require slower speed operation depending on terrain.	4-5	Six independant damper units lessen possibility of significant problem.

Component Identification	Function	Modes of Failure and causes	EFFECTS on component	EFFECTS on subsystem	Criticality Number	Alternates
Suspension (continued)	(continued).....	Suspension arm bends: (a) excessive load transmitted thru wheel. (b) excessive load from obstacle impacting directly against arm.	Functions degraded on damage.	Mobility degraded depending on extent of damage.	3-4	Six-unit design reduces probability of significant problem.
		Suspension arm, pivot points, or brackets fail by fracture: (a) Member fails due to excessive transient load, (e.g. obstacle impact at high velocity). (b) Member damaged, as above, or nicked to produce failure at normal operating stresses.	Functions severely degraded	High probability of excessive dislocation of wheel, causing vehicle abandonment.	2-3 (possible 1 outside wall back radius)	Structural design has some built-in redundancy with respect to failure of certain parts.
		Torsion bar fails: (a) Bar fractures at normal stress level at point of defect or damage. (b) Bar becomes detached at anchor points (c) bar fails from overstressing due to damper failure.	Shock absorbing capability lost.	Subsequent traverse would result in increased stresses on suspension arms, unless velocity reduced. Vehicle abandonment would result if failure follows (c).	2-4	If intact, damper will act to restrain suspension unit in the absence of torsion bar restrainment.

LSSM MOBILITY SUBSYSTEM - Failure Mode and Effect Analysis

Component Identification	Function	Modes of Failure and causes	EFFECTS on component	EFFECTS on subsystem	Criticality Number	Alternates
Chassis-Frame	Restrains suspension assemblies. Base for vehicle. (chassis)	Chassis bends or fractures: Inadvertent overstress during obstacle traverse, either through suspension or direct impact against frame.	Degrades functions depending on extent of damage.	Minor effects, to vehicle abandonment	2-4 (possible 1-if outside walk-back radius)	Vehicle speed reduction could be affected to increase probability of returning to shelter.
		Suspension mounting brackets fail: Overstressed during obstacle traverse.	Function severely degraded	High probability of causing excessive dislocation of wheel.	2-3 (possible 1-if outside walk-back radius)	Multiple hinge point may provide some protection against complete disablement.
	Connects forward and rear units. Provides vehicle flexibility (frame)	Flexible frame bends (yields): (a) Overstressed during obstacle crossing from direct contact (impact) with lunar surface. (b) Overstressed due to loss of pitch limiter restraint.	Degrades functions depending on extent of damage.	Traverse length might be reduced depending on extent of damage, position of vehicle in traverse, and roughness of surface remaining to be traverse	3-4	A bent frame would reduce obstacle crossing mobility but would not incapacitate the vehicle unless the bent frame members subsequently fractured.
		Flexible frame fractures: (See above comments). Overstressed from normal loads due to previous frame member damage	Frame functions lost.	Vehicle disabled.	2 (1- if outside walk-back radius)	Failure of damaged frame may be avoided by careful selection of terrain to be traversed

LSSM MOBILITY SUBSYSTEM - Failure Mode and Effect Analysis

Component Identification	Function	Modes of Failure and causes	EFFECTS on component	EFFECTS on subsystem	Criticality Number	Alternates
Chassis-Frame (continued)...	Restrains trailer movement with respect to 4 x 4. (pitch limiter)	Pitch limiter seizes: (a) Bearing surfaces cold weld. Sealing members fail. (b) Bearing surface damaged due to foreign particles.	Limiter becomes rigid non-moving member.	Traction and obstacle crossing capability adversely effected in other than flat terrain.	4	Driver can avoid obstacles and/or disconnect seized limiter.
		Pitch limiter becomes detached: Connecting points or limiter components fail due to over-stressing caused by bottoming after rapid excursion.	Limiter function lost	Could result in overstressing of frame in rough terrain.	4	Subsequent damage to flex frame could be avoided by careful selection of path to be traversed.
Steering	Provides steering control to front and rear wheels.	Steering torque lost: (a) Motor shorts out. (b) Bearing surfaces seize following seal or lubrication failure. (c) Gear train fails and seizes. (d) Ball screw fails and seizes.	Steering function lost.	Steering capability degraded partly or completely depending if one or both steering assemblies fail.	3	Safety features of steering unit allows disconnecting of seized mechanism and manual alignment of wheels. Subsequent steering accomplishes via two-wheel steering with assist from scuff-steering mode as required.

LSSM MOBILITY SUBSYSTEM - Failure Mode and Effect Analysis

Component Identification	Function	Modes of Failure and causes	EFFECTS on component	EFFECTS on subsystem	Criticality Number	Alternates
Steering (continued)...	Synchronizes steering of front and rear units.	Steering synchronizing lost: (a) Synchronizing rod seizes with subsequent manual disconnection to free steering motors. (b) Rod fractures from over-stressing.	Function lost.	Minor effects on control; some wheel skuffing will occur during turns depending on differences in wheel resistance to turning.	4	Steering units can be operated unsynchronized without excessive degradation of control.
	Restrains front and rear wheels during periods between steering commands.	Wheel restrainment lost: (a) Connecting rods or joints fail from excessive loads. (b) Housing restrainments shear (disconnect pins and gear-rack assembly).	Function Lost.	Vehicle mobility severely degraded.	2-3	Manual repair of failure, to lock wheel into zero-turn position.

LSSM MOBILITY SUBSYSTEM - Failure Mode and Effect Analysis

Component Identification	Function	Modes of Failure and causes	EFFECTS on component	EFFECTS on subsystem	Criticality Number	Alternates
Drive Electronics System (two controller/inverter system assumed).	Control & distribute power to wheel drive motors.	Cabling to wheel drive motor fails: (a) short develops & fuze opens. (b) cabling damaged during obstacle crossing	Function lost	Tractive power lost at corresponding wheel. Head for shelter with second similar failure.	4 - one failure 3 - two failure	Six-wheel configuration gives good drive redundancy. Disconnecting of affected drive unit would minimize drag.
		Critical component of right or left side of system fails: (a) random failure (b) damaged from excessive environmental conditions	Function on one side lost.	Significant tractive power and mobility capability lost. Head for shelter.	3 2 - in rough terrain	Traverse could continue with one side still functioning unless terrain was very rough.
		Both sides of system experience failure of critical component.	Total capability lost.	Vehicle tractive power lost.	2 (Probable 1 - if outside walkback radius)	Depending on failure mode and spare units which may be included in the final configuration, failure might be by-passed to restore operation.

8.2 RELIABILITY ANALYSIS

8.2.1 Introduction

The reliability analysis results presented herein are based on the "Alphonsus Single LSSM Mission" as defined in "Preliminary Design Study of a Lunar Local Scientific Survey Module (LSSM)", First Interim Report, September, 1965, Boeing Document D2-36072-4. This mission consists of twelve manned sorties with travel times ranging from 0.4 hours to 4.0 hours, followed by a remote traverse of 50 hours travel time. Total travel time for the twelve sorties is approximately 38 hours.

Assuming the usual rigorous development program the numerical results of this study represent an estimate of the achievable level of mobility system reliability for the twelve sorties. The remote portion of the mission is not considered.

The reliability values contained in this report are based on related MOLAB data and currently available failure rate data. The analysis assumes that the design is adequate to perform as intended in the environment to be encountered. Further, it is assumed that wear and fatigue, are not significant factors for the relatively short operating times described above, except as adversely influenced by quality defects.

8.2.2 Conclusions

With respect to the "Alphonsus Single LSSM Mission", it was estimated that the reliability of the mobility system would be 0.99218 for the 12 sorties. This value represents the probability of the mobility system not causing mission abort during the 38-hour total operating time. This value may be conservative since some failures may be repairable, depending on the nearness of the vehicle to the shelter when the failure occurs if provisions for repair are included.

Figure 8.2.1 shows the LSSM baseline concept. Figure 8.2.2 presents a block diagram of the mobility system with the probability of success values for each subsystem. The values apply to the 12 manned sorties.

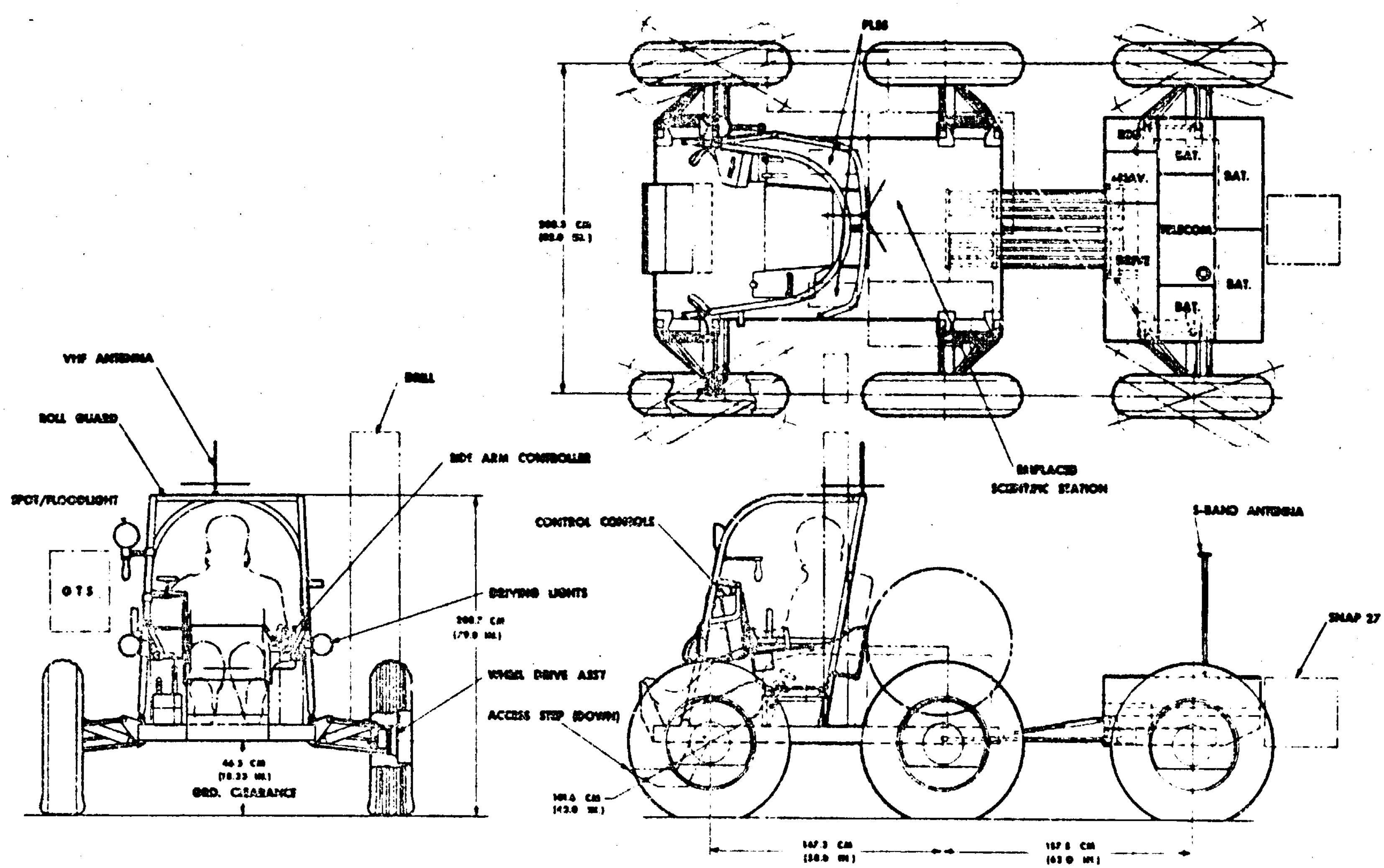

Figure 8.2.1 - Baseline LSSM Concept - Deployed

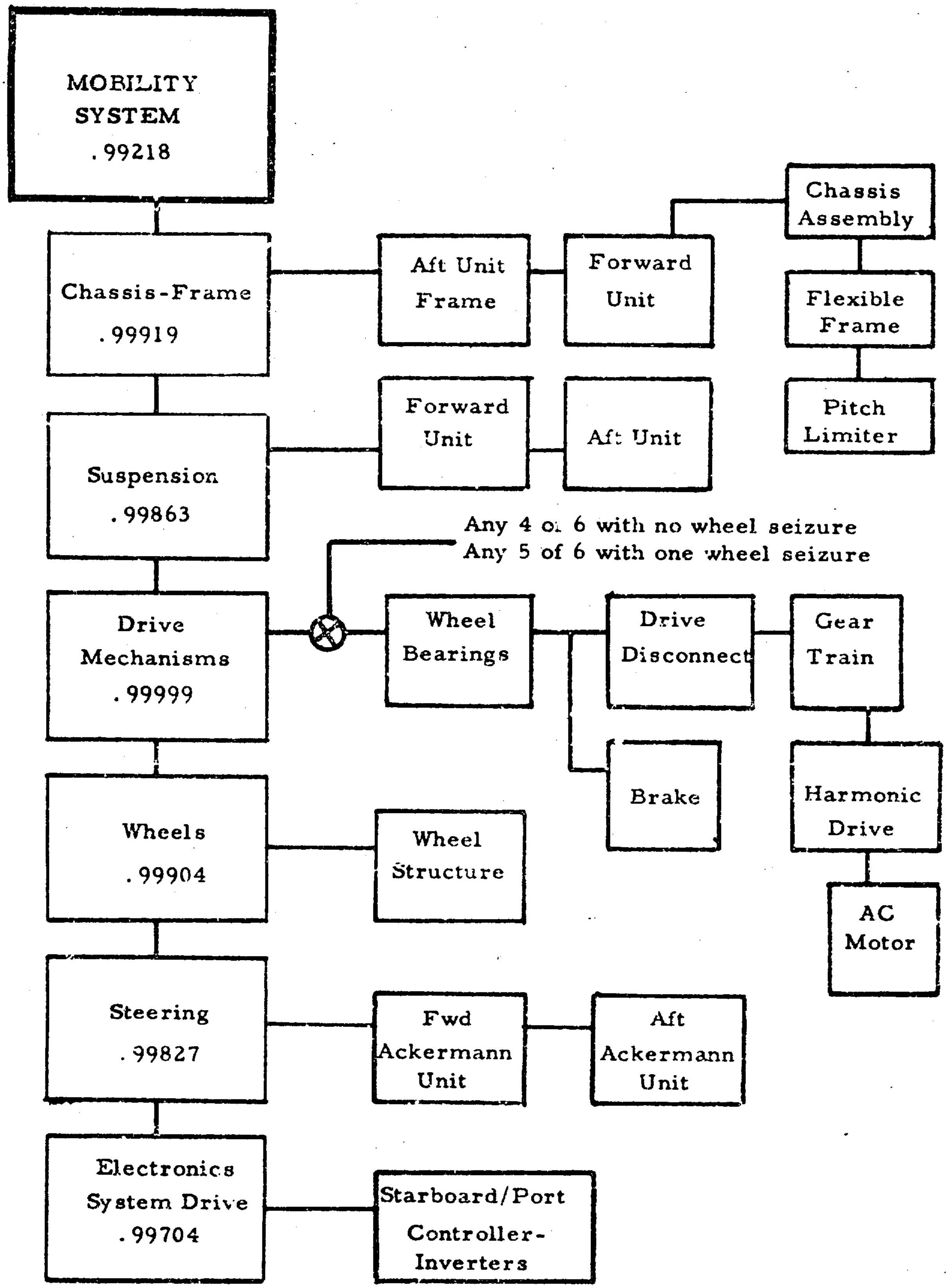

Figure 8.2.2- LSSM Mobility System Reliability Estimates - 12 Manned Sorties Mission

The reliability estimates determined for the mobility system emphasize the value of redundancy in design. The wheel drive mechanisms, the most complex of the subsystems, were determined to have a negligible probability of failure as a subsystem. This is due to the ability of the subsystem to continue adequate functioning with, conservatively, only four drive mechanisms driving.

8.2.3 Discussion

The following discussion presents a statement of the problem, a definition of the mission, the approach used, and comments relative to determining the reliability of the mobility system components.

a. Definition of Problem

In order to gain insight into what attainable probability of mission success might be expected of a LSSM vehicle, the Boeing Company has undertaken to estimate the achievable level of reliability of the LSSM system, assuming a normally rigorous development program. In order to determine the over-all mission reliability, a similar estimate was required for the mobility system, the results of which are presented herein.

b. Baseline Mission Definition

The mission operating profile chosen for this estimate is shown in Figure 8.2.3. The remote portion of the mission is not considered in this reliability estimate. The mission involved in this estimate can be simplified to one operating period of 38 hours.

c. Approach to Estimating Reliability

Use of Failure Rate Data - A review of all known sources of mechanical failure rate data resulted in the selection of the following data sources for the subject estimation:

- Compendium of Failure Rate Data for Polaris Missile Hardware, LMSC-803280, 1 November 1963.
- Reliability Stress and Failure Rate Data for Electrical Equipment, MIL-HDBK-217, 8 August 1962.

SORTIE NO.	MISSION DAY	SORTIE DURATION (HR)	DISTANCE TRAVERSED (KM)	EXPERIMENT TIME (HR)	TRAVEL TIME (HR)	AVERAGE VELOCITY (KM/HR)	SCIENTIFIC PAYLOAD MASS (KG)
1	2	3	5	1.7	1.3	3.8	134
2	2	3	2	2.6	0.4	5.0	270
3	3	6	20	2.0	4.0	5.0	134
4	4	6	20	2.0	4.0	5.0	134
5	5	6	26	1.3	4.6	5.5	134
6	6	6	19	2.2	3.8	5.0	142
7	7	6	20	2.0	4.0	5.0	134
8	8	6	20	2.0	4.0	5.0	142
9	9	6	14	3.5	2.6	5.6	134
10	10	6	16	3.0	3.0	5.3	180
11	11	6	18	2.4	3.6	5.0	138
12	12	6	12	3.6	2.4	5.0	164
					37.7		
MISSION EXTENSION (REMOTE CONTROL)	—	186 ✡	150	74.5	50.0	3.0	88

✡ INCLUDES RECHARGE-TIME

Figure 8.2.3- Alphonsus Single LSSM Mission - LSSM Sortie Summary

Although it is not an objective of this memorandum to explain the detailed procedures of a reliability estimation effort, some comments relative to the failure rate data seem appropriate.

Failure rate data must be construed to be data accumulated for "random" failures which were not time dependent. Time independence implies a constant probability of instantaneous failure. Only with the condition of time independence can the available failure data be used in a logical and correct manner. When using such data, the following assumptions are made: (1) the design is adequate to perform as intended in the environment to be encountered, and (2) wear and fatigue are not reflected by the failure rates except as the result of quality defects.

Failures which are used in compiling failure rate tables would be expected to be caused by one or more of the following: (1) quality defects, (2) abnormal environmental spikes, (3) undetected design deficiencies, and (4) wear and fatigue. A descending order of frequency of encounter would be expected. Wear and fatigue-induced failures would be expected to be infrequent since much of the basic data are from areas of use where preventative maintenance by replacement of parts is common. The significance of the error caused by the inclusion of wear/fatigue failures in the basic data should be materially reduced by the "perfect design" assumption applied to the components under consideration.

Factors to Modify Basic Failure Rates - Several factors were used to modify the basic failure rate data to bring them in line with the conditions of use on LSSM. These factors, as appearing in Attachment 8.2.1 are explained as follows:

t - mission time.

Mission time is usually considered to be 38 hours as previously discussed. Rather than using a full 38-hour mission time for intermittent-operating components, estimated cumulative operating times are used. Periods of non-operation are logically considered to be characterized by zero failure rates for short periods.

K - factor to account for effects of environment.

Basic failure rates are considered to be directly applicable to parts designed and produced under reasonably close controls and subjected to normal operating stresses with reasonable safety factors and at ambient conditions of $70^{\circ}F$ and one atmosphere. With respect to LSSM, normal operating stresses would be considered to be induced via a traverse over a moderately smooth undulating surface at a velocity of 5 km per hour. Possible significant deviations from this would be reflected in the K factor. Estimated effects of temperature and vacuum conditions are also reflected in this adjustment factor.

It should be noted here that the LSSM hardware will undoubtedly receive more extensive reliability and quality control, test, and checkout efforts than received by the parts represented in the basic failure-rate data. It might be concluded that the basic failure rates could, therefore, logically be reduced to reflect an expected lower rate. However, due to critical weight considerations, the LSSM safety factors are expected to be smaller than those related to the basic data. This and the fact that the LSSM will be operating in a more severe environment are believed to reasonably balance the situation.

E - probability of failure of component to cause failure of "12-sortie" mission.

Since a component failure may not always result in failure of the mission, this factor is necessary to reflect in the system reliability figure only those failures which effect system reliability. As an example, failure of a damper might result in subsequent mission failure only five per cent of the time. Therefore, system reliability may be penalized for only five percent of the probability of failure of the damper.

d. Comments on Subsystem Failure Estimates

The following discussion briefly explains the assumptions used in the estimation of reliability of each subsystem and comments on some of the details.

Chassis - Frame - The assumption is made here that a separation of the chassis structure or failure of a suspension arm mounting bracket would have a high probability of causing the detachment of a suspension and wheel assembly shortly thereafter. Loss of one such assembly would be expected to terminate the traverse, causing mission failure. The pitch limiter is considered to be a non-critical component with a failure resulting in loss of pitch restraint of the trailer. This loss could conceivably result in over-stress of other components.

Suspension - Failure of a structural member of a suspension unit is assumed to have a significant probability of causing catastrophic dislocation of a wheel and drive assembly. Four attachment points offer some redundancy. A torsion bar failure might be prevented from causing excessive displacement of the wheel by the damper stop; however, the structural member would be subjected to increased dynamic loads without the "cushion" of the energy-absorbing torsion bar.

Drive Mechanism - Because of the redundancy associated with six-wheel drives, the wheel-drive subsystem can sustain, without mission failure, the following: (1) one wheel drive seizure, or (2) two wheel drives failing to drive. The redundancy of this subsystem complicates the procedure; the details of the work are appended as Attachment 8.2.2. The (E) factor, with respect to this subsystem only, takes on a slightly different meaning. It is used as the probability of the failure of the component to cause the indicated mode of failure. Comments worth mentioning here with respect to reliability estimation of this mechanism are:

(a) Failure rates for the flexspline, circular spline, and wheel bearings were doubled, when considering seizure, to account for possible adverse effects of low pressure operation.

(b) It was assumed that gear teeth failures would be equally divided between gear seizure and all interfering teeth stripping from the gears.

(c) Failure of the drive disconnect would take the form of seizure of the mechanism prior to or during attempted actuation.

(d) High speed bearings would probably fail by seizure.

The redundancy of the wheel drive subsystem is a major factor in the overall system reliability. The reliability of a single drive mechanism was estimated as 0.99898. This value is not significantly better than any of the other subsystem reliabilities. With the six-wheel redundancy the wheel drive subsystem exhibits a negligible unreliability.

Wheels - The assumption here is that mission failure would occur with the failure of one wheel. A wheel failure would be considered as an event more critical than a wheel seizure with essentially total collapse of the wheel structure. A wheel failure could be visualized as resulting in the dragging of the drive mechanism on the lunar surface.

The built-in redundancies of the wheel design make a mathematical model of the wheel reliability highly complex. Therefore, rough approximations were used in arrivi .g at a reliability figure.

Comments appropriate here are:

(a) Failure of the tread and mesh covering, although resulting in a reduction in traction, is considered to have no adverse effect on mission success.

(b) Although there are many parts in the spring wire outer frame to fail, the probability of enough adjacent wires failing to produce a significant area of failure is very remote.

(c) The stiff inner frame has a low operation time, especially at slow speed. Total failure of the outer frame would be backed up by this more rigid inner frame. However, if the wheel were to operate on this inner frame, the probability of failure of the inner frame, rim, and wheel disc would be significantly increased.

(d) The rim and wheel disc are considered to be the only critical parts of the wheel since failure of either would probably cause a wheel loss.

Steering - With respect to steering reliability it is assumed that the mission would be aborted with failure of either steering actuator assembly. Actually, the mission could proceed with certain components inoperative. If one steering motor fails to operate, the second motor can be used to power both steering units via the interconnecting shaft. In addition, the front unit includes an emergency manual steering mode. A third steering mode is skid steering.

Failure modes considered include loss of steering torque and loss of wheel restrainment. It was assumed that the steering motors would be operating about one-third of the vehicle operating time. Bellows failure, excluding the two redundant bellows, could result in failure due to cold welding of bearing surfaces. Bellows fatiguing would be retarded by the vacuum environment.

Referring to Figure 8.2.2, the steering subsystem reliability of 0.99827 would be increased to 0.99999 if one steering unit failure could be tolerated without causing mission failure. Mobility system reliability would be increased from 0.99218 to 0.99390.

Because of the back-up modes of operation, in actual operation on the lunar surface the vehicle would have a high probability of completing a sortie even after sustaining a steering failure. System effectiveness could be enhanced by providing for repair of failures at the lunar base.

Drive Power Distribution - A two controller-inverter power distribution and control configuration was assumed for this subsystem. One controller-inverter feeds the starboard wheels and the other, the port wheels. The control of all six wheels with one controller-inverter has not been considered as a backup mode of operation in this evaluation. However, this is possible with incorporation of a simple switching system.

If a spare controller-inverter were included in this subsystem, the subsystem reliability of 0.99704 would be increased to 0.99999 and the system reliability of 0.99218 would increase to 0.99512.

LSSM FAILURE RATE ESTIMATE: 12- SORTIE MISSION (Part 1)

SUBSYSTEM/COMPONENT	Failures/ 10^6 hrs.	t hrs.	K	E	Failures/10^6
CHASSIS - FRAME					
Forward Unit					
Chassis Assembly					
Structure	3	38	1.0	.8	91
Mounting Brackets (8)	8	38	1.0	.3	91
Flexible Frame Assembly	15	38	1.0	.8	456
Pitch Limiter	10	38	1.0	0.1	38
Aft Unit					
Frame	3	38	1.0	.8	91
Mounting Brackets	4	38	1.0	.3	45
				TOTAL:	812
SUSPENSION					
Forward & Aft Unit					
Damper	10	38	2.0	0.05	38
Upper Arms	2	38	1.0	.3	23
Wheel Drive Brackets	3	38	1.0	.5	57
Lower Arms	2	38	1.0	.3	23
Torsion Bar	5	38	1.0	0.1	19
Joints (6)	6	38	1.0	.3	68
				TOTAL:	228
				(6) units	1368

SUBSYSTEM/COMPONENT	Failures/ 10^6 hrs.	t hrs.	K	E	Failures/10^6
DRIVE MECHANISM	Failure Mode: Disconnect Fails to Operate				
Disconnect					
Pins	1.0	1	2	1	2
Pin Springs	0.5	1	1	1	.5
Restraining Ring	1.0	38	2	1	76
					78
	Failure Mode: Connected Components Sieze				
Electric AC Motor					
Bearings	2 @ 4000 rpm	38	2	1	152
Gear Train (4 gears)	8	38	2	.5	304
Harmonic Drive					
Wav- Generator Bearings	1	38	1	1	38
Flexspline/Circular Spline	6	38	2	.8	365
					859
	Failure Mode: Unconnected Components Sieze				
Brake (fails "on")					
Actuator	1	1	1	1	1
Spring	2	38	1	.5	38
Wheel Bearings (2)	12	38	2	.5	456
					495

LSSM FAILURE RATE ESTIMATES: 12-SORTIE MISSION (Part 3)

SUBSYSTEM/COMPONENT	Failures/ 10^6 hrs.	t hrs.	K	E	Failures/10^6
	Failure Mode: Components Fail to Drive				
Electric AC Motor					
Stator Windings	1 @ 165° C	38	2	1	76
Gear Train (4 gears)	8	38	1	.5	152
Harmonic Drive					
Flexspline Structure	3	38	.5	1	57
Flexspline/Circular Spline	6	38	1	.2	46
Structure					
Housings	2	38	1	1	76
Drive Disconnect					
Pins	3	38	1	1	114
					521

SUBSYSTEM/COMPONENT	Failures/ 10^6 hrs.	t hrs.	K	E	Failures/10^6
WHEELS					
Wheel Structure					
Tread	10	38	.8	0.0	0
Mesh Cover	8	38	.8	0.0	0
Spring Wire Outer Frame	5x360x.005	38	.5	0.2	34
Stiff Inner Frame	15	1.0	.5	0.8	6
Rim	3	38	.5	1.0	57
Wheel Disc	3	38	.5	1.0	57
Fasteners	1	38	.5	0.3	6
					160
				TOTAL: (6) units	960
STEERING					
Motor	18	10	1.3	1	234
Bearing & Bearing Surfaces (9)	9	10	1	.5	45
Gear Train (4)	8	38	1	1	304
Ball Screw & Nut	4	38	1	.5	76
Steering Link (2)	2	38	1	..5	38
Bellows (2)	6	38	.8	.9	164
Hsg.-Restrainments	3	38	1	.05	6
					867
				TOTAL: (2)units	1734
DRIVE POWER DISTRIBUTION					
Controller-inverters	78*	38	1	1	2964

* From Reference (e)

ESTIMATE OF LSSM WHEEL DRIVE MECHANISM RELIABILITY

uccess Definition: Mission may continue with one wheel drive seizure or two heel drive failures to drive. (This redundancy allowance is less conservative han that reflected in reference (d); results using other criteria are included in his enclosure).

$R_{subsystem} = P_r$ (exactly one wheel seizure will occur)

$+P_r$ (no more than two failures-to-drive occur).

let: $P_s = P_r$ (seizure)

$P_F = P_r$ (failure to drive)

$P_C = P_r$ (good)

$$R_s = \binom{6}{1} P_s P_6^5 + \sum_{i=0}^{2} \binom{6}{1} P_F^i P_G^{6-i} = 6 P_s P_G^5 + 6 P_F P_G^5 + 15 P_F^2 P_G^4$$

P_r (seizure):

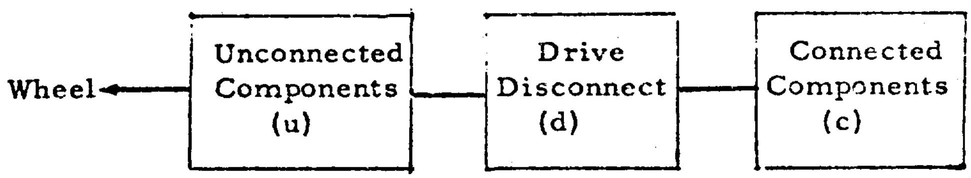

$P_s = P_r$ (connected components seize and disconnect cannot be operated r unconnected components seize or both connected and unconnected components eize).

$P_s = P_r$ (c seizes) x P_r (d cannot be operated) x P_r (u does not seize) + P_r (u seizes) + (o).

$P_s = (.000859)(.000080)(.999505) + (.000495)$

$P_s \cong .000495$

(Note: Values obtained from enclosure (4), pgs. 2 & 3, developed using ref (d)).

Subsystem R:

$$P_s = .000495$$

$$P_F = .000521$$

$$P_G = .998984$$

$$R_s = 6\,(.000495)\,(.998984)^5 + (.998984)^6 + 6\,(.000521)\,(.998984)^5$$
$$+ \ 15\,(.000521)^2\,(.998984)^4$$

$$R_s = \underline{.999988}$$

For other "success" criteria:

Failure Allowance w/o Mission Failure	Drive Reliability	Mobility System Reliability
None — All Wheels operate:	.993919	.986155
One Wheel Seizes:	.996874	.989087
One wheel fails to Drive:	.997029	.989241
Two wheels fail to Drive:	.997033	.989245

9.0 CONCLUSIONS

This report has discussed the process leading to the selection of a 6 x 6 semi-flexible frame vehicle as the preferred LSSM baseline concept. Analytical, scale-model and computer techniques for evaluating the mobility performance of vehicles in general, and the baseline LSSM in particular, were described. A preliminary design was performed, in sufficient detail to demonstrate feasibility and to develop a substantial degree of confidence in the ability to implement the design. the LSSM mobility system consisting of the following subsystems:

- Flexible wire frame wheels
- Individual wheel drive mechanisms with AC induction motors and harmonic drive reduction
- Identical parallel arm suspensions with torsion bar spring element and linear hydraulic damper
- Identical DC motor drive Ackermann-type cross-link actuators for front and rear sets of wheels
- Chassis-Frame consisting of forward and unit box structures, flexible tubular rods connecting the two units, and a telescoping pitch limiter.
- Electric drive inverter-modular control system

Some of the major conclusions reached during the course of this study were:

- Based on considerations of mobility and reliability to increase the probability of mission success and crew safety, the preferred concept for the baseline LSSM is a 6 x 6 articulated frame vehicle.
- The use of six individually powered wheels and two-axle steering provides important redundancies in case of mechanism failure.